**Harm-Gerd Karl Blaas**

# THE EMBRYONIC EXAMINATION

## Ultrasound studies on the development of the human embryo

NTNU Trondheim
Norwegian University of Science and Technology
Faculty of Medicine

TAPIR

**Harm-Gerd Karl Blaas**

# THE EMBRYONIC EXAMINATION

## Ultrasound studies on the development of the human embryo

TAPIR

Publication from the Norwegian University
of Science and Technology
National Center for Fetal Medicine
Department of Gynecology and Obstetrics
N–7006 Trondheim, Norway



ISBN 82-519-1515-5
ISSN 0805-7680

Printed by TAPIR trykkeri

*TAPIR forlag*
*N–7005 TRONDHEIM*
*Tel.: + 47 73 59 32 10*
*Fax: + 47 73 59 32 04*
*Email: tapir.forlag@tapir.ntnu.no*
*http://www.tapir.ntnu.no*

# Contents

## 1.1 Acknowledgments

This work was performed at the National Center for Fetal Medicine from the Department of Obstetrics and Gynecology, University Hospital of Trondheim. Many people have supported my efforts, and I wish to express my gratitude to them all.

My sincere thanks to Professor Kåre Molne, Head of the Department of Gynecology, and to Dr. Thomas Knoff, Head of the Department of Obstetrics, for their kind support and enduring encouragement.

This work would have been impossible without my tutor, co-writer and friend Professor Dr. med. Sturla Hall Eik-Nes. He offered me the chance to come to Trondheim, where he provided the foundation for my work: a laboratory with tremendous possibilities for research, the equipment and assistance which was essential in performing these studies. He introduced me into scientific work, and contributed decisively to the progress of my studies by constant positive and constructive criticism. His sense for proportions, order and perfection and his extensive knowledge improved my papers and this book. I am greatly indebted to him for his valuable teaching, his generous friendship, and his never-ending readiness to help and support me.

My honest thanks go to my friend and co-writer Dr. med. Torvid Kiserud. We shared an office for several years, where we had fruitful and constructive professional discussions during long evening hours, now and then interrupted by a refreshing match of quick-chess. Many ideas for our research were hatched during these inspiring evening and night hours.

I also wish to express my gratitude to the indispensable technical and statistical help that I have received from Leif Rune Hellevik, MSc, John Bjørnar Bremnes, MSc, and Sevald Berg, MSc.

Many thanks, too, to Professor Dr. techn. Hans Torp, Professor Dr. techn. Bjørn Angelsen and Professor Dr. techn. Bjørn Olstad who gave me valuable ideas, suggestions and support to my 3D ultrasound studies.

The 3D studies would not have been performed without the technical assistance from the firm Vingmed Sound, Horten. Ditlev Martens, MSc, Christian Michelsen Research,

Bergen, made major contributions for the development of the EchoPAC-3D software from Vingmed Sound. Provision of this EchoPAC-3D software, and the specially designed 3D transvaginal transducer, and the valuable help from Dr. techn. Kjell Arne Ingebrigtsen, Arve Stavø, MSc, and Dr. ing. Erik Steen was essential for these studies.

I want to thank my co-workers Dr. med. Kjell Åsmund Salvesen, and mid-wives Eva Tegnander, Gerd Inger Lånke, Bente Simensen, Josefa Anonuevo Berit Albriktsen, Kjerstin Eriksson, Randi Ytre-Eide, Lise Svaasand and Wenche Willassen for their inexhaustible enthusiasm and co-operation which made daily life at the department so pleasant.

I am very grateful to the extraordinarily co-operative and friendly staff of the ultrasound department, in particular to Mari Schille, Unni Hansen, Kristin Trondsetås Græsli, Christine Østerlie and Laila Småvik for their crucial assistance in finding patients for the studies. And I want to thank all the patients who were willing to participate in my studies making this research possible.

I owe special thanks to Nancy Lea Eik-Nes for her indefatigable readiness to revise the language of the papers and this book. Her knowledge of the art of medical writing has improved my manuscripts significantly.

Finally, my warm thanks go to my beloved family. My wife Sissel, who stood patiently at my side during all these years, though my studies restricted spare time for my family to a minimum. She has become so used to hearing me saying «I'm busy» – has she? And my daughters Fey-Constanze, Ewa Simone and Ine Gerlinde, who were and are my constant source of joy, and who with loving forbearance have not given up on their stressed and absent-minded father.

Trondheim, October 1998

Harm-Gerd Karl Blaas

## 1.2 Summary


### Introduction
Embryology is the description of the anatomy, the normal anatomic relations and the development of abnormalities of the embryo. The developmental steps of the human embryo have been described and staged by the classical human embryologists. More than 30 years ago ultrasound was introduced as a mean to evaluate the pregnancy. In the 70's, measurements of the embryo and extra-embryonic structures were presented. This initiated many studies that described the normal and abnormal early pregnancy. When real-time ultrasound was put into use, the interest for the morphological development of the embryo and fetus increased. At the end of the 80's, the introduction of high-frequency transvaginal ultrasound made the anatomical description of the living embryo possible.

### Purpose
The objective of the thesis was to give a detailed description of the normal development of the human embryo by using high-frequency 7.5 MHz ultrasound and employing two-dimensional and three-dimensional imaging techniques.

### Subjects and methods
Twenty-nine normal early singleton pregnancies were included in a longitudinal study and examined 5 times each, with intervals of approximately one week between the examinations. All pregnancies were examined between 7 and 12 weeks of gestation with two-dimensional ultrasound. Multiple measurements were carried out, including the brain (lateral ventricles, cavities of diencephalon, mesencephalon and rhombencephalon, choroid plexuses of lateral ventricles and of fourth ventricle, and cerebellum), embryonic and extra-embryonic biometry (CRL, BPD, OFD, MAD, chorionic cavity, amniotic cavity, yolk sac), and truncal structures (heart diameter and heart rate, stomach, midgut herniation) (Papers I–IV).

Three normal healthy early pregnancies (7-, 9- and 11-week-old) were included in a pilot-study and evaluated by three-dimensional ultrasound in a new 3D prototype set-up. The brain cavities were reconstructed from the ultrasound recordings (Paper V).

Thirty-four normal early singleton pregnancies were included in another three-dimensional study (7- to 10-week old; 9.3–39 mm CRL). A new specially designed 7.5 MHz 3D transvaginal probe was developed and was used for the ultrasound recordings. The ultrasound data were digitalized and transferred to a PC for further analysis with 3D software (EchoPAC 3D). After manual segmentation of embryonic structures in the 3D volume, reconstructions of the bodies and the brain compartments of the specimens could be made (Paper VI).

### Results and comments
It was possible to describe the anatomy of embryos and embryonic organs longitudinally from week seven on.

At week seven all brain compartments were visible. Initially, the rhombencephalic cavity was the largest, while the hemispheres were the smallest brain compartment. The hemispheres grew exponentially and dominated the brain after week eight. The cavities of the mesencephalon (future Sylvian aqueduct) and diencephalon (future third ventricle) had approximately the same size during week seven. At the end of the first trimester, the cavity of the diencephalon had become very narrow, while the future Sylvian aqueduct still was a relatively large cavity. The choroid plexuses of the fourth and of the lateral ventricles appeared during week eight. The cerebellum became distinct during week nine. The first sign of the midgut herniation appeared during week seven. The stomach and the

heart chambers became visible during week eight. The reciprocal movements of the atrial and ventricular walls of the heart made the identification of the atria and ventricles possible. The heart rate increased from mean 138 bpm at week seven to mean 175 bpm at week nine. The embryos and their associated structures showed virtually identical growth velocities. The growth of the yolk sac was uniform until 10 weeks when it degenerated either by shrinking or by enlarging before dissipating; the alteration of the shape is believed to reflect the cessation of the physiological function at that time. The spread of the parallel growth curves between the individuals varied more than expected. This may have been due to a discrepancy between the LMP-based age and the true age, caused by variations of the time of ovulation, fertilization and nidation, and/or of the growth at very early stages. Once the growth velocity picked up, the embryos seemed to follow the same growth curve.

The development of the size of the specimens and the shape both of the body and the brain cavities showed good agreement with images from the embryological literature. Three-dimensional reconstructions of the slender body and the tiny ventricles during week seven highly resembled the images from classic embryological literature. With increasing age and size the shape of the bodies gradually changed from cuboid to elongated ellipsoid. The brain cavities altered their shape and their relative proportion. In the largest specimens the lateral cerebral ventricles dominated the brain and concealed the third ventricle. The cavity of the mesencephalon was relatively large throughout the first trimester. In the smallest embryos, the rhombencephalic cavity was the largest cavity in the top of the head. In the largest fetuses, it had changed its form and position and was located posteriorly in the head.

## Conclusion

The in-vivo two-dimensional and three-dimensional ultrasound findings were in agreement with the descriptions and the «developmental time schedule» of human embryos as described in the Carnegie staging system. A remarkable uniformity of the development could be registered: Specimens of the same size (CRL) looked virtually identical. The developmental degree and the size of the organs and the relative proportions of these structures to each other were similar in embryos of the same size. The volume reconstructions of living embryos and their CNS represent new information which has not been possible before in human embryology.

## Future aspects

It has become possible to produce ultrasound images with such a quality that the interest has gone beyond the practical diagnostic use towards the use of sonoembryology as a research tool in the basic evaluation of the growing embryo. The embryo can now be followed in vivo and be displayed in both two and three dimensions. The overview of normal embryological development gives an idea of the manifold dramatic processes that take place during the first trimester. High frequency transvaginal ultrasound will help disclose developmental disorders of the embryo and the early fetus; it is already a technique that has become invaluable for women with increased risk of hereditary conditions.

There is no reason to believe that the technological development of ultrasound has reached its end-point or even come close to it. An increase of the transmitted ultrasound frequency is to be expected, which in turn will increase the resolution. Computer technology will be increasingly used to handle the pre- and postprocessing of ultrasound imaging. There is reason to believe the three-dimensional technique, too, will be developed and have practical use in the evaluation of the early pregnancy.

## 1.3 List of the papers

The thesis is based on studies reported in the following papers, and referred to in the text as Paper I to VI:

Paper I
Harm-Gerd Blaas, Sturla H. Eik-Nes, Torvid Kiserud, Leif Rune Hellevik. Early development of the forebrain and midbrain: a longitudinal ultrasound study from 7 to 12 weeks of gestation.
Ultrasound Obstet Gynecol 1994; 4:183–92.

Paper II
Harm-Gerd Blaas, Sturla H. Eik-Nes, Torvid Kiserud, Leif Rune Hellevik. Early development of the hindbrain: a longitudinal ultrasound study from 7 to 12 weeks of gestation. Ultrasound Obstet Gynecol 1995; 5:151–60.

Paper III
Harm-Gerd Blaas, Sturla H. Eik-Nes, Torvid Kiserud, Leif Rune Hellevik. Early development of the abdominal wall, stomach and heart from 7 to 12 weeks of gestation: a longitudinal ultrasound study. Ultrasound Obstet Gynecol 1995; 6:240–49.

Paper IV
Harm-Gerd Blaas, Sturla H. Eik-Nes, John Bjørnar Bremnes. The growth of the human embryo. A longitudinal biometric assessment from 7 to 12 weeks of gestation.
Ultrasound Obstet Gynecol 1998; 12:346–54.

Paper V
Harm-Gerd Blaas, Sturla H. Eik-Nes, Torvid Kiserud, Sevald Berg, Bjørn Angelsen, Bjørn Olstad. Three-dimensional imaging of the brain cavities in human embryos.
Ultrasound Obstet Gynecol 1995; 5:228–32.

Paper VI
Harm-Gerd Blaas, Sturla H. Eik-Nes, Sevald Berg, Hans Torp. In-vivo three-dimensional ultrasound reconstructions of embryos and early fetuses. Lancet 1998; 352:1182–6.

## 1.4 Abbreviations

| | |
|---|---|
| 2D | two-dimensional |
| 3D | three-dimensional |
| A-scan (mode) | amplitude scan (mode) |
| AC | abdominal circumference |
| B-scan (mode) | brightness scan (mode) |
| BPD | biparietal diameter |
| bpm | beats per minute |
| CNS | central nervous system |
| CRL | crown-rump length |
| GL | greatest length |
| HC | head circumference |
| M-mode | motion mode |
| MAD | mean abdominal diameter |
| MHz | Megahertz |
| OFD | occipito-frontal diameter |

# 2 Background

## 2.1 Classic human embryology

### 2.1.1 History of classic human embryology

More than 100 years ago, Wilhelm His thoroughly described the anatomy of individual human embryos with the help of fixation and sectioning techniques, and reconstructions from the resulting histological slices (His, 1880-85; His, 1887). Through this founding work based on the examination of chicken embryos and aborted human embryos and fetuses, he has come to be known as the «Vesalius of human embryology» (O'Rahilly and Müller, 1987).

Keibel and Mall continued His' efforts to describe the early human development (Keibel and Mall, 1910; Keibel and Mall, 1911). In 1914 Mall proposed a staging system based on the external features of embryos (Mall, 1914). The staging system used today, the Carnegie staging system, was originally devised in the 1940's by Streeter [(Streeter, 1942; Streeter, 1945; Streeter, 1948) who called the stages 'horizons'. In 1987, O'Rahilly and Müller revised the staging system, and introduced 'stages' instead of 'horizons' (O'Rahilly and Müller, 1987). In the Carnegie staging system for dating and staging of human embryos, the first eight postovulatory weeks are divided into 23 stages based on the external and internal morphological status of the embryos. The onset of marrow formation in the humerus was arbitrarily adopted as the completion of the embryonic period and the beginning of the fetal period of prenatal life (Streeter, 1949). Streeter believed that the time range in each of the 'horizons' 10 to 23 was only ± 1 day, but it is now known that the range becomes increasingly greater from Carnegie stage 14 onwards (O'Rahilly and Müller, 1987).

According to O'Rahilly (O'Rahilly and Müller, 1994), an embryo of 10 post menstrual weeks is less than half the length of an adult thumb, but already possesses several thousands named structures, practically any of which may be subject to developmental deviations. Thus, the embryonic period proper is particularly important because, during that time, the majority of congenital anomalies make their appearance. The knowledge of the normal development of the human embryo is a prerequisite of all first trimester ultrasound diagnosis.

### 2.1.2 Definition of embryonic/fetal age

This thesis deals with the transvaginal two-dimensional and three-dimensional ultrasound examination of embryos and young fetuses aged about seven to 12 weeks of gestation as based on the last menstrual period (LMP). The determination of the age of an embryo or fetus is a prerequisite for assessing its development. Age can be expressed in different ways: Obstetricians use the gestational age based on the LMP for the dating of the pregnancy. The «Nägele's rule» was introduced over 150 years ago by Nägele, who was well aware of the uncertainties associated with his method (Nägele FC. Lehrbuch der Geburtshülfe für Hebammen. Heidelberg: Akademische Buchhandlung von JEB Mohr, 1833) (Geirsson, 1997). It took many decades to recognize the correlation between the last menstrual period and the ovulation. In 1918 it was still believed that ovulation occurs between the 4$^{th}$ and the 13$^{th}$ post menstrual day, with fertilization approximately one day after copulation (Mall, 1918). Mall's analysis of his own studies and of the literature confirmed the biological variations of the time period between menstruation and the beginning of the pregnancy (Mall, 1918). Today, large studies plead for the advantageous use of ultrasound measurements in assessing the gestational age (Tunón *et al.*, 1996). This is also discussed in-extenso in a recently published review article (Geirsson, 1997). Embryologists prefer to use postovulatory age, which refers to the length of time since the last ovulation prior to the pregnancy, because fertilization must occur very close to the time of ovulation (O'Rahilly and Müller, 1987). O'Rahilly recommends avoiding the word «conception» (post conceptional age), as fertilization is not universally accepted as the commencement of the pregnancy: some authors even use «implantation» as the start of the pregnancy (O'Rahilly and Müller, 1987).

In order to use a uniform terminology, all statements of time in this thesis are based on the last menstrual period, expressed in completed weeks and completed days, assuming a regular cycle with ovulation at 2 weeks 0 days. This means that both the length of the pregnancy and the age of the embryo are expressed in the same way making the comparison of embryonic development with first trimester ultrasound findings easy. For example, 'during week 8' means 8 completed weeks plus 0 to 6 days, and 'at the end of week 9' means 9 completed weeks plus about 4 to 6 days from the last menstrual period.

### 2.1.3 The development of the human embryo

The human embryo develops from the fertilized ovum, through the bilaminar and three-laminar disc, into a cylindrical body, and only at the end of the embryonic period does it look like an immature human being with its unique structural proportions. In the

following overview, the chronological development is described based on modern embryological text books (O'Rahilly and Müller, 1987; Hinrichsen, 1990; Larsen, 1993; O'Rahilly and Müller, 1994) when not annotated otherwise in the text. The description is limited to the organs and organ systems which are of interest for the understanding of this thesis.

#### 2.1.3.1 2 weeks 0 days to 4 weeks 6 days

These first three weeks of embryonic development are described by Carnegie stages 1 to 9. The first unicellular stage is characterized by the fertilization. An outline of the main embryonic developmental steps until week four are: blastomere (stage 2); blastocyst (stage 3, ≈ 2 weeks 1 1/2 – 3 days, and stage 4, ≈ 2 weeks 5 - 6 days), implantation (stage 4); amniotic cavity and primary yolk sac, also called umbilical vesicle (stage 5, ≈ 3 weeks 0 - 5 days); primitive chorionic villi, secondary yolk sac and occurrence of the primitive streak (stage 6, ≈ 3 weeks 6 days); «gastrulation»: cells from the epiblast substitute the hypoblast and migrate between the two existing cell layers establishing the mesoderm; notochordal process (stage 7, ≈ 4 weeks 2 days); initiated by the appearance of the primitive streak, this event starts the transformation of the embryonic cell clot into an individual with bilateral symmetry, with dorsal and ventral surfaces, with rostral and caudal ends and left and right sides; appearance of the oropharyngeal and the cloacal membrane, start of the neurulation (stage 8, ≈ 4 weeks 4 days); appearance of the primitive heart tube (stage 9, ≈ 4 weeks 6 days).

#### 2.1.3.2 5 weeks 0–6 days

External form: The folding process which transforms the embryonic disc into a cylindrical body takes place from Carnegie stage 9 (≈ 4 weeks and 6 ± 1 days) to Carnegie stage 12 (≈ 5 weeks and 5 ± 1 days) (O'Rahilly and Müller, 1987). The edges of the embryonic disc continue dorsally into the amniotic membrane, and ventrally into the wall of the umbilical vesicle (yolk sac). By the folding process of the embryo, the amniotic membrane, and thus, the amniotic cavity, is drawn over the embryo. At the end of this process the amniotic membrane ensheathes the body stalk, in other words, the umbilical cord, which contains remnants of the allantois, the umbilical vessels, and the vitelline duct. From this time, the embryo grows more rapidly than the yolk sac. The initially wide connection between the yolk and the embryo narrows into the vitelline duct, keeping a continuous connection to the developing gut tube. At the end of the week the body stalk is established. CNS: At Carnegie stage 10 (≈ 5 weeks 1 day), the neural folds begin to fuse in the adjacent rhombencephalic and spinal regions. The site of the final closure of the

rostral neuropore at Carnegie stage 11 (≈ 5 weeks 3 days) is probably the future commissural plate in the middle of the lamina terminalis. The closure of the neural tube heralds the onset of the ventricular system and separates the ependymal from the amniotic fluid (O'Rahilly and Müller, 1990). In studies of chicken embryos it was found that the embryonic brain compartments start to enlarge abruptly immediately after closure of the neural tube. In the study group of chicken embryos, where the cavity of the mesencephalon was drained, the development of the brain tissue was reduced. This indicates that fluid pressure is a necessary driving force for normal brain enlargement (Desmond and Jacobson, 1977). A series of ring-like constrictions mark the approximate boundaries between the primordia of the major brain regions: the forebrain, the midbrain, and the hindbrain (Rubenstein *et al.*, 1998). Heart: The heart tube folds into the primitive atria (sinus venosus) and the ventricular compartment. Cardiac contractions are believed to commence at the beginning of Carnegie stage 10 (≈ 5 weeks 1 ± 1 days) (deVries and Saunders, 1962). Peristaltic flow is shown at Carnegie stage 11 (≈ 5 weeks 3 days). Intestinal tract: The oropharyngeal membrane ruptures at 38 days (O'Rahilly, 1978).

#### 2.1.3.3 6 weeks 0–6 days

External form: At Carnegie stage 13 (≈ 6 weeks 0 days), all four limb buds become visible. They become paddle-shaped during the next two Carnegie stages, where the upper limb develops first. CNS: At Carnegie stages 14 (≈ 6 weeks 4 days) and 15 (≈ 6 weeks 5 days) the forebrain divides into the telencephalon, with the cerebral hemispheres as small evaginations, and into the diencephalon (Yokoh, 1975; O'Rahilly and Müller, 1994). Heart: The septum primum and the foramen primum appear in the heart. Intestinal tract: The stomach appears fusiform at Carnegie stage 13 (Streeter, 1945).

#### 2.1.3.4 7 weeks 0–6 days

External form: The thighs, legs and feet are becoming distinguishable at Carnegie stage 16 (≈ 7 weeks 2 days). The digital rays of the hand appear. CNS: No longitudinal fissure is found between the laterally bulging cerebral hemispheres at this Carnegie stage. At the end of the week, at Carnegie stage 17 (≈ 7 weeks 5 days), the interventricular foramen is delimited by the corpus striatum and the ventral thalamus. The cerebellar primordium grows, the isthmus rhombencephali is evident. Heart: The atrioventricular cushions are fusing. The foramen secundum and the semilunar cusps appear. The innervation of the heart starts in the embryo of 10 mm - 13 mm CRL (7 weeks) where branches of the vagal nerve and cervical sympathicus are found in the region of the sinus venosus and with the trunks of the aorta and the pulmonal artery (Steding and Seidl, 1990). Intestinal tract: In

1817, Meckel reported on the development of the embryonic gastro-intestinal tract (Meckel, 1817). He stated that the midgut herniation in embryos was physiological and not an early malformation. Sometimes a diverticle (Meckel's diverticulum), which represents a remnant of the vitelline duct, is found at the ileum. The primary bowel loop was described entering the umbilical cord in embryos of 7 mm - 10 mm CRL (Kiesselbach, 1952). At Carnegie stage 17, approximately 7 weeks 6 days, the primary intestinal loop can be seen, projecting further into the umbilical cord as the normal umbilical hernia (Streeter, 1948). The counterclockwise rotation of the intestine commences.

#### 2.1.3.5 8 weeks 0–6 days

External form: The cuboidal body elongates during this week, the limbs extend in the forward direction. At Carnegie stage 18 (≈ 8 weeks 2 days) the elbow region becomes discernible. The toe rays may be identified. CNS: In the rhombencephalon the choroid plexuses are present in most embryos. Half of the diencephalon is covered by the hemispheres. The mesencephalon is on the top of the brain. Heart: In the heart the membranous part of the interventricular septum takes form. The septum secundum and the foramen ovale are appearing. At Carnegie stage 19 (≈ 8 weeks 5 - 6 days) the ventricles lie ventrally to the atria. The endocardial cushions fuse. Extraembryonic structures: The embryonic hematopoiesis shifts from the yolk sac to the liver. Intestinal tract: Already in about 15 mm CRL embryos, the stomach shows the fornix, corpus and pars pylorica (Pernkopf, 1923). The cloacal membrane ruptures from urinary pressure in embryos of 16-17 mm CRL (Ludwig, 1965), the anal membrane breaks down after 62 (deVries and Friedland, 1974) to 65 days (O'Rahilly, 1978). The question of epithelial plugging and/or vacuolization in the embryological development of the duodenum has been discussed. Some authors believe that non-recanalisation of complete plugging of the lumen at Carnegie stage 19 is responsible for the duodenal atresia (Boyden *et al.*, 1967), while other authors doubt the existence of a complete plugging (Moutsouris, 1966).

#### 2.1.3.6 9 weeks 0–6 days

Carnegie stages 20 to 23 describe the final week of the embryonic development. External form: During this week the head becomes more rounded and set upright, while the body, the arms and the legs further elongate. The elbows bend laterally, the fingers on opposite hands may touch over the mid-line. At the end of the week the soles of the feet are still in a sagittal position. CNS: The chondrocranium and the skeletogenous layer of the head become recognizable. At the end of the embryonic period the falx cerebri starts to develop

from the skeletogenous layer. The cerebral hemispheres nearly conceal the diencephalon. Fusion of the medial walls of the hemispheres does not occur during the embryonic period. The foramina of Monro reduce to dorsoventral slits. The insula appears. The thalami are thickening. The cavity of the mesencephalon is still wide. The rhombic lips have developed into cerebellar hemispheres. The choroid plexuses of the fourth ventricle divide the roof into the pars membranacea superior and inferior. Heart: The truncoconal swellings grow down onto the upper ridge of the ventricular septum and onto the inferior endocardial cushion, separating the right and left ventricles. The formation of the foramen ovale by the septum secundum is completed during week nine (Moore, 1988). The expansion of the cardiac nerves and ganglions is completed late in the fetal period. Body cavities: The diaphragm is established dividing the pleuro-peritoneal cavity. At Carnegie stage 20 (≈ 9 weeks 2 days), the narrow pleuro-peritoneal duct still connects the pleural and peritoneal cavities (Duncker, 1990). At Carnegie stage 23 (≈ 10 weeks 0 - 1 days), the lungs fill less than half of the pleural cavity. Intestinal tract: According to Ludwig, the anal membrane ruptures in embryos of 27 mm to 33 mm CRL (Ludwig, 1965).

#### 2.1.3.7 10 weeks 0–6 days and 11 weeks 0-6 days

Early postembryonic period

The distinction between the embryonic period and the fetal period is arbitrarily chosen at the onset of marrow formation in the humerus (Streeter, 1949). External form: The body and the limbs achieve the typical fetal shape. The feet gradually obtain the adult position. CNS: Among the most noticeable external changes of the brain are the union of the cerebellar hemispheres with the definition of the vermis and the increasing concealment of the diencephalon and mesencephalon by the cerebral hemispheres. The cerebellum enlarges, drawing the roof of the fourth ventricle beneath its caudal border. The development of the corpus callosum begins at about 12 - 13 weeks. The mesencephalic cavity is still wide. Intestinal tract: After a rotation of a total of $270^0$, the intestine returns into the abdominal cavity during week 11. Lauge-Hansen found that the last bowel loop had returned into the abdominal cavity in fetuses with a 44 mm CRL (Lauge-Hansen, 1973), while Kiesselbach stated more generally, after reviewing the embryological literature, that the midgut returned into the abdomen in fetuses of 40 mm to 50 mm CRL (Kiesselbach, 1952). Thus, at approximately the end of week 11 the physiological herniation is completed.

## 2.2 Ultrasound in medicine

### 2.2.1 Development of ultrasound in medicine

In 1880, Wilhelm His' contemporaries, the Curie brothers, detected the piezoelectric or pressure-electric effect, «le phénomène de pyroélectricité» as the Curie brothers described it. The effect was detected on the surface of a specially cut piece of quartz which was exposed to mechanical stress, and thus the potential for creating ultrasonic waves was recognized (Curie and Curie, 1880). In 1937, inspired by a review article about ultrasound application in underwater techniques, the Austrian neurologist K. Th. Dussik made the first attempts to use ultrasound in medical diagnosis, which he discussed in a paper in 1942 (Dussik, 1942). The pulse-echo technique was developed in USA by Howry and Bliss at the end of the forties and the beginning of the fifties. They developed a forerunner to the compound scanner, which they called Somascope ('tissue vision') (Howry and Bliss, 1952). Howry later described compound-scanning which made it possible to obtain both uni-dimensional A-mode and two-dimensional B-mode images (Howry, 1957).

The A-mode displayed the amplitude of the echoes detected by the transducer as jags on the screen of the oscillograph. The echo-pattern on the oscilloscope screen altered with the angle of the sound beam. The relative direction of the beam could not be shown, therefore, the information was limited to these structures that caused the echoes. In B-mode, the signals were displayed with varying brightness according to the height (intensity) of the amplitude of the returning echo. Using the compound-scan, segment-shaped echoes were obtained from an object from several positions. These segments met forming a rosette, with the object at the center. Since the object was crossed by all segments, most light and enhancement was generated at and around the object on the ultrasound image. At the same time, most of the object was displayed in the axial direction of the beam giving a rather good quality of the image.

In the field of obstetrics and gynecology, Ian Donald's pioneering article about «The investigation of abdominal masses by pulsed ultrasound» in 1958 was a breakthrough. He introduced the world's first direct-contact two-dimensional ultrasonic scanner which would revolutionize the every day life of the gynecologist and obstetrician (Donald *et al.*, 1958; Donald, 1964).

Real time 2D imaging was described in the late sixties: The Siemens Vidoson echoscope

achieved a fast real-time linear scan by utilizing a rotating transducer situated at the focus of a parabolic reflector (Krause and Soldner, 1967). The development of transducer arrays and the associated circuitry for steering and shaping of the ultrasound beam had a major clinical impact for the future of real-time ultrasound: The principle of linear phased array was introduced in 1968 by Somer, who showed that fast electronic sector scanning could be obtained with a stationary linear array transducer (Somer, 1968). An array of transducers which operated sequentially as single elements (linear switched array) was first applied by Bom and co-workers in 1971 (Bom *et al.*, 1971). The principle of the annular array transducer with its improved lateral resolution was described in the early seventies (Hubelbank and Tretiak, 1970; Thurstone and Melton, 1970; Robinson, 1972).

Improvement of the imaging technique was accomplished early in the seventies by the Australian group at the CAL (Commonwealth Acoustic Laboratories) led by Kossoff (Kossoff, 1971; Kossoff, 1972). Kossoff and co-workers presented various gray scale images from intact and abnormal early pregnancies (Kossoff *et al.*, 1974). The same group also developed the Octoson, a high resolution ultrasound machine consisting of eight transducers with large apertures mounted on an arm (Kossoff, 1976). This ultrasound system obtained a compound scan echogram by simultaneously oscillating all transducers and sequentially switching through the transducers.

3D ultrasound imaging was already proposed in the fifties (Howry *et al.*, 1956). The first report of a three-dimensional ultrasonogram of a supra-orbital tumor made of serial photographic ultrasound plates stacked together was published in 1961 (Baum *et al.*, 1961). In 1974, Szilard showed a 3D image of a fetus in utero by using 15 ultrasound tomograms recorded at intervals of 1 cm each (Szilard, 1974). It was not until the development of computer raster displays in the seventies that the visualization of 3D ultrasound data initiated 3D reconstructions of the fetus: In 1976, Moritz and Shreve described a spark gap position location system (Moritz and Shreve, 1976) which later was used for the 3D studies in obstetrics of Brinkley and co-workers, who reconstructed geometrical models of the fetus (Brinkley *et al.*, 1978; Brinkley *et al.*, 1982; Brinkley, 1984). Since the end of the 1980's, 3D ultrasound became a major field of research in obstetrics and gynecology, applying new visualization techniques such as creating new 2D sections (Kratochwil, 1992), surface shading (Baba *et al.*, 1989) and the transparency mode (Sohn *et al.*, 1991).

### 2.2.2 Milestones of first trimester ultrasound evaluation

In diagnostic ultrasound, the proximity between the transducer and the target is crucial for the quality of the imaging. In 1958, the history of the early pregnancy ultrasound evaluation started with the detection of a 14 week-old pregnancy (Donald *et al.*, 1958). A few years later, during the sixties, systematic evaluation of first trimester pregnancies started.

#### 2.2.2.1 Early sixties. Visualization of the embryo

In 1961, Donald and Brown showed images of a 10 1/2 week-old twin pregnancy. Two years later, MacVicar, a co-worker of Donald, reported on the sonographic detection of 135 pregnancies before 20 weeks of gestation, using a 2.5 MHz pulsed ultrasound (MacVicar and Donald, 1963). The earliest age at which embryonic echoes could be obtained was between 8 and 9 weeks of gestation. MacVicar and Donald also gave an account of the diagnosis of incomplete abortion and of hydatidiform mole. Sundén described in his extensive thesis «On the diagnostic value of ultrasound in obstetrics and gynæcology» (Sundén, 1964), the first trimester ultrasound findings in 37 normally developing pregnancies and in 19 abortions. He was also able to detect embryonic echoes at the end of week eight. The earliest identification of the fetal skull was made at week 13.

#### 2.2.2.2 Late sixties. Registration of the heart activity; measurement of the gestational sac; transvaginal ultrasound

At the end of the sixties, the first measurements of pregnancy structures, such as the gestational sac, were published (Hellman *et al.*, 1969). A great innovation became introduced in 1967, namely the transvaginal approach of the gynecological examination and, thus, the first trimester examination (Kratochwil and Eisenhut, 1967; Kratochwil, 1969). Jouppila used a transvaginal transducer for his studies on the uterus, the gestational sac and on fetal heart activity, which were published in a thesis in 1971 (Jouppila, 1971). Soon after Kratochwil's paper on the very early detection of embryonic heart activity (Kratochwil and Eisenhut, 1967), measurements of the heart rate by Doppler ultrasound were published (Takeuchi *et al.*, 1968; Müller and Osler, 1969; Jouppila, 1971).

#### 2.2.2.3 Early seventies. Embryonic & early fetal biometry

Robinson's evaluation of the CRL established the biometry of the embryo and early fetus (Robinson, 1973; Robinson and Fleming, 1975). Robinson also showed the particular

course of the heart rate curve with a maximum heart rate at 9 weeks in the first trimester (Robinson and Shaw-Dunn, 1973).

#### 2.2.2.4 Late seventies. Visualization of small structures

It was not until the end of the seventies that grey-scale real-time ultrasound became generally available. For example, before 1977, studies on CRL measurements were performed with a compound-scanner (Robinson, 1973; Drumm *et al.*, 1976; Hansmann *et al.*, 1977), while in later studies, real time scanners were used (Hansmann *et al.*, 1979). At the end of the seventies and the beginning of the eighties, the improved quality of ultrasound equipment made it possible to detect tiny structures such as the yolk sac by transabdominal ultrasound (Mantoni and Pedersen, 1979; Sauerbrei *et al.*, 1980).

#### 2.2.2.5 Middle of the eighties. Description of embryonic organs

Little by little, small embryonic structures such as the midgut herniation (Cyr *et al.*, 1986) and the rhombencephalic cavity (Cyr *et al.*, 1988) were identified. In an article composed of several studies an attempt was made to decode ultrasound images obtained with 5 MHz transabdominal transducers and describe the development of embryonic organs (Green and Hobbins, 1988).

#### 2.2.2.6 Late eighties. Sonoembryology

Transvaginal ultrasound became generally introduced. The report «A close look at early embryonic development with the high-frequency transvaginal transducer» (Timor-Tritsch *et al.*, 1988), followed by «First trimester transvaginal sonographic diagnosis of fetal anomalies» describing fetal anomalies at 11 weeks (Rottem *et al.*, 1989), initiated a new era with many studies and reviews about detailed images and descriptions of normal first trimester conceptuses (Blumenfeld *et al.*, 1988; Krone *et al.*, 1989; Timor-Tritsch *et al.*, 1989; Warren *et al.*, 1989) and abnormal (Bronshtein *et al.*, 1990; Cullen *et al.*, 1990; Rottem and Bronshtein, 1990; Achiron and Tadmor, 1991). The term «sonoembryology» was coined in 1990 by Timor-Tritsch to describe the study of the embryo by means of transvaginal sonography (Timor-Tritsch *et al.*, 1990).

#### 2.2.2.7 Nineties. Three-dimensional ultrasound

In the beginning of the nineties, the first 3D images of first trimester pregnancies were presented by Kelly and co-workers (Kelly *et al.*, 1992). Bonilla-Musoles showed 3D images of the embryo and young fetus using the orthogonal slice mode, surface shading mode and transparency visualization mode (Bonilla-Musoles *et al.*, 1995).

## 2.3 Physics

### 2.3.1 The transabdominal transducer

Sound waves with frequencies above the audible range of the human ear are called ultrasound. Diagnostic medical ultrasound usually operates in the range of 2 MHz to 10 MHz for a transcutaneous approach. In obstetrical ultrasound, 3.5–5 MHz transducers are used for the transabdominal approach, but frequencies up to 7.5 MHz may be used. The growing interest of the imaging of the young human conceptus in the first trimester during the eighties made especially high demands on image resolution. For example, at Carnegie stages 15 and 16, which extend from the end of week 6 to the beginning of week 7, the total embryonic length ranges from about 7 mm to 14 mm (O'Rahilly and Müller, 1987), with proportionally smaller dimensions of the developing organ systems in such small specimens.

Using the transabdominal approach for imaging the embryo well-known physical problems were encountered: The abdominal wall with its different layers consisting of muscles, tendon and fat leads to acoustic noise, such as reverberations and phase front aberrations, in the ultrasound image. In early pregnancy, the distance between the embryo, lying concealed in the pelvis, and the transducer necessitates the use of low ultrasound frequencies. Practically, the resolution of the ultrasound image will become too coarse.

### 2.3.2 Resolution of the ultrasound image

The quality of the ultrasound image depends on two main factors: 1. The spatial resolution is determined by the smallest distance between two points or surfaces at which two identifiable signals can be separated. 2. The contrast resolution describes the ability to detect small variations in the intensity of the back-scattered signals from targets that are close to each other.

The ultrasound beam consists of a main lobe, which is the central core of the beam in the far field, and side lobes, which are field intensities outside the main lobe of the far field. Under optimal test conditions, where the ultrasound beam passes through water, the width of the main lobe of the beam is narrow. The width increases by phase front aberrations when the beam passes tissue with variable sound velocity, for example tissues with a complex mixture of fat and muscles as may be found in the body wall. The phase front aberrations also increase the side lobe level, which is acoustic energy outside the

main lobe of the beam. These signals from the side lobe appear as acoustic noise in the image. This noise is produced by the transmitted pulse, and hence cannot be reduced by increasing the transmit power.

Another source of acoustic noise is multiple scattering, or reverberations of the transmitted pulse. Scattering produces echoes at time delays different from the scatterer position causing noise in the image. These echoes are specially strong from layers of fat and muscles in the body wall.

As the pulse is traveling through the tissue, attenuation of the amplitude of the beam occurs not only by reflections and scattering, but mainly by absorption of acoustic energy.

If we take an ultrasound picture of two point targets we will see two ellipsoid specks smeared out on the screen transverse to the axis of the ultrasound beam (Figure 2.3.2 a). In other words, the points appear slightly larger and more distorted than they are in reality, and they are surrounded by a halo. In the same way, the ultrasound image of an object with a smooth surface will show a blurred surface. This phenomenon is caused by the point spread function and shows the radial resolution and the lateral resolution of the ultrasound system.

**Figure 2.3.2 a**
The definition of the spatial resolution in the 2D image: a) The ultrasound beam sweeps over two point targets b) The two point targets are smeared-out in the ultrasound image and appear as ellipsoid specks (with permission from Angelsen (Angelsen, 1996)).

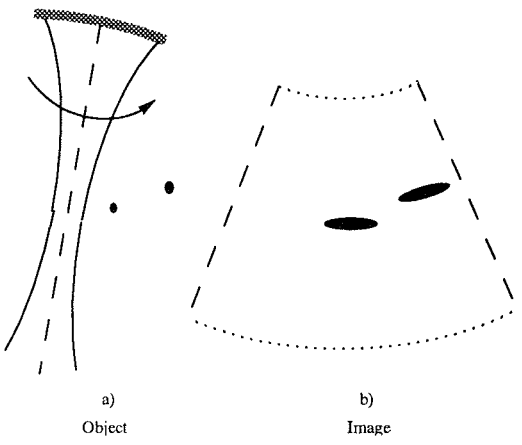


The radial resolution ($\Delta$ rad) along the ultrasound beam is determined by the length of the transmitted pulse '$T_p$', and is expressed by the formula $\Delta rad = \frac{cT_p}{2} = \frac{c}{2B}$, where 'B' is

the bandwidth of the pulse and 'c' is the sound velocity. From physical modifications in the transducer (see 2.3.3.1), '$T_p$' always has only a few oscillations, e.g. $T_p = 3T$, where $T$ is the period of the pulse oscillation, and is defined by $T = 1/f$, where $f$ is the ultrasound frequency. The absolute length of a pulse can be shortened by increasing the frequency (Figure 2.3.2 b).

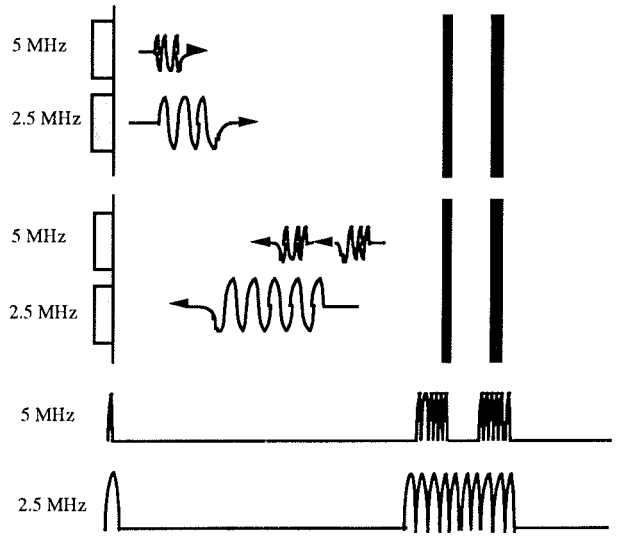


**Figure 2.3.2 b**
Radial resolution. An impulse consisting of three oscillations is transmitted. Using a pulse of 2.5 MHz, the two targets appear as one structure on the ultrasound image. The figure illustrates how the shorter pulse with higher frequency (5 MHz) can resolve the two targets close to each other (with permission from Angelsen (Angelsen, 1996)).

**Table 2.3.2** The radial (Δ rad) and the lateral (Δ lat) resolutions at the focus of annular array transducers with different ultrasound frequencies, where the aperture is 11.5 mm and the focal distance is 25 mm, and where the ultrasound pulse is assumed to have three oscillations.

| MHz | 3 | 4 | 5 | 6 | 6.5 | **7.5** | 10 |
|---|---|---|---|---|---|---|---|
| Δ rad (mm) | 0.77 | 0.58 | 0.46 | 0.39 | 0.36 | **0.31** | 0.23 |
| Δ lat (mm) | 2.23 | 1.67 | 1.34 | 1.12 | 1.03 | **0.89** | 0.67 |

The lateral resolution (Δ lat) describes the resolution transverse to the ultrasound beam, and is determined primarily by the width 'D' of the aperture of the transducer and the distance 'F' between the transducer and the focus. The lateral resolution determines the lateral blurring of the point targets. It increases with the distance 'F' and decreases with increasing size 'D' of the aperture and with the increasing frequency (Table 2.3.2). The good quality of the compound scan images which were obtained with the Octoson

(Kossoff, 1976) was partly based on the large apertures of the transducers.

### 2.3.3 High frequency transvaginal transducer

As early as in 1954, Edler and Hertz discussed the choice between high frequencies and sharp echoes versus low frequencies and better penetration of the sound beam (Edler and Hertz, 1954). This problem clearly points out the demands on the ultrasound equipment for the imaging of the tiny human embryo:

1. It is important to avoid the maternal abdominal wall and come as close as possible to the target, in other words we have to use the transvaginal approach. Then acoustic noise (phase front aberrations and reverberations) and attenuation is reduced, thus improving the contrast resolution.

2. Highest possible frequencies have to be applied to obtain the best possible spatial resolution.

#### 2.3.3.1 Linear array

Modern transducers form the ultrasound beam with electronic arrays. In the array transducers, the bars of elements are mounted on a backing with fill-mass between the elements. The linear array transducers have one-dimensional arrays where the ultrasound beam is focused in the scan plane only (the azimuth plane) by controlled delay of the excitation of the elements. In the plane perpendicular to the scan plane (elevation plane) the beam has a fixed focal distance with a relatively thick slice (Figure 2.3.3 b). Imaging and measurements of very small structures may be affected by the poor resolution in the elevation plane. An impedance matching layer is usually a single layer $\lambda/4$ thick, and is placed in front of the elements. This layer restrains the «ring-down» of the emitted pulse and thus shortens it. The distance between the center of the elements is called «pitch», which also includes the fill mass between the elements.

Linear arrays can steer the ultrasound beam in two different ways: either by the phased array or by the switched array principle.

1. The phased linear array transducer was introduced by Somer (Somer, 1968). These transducer types are multiple-element transducers whose purpose is to steer the ultrasonic beam in various angles (Somer, 1978). To achieve this, the distance

between the center of the single elements, the pitch, must be less than $\lambda/2$. A parabolic delay of the elements focuses the beam electronically. This transducer has a small aperture and produces a sector scan. Due to the short distance between the elements ($<\lambda/2$) the manufacturing of this transducer is not possible for very high frequencies.

2. In the switched linear array transducer only subsets of the elements are activated. By switching to another subset of elements the ultrasound beam can be swept horizontally (Bom *et al.*, 1971). The elements of the switched array transducer can be several wave lengths wide; this facilitates the manufacturing of such high frequency transducers. The switched linear array generates a rectangular image format.

   Curving the linear array transducer creates the curved switched array, which gives a better image format in high frequencies and makes this transducer type suitable for the transvaginal approach: the sector image has a sufficiently large width of the image at the region of interest, while the length of the array can be kept short.

#### 2.3.3.2 Annular array

The annular array transducer consists of an array of relatively large elements which are arranged as concentric rings and a central plate (Hubelbank and Tretiak, 1970; Thurstone and Melton, 1970; Robinson, 1972). Due to the wide elements, high frequencies can be applied, as with the switched array. The annular array transducer focuses the beam electronically by delaying the signals from the different elements. The beam must be sectored mechanically because the concentric elements are incapable of steering the beam. Rapid to and fro rotation movements of the annular array create the sector image. The advantages of the annular array principle are the possibility for high frequency imaging and symmetric focusing (Figure 2.3.3 a). The symmetric focusing improves the spatial resolution also in the elevation plane, creating thin ultrasound slices of high quality. Small structures as embryonic brain cavities will be depicted with relatively sharp contours. This facilitates the interpolation between these slices in the 3D reconstruction process and makes the annular array transducer type favorable for 3D imaging.

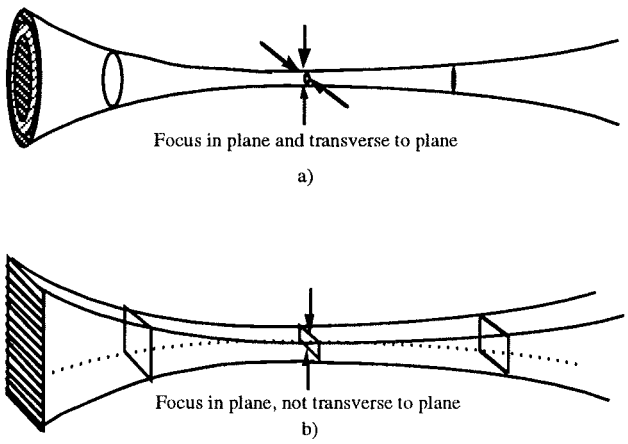


**Figure 2.3.3**

a) The symmetric electronic focus for annular array

b) The one-dimensional electronic focus for linear array, which has a thick elevation plane (with permission from Angelsen (Angelsen, 1996)).

## 2.4 3D imaging

The reduced mobility of the transducer at the transvaginal examination limits the access of 2D scan planes. During the examination of the early pregnancy we often obtain unsuitable sections through the embryo which are difficult to interpret, and where correct measurements are not possible (Figure 2 A in appendix). Therefore, 3D ultrasound is particularly advantageous for the transvaginal ultrasound examination, as 3D ultrasound techniques enable us to obtain new cross-sectional 2D sections which would not have been possible to obtain with the 2D probe. Additionally it offers new visualizing and measurement modes such as surface rendering and volume rendering, and the possibility of volume calculation.

### 2.4.1 Acquisition of 3D data

3D data are acquired as a set of consecutive 2D ultrasound slices created through movement of the 2D ultrasound scan planes and continuous storing of the images. The transducer can be moved by a motor or with a free-hand technique. The motor-controlled scanning can be parallel, fan-like scanning or rotation, the latter usually applied for the transvaginal access. It is necessary to know the orientation of the transducer in space in order to determine the relative positions of the ultrasound slices before the scans are converted into a 3D volume. This is not a problem as long as the scan movements are steered by a motor which is synchronized with the scanner. In the free-hand movement of the transducer, position-sensing techniques have to be used, such as the acoustic technique already described in the seventies (Moritz and Shreve, 1976), or the

electromagnetic technique used by Kelly and co-workers (Kelly *et al.*, 1992). We used the rotation technique where the transducer was coupled to a step motor. The recording time of such a scan depends on the velocity and the angle of the rotation. It usually takes a few seconds to acquire a 3D data set. The object should be still during the data acquisition, in order to avoid reconstruction errors. Likewise, the probe must be kept in a stable position. For the 3D reconstructions, the raw digital ultrasound data are transferred directly from the scanner to an external PC. The first system for data acquisition described by Brinkley and co-workers was extremely time consuming: each scan had to be acquired separately, including the segmentation process (Brinkley *et al.*, 1978). The time required was approximately 1/2 hour per ultrasound tomogram (Brinkley, 1984). Brinkley and co-workers later developed an improved system where the scanning time could be held within the order of an ordinary ultrasound examination (Brinkley, 1984). Still, the segmentation and volume calculation process (see 2.4.2.4) lasted for many hours. Today, the data acquisition is very short and approaches fractions of a second. To obtain 3D images of good resolution and sufficient quality, the width of the original 2D ultrasound tomograms (slices) should be narrow (Baba and Okai, 1997). The 2D tomograms are converted into a regular grid of voxels (Steen and Olstad, 1994). For the 3D volume, the gaps between the 2D tomograms are filled by interpolation of the neighboring pixels.

### 2.4.2 Visualization and calculation of 3D data

After the 3D reconstruction, the visualization of 3D data is made as projections onto a 2D screen. Different methods or algorithms are used for displaying 3D data: 3D navigation is done for section reconstruction, while surface shading and volume rendering are modes that can display the surface or the volume e.g. of whole organs (Steen, 1996; Baba and Okai, 1997). There are also techniques that can be used to build geometric models of the organs so that precise volume estimates can be made (Steen, 1996; Thune *et al.*, 1996).

#### 2.4.2.1 3D navigation

In 3D navigation, new 2D planes are obtained from the 3D volume for visualization, measurements and, eventually, volume analysis (see 2.4.3.4). Orthogonal planes (X, Y and Z axis), parallel planes and anyplane slices can be obtained. Anyplane slicing is made by freely extracting new 2D planes at different positions from the 3D volume (Figures 2 B-D in appendix).

#### 2.4.2.2 Surface rendering

In surface rendering, after regional extraction from the 3D data set, an intermediate 3D geometrical data set is projected on a 2D plane (Baba and Okai, 1997). The visualization of the surface of the extracted object is made with different algorithms. These are, for example, algorithms for varying the viewing direction, for projecting the data parallel or perspectively, and for different modes of shading (Figure 2 I in appendix). The voxels behind the surface of interest are not taken into account when generating the 3D image. Surface shading of embryos and young fetuses were shown by Kelly and co-workers (Kelly *et al.*, 1992) and by Bonilla-Musoles and co-workers (Bonilla-Musoles *et al.*, 1995).

#### 2.4.2.3 Volume rendering

In the volume rendering technique, 3D data are projected on a 2D plane directly, without regional extraction and without construction of intermediate geometrical data sets. For visualization the «ray casting» technique is applied (Steen, 1996). An image is constructed in a view plane which is thought to be outside the space-limited 3D scene. Each pixel of the new image is associated with a ray through the 3D volume. The value of the pixel is then calculated as a function of all voxels through which the ray passes. There are different algorithms that can be applied, for example the maximum data value, the average data value, the maximum data gradient or other algorithms (Steen and Olstad, 1994). Transparency visualization of organs is an example of volume rendering as shown in the visualization of fetal hands (Steen and Olstad, 1994). Bonilla-Musoles showed the fetal spine at 13 weeks of gestation computed in the X-ray/maximum transparency mode (Bonilla-Musoles, 1996).

#### 2.4.2.4 Geometry visualization

If we want to build a geometric model from the 3D data set, the object of interest needs to be delineated or segmented from its surroundings. This process is called segmentation and is done by tracing contours in a number of 2D-slices (Figures 2 E & F in appendix). Segmentation is done manually. Research has been done on semi-automatic or automatic tracing, but because of the relatively poor image quality of the ultrasound tomograms, due to a lot of acoustic noise, such research has not been successful. From the given set of segmented contours (Figure 2 G in appendix), a polyhedron can be reconstructed (Thune *et al.*, 1996). The reconstructed geometrical object can then be visualized as 3D images by rendering the surface using different colors and different opacity values (Figure 2 H in appendix).

### 2.4.2.5 Volume calculation

The volume of the geometrical object can be calculated (Gilja *et al.*, 1994; Thune *et al.*, 1996). The point spread function blurs the outline of an object, thus the manually drawn segmentation lines may lie somewhat outside the true surface of the object of interest (Figures 2 D & E in appendix). This has to be taken into account for the estimation of the volume. Thus, volume estimations of structures with outer surfaces may be overestimated, whereas cavities with inner surfaces may be underestimated.

## 2.5 Safety

### 2.5.1 Output levels of diagnostic ultrasound equipment

For many years, diagnostic ultrasound has been widely used in clinical medicine with no proven deleterious effects. It is partly its lack of adverse effects which has allowed its use to grow to the point where «more than one out of every four imaging studies in the world is an ultrasound study» (WFUMB, 1997). However, there is evidence of an upward trend in output levels of diagnostic ultrasound equipment (Duck and Martin, 1991; Henderson *et al.*, 1995) such that the safety issue continues to attract our attention.

There are many different measures to quantify output levels. Common acoustic output parameters are peak negative pressure «p-» (unit: megapascals = Mpa) and spatial peak temporal average intensity «$I_{SPTA}$» (unit: mW $cm^{-2}$). The peak negative pressure gives an indication of the capability for producing cavitation, one of the principal mechanisms by which ultrasound can damage tissue. Ultrasonically-induced cavitation can occur in tissue where gas bubbles (air or contrast agents) are present (Rott, 1997; ter Haar, 1997). For example, ultrasonically-induced capillary bleeding has been recorded in inflated lungs (Dalecki *et al.*, 1997). As there are no gas bubbles in the embryo or the fetus, the risk for cavitational effects by diagnostic ultrasound is negligible (Rott, 1997).

$I_{SPTA}$ can be taken as a rough indicator of the likelihood of tissue heating caused by ultrasound. At the beginning of the 1990's the average value of $I_{SPTA}$ intensity for B mode imaging was typically around 10 mW $cm^{-2}$, while the intensities for M mode, Color Doppler and continuous wave Doppler were around 100 mW $cm^{-2}$. The $I_{SPTA}$ of pulsed Doppler (PD) was several times higher, and values of more than 1000 mW $cm^{-2}$ have been measured (Duck and Martin, 1991). From 1991 to 1997, Henderson and co-authors analyzed the «worst case» values of peak negative pressure and spatial peak temporal average intensity in a survey of 50 different types of scanners having between them over 350 different probes from more than 20 different manufacturers (Henderson *et al.*, 1997).

They found that the highest $I_{SPTA}$ values, produced in B and Color Flow modes were at levels which overlapped with those found in PD mode. They concluded that it was no longer safe to assume that the highest acoustic output values would always be greatest for the PD mode. In light of these results, even the users of B mode must be aware of the output levels from their own ultrasound machine (Henderson *et al.*, 1997).

### 2.5.2 Possible adverse effects on the early conceptus

Fetal bone has a high absorption coefficient, and this tissue is most likely to experience the greatest temperature rise during a second or third trimester ultrasound examination. Duck and Martin studied the effect of PD beams on fetal vertebrae and found a temperature rise of 0.6°C - 1.8°C in fetuses of 14 to 39 weeks of gestation (Duck and Martin, 1991). The first ossification centers of the clavicle and mandible appear at Carnegie stages 18 to 20, during week 8 (O'Rahilly and Müller, 1987; Ashhurst, 1997). Thus, it might be possible to produce a measurable temperature rise in bone by the end of the first trimester (Doody, 1997). It has also been claimed that there may be non-thermal and non-cavitational bioeffects of ultrasound due to radiation force effects (Starritt, 1997).

Data on ultrasound effects in the embryonic period are scarce, but since the embryo consists of approximately 92.7% water (Jirásek *et al.*, 1966), the possibility of thermal effects that are dependent on the presence of absorbing tissue, such as bone, is small. Studies on rat embryos demonstrated developmental abnormalities at in-vitro exposures by PD with intensities above 5000 mW $cm^{-2}$ $I_{SPTA}$ and 1.9 Mpa p- (Ramnarine *et al.*, 1997).

### 2.5.3 Output regulations

The previous upper limit of output intensity of 94 mW $cm^{-2}$ for diagnostic ultrasound, was put forward by the Food and Drug Administration (USA). No significant biological effects have ever been proven from in vivo or in vitro experiments with output values below 100 mW $cm^{-2}$. According to the new output regulations from the FDA, the output display standard (ODS), an ultrasound machine has to display the emitted energy presented as a mechanical index (MI) and a thermal index (TI) on the screen (AIUM/NEMA, 1992). MI expresses the risk for cavitational effects, and TI that of warming up the tissue.

The clinical safety statement from the EFSUMB Radiation Safety Committee in 1984 concluded that numerous investigations of various degrees of sophistication had been

undertaken in an endeavor to detect adverse effects. None of these studies had shown that ultrasound at diagnostic intensities in use at that time had led to any deleterious effect to the fetus or mother (EFSUMB, 1984). In 1998 in Tours, the European Committee for Medical Ultrasound Safety (ECMUS) maintained this statement: «Based on scientific evidence of ultrasonically induced biological effects to date, there is no reason to withhold B- or M-mode scanning for any clinical application, including the routine clinical scanning of every woman during pregnancy» and «The embryonic period is known to be particularly sensitive to any external influences. Until further scientific information is available, investigations using pulsed or color Doppler ultrasound should be carried out with careful control of output levels and exposure times. With increasing mineralization of the fetal bone as the fetus develops the possibility of heating fetal bone increases. The user should prudently limit exposure of critical structures such as the fetal skull or spine during Doppler studies» (ECMUS, 1998).

The total ultrasound exposure during 3D studies is likely to be lower than during ordinary 2D scans. When the object of interest has been put in focus, the 3D data acquisition takes about 2 - 8 seconds. As the analysis of the 3D data set is done off-line, the total scan time will be short.

## 2.6 Measuring the embryo/early fetus. A comparison of embryological and ultrasound measurement methods

Both embryologists and sonographers make measurements in order to quantify the young conceptus or part of it. In the present chapter, different methods of measurement in embryology and sonography are described, and similarities and differences between these are discussed.

### 2.6.1 The embryo/fetus

#### 2.6.1.1 Body

Embryology: The most common measure used by embryologists is the length of the embryo, excluding the lower limbs, which are flexed during prenatal life. George LeClers, Count of Buffon (1707–1788), was probably the first to measure human embryos (Tanner, 1981): «I take the fetus at 1 month, when all the parts are developed. It then is one pouce (French thumb, inch = 2.7 cm) in length».

The crown-rump length (CRL) seems to have been introduced into embryology by Fr. Arnold, 1851, Handbuch der Anatomie des Menschen. Freiburg im Breisgau. Volume II, page 1210 (His, 1904). His himself used the «Nackenlänge» («neck length»), a measure from the embryonic breech to the flexure of the neck in embryos from 6 to 9 weeks before he went over to the CRL in older embryos and fetuses (His, 1904). The CRL which corresponds to the sitting height in postnatal life (O'Rahilly and Müller, 1984) was described by Mall in 1907: He assumed that the CRL extended from "a point just over the mid-brain" to "the lowest point of the breech" (Mall, 1907). He recommended measuring the CRL even in small embryos. Doing so one should have in mind the natural curvature of the embryonic/fetal body and brain at different ages: At seven weeks the rhombencephalon lies on top of the embryo and the midbrain is positioned anteriorly, while, one week later, the midbrain is the cranial end-point (O'Rahilly and Müller, 1984; O'Rahilly and Müller, 1987). In later publications, Mall recommended measuring the total length of the fetus including the legs. He described how to take this measurement in the embryo without destroying it (Mall, 1910). In his large biometric study on 704 embryos and fetuses, the weights of which ranged from 0.012 g - 4298 g, Streeter used the CRL as defined by Mall (Streeter, 1920). He stated that the body could safely be straightened for CRL measurement of fetuses down to 35 or 40 mm length, and that specimens smaller than this should be measured without disturbing their natural curvature. Streeter took into account the fact that the CRL was less than the greatest length (GL) in the smaller embryos, in which he measured the GL. Later, in his extensive work on the 'developmental horizons' from the 1940's, he avoided the term 'crown-rump length' and instead made use of the term 'greatest length' (Streeter, 1942; Streeter, 1945; Streeter, 1948; Streeter, 1949).

O'Rahilly and Müller compared the GL with the CRL in 43 staged embryos and concluded that the GL exceeded the CRL between Carnegie stage 13 (about 6 weeks - 0 days) and Carnegie stage 18 (about 8 weeks - 2 days to 8 weeks - 4 days) with up to 1.5 mm. Thereafter the two lengths were basically equal (O'Rahilly and Müller, 1984). They concluded that the exact points for the measurement of the CRL, both the cranial end-point at the midbrain and the caudal end-point at the breech, sometimes were difficult to locate, rendering the crown-rump measurement unsatisfactory (O'Rahilly and Müller, 1984). Thus, the GL, which is independent of fixed points, and which is much simpler to measure than the CRL, is commonly used in the embryological literature (O'Rahilly and Müller, 1987; O'Rahilly and Müller, 1994).

The size of embryos and fetuses expressed in weight (grams) has been studied on a large scale by Streeter (Streeter, 1920). Twenty-eight of the specimens with CRL 9 mm to 40 mm had a weight range from 110 mg to 5 200 mg. The difference between the fetal weight in grams and the volume in cubic millimeters is less than 2% (Meban, 1983).

Ultrasound: In 1973 the term 'crown-rump length' was introduced by Robinson for the ultrasonic measurement of the embryonic size (Robinson, 1973). His nomogram of the correlation between the CRL and the gestational age is still widely used for the evaluation and dating of the early pregnancy (Robinson and Fleming, 1975). Although they used the term 'crown-rump length', Robinson, as well as all other authors of more recent ultrasound studies about the embryonic/fetal length, actually measured the 'greatest length' as defined by Streeter (Streeter, 1920) and O'Rahilly (O'Rahilly and Müller, 1984) instead of Mall's 'crown-rump length' (Mall, 1907).

When comparing measurements made by ultrasound with measurements made directly on the embryo, one must bear in mind that due to the fixation procedures the length of embryos as measured in embryological studies may be about 1 to 5 mm less than according to equivalent in-vivo CRL measurements (Drumm and O'Rahilly, 1977).

There is no reason to change the use of the generally applied term «CRL» in clinical praxis although the term «GL» would be correct in many cases.

#### 2.6.1.2 Head

Embryology: The measurement of the width of the head is not common in classical human embryology. His described the measurement of the embryonic «Kopflänge» (= head length), which is the longest diameter in a plane parallel to the eye-ear line (His, 1904; Mall, 1907). In addition to the 'Kopflänge' His introduced the 'Kopftiefe' (= head depth), which corresponds approximately to the height of the head, measured from the chin to the crown (His, 1904; Mall, 1907). Streeter recommended the 'head modulus', a parameter consisting of the mean between the greatest horizontal circumference of the head and the biauricular transverse arc (Streeter, 1920). He obtained the biauricular transverse arc by placing a thin strip of paraffined paper at the external auditory meatus (in older specimen tragus) of one side and extending it over the apex of the head to the opposite external meatus, the paper then being laid along a millimeter rule. Similar paper strips were used for obtaining the head circumference (Streeter, 1920).

Ultrasound: The report by the Glasgow group that the fetal biparietal diameter (BPD) could be measured accurately with a uni-dimensional A-scan technique introduced the fetal cephalometry (Donald and Brown, 1961; Willocks, 1962; Willocks *et al.*, 1964). Today, it is common to measure the size of the head by ultrasound. Hellman and co-worker evaluated cephalometry in a larger scale and analyzed the correlation between head size measured by ultrasound near term and the head size and weight of the newborn (Hellman *et al.*, 1967). Thompson and co-workers were the first to estimate fetal weight by measurements of the BPD (A-scan) and the thoracal circumference (B-scan) (Thompson *et al.*, 1965). Campbell correlated the BPD with gestational age (Campbell, 1969). Campbell and Thoms described the reference points in the second and third trimester for the measurement of the biparietal diameter from the edges of the parietal bones to the cavum septi pellucidi, the thalami and midbrain and a point just above the cerebellum in the horizontal plane perpendicular to the body axis (Campbell and Thoms, 1977). One of the latest studies on 587 fetuses from 12 to 42 weeks of gestation presented charts of the biparietal diameter both for outer-outer and outer-inner measurements (Chitty *et al.*, 1994a). The occipito-frontal diameter (OFD) is measured between the leading edge of the frontal bone and the outer border of the occiput in the same plane as the biparietal diameter (Hansmann *et al.*, 1972; Chitty *et al.*, 1994a). His' parameter 'Kopflänge' is comparable to the occipito-frontal diameter. The head circumference (HC) is obtained in the same plane as the BPD and OFD.

The reference points for the head measurement of the second trimester fetus (BPD, OFD and HC) such as the cavum septi pellucidi and thalami are not formed in the first trimester. The shape of the embryonic head and the position of the intracranial structures change significantly during the early development, as described in the embryological literature (Streeter, 1942; Streeter, 1945; Streeter, 1948; Streeter, 1949; O'Rahilly and Müller, 1987; O'Rahilly and Müller, 1994). At seven weeks, at Carnegie stages 16 and 17, the horizontal plane through the embryonic head includes the rhombencephalon and the posterior part of the mesencephalon. This plane lies above the diencephalon and the hemispheres. The largest width is found at the height of the rhombic lips, the future cerebellum. The largest length extends from the cervical flexure to the anterior wall of the bent mesencephalon. Due to the development of the brain, characterized by uneven growth of the brain compartments and by the 'deflection' of the brain, the largest width alters its position during the embryonic and early fetal period. At the beginning of week nine, Carnegie stages 21 and 22, the plane for the measurement of the head size includes the hemispheres anteriorly, the diencephalon in the middle of the head, and the cerebellum

posteriorly. At the end of the embryonic period, at Carnegie stage 23, the measurement plane involves the hemispheres, the diencephalon and the upper part of the cerebellum. In the early fetal period, the future cranium becomes successively distinguishable.

The terms biparietal diameter and occipito-frontal diameter are basically not suitable for the embryonic period, and it would be more correct to use terms like width of the head and antero-posterior diameter. There is a sliding transition from the embryonic 'head width' to the fetal 'biparietal diameter', therefore the historically oldest term BPD was kept for the measurement of the head when the measurement of the head width was introduced in the first trimester (Krone *et al.*, 1989; Rempen, 1991a; Rempen, 1991b; Kustermann *et al.*, 1992; Grisiola *et al.*, 1993; Lasser *et al.*, 1993). Anatomical reference points for the measurement were not given in these papers; it is likely that the calipers were placed at the outer borders of the largest width of the embryonic head.

A certain aspect has to be considered in connection with BPD measurements at the end of the first trimester. As referred to above, there are nomograms for the BPD-values both obtained by outer-outer and outer-inner measurements. The outer-inner placement of the calipers has historical reasons: The early cephalometric studies were done with the A-scan technique (Donald and Brown, 1961; Willocks, 1962; Willocks *et al.*, 1964), where the amplitudes of the walls of the cranium and of the falx were depicted. Here, the markers were placed at the beginning of the rising amplitudes, which actually represented an outer-inner measurement. Willocks analyzed the average thickness of the neonatal skull in 18 post-mortem specimens weighing over 2000 g, and found a mean thickness of 1.3 mm (Willocks *et al.*, 1964). The introduction of the Compound scanner and, later, of the real-time ultrasound scanner gave B-images of the horizontal section through the head, showing the wall of the cranium as an ellipse. Postnatally, the true BPD is given by measuring the outside of the head from one side to the other side. It would seem natural, to measure the width of the fetal head by placing the calipers on the outer sides of the head, too, but in many places, for example Sweden, the practice of outer-inner measurements (Eik-Nes *et al.*, 1982) was maintained. Though the outer-inner BPD does not correspond to the «true» BPD, estimations of age or weight will give the same results as those obtained from outer-outer measurements, as long as the nomograms based on this method are uniformly used in the population. Now, a new difficulty appears concerning the measurement of the width of the head in the first trimester: at which gestational age or which CRL should the distal caliper be moved away from the outside of the embryonic/fetal head into the inside of the developing wall of the cranium?

The embryonic HC measurement was presented starting at seven (Kustermann *et al.*, 1992) and nine weeks (Lasser *et al.*, 1993), calculated from the BPD and the OFD (also called antero-posterior diameter), using the formula for an ellipse.

It is important that the user of early biometry is aware of the changing embryonic anatomy. For the BPD measurement the calipers should be placed at the outer contour of the embryonic head at its broadest extension. The logical continuation of this measurement for the later pregnancy is the outer-outer position of the calipers at the fetal skull. An international agreement on this measurement procedure is desirable.

#### 2.6.1.3 Abdomen

Embryology: In the classical embryological literature (Mall, 1907; Mall, 1910; Streeter, 1920; Streeter, 1948; O'Rahilly and Müller, 1987), measurement of the abdomen was not described.

Ultrasound: Abdominometry was introduced as part of the biometric assessment of the fetus (Thompson *et al.*, 1965; Hansmann *et al.*, 1972; Campbell, 1975; Eik-Nes *et al.*, 1982). The possibility of evaluating the diameter of the abdomen and thus calculating the circumference was first shown by Thompson and co-workers (Thompson *et al.*, 1965). The thoracal transverse diameter (Thoraxquerdurchmesser = ThQ) (Hansmann *et al.*, 1972), the mean abdominal diameter (MAD) (Eik-Nes *et al.*, 1982) and the abdominal circumference (AC) (Campbell, 1975) were described in the second and third trimester pregnancy. The plane of the ThQ is taken at the level of the lower thoracic aperture (Hansmann, 1976) and is identical with the MAD plane (Eik-Nes *et al.*, 1982). The mean abdominal diameter consists of two perpendicular measurements (antero-posterior and transverse diameter) taken in the horizontal section through the fetal body below the heart and above the umbilicus at the level of the stomach and the entrance of the umbilical vein in the liver sinus. This parameter is often used as the basis for the calculation of the circumference (Chitty *et al.*, 1994b). The embryonic trunk circumference was introduced in the first trimester biometry as a possible parameter for the estimation of the embryonic age (Reece *et al.*, 1987). Reece and co-workers used an abdominal 5 MHz transducer and based the calculation of the circumference on two perpendicular measurements taken just «caudal to the cardiac pulsation». In three first trimester studies, the measurements of the AC were taken at the umbilical cord insertion (Green and Hobbins, 1988; Kustermann *et al.*, 1992; Lasser *et al.*, 1993). It is likely that the AC was calculated from two perpendicular measurements in these studies, but this is not clearly specified in two of the

papers (Kustermann *et al.*, 1992; Lasser *et al.*, 1993). Taking the measurement at the umbilical cord insertion may be imprecise, as the physiological midgut herniation comprises a relatively large part of the abdominal wall, thus making a precise placement of the calipers impossible. During the first trimester, the ThQ is taken just below the heart (Wisser, 1995). Rempen used the term «größter Abdomendurchmesser» (= largest abdominal diameter) for the same measurement (Rempen, 1991b).

It is advantageous to use comparable parameters when describing embryonic and fetal biometry. Instead of measuring the mean diameter of the abdomen and multiplying it with the constant $2\pi$ to obtain the abdominal circumference, one might as well use the simpler parameter mean abdominal diameter.

#### 2.6.1.4 Limbs

Embryology: Mall proposed a method to measure the length of the lower limbs in embryos in order to calculate the stand height (Mall, 1907; Mall, 1910). According to his figures, this method would be applicable in embryos from Carnegie stage 17 onwards, which is approximately 7 weeks 5 days based on the LMP. Streeter took measurements of the foot length, starting in embryos/fetuses of 25 mm CRL (Streeter, 1920). The first ossification centers of the clavicle and mandible appear at Carnegie stages 18 to 20, which is during week 8. The ossification centers in the femoral diaphysis and in the maxilla (Carnegie stages 19 and 20) develop at about 9 LMP-based weeks (O'Rahilly and Müller, 1987; Ashhurst, 1997).

Ultrasound: The echogenic ossified part of the developing long bone is measured by ultrasound. The earliest paper on ultrasound evaluation of limb length was a study of the fetal femur length as a function of age between 12 and 22 weeks (Queenan *et al.*, 1980). Today, the femur length has become part of the standard biometric evaluation at the second trimester routine ultrasound as a parameter for the bone growth. According to the embryological development (O'Rahilly and Müller, 1987; Ashhurst, 1997), a significant ossification of the long bones does not appear before the fetal period at 10 LMP-weeks and later. This was confirmed in a study on the development of the skeleton comparing longitudinal ultrasound imaging from living embryos/fetuses with radiographs obtained from aborted silver nitrate impregnated embryos and fetuses (Zalen-Sprock *et al.*, 1997). At 10 1/2 weeks the ossified part of the femur was just measurable to 2.1 mm by ultrasound. In a 10 week-old silver nitrate impregnated embryo the femur length was even shorter. There are first trimester studies which presented limb measurements from about

9 to 10 weeks on (Rempen, 1991b; Kustermann *et al.*, 1992; Zorzoli *et al.*, 1994). In these papers the exact method of measurement was not defined nor were exemplifying figures shown. The presented lengths of the femur at 10 weeks 0 days were approximately 4 mm to 6 mm, which seems unexpectedly long. Zorzoli and co-workers also described the foot length, measured from 10 weeks on.

### 2.6.2 Embryonic and fetal organs

#### 2.6.2.1 Brain cavities

Embryology: Images from histological slices of embryonic brain ventricles show that there are large fluid-filled cavities throughout the embryonic period (Bartelmez and Dekaban, 1962; O'Rahilly and Müller, 1990; O'Rahilly and Müller, 1994). Different two-dimensional measurements for the embryonic/fetal brain and brain cavities have been proposed (Day, 1959; Westergaard, 1971; O'Rahilly and Müller, 1990), but no systematic standardized measurements of the embryonic brain have been adopted. The development of the form of the brain compartments were demonstrated by 3D reconstructions from histological slices as shown by Hochstetter (Hochstetter, 1919; Kostovic, 1990) using the technique described by Born (Born, 1883), or by 3D casts from the lateral ventricles of aborted specimens (Woollam, 1952; Day, 1959; Westergaard, 1971). In an extensive study on the phylogenetic and ontogenetic development of the cerebral ventricles (Kier, 1977), a barium-gelatin contrast medium was injected into the ventricular system of aborted animal fetuses and human fetuses for radiographic imaging. Jenkins calculated the volumes of embryonic and fetal brain compartments obtained from 3D reconstructions of a few specimens from the Carnegie collection (Jenkins, 1921).

Ultrasound: Transabdominal ultrasonography has been used to describe embryonic cerebral ventricles such as the rhombencephalic cavity (Cyr *et al.*, 1988) and the lateral ventricles (Green and Hobbins, 1988). The first detailed transvaginal sonographic imaging of the embryonic development with descriptions of the brain at different gestational age was published in 1988 (Timor-Tritsch *et al.*, 1988). Except for a study on the development of the rhombencephalic cavity (Zalen-Sprock *et al.*, 1996), no measurements of embryonic brain compartments have been done.

#### 2.6.2.2 Heart

Embryology: During the embryonic period, the heart undergoes profound developmental changes during which it is transformed from the paired tubular phase at about four to five

weeks (Carnegie stages 9 - 10) (Davis, 1927; O'Rahilly and Müller, 1987) into the four chambers of the heart, usually completed at the end of week eight by the closure of the interventricular foramen (Moore, 1988). Cardiac contractions are believed to commence at the beginning of Carnegie stage 10 (≈ 5 weeks 1 ± 1 days) (deVries and Saunders, 1962). Estimated from images of embryos (O'Rahilly and Müller, 1987), the heart diameter is about 0.4 mm at Carnegie stage 10 (≈ 4 weeks 6 ± 1 days, CRL 1.5 mm - 3 mm), about 1.7 mm at Carnegie stage 14 (≈ 6 weeks 4 days, CRL 5 mm - 7 mm) and about 2.2 mm at Carnegie stage 18 (≈ 8 weeks 2 days, CRL 13 mm - 17 mm).

Ultrasound: When Edler and Hertz introduced ultrasound as a diagnostic tool for the evaluation of the heart, they used the uni-dimensional A-scan and M-mode (Edler and Hertz, 1954). In 1962, fetal heart activity was recorded by electrocardiography at 12 weeks of gestation (Lamkee *et al.*, 1962). The Doppler technique made its entry in first trimester diagnosis during the sixties: As early as in 1964, the possibility of detecting fetal heart activity by Doppler was described (Callagan *et al.*, 1964), and in 1965, the earliest proof of first trimester fetal heart activity was made during the 10$^{th}$ week (Johnson *et al.*, 1965). In 1968, Takeuchi and co-workers described the transvaginal approach by using a fingerprobe for the detection of embryonic and fetal heart activity with Doppler ultrasound. They detected heart activity as early as the 47$^{th}$ day after the rise of basal body temperature (Takeuchi *et al.*, 1968), which corresponded to a pregnancy at the end of week eight (LMP-based). Other first trimester Doppler studies evaluating the heart activity described the heart rates (Müller and Osler, 1969; Jouppila, 1971). At the end of the sixties the M-mode technique was introduced for the identification of the first trimester heart activity: In 1967, the detection of embryonic heart activity at six weeks of gestation using a transvaginal transducer was described by Kratochwil and Eisenhut (Kratochwil and Eisenhut, 1967), and in 1968, Bang and Holm published a study about the M-mode technique applied transabdominally, where the detection of heart activity at the 10$^{th}$ week was registered (Bang and Holm, 1968).

#### 2.6.2.3 Stomach

Embryology: The intestine is sufficiently developed during the embryonic period to be filled with fluid. The lumen of the primitive gut is well defined throughout its length after six weeks. In a study of 162 well-preserved normal embryos and fetuses with CRL of 22 mm - 250 mm Nour-El-Din Hawass and collaborators (Hawass *et al.*, 1991) performed careful measurements of the esophagus and the stomach and demonstrated that the stomach already had a considerable lumen (mean 2.3 mm) in the transverse section in

embryos of 22 mm CRL (nine weeks). Liebermann-Meffert (Liebermann-Meffert, 1969) studied 75 well-preserved embryos and fetuses with a CRL of 8 mm - 200 mm and found that the position of the stomach remained fundamentally unaltered from the early stage of the embryonic period. The relative growth rate of the stomach, compared to body length and abdominal cavity volume, was greater in younger embryos. During week eight (CRL 15 mm - 21 mm) she found that the peritoneal cavity was completely occupied by the liver anteriorly and by the growing stomach dorsally, while the intestinal loops were herniated into the umbilical cord.

Ultrasound: Using abdominal ultrasound, the stomach was occasionally identified at 10 weeks of gestation (Green and Hobbins, 1988). With the transvaginal approach the stomach was seen as a well-delineated hypoechogenic structure on the left side of the abdomen at 10 - 11 weeks (Cullen *et al.*, 1990). Measurements of the stomach such as the longitudinal and the antero-posterior diameter were described in older fetuses from 16 weeks on (Nagata *et al.*, 1989).

#### 2.6.2.4 Midgut herniation

Embryology: The development of the midgut herniation has caught the interest of the embryologists since the beginning of the last century (Meckel, 1817). Measurements of the extension of the midgut herniation have not been described.

Ultrasound: The ultrasound detection of the physiological herniation was first described by Cyr and co-workers (Cyr *et al.*, 1986). The dimensions of the echogenic mass varied from 5 mm to 10 mm, but the measuring method was not presented. Another longitudinal study presented the mean diameter of the midgut herniation (Schmidt *et al.*, 1987). Bowerman measured the maximum transverse and longitudinal dimensions of the umbilical cord where it contained bowel (Bowerman, 1993). The first transvaginal study of the physiological herniation (without measurements) was carried out in 1988 (Timor-Tritsch *et al.*, 1989). Van Zalen-Sprock and co-workers determined the extension of the midgut herniation by measuring the circumference of the herniated bowel in the transverse (= horizontal) section through the abdomen (Zalen-Sprock *et al.*, 1997).

### 2.6.3 The extra-embryonic structures

#### 2.6.3.1 Chorionic cavity

Embryology: The blastocystic cavity, which occurs at Carnegie stage 3, develops into the chorionic cavity at Carnegie stage 5 a-c (O'Rahilly and Müller, 1987). In measurements

obtained from eight pregnancies described by Hertig and Rock and from one pregnancy described by Heuser, the mean diameter of the chorionic cavity ranged from 0.15 mm to 0.49 mm at Carnegie stage 5 (O'Rahilly and Müller, 1987). At 6 weeks (CRL ≈ 5 mm, Carnegie stages 12 to 14), the diameter of the chorionic cavity is about 25 mm, and at 10 weeks (CRL ≈ 30 mm, Carnegie stage 23), the mean diameter has increased to about 65 mm (O'Rahilly and Müller, 1987). Streeter described the variability and uncertainty of measuring the chorionic sacs of aborted specimens, which usually had been opened and were obtained more or less collapsed before the examination (Streeter, 1942; Streeter, 1945; Streeter, 1948). O'Rahilly and Müller used the mean of the greatest and least diameters as an average diameter of the chorionic cavity in early Carnegie stages. From Carnegie stage 13 on, three diameters were usually presented (Appendix I in (O'Rahilly and Müller, 1987)).

Ultrasound: In 1958 Donald and co-workers were the first to visualize a fourteen week old pregnancy and the gestational sac (Donald *et al.*, 1958). The first measurements of the gestational sac, in other words of the chorionic cavity, were presented by Hellman and co-workers (Hellman *et al.*, 1969) and by Jouppila (Jouppila, 1971). Hellman and co-workers took the mean of three perpendicular measurements (anterior-posterior, longitudinal and transverse) from 5 to 10 weeks of gestation based on the last menstrual period (Hellman *et al.*, 1969). Jouppila studied the gestational sac transvaginally and calculated the mean diameter by averaging the length and the depth. He performed the actual measurements on a Polaroid photograph taken from the B-scan oscilloscope (Jouppila, 1971). In 1974, Kohorn and Kaufman analyzed the gestational sac diameter in 50 pregnancies (Kohorn and Kaufman, 1974) applying Jouppila's method, and obtained 'on occasion transverse scans to provide a three-dimensional study'. In 1975, Robinson introduced a new concept of calculating the volume of the gestational sac (Robinson, 1975). The technique employed involved the use of parallel section scans taken in series from one end of the gestational sac to the other, followed by planimetric measurements from ultrasound photographs of the sac areas produced (Robinson, 1975). Though this method promises relatively precise volume calculations, it was time consuming. Therefore studies of the chorionic cavity usually apply the simple method of measuring three perpendicular diameters, either using the geometric mean (Rossavik *et al.*, 1988) or the arithmetic mean (Nyberg *et al.*, 1988; Goldstein *et al.*, 1991; Rempen, 1991b; Daya, 1993). With the introduction of real-time scanner electronic measurement became possible. For the measurements, the calipers were often placed right inside of the chorionic membrane (Nyberg *et al.*, 1988; Goldstein *et al.*, 1991; Rempen, 1991b;

Daya, 1993).

#### 2.6.3.2 Amniotic cavity

Embryology: Abramovich measured the amniotic fluid volume from early pregnancies, where the specimens were obtained by abdominal hysterotomy with the amniotic sac intact (Abramovich, 1968; Abramovich, 1981). He described the close correlation between amniotic fluid volume and fetal size (length and weight).

Ultrasound: In his study about the gestational sac, Robinson stated that at no time did he observe any structure that could definitely be recognized as the amniotic membrane (Robinson, 1975). He believed that the ultrasound equipment at that time was insufficient to discern the thin membrane on the ultrasound image. Using modern transvaginal ultrasound, the amniotic membrane is easily depicted (Rempen, 1991b; Grisiola *et al.*, 1993). As with the chorionic sac, the amniotic sac is measured by three perpendicular diameters. Rempen placed the calipers on the thin membrane of the amnion (Rempen, 1991b).

#### 2.6.3.3 Yolk sac

Embryology: The so-called primary yolk sac (O'Rahilly and Müller prefer the term 'umbilical vesicle' instead of 'yolk sac') occurs at Carnegie stage 5 b (O'Rahilly and Müller, 1987). It is transformed into the secondary yolk sac from Carnegie stage 5 c to Carnegie stage 6 (approximately 27 post menstrual days) (O'Rahilly and Müller, 1987). Systematic measurements of the yolk sac are not presented in the classical embryological literature (His, 1880-85; Keibel and Mall, 1910; Keibel and Mall, 1911; Streeter, 1942; Streeter, 1945; Streeter, 1948; O'Rahilly and Müller, 1987). There are a few embryos in early developmental stages in Keibel and Mall's «Handbuch der Entwicklungsgeschichte des Menschen» (Keibel and Mall, 1911) where the size of the yolk sac is given: one embryo (CRL 1.8 mm) had a mean yolk sac diameter of 1.3 mm, while another embryo (CRL 4.9 mm) had a yolk sac with a diameter of only 0.58 mm. The method for the yolk sac measurement was not described. In O'Rahilly and Müller's «Developmental Carnegie stages in human embryos» photographs of four embryos with known CRL (Prague embryo No. 2008, CRL 1.7 mm, Carnegie stage 9; H98 embryo No. 7251, CRL 1.2 mm, Carnegie stage 10; embryo No. 6050, CRL 3.0 mm, Carnegie stage 11; embryo No. 5923, CRL 4.0 mm, Carnegie stage 12) along with their yolk sacs were shown (O'Rahilly and Müller, 1987). From the photographs, the diameters of the yolk sacs can be estimated to be about 1.0 mm, 1.0 mm, 2.6 mm and 3.8 mm respectively.

After the completion of the embryonic folding, the initially broad communication of the yolk sac with the embryo is reduced to the vitelline duct. The yolk sac itself grows slowly but «never reaches a diameter of much more than 5 mm» (Hamilton and Mossman, 1972). The wall of the yolk sac has three cell layers (endodermal, mesenchymal, mesothelial). In a study on the ultrastructure of the human yolk sac the thickness of the wall was measured to be 40 µ - 50 µ (= 0.04 mm - 0.05 mm) at about five weeks, and 150 µ - 200 µ (= 0.15 mm - 0.2 mm) at about nine weeks (Hesseldahl and Larsen, 1969). According to histological images, the thickness of the wall varies from approximately 0.01 mm (in young specimens) to 0.3 mm (O'Rahilly and Müller, 1987; Takashina, 1989; Jauniaux and Moscoso, 1992). In conclusion, the wall of the yolk sac is very thin, namely ≤0.3 mm.

Ultrasound: The yolk sac appears as a small ring with rather bright walls lying within the chorionic cavity (extra-embryonic coelom). The visualization of the yolk sac by ultrasound was first described in 1979 (Mantoni and Pedersen, 1979). Using 3.5 - 5 MHz real-time ultrasound Sauerbrei and co-workers demonstrated the yolk sac with a mean diameter of 5 mm - 7 mm in all 18 patients examined (Sauerbrei *et al.*, 1980). For the measurements the calipers can be placed on the outside (Rempen, 1991b; Zalen-Sprock, 1997) or on the inside (Lindsay *et al.*, 1992; Stampone *et al.*, 1996) of the echogenic wall. In studies, where information about different measurement methods were given, relatively large differences of the yolk sac size were found (Rempen, 1991b; Lindsay *et al.*, 1992; Stampone *et al.*, 1996); see also Results and comments.

The measurement which most likely represents the true diameter is obtained by 'outer - inner' or 'middle - middle' placement of the calipers.

# 3 Aims of the present studies

The early ultrasound studies which started the comparison of ultrasound images with the embryonic anatomy were done either transabdominally (Green and Hobbins, 1988) or transvaginally with 5 to 6.5 MHz transducers (Timor-Tritsch *et al.*, 1988; Timor-Tritsch *et al.*, 1990). There was a need to obtain even more detailed ultrasound images and study the development of living human embryos by comparing the findings with descriptions from classical human embryology. This could be done by systematic studies with transvaginal transducers where higher frequencies were applied. For the basic study of the embryonic development it seemed appropriate to observe normal early pregnancies longitudinally.

The aims of the ultrasound studies were

1. to give a detailed two-dimensional description of the anatomy and the size of the embryo, its organs and of the extraembryonic structures at very early stages;

2. to describe the development and growth of the anatomy and compare the in-vivo ultrasound findings with descriptions from classical embryology;

3. to describe the development of both the shape and the volume of the embryo and early fetus and the brain cavities with the aid of three-dimensional imaging.

# 4 Material and methods

## 4.1 Study populations

### 4.1.1 2D descriptions

Thirty-six healthy pregnant women were recruited to be included in a longitudinal study of the embryonic development (Papers I - IV). Five women were excluded because of deviations from the protocol (three early pregnancy losses, one bleeding during week nine, one preterm delivery at 36 weeks due to pre-eclampsia), and two women decided to discontinue after the first examination. The 29 women finally included in the study (mean age 28 years, range 19–38) all had uneventful pregnancies and gave birth to 16 male and 13 female children with a mean gestational age of 40 weeks 0 days (range 37 weeks 2 days–42 weeks 1 day LMP-based age). The mean birth weight was 3610 g (range 2610–4890 g). All but two delivered spontaneously. Those two were delivered by cesarean section at 40 weeks 2 days and 40 weeks 4 days, respectively, because of mechanical disproportion. All children proved to be healthy.

### 4.1.2 3D evaluation, pilot study

In this pilot study, the 3D scans were made on three women with no pregnancy complications referred for an ultrasound evaluation to confirm and date the pregnancy. The transvaginal ultrasound examination showed normal development of the embryonic or fetal anatomy. The gestational age was based on the CRL.

### 4.1.3 3D evaluation

Thirty-five healthy pregnant women with no pregnancy complications were recruited for a cross-sectional 3D ultrasound study of the embryonic development with emphasis on the body and the brain (Paper VI). One pregnancy was excluded from the study because the child died of total anomalous pulmonary venous return a few days after delivery. The 34 women included in the study gave birth to 17 male and 17 female children with a mean gestational age of 40 weeks 3 days based on the CRL (range 38 weeks 0 days–43 weeks 0 days). The mean birth weight was 3652 g (range 2770–4970 g). All but three delivered spontaneously. Two were delivered by Cesarean section at 39 weeks 2 days and at 39 weeks 4 days, respectively; the first one because of pre-eclampsia, the second one because of mechanical disproportion. One breech delivery was induced with oxytocin at 39 weeks 3 days. All children proved to be healthy.

## 4.2 Methods

### 4.2.1 Ultrasound equipment

The slightly curved switched array 7.5 MHz transvaginal transducer (Dornier AI 3200), which was used for studies I - IV, consisted of 96 elements. The transducer produced an $I_{SPTA}$ of 1.92 mW $cm^{-2}$. This output level was reduced to 30% (0.58 mW $cm^{-2}$) in the B mode.

The 7.5 MHz annular array transvaginal scanners (Vingmed Sound) used in studies V and VI had apertures of 11.5 mm diameter. The scan-plane of the transducer used in study V had an end-fire position. The 3D transvaginal probe applied in study VI was specially developed to enable 3D recordings. It had a scan-plane which was tilted 45 degrees from the end-fire position, rotating inside a fixed dome. The annular arrays in both transducers consisted of 4 active elements. They produced an $I_{SPTA}$ of maximal 12.1 mW $cm^{-2}$ in the B mode.

Thus, both transducer types emitted intensities which were far below the previously upper limit of output intensity of 94 mW $cm^{-2}$ that had been recommended by the FDA.

### 4.2.2 2D imaging

In order to use uniform terminology all statements of time in this thesis are based on the last menstrual period, expressed in completed weeks and completed days, assuming a regular cycle with the ovulation at 2 weeks 0 days. Gestational age was based on the LMP (Papers I - IV), or assessed by the CRL (Papers V - VI).

The measurements of the brain compartments (Papers I - II) were made according to Figures 4.2.2.a - c.

Methodological considerations about measuring the CRL, BPD, OFD, MAD, heart diameter, extension of the midgut herniation, diameters of the yolk sac, the amniotic cavity, and the chorionic cavity are described in chapter 2.6.

We measured the CRL, which actually was the GL, in a straight line from the cranial to the caudal end of the body in the straightest possible position of the embryo/fetus (Paper IV).

**Figure 4.2.2** a Sketch of the embryonic central nervous system at 7 weeks (Carnegie stage 16). A = sagittal section; B = sagittal measurements of the cavities of the rhombencephalon, mesencephalon, diencephalon and hemisphere; C = horizontal section superior through the embryonic head with the measurements of the width and length indicated by the arrows.

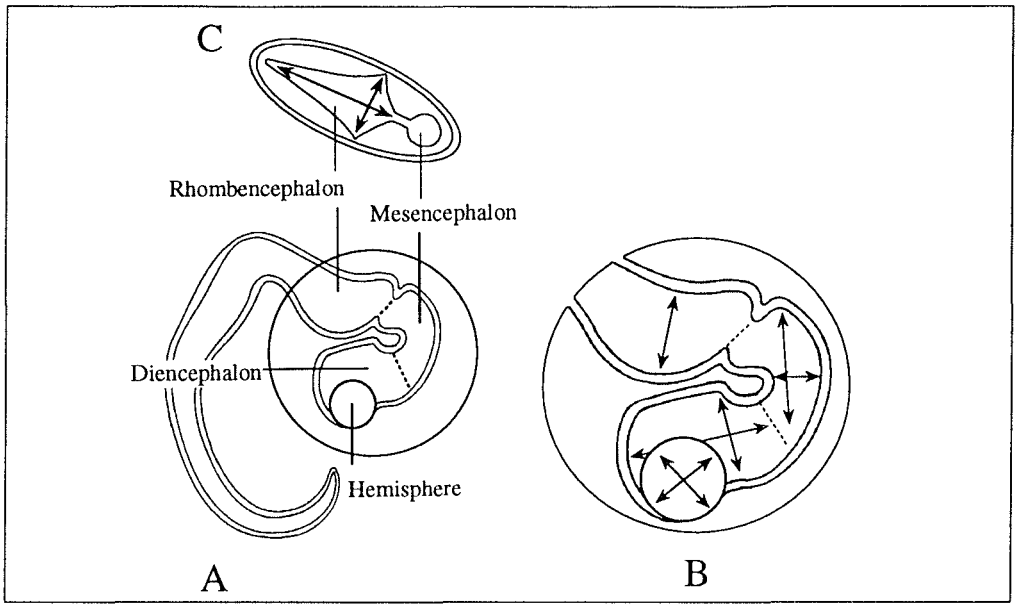


For the measurement of the width of the head (BPD, Paper IV), the calipers were placed at the outer contour of the embryonic head at its broadest extension. The same plane was used for the antero-posterior diameter (OFD, Paper IV). In the early fetal period the future cranium became successively distinguishable such that the biparietal diameter was obtained by placing the calipers at the outer border of the not-yet-ossified cranium in a horizontal section at the level of the thalami. The plane then involved the anterior hemispheres, the ventral thalami and the posterior part of the mesencephalon just above the cerebellum.

The MAD (Paper IV) was measured above the umbilical cord insertion just below the heart.

The heart rate was evaluated electronically using the M-mode (Paper III). The heart size was measured in the largest two perpendicular diameters in the horizontal thoracal section on the real-time image. When the level of the atrio-ventricular valves became visible (approximately 9 weeks and later), the measurements were taken at the level of the valves and through the apex of the heart (Paper III).

**Figure 4.2.2 b** Sketch of the sagittal (A) and parasagittal (B) sections through the brain at about 10 weeks (Carnegie stage 23). The arrows show the measurements. Hem = hemisphere; Di = diencephalon; Mes = mesencephalon; Chor plexus = choroid plexus.

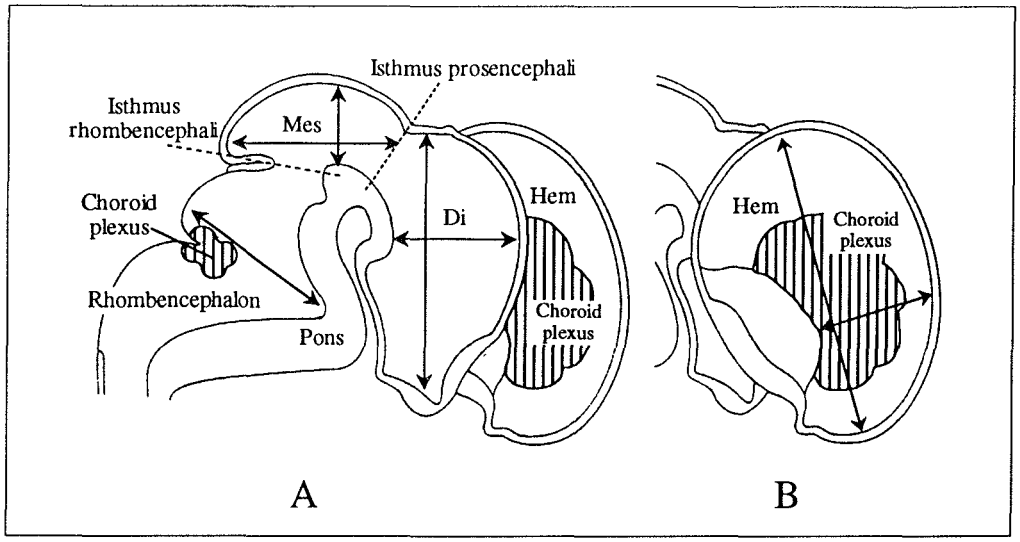


**Figure 4.2.2 c** Sketch of the horizontal (A) and posterior coronal (B) planes through the embryonic and early fetal brain. The brain compartments in sketch A are projected on each other (compare Figure 4.2.2.b A)

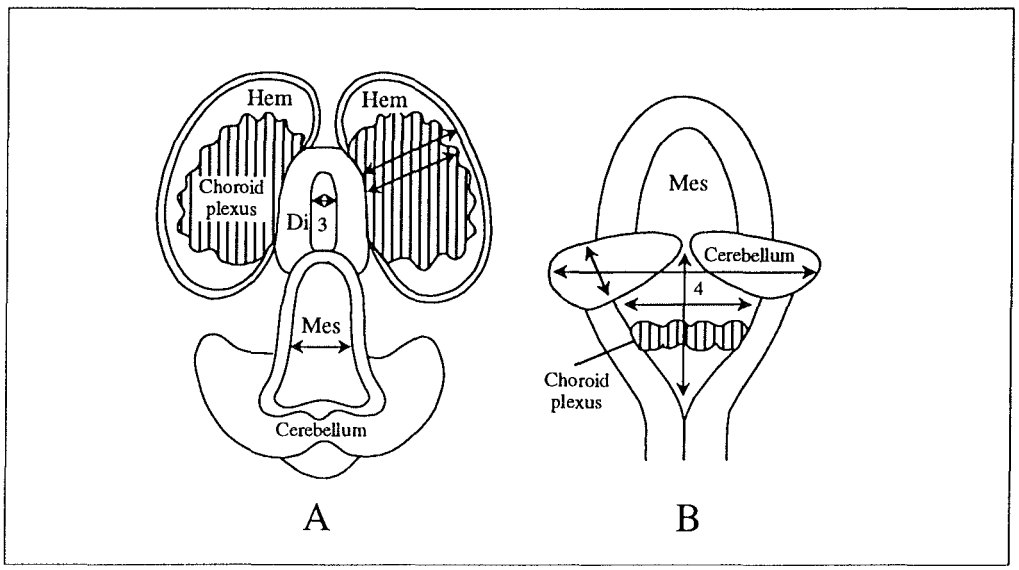


The mean diameter of the stomach was measured in the horizontal plane, using the antero-posterior and transverse diameter (Paper III).

The thickness of the umbilical cord and the length of the protruded intestine into the cord were measured close to the abdomen (Paper III).

For the measurement of the chorionic cavity the calipers were placed on the thin chorionic membrane (Paper IV). The amniotic cavity was analyzed in the same way with the calipers placed on the thin membrane (Paper IV). Also for the measurement of the yolk sac the calipers were placed on the middle of its wall (Paper IV). The mean diameters were calculated from diameters obtained in three perpendicular planes. We have not included measurements of the limbs in our studies because of the relatively late onset of bone ossification.

### 4.2.3 3D imaging

In study IV the transducer was attached to a rotating stepper motor coupled to a PC-based TomTec Echo-Scan unit (Boulder, Co, USA). During a period of 4 seconds, the stepper motor rotated the transducer 180 degrees. A complete 3D scan consisted of 132 two-dimensional sector images rotated around the central axis of the transducer. The TomTec unit converted the output video signals from the Vingmed scanner into digital representations. The unit then scan-converted the images into a regular volumetric data set which was then transferred to a UNIX workstation running AVS, a general purpose computer graphics system from Advanced Visualization Systems. The visualization and volume calculation were performed with a prototype AVS module developed by Chr. Michelsen Research, Bergen, Norway. An in vitro evaluation of this volume estimation method has been described (Gilja *et al.*, 1994). The volumes of the brain cavities were obtained by manually drawn segmentation. This process required many hours per brain reconstruction.

For the 3D reconstructions of the study presented in Paper VI, the raw digital ultrasound data, acquired with a specially designed 3D transvaginal probe, were transferred directly from the scanner to an external PC for further processing with the Vingmed Echopac3D software. The volume calculation algorithm that had been used for the AVS models in the pilot study (Paper V) was also used for the 3 D reconstructions in this study. The data acquisition (181 frames/volume, range 89–297) took an average of 5.3 seconds (range 2.3–8.6). In the PC, the original 2D-planes were scan-converted into a regular 3D data set (geometrical data set construction). This means that the raw ultrasound data were fitted into a regular array of small volume elements (voxels).

The embryos/fetuses and their brains were examined by 3D navigation in the 3D data set, manual segmentation in the anyplane mode, and surface and volume rendering of the geometrical 3D reconstructions. The segmentation process for the volume rendering of the brain cavities and the body lasted 1 to 2 hours per embryo or fetus. The surface of an embryo does not appear as a sharp silhouette, but rather as a blurred line. This is due to the so-called point spread function, which again is a result of the resolution of the ultrasound system (see chapter 2.3.2). Especially small structures appear larger than they are, and the outlining results in volume overestimation proportional to the surface of the subject. Conversely, the volume estimation of, for example, brain cavities, where the surface turns to the inside, results in underestimation. Therefore, the volume calculations were tested in a test series of 10 cylindrical phantoms with known volumes. Each test phantom was recorded from different angles and analyzed three times. By comparing the volume estimates with the true volumes, the deviation factor due to the point spread function was calculated (= 0.2 mm in the present study). We corrected for the point spread function in the embryos and its brain structures by modeling the surface using the formula for a cube.

## 4.3 Statistical analysis

### 4.3.1 2D measurements

Cross-sectional regression analysis was used to examine the associations between the measured values and gestational age in studies I-III. Simple models to fit the data were searched for, but transformation of the responses were necessary in some analyses to remove the heteroscedasticity. The normality of the residuals was confirmed both by visual inspection and by the Shapiro Francia W' test (Altman, 1991). The assumption of independency and constant variance of the residuals was confirmed by the residual plots. In paper II, the regressions and the normal distribution of the residuals were additionally evaluated by the Kolmogorov-Smirnov one-sample test and the Chi-square test of goodness of fit (STATISTICA, StatSoft). As serial measurements on individual embryos are highly correlated, the effective sample size was likely smaller than the total number of observations and therefore the prediction intervals should be interpreted with caution (Altman and Chitty, 1993).

#### 4.3.1.1 Intra-observer study

The reproducibility of measurements was evaluated by an intra-observer study in pregnant women who were not included in the longitudinal study. All measurements were recorded

on video print pictures, the values hidden for the examiner. The participants were scanned, then left the examination room for about 5 to 10 minutes before they were rescanned. The intra-observer variation was evaluated by repeated measurements of brain structures, the CRL and the BPD (Table 5.3). Limits of agreement (± 2 SD) for intra-observer measurements were calculated (Bland and Altman, 1986).

### 4.3.2 Growth analysis

The growth of the embryos/fetuses was evaluated by longitudinal measurements of the CRL, BPD, OFD, MAD, and diameters of the chorionic cavity, amniotic cavity and yolk sac (Paper IV). Hierarchical data occur when individuals are measured on more than one occasion, as it is the case in a longitudinal study. The variation of the data in this study was differentiated into two levels: the variation of each individual (level 1) and the variation between the individuals (level 2). The program MLn (Multi-Level n, Woodhouse, G., Rasbash, J., Goldstein, H., Yang, M., Howarth, J. and Plewis, I. (1995). MLn command reference. London, Institute of Education) was used for the statistical evaluation of these hierarchical data (Paper IV).

The statistical model for the data had to take into account the difference in size between the individuals

$$Y_{ij} = \alpha + \alpha_j + \alpha_{ij} + \beta x_{ij} \qquad \text{(A)}$$

where the index $ij$ meant observation number $i$ on the $j$th individual. Here $\alpha ij$ were the intercept residuals for observations and $\alpha j$ the intercept residuals for individuals. Both residuals were assumed to be independent and normally distributed, with zero means and constant variances $\sigma^2_{1\alpha}$ and $\sigma^2_{2\alpha}$ respectively. Levels 1 and 2 were assumed to be independent.

The next step was to check whether the slope for each individual was identical; this was done by adding slope residuals for individuals ($\beta_j$) at level 2 to the slope coefficient ($\beta$). The model became

$$Y_{ij} = \alpha + \alpha_j + \alpha_{ij} + (\beta + \beta_j)x_{ij}. \qquad \text{(B)}$$

The new random coefficients $\beta_j$ were assumed to be independent and normally distributed, with zero mean and variance $\sigma^2_{2\beta}$. Since there were two random variables ($\alpha_j$ and $\beta_j$) at level 2, a possible covariance $\sigma^2_{2\alpha\beta}$ was included.

The -2*log likelihoods for models (A) and (B) were computed. It was possible to test the significance of the parameters $\beta j$ since the difference in the likelihoods was $\chi^2$ with the number of new parameters as degree of freedom (Goldstein, 1995), in this case there were 2 degrees of freedom ($\sigma^2_{2\beta}$ and $\sigma^2_{2\alpha\beta}$).

The described procedure was applied for the analysis of the BPD, OFD, MAD, chorionic cavity diameter, amniotic cavity diameter and, after square root transformation, of the CRL.

The stepwise analysis of the longitudinal plot of the yolk sac diameter resulted in the model

$$Y_{ij} = \alpha + \alpha_j + \alpha_{ij} + (\beta + \beta_j + \beta_{ij})x_{ij} + (\gamma + \gamma_j)x_{ij}^2 + \eta x_{ij}^3, \qquad \text{(C)}$$

where the fixed part was a third degree polynomial.

The model assumptions were examined visually by constructing normal and residual plots for all random variables.

The statistical analysis was based on the LMP-based gestational age. The LMP-values of the study were centered at 9 weeks–4 days (9.5862 weeks) before the statistical analysis. Thus, the constants $\alpha$ are not related to the y-axis in x=0 days, but in x=9.5862 days.

### 4.3.3 3D measurements

Cross-sectional regression analysis was used to examine the associations between the calculated volumes and the size (CRL) of the embryos/fetuses (Paper VI). Simple models to fit the data were searched for, but transformation of the responses was necessary in some analyses to remove the heteroscedasticity. The normality of the residuals was confirmed both by visual inspection and by the Shapiro Francia W' test (Altman, 1991). The assumption of independency and constant variance of the residuals was confirmed by the residual plots.

# 5 Results and comments

## 5.1 2D measurements

A total of 145 examinations were performed in 29 individuals. The developmental changes of the embryo during 3 weeks are illustrated in Figures 1 A - C in appendix.

### 5.1.1 Hemispheres, lateral ventricles

The lateral ventricles could be measured in five embryos (17%) during week seven, in 23 embryos (79%) before 9 weeks 0 days, and in all individuals from 9 weeks on. At 7 weeks 4 days, the mean length (n = 115), width (n = 115) and height (n = 114) of the lateral ventricles were 1.7 mm (0.6 mm - 3.4 mm), 1.0 mm (0.4 mm - 2.1 mm), and 1.8 mm (0.8 mm - 3.2 mm) respectively. At 12 weeks 0 days, the mean length was 16.4 mm (12.4 mm - 20.9 mm), the mean width was 6.1 mm (4.2 mm - 8.4 mm), and the mean height 8.2 mm (5.9 mm - 10.9 mm). The growth of all these parameters was curvilinear.

Assuming the lateral ventricles to have an ellipsoid configuration, it was possible to estimate the volume from the 2D measurements using the formula for an ellipsoid $V_{2\text{Hem}} = 2\frac{4}{3}\pi\frac{L}{2}\frac{W}{2}\frac{H}{2}$, where L, W and H were the length, width and height of the hemispheres: The volume increased exponentially from 4.6 $mm^3$ at 8 weeks 0 days to 734.4 $mm^3$ at 12 weeks 0 days (cubic root transformation).

### 5.1.2 Choroid plexuses of lateral ventricles

The choroid plexus in the lateral ventricles became visible during week eight as tiny echogenic areas within the relatively hypoechogenic hemispheres in 16 embryos (53%). At 9 weeks 0 days the mean length (n = 108), width (n = 108) and height (n = 108) of the choroid plexuses were 2.8 mm (1.2 mm - 5.1 mm), 1.3 mm (0.5 mm - 2.4 mm), and 1.8 mm (0.9 mm - 3.0 mm) respectively. At 12 weeks 0 days, the mean length was 12.7 mm (8.9 mm - 17.2 mm), the mean width 4.4 mm (2.8 mm - 6.3 mm), and the height 5.4 mm (3.7 mm - 7.3 mm). The growth of all these parameters was curvilinear.

### 5.1.3 Diencephalic cavity

The diencephalic cavity was detectable in 17 embryos (59%) during week seven, and in all 29 embryos of the 2D study before 9 weeks 0 days. The mean length (n = 72) of the

cavity of the diencephalon at 7 weeks 3 days was 2.1 mm (0.8 mm - 3.4 mm) increasing to 3.6 mm (2.3 mm - 4.9 mm) at 10 weeks 0 days. The reduction of the mean width (n = 133) was linear, initially 1.2 mm (0.7 mm - 1.7 mm) at 7 weeks 0 days, decreasing to 0.8 mm (0.3 mm - 1.3 mm) at 12 weeks 0 days. The mean height (n = 73) was 1.1 mm (0.3 mm - 1.8 mm) at 7 weeks 0 days, and increased to 1.9 mm (1.2 mm - 2.6 mm) at 10 weeks 0 days. The data could best be fitted to a linear regression.

### 5.1.4 Mesencephalic cavity

The mesencephalic cavity could be recognized during week seven in 17 of 29 embryos (57%). The mean length of the mesencephalic cavity (n = 134) increased from 2.8 mm (1.7 mm - 3.9 mm) at 7 weeks 2 days, to 4.8 mm (3.7 mm - 5.9 mm) at 12 weeks 0 days. At 7 weeks 2 days, the mean width (n = 133) was 1.3 mm (0.7 mm - 1.8 mm) and the mean height (n = 136) was 1.2 mm (0.6 mm - 1.7 mm). The width increased to 1.7 mm (1.2 mm - 2.3 mm) at 12 weeks 0 days, the height to 2.0 mm (1.4 mm - 2.5 mm). The parameters were analyzed linearly.

### 5.1.5 Rhombencephalic cavity

Measurement of the length of the rhombencephalic cavity (n = 145) showed a relatively large variation with a mean length from 3.8 mm (2.2 mm – 5.3 mm) at 7 weeks 0 days, to 4.4 mm (2.8 mm – 5.9 mm) at 12 weeks 0 days. The mean length increased only 0.6 mm during five weeks. Using the CRL as the independent variable there was an increase and a decrease of the mean length of the rhombencephalic cavity from 3.1 mm (CRL 8 mm) to 4.4 mm (CRL 16 mm) and to 2.9 mm (CRL 24 mm). The width of the rhombencephalic cavity (n = 145) increased from 2.1 mm (0.6 mm – 3.7 mm) at 7 weeks 0 days to 4.5 mm (2.9 mm – 6.1 mm) at 12 weeks 0 days. The data could best be fitted to a polynomial of the second degree. The depth of the rhombencephalic cavity (n = 141) was 1.5 mm (0.4 mm – 2.6 mm) at 7 weeks 0 days. The increase was curvilinear to 3.2 mm (2.2 mm – 4.3 mm) at 12 weeks 0 days. Also these data could best be fitted to a polynomial of the second degree.

We assumed that the rhombencephalic cavity had a pyramid-like configuration, and estimated the volume from the 2D measurements by the formula $V_{\text{Rhomb}} = \frac{1}{3}\frac{LW}{2}D$: It increased slowly from 21.2 $mm^3$ at 7 weeks 0 days to 75.3 $mm^3$ at 12 weeks 0 days (cubic root transformation).

### 5.1.6 Cerebellum

The cerebellum, consisting of the anterior rhombic lips, could be measured in 6 of 29 embryos (20%) before 9 weeks 0 days. Before 10 weeks 0 days the cerebellum was distinguishable in 80% of 29 embryos, and after 10 weeks 3 days it could always be seen. The width of the cerebellum (n = 93) was 4.8 mm (3.0 mm – 7.1 mm) at 9 weeks 0 days. At 12 weeks 0 days the width had increased to 8.1 mm (5.7 mm – 11.0 mm). The data could best be fitted to a square root transformation. The height of the cerebellum (n = 93) grew linearly from mean 1.4 mm (0.7 mm – 2.1 mm) at 9 weeks 0 days to mean 2.5 mm (1.8 mm – 3.2 mm) at 12 weeks 0 days.

### 5.1.7 Choroid plexuses of fourth ventricle

The choroid plexuses of the fourth ventricle became visible in 13 embryos (43%) during week 8. The width of the choroid plexuses of the rhombencephalon (n = 100) was 3.2 mm (1.8 mm–4.6 mm) at 9 weeks 0 days and increased linearly to 4.1 mm (2.7 mm – 5.6 mm) at 12 weeks 0 days. The height of the choroid plexuses (n = 102) was 1.1 mm (0.6 mm – 1.6 mm) at 9 weeks 0 days. The height reached 1.3 mm (0.8 mm – 1.8 mm) at 12 weeks 0 days.

### 5.1.8 Comments concerning brain structures

Several papers have been published about the ultrasound evaluation of the embryonic development. Two of these papers dealt exclusively with the brain development, one presented a cross-sectional descriptive ultrasound study (Timor-Tritsch *et al.*, 1991), while the other was an overview article (Achiron and Achiron, 1991). All studies demonstrated the possibilities of studying embryonic CNS structures using the transvaginal approach, and showed that the features changed specifically from week to week. Still there were divergences in interpreting the appearance and significance of certain structures seen by ultrasound, such as the so called "single ventricle" (Blumenfeld *et al.*, 1988; Cyr *et al.*, 1988; Timor-Tritsch *et al.*, 1988; Bree and Marn, 1990; Timor-Tritsch *et al.*, 1990; Achiron and Achiron, 1991; Timor-Tritsch *et al.*, 1991). Cyr and colleagues, who examined 25 embryos from eight to 10 weeks using a 5 MHz transabdominal transducer, believed that a relatively large cystic structure in the head presented the rhombencephalic cavity (Cyr *et al.*, 1988). Timor-Tritsch and colleagues (Timor-Tritsch *et al.*, 1991) presented a cross-sectional study of 133 observations between six and 14 weeks of gestation, examined with a 6.5 MHz transvaginal transducer. They described the telencephalic and mesencephalic vesicle during week seven, followed by the occurrence of the myelocele (lower funneling of the fourth

ventricle) at the end of the same week. The developing rhombencephalon was clearly imaged at week 8 and later. Both the metocele and the myelocele were registered during week eight. Achiron and Achiron (Achiron and Achiron, 1991), who also used a 6.5 MHz transducer, and Bree (Bree and Marn, 1990) described brain development in a review report. They interpreted the single ventricle in the embryonic brain during week seven as the forebrain dividing during week eight. Cullen and colleagues (Cullen *et al.*, 1990) interpreted a single ventricle visible at eight weeks of gestation as the rhombencephalon. Takeuchi (Takeuchi, 1992), who used a 7.5 MHz transvaginal transducer, placed the visibility of the fourth ventricle at seven weeks. An invasive approach by a catheter-based 12.5 MHz ultrasound transducer introduced through the cervix into the chorionic cavity was described by Ragavendra and co-workers in the early 90's (Ragavendra *et al.*, 1991). In 1995, another group demonstrated the imaging of embryonic structures applying a 20 MHz catheter-based intra-uterine transducer (Fujiwaki *et al.*, 1995). The authors concluded that 6 of the 12 embryos at seven weeks still had primary brain vesicles which represented the unpartitioned prosencephalon and the rhombencephalon. This is not in agreement with the embryological literature which places the development of the cerebral hemispheres, and thus the «five vesicle stage», at Carnegie stages 14 and 15, in other words at six weeks (Yokoh, 1975; O'Rahilly and Müller, 1987; O'Rahilly and Müller, 1994). The limited access for 2D imaging by the transvaginal approach may explain the difficulty of detecting all structures. Van Zalen-Sprock analyzed the mean diameter of the rhombencephalic cavity from eight to 12 weeks and showed that in some congenital conditions affecting the rhombencephalon the fourth ventricle was enlarged significantly (Zalen-Sprock *et al.*, 1996).

In our 2D study we could not take measurements of the hemispheres in all embryos during week seven, but the large rhombencephalic cavity was always measurable. In our 3D studies it was always possible to identify all five brain cavities in all specimens at seven weeks, even in the smallest specimen of 9.3 mm CRL (Papers V and VI). At week eight, the hemispheres reached a considerable size, at which time they have been mistakenly interpreted as the orbits (Bree and Marn, 1990). The optic primordium becomes detectable by light microscope at Carnegie stage 10 (O'Rahilly and Müller, 1987), which is approximately at the beginning of week five. Initially, the eyes do not look like hypoechogenic areas as in the third trimester fetus; they become visible by high-frequency ultrasound at approximately eight weeks. The walls of the hemispheres have a thickness of about 1 - 2 mm at the end of the first trimester. The posterior horns of the lateral ventricles do not develop before the second trimester (O'Rahilly and Müller, 1994).

O'Rahilly analyzed the size of the CNS-structures in four embryos which were 10 weeks old (Carnegie stage 23) (O'Rahilly and Müller, 1990), and found the distance from the anterior horn to the future posterior horn to be 9.5 mm (range 7.3 - 10.9 mm). At 10 weeks 0 days we found a mean length of 7.9 mm with a 95% prediction interval of 5.3 mm to 11.1 mm.

The choroid plexus of the lateral ventricle develops from a choroid fold, and can be observed in Carnegie stage 18. The growth is rapid, and at Carnegie stage 23 the choroid plexus occupies approximately one third or more of the lateral ventricle (O'Rahilly and Müller, 1990). By ultrasound it became visible during week eight, and showed a growth corresponding to that of the hemisphere (Paper I).

The cavity of the diencephalon, the third ventricle, is in continuity with the anterior part of the forebrain. The epithalamus, ventral and dorsal thalamus and hypothalamus are present at Carnegie stage 15, but the diencephalic wall is still thin at Carnegie stage 17 (Streeter, 1948). The dorsal thalamus grows rapidly after Carnegie stage 20, and in 80% of the brains the two bulges fuse in the midline, forming a bridge of grey matter across the third ventricle; this bridge is called the massa intermedia, and it almost fills the third ventricle by 14 to 15 weeks (Lemire, 1975). The cavity of the diencephalon is easily seen by ultrasound during the embryonic period from week seven on. Its width decreases slowly during the first trimester. This can be explained by the growth of the wall of the diencephalon, especially the posterior thalamus. Because of the decreasing width, measurement of the height and the length proved to become more difficult after 9 to 10 weeks. This phenomenon made the measurements of height and length of the third ventricle less reliable towards 12 weeks. Therefore we included only measurements of the length and height obtained up until 10 weeks 0 days. It might be more appropriate to estimate the extension of the diencephalon by measuring only the length and height of the whole hypoechogenic diencephalon. The third ventricle must not be misinterpreted as the cavum septi pellucidi. According to the embryological literature, the corpus callosum and cavum septi pellucidi are not yet developed at the end of the first trimester (England, 1988).

The midbrain cavity is known as the aquaeductus Sylvii in the adult brain. It is relatively wide throughout the embryonic period proper (O'Rahilly and Müller, 1990). Originally, the mesencephalon has thin walls, and its lumen is a continuation of the third ventricle (England, 1988), separated from the diencephalon by a slight constriction. At Carnegie

stages 22 to 23 this constriction is found immediately rostral to the midbrain; it is called the isthmus prosencephali, and could easily be seen by ultrasound. The border towards the rhombencephalon is the distinct isthmus rhombencephali. The midbrain shows bilateral evaginations at Carnegie stage 19 in the caudal part of the cavity (called "Blindsäcke" by Hochstetter in 1929) (O'Rahilly and Gardner, 1971; Müller and O'Rahilly, 1990). O'Rahilly and Müller (O'Rahilly and Müller, 1990) measured the cavity of the mesencephalon, the mesocele, and found a mean size of 2.2 mm x 2.5 mm x 5.3 mm in preparations of embryos at Carnegie stage 23. This indicates that the cavity "clearly is still in no sense a narrow aqueduct" (O'Rahilly and Müller, 1990). We found both height and width increasing slightly throughout the first trimester. The mean inner diameter at 10 weeks in our study (Carnegie stage 23) was 1.5 mm x 1.6 mm x 3.9 mm. A study on the size of embryonic and fetal brain compartments was presented by Jenkins as early as in 1921 (Jenkins, 1921). In the embryo of 4.3 mm CRL (≈ 6 weeks 1 day) the rhombencephalon accounted for 54.4% of the brain, the mesencephalon for 14.3%, the diencephalon for 24.3%, and the telencephalon for 7.0%. In the embryo of 25 mm CRL (≈ 9 weeks 3 days) these proportions had changed to rhombencephalon, 36.6%, mesencephalon, 14.8%, diencephalon, 19.8%, and telencephalon, 28.8%.

### 5.1.9 Heart

The mean diameter of the heart (n = 144) increased linearly with gestational age. The relationship of the mean heart diameter to the CRL could best be expressed by a polynomial regression of the second degree after square root transformation. There was a linear dependence of the mean heart diameter on the mean abdominal diameter (n = 143).

The ratio between the mean heart diameter and the CRL was 0.22 at 7 weeks 0 days, decreasing to 0.17 at 9 weeks 0 days, and further to 0.13 in the fetus at 12 weeks 0 days. We found a similar ratio between the mean heart diameter and the MAD: It fell from 0.57 at 7 weeks 0 days to 0.47 at 9 weeks 0 days, and to 0.42 at 12 weeks 0 days.

### 5.1.10 Heart rate

The mean heart rate (n = 144) increased from 138 beats per minute (122 bpm - 154 bpm) at 7 weeks 0 days to 166 bpm (150 bpm - 182 bpm) at 8 weeks 0 days, and to 175 bpm (159 bpm - 190 bpm) at 9 weeks 0 days. The peak of the curve (fourth degree polynomial), 175 bpm (159 bpm - 191 bpm), was found at 9 weeks 3 days. At 12 weeks 0 days the mean heart rate had decreased to 166 bpm (150 bpm - 182 bpm).

### 5.1.11 Comments concerning heart

During the embryonic period, the heart undergoes profound developmental changes which transform its simple tubular cavity at five weeks into the four chambers of the heart, usually completed at the end of week eight by the closure of the interventricular foramen.

As expected, the size of the human embryonic heart was correlated to that of the crown-rump length and the abdominal diameter. Compared to the body size, the heart was relatively large in the early embryonic period. The heart size became a relatively smaller part of the embryo with increasing age. Clark described similar conditions in chick embryos (Clark, 1985). He found a 15-fold increase of the embryonic dry weight compared to a nine-fold increase of the heart weight from three days to six days gestational age, and he concluded that the larger the embryo the smaller the relative size of the heart. Bronshtein and colleagues (Bronshtein *et al.*, 1992) presented biometric data of the fetal heart in a cross-sectional study of 120 normal fetuses from 10 to 17 weeks. The estimated heart size at 11 - 12 weeks was lower than in our study, possibly because the heart diameter was only measured at the level of the atrio-ventricular valves in Bronshtein's study. The size increased by about 1.2 mm a week. They also calculated the heart size/chest diameter ratio, which corresponds with our heart size/MAD ratio, finding a slight increase of this ratio instead of a decrease.

The heart rate of the embryo has been analyzed with ultrasound by others. Jouppila, who examined the rate transvaginally, found a frequency of 170 bpm - 179 bpm at the $8^{th}$ to $11^{th}$ weeks of gestation, decreasing to mean 149 bpm at the $16^{th}$ week of gestation (Jouppila, 1971). Müller and Osler found similar values, namely about 170 bpm at the $10^{th}$ week, decreasing to about 150 bpm at 15 weeks and later (Müller and Osler, 1969). At the end of the sixties the M-mode technique was introduced for the identification of the first trimester heart activity by Kratochwil and Eisenhut (Kratochwil and Eisenhut, 1967). Bang and Holm published a study about the M-mode technique applied transabdominally, where the detection of heart activity at the $10^{th}$ week was registered (Bang and Holm, 1968). By this method, the particular course of the heart rate curve with a maximum heart rate at 9 weeks in the first trimester was shown five years later (Robinson and Shaw-Dunn, 1973). In some real-time ultrasound studies the fetal heart rate was counted for periods of 15 seconds and then multiplied by four (Hertzberg *et al.*, 1988; Merchiers *et al.*, 1990): Hertzberg (Hertzberg *et al.*, 1988) found the highest mean frequency of 144 bpm at eight weeks, while Merchiers (Merchiers *et al.*, 1990) recorded the highest

mean frequency of 157 bpm during week 10. In general the heart rate obtained by visual counting is lower (Hertzberg *et al.*, 1988; Merchiers *et al.*, 1990) than the heart rate obtained by M-mode measurements (Robinson and Shaw-Dunn, 1973; DuBose *et al.*, 1990). As visual measurements of very high heart rates are difficult to obtain, DuBose (DuBose *et al.*, 1990) suggested using M-mode measurements to improve the accuracy of the counting. Similar to our findings, Robinson (Robinson and Shaw-Dunn, 1973), DuBose (DuBose *et al.*, 1990) and Wisser (Wisser and Dirschedl, 1994) recorded the highest mean heart rate at the beginning of week nine, with mean values of 177 bpm found by Robinson and 175 bpm calculated by DuBose. By transforming the time-axis (gestational age) to a logarithmic scale, Wisser revealed that the embryonic heart rate could be divided into an ascending and a descending linear part with the peak at 9 weeks 0 days of gestation (Wisser and Dirschedl, 1994).

The regularity we found in the pattern of the initial increase of the heart rate, the initial distinct decrease of the ratio between heart size and crown-rump length and the ratio between heart size and abdominal diameter, followed by the slow decrease of these parameters, suggests a fundamental association in the anatomical and physiological development of the heart. The size of the heart and the frequency of the heart activity are factors that are modified by the structural development and actual physiological demands of the early blood circulation. In the early embryo with its developing heart architecture, a certain heart size and muscle mass may be necessary to maintain a sufficient pump power. Clark assumed that the energy delivered to the intracardiac blood may be relatively less in the complex heart than in the early muscular tube (Clark, 1985). As already suggested by Wisser (Wisser and Dirschedl, 1994), maximal heart rate is reached when the morphological development of the embryonic heart is completed. It may be speculated that developmental changes in the embryonic period have improved and economized the function of the heart and peripheral vasculature, and optimized the heart rate so that at nine weeks and later, proportionally less muscle mass and fewer heart beats are required to meet the demands of the fetal blood circulation.

Alterations of the heart rate can be associated with embryonic maldevelopment (Schats *et al.*, 1990; Achiron *et al.*, 1994). Gross defects of the heart such as an ectopia cordis should be detectable at the end of the embryonic period, while defects such as a large AV-canal may be detectable at the very beginning of the fetal period.

### 5.1.12 Stomach

In 9 of the 29 embryos (31%) the stomach could be identified before 9 weeks 0 days. The stomach could be detected in 22 embryos (76%) before 10 weeks 0 days. We measured the stomach in the horizontal section. The mean diameter (n = 88) was 1.2 mm (0.5 mm - 2.1 mm) of those identified at 9 weeks 0 days, increasing to 2.4 mm (1.4 mm - 3.7 mm) at 12 weeks 0 days. The data could best be fitted to a square root transformation.

### 5.1.13 Comments concerning stomach

Embryonic studies have shown that there is a considerable lumen in the developing embryonic stomach which may be filled with fluid and, thus, should be detectable by ultrasound. We could observe the appearance of the stomach earlier than described by other authors, likely due to the use of the 7.5 MHz transvaginal transducer. Cullen (Cullen *et al.*, 1990) and Green (Green and Hobbins, 1988) identified the stomach at ten weeks, but they did not measure its size. The human fetus initiates swallowing movements at 11 weeks (Diamant, 1985). We found fluid in the stomach of embryos as early as at eight and half weeks. Since the embryo does not swallow amniotic fluid at that stage, fluid production from the intestinal epithelium is most likely present already in the embryonic period. Thus, the physiology of the intestinal tract fluid production in the first-trimester conceptuses is different from that in older fetuses. As demonstrated, the finding of an empty stomach during the first trimester is a normal feature. Developmental disorders of the intestinal tract such as intestinal or esophageal atresia may affect the amount of fluid in the stomach during the first trimester and thus provide a sign for detection. Tsukerman and colleagues (Tsukerman *et al.*, 1993) described a 12-week-old fetus with a grossly dilated stomach and duodenum. This fetus had a complete atresia both of the esophagus and the duodenum. Here the fluid accumulation probably originated from the gastric and duodenal epithelium itself. We found a similar case with a grossly enlarged stomach and even dilated bowel in an IVF-triplet pregnancy at 10 weeks 6 days. The fluid accumulation in the intestine disappeared after the completion of the midgut herniation and the stomach became empty for the rest of the pregnancy. Our suspicion of esophageal atresia was confirmed after birth. One might hypothesize that intestinal fluid had no possibility of becoming evacuated due to the proximal atresia and a sort of distal occlusion in form of the physiological midgut herniation.

### 5.1.14 Midgut herniation

In accordance with the regression line (polynomial of the third degree) the longest elongation of the midgut herniation (n = 96) was estimated at 10 weeks 2 days - 10 weeks

4 days (4.1 mm, range 2.4 mm - 5.8 mm). The gut projected at the most 6.3 mm into the cord in a 10 week-0 day-old fetus. The cord diameter at the level of the abdominal insertion (n = 143) showed an increased thickness between 8 weeks and 11 weeks; the thickness of the cord registered at a free loop showed no increase.

### 5.1.15 Comments concerning midgut herniation

The physiological herniation of the midgut has been described in several ultrasound studies, some used a 3.5 MHz or a 5 MHz transabdominal ultrasound transducer (Cyr *et al.*, 1986; Schmidt *et al.*, 1987; Green and Hobbins, 1988; Timor-Tritsch *et al.*, 1989; Bowerman, 1993), while Timor-Tritsch and colleagues (Timor-Tritsch *et al.*, 1989) applied a 6.5 MHz transvaginal probe. Green and colleagues (Green and Hobbins, 1988) and Timor-Tritsch and colleagues did not quantify the extension of the herniation. Timor Tritsch and colleagues suggested that the presence of a midgut herniation was indicated if the diameter of the cord immediately at the abdominal insertion was 1.5 times larger than the cord peripherally. They found the earliest midgut herniation at eight weeks. The midgut herniation was present in pregnancies until 11 weeks of gestation. Cyr and colleagues (Cyr *et al.*, 1986) examined transabdominally 10 pregnancies between 7 and 10 weeks and found in all cases herniated bowel mass in the umbilical cord with a mean diameter of 6.3 mm (5 mm - 10 mm). Schmidt and colleagues (Schmidt *et al.*, 1987) examined 14 cases longitudinally. They found larger herniated masses in eight-week-old embryos than in older embryos or fetuses. In their study the mean diameter of the protruded mass was 6 - 9 mm at eight weeks; it decreased to 5 mm - 6 mm at nine weeks. Bowerman measured the largest dimension of the protruding «mass» of the midgut herniation in 48 specimens ranging from 19 mm to 82 mm CRL (Bowerman, 1993) finding a linear increase of the dimension of the midgut herniation from 4 mm at 8 weeks 4 days to 7 mm at the end of 10 weeks. We found the largest mass of the midgut herniation in a ten-week-old fetus, but the length of the mass never exceeded 6.3 mm. Already in 1989, Brown and colleagues (Brown *et al.*, 1989) presented the diagnosis of an epigastric omphalocele as early as at 10 weeks 2 days (CRL 35 mm). The transverse diameters of the herniated mass measured 8 and 9 mm. Van Zalen-Sprock and co-workers presented 17 cases of omphaloceles which were diagnosed at 11 weeks 6 days up to 15 weeks 3 days (Zalen-Sprock *et al.*, 1997). Though smaller medial omphaloceles may not be detectable during the period of the physiological midgut herniation we suggest that large omphaloceles, especially the epigastric omphaloceles containing the liver (Brown *et al.*, 1989), and gastroschises may be detectable towards the end of the embryonic period, namely at nine weeks of gestation. Larger defects such as the limb-

body-wall complex should be detectable even earlier.

## 5.2 Embryonic growth

### 5.2.1 Measurements

The CRL values at the first examination varied from 8 to 18 mm. In embryos of 12 mm CRL the range of the LMP-based age was at most 8 days. Correspondingly, the BPD values varied from 3 to 8 mm. The largest age range of 9 days was found in embryos with a BPD of 4 mm. The longitudinal plot of the CRL measurements (145 observations) were curvi-linear and showed a heteroscedastic distribution of the data. For the analysis of the CRL development, a square root transformation of the data was performed. The variation of the slope between the individuals was hardly visible using model B and did not describe the data significantly better than model A ($p = 0.08$). The total variation of the data was made of 85% variation in level 2 (between the individuals), and 15% variation in level 1 (of each individual).

The longitudinal plots of the measurements of the BPD (139 observations), the OFD (139 observations), the MAD (142 observations), the chorionic cavity diameter (145 observations) and the amniotic cavity diameter (143 observations) revealed a linear flow of the data. The statistical analysis showed non-significant differences of the slopes at level 2. The corresponding p-values were $p = 0.375$ (BPD), $p = 1$ (OFD), $p = 0.45$ (MAD), $p = 0.067$ (chorionic cavity diameter) and $p = 0.062$ (amniotic cavity diameter). Therefore, model A was used for the description of the data. The variations of the data at level 2 expressed as percentage of the total variation, were 81% for BPD, 69% for OFD, 59% for MAD, 56% for the chorionic cavity diameter and 75% for the amniotic cavity diameter. The variation, then, consisted mainly of variation between individuals.

The mean growth curve of the CRL and that of the mean amniotic cavity diameter showed very similar absolute values in millimeters throughout the observation period.

The yolk sac (142 observations) appeared as a round structure with a rather echogenic wall during the embryonic period. The longitudinal plot of the yolk sac diameter initially showed a slightly increasing linear course of the growth until 10 weeks of gestation. During weeks 10 to 11 the shape of the yolk sac altered and its wall became thinner. The yolk sac became enlarged in some cases, while it shrank in other cases. The data were fitted by a polynomial of third degree.

While cross-sectional data give information on the size of an individual at known gestational age, longitudinal data provide the ability to assess typical growth patterns over a time period. There are only a few longitudinal studies addressing the growth in the early pregnancy (Rossavik *et al.*, 1988; Rabelink *et al.*, 1994). Rossavik used two CRL measurements to calculate the growth (Rossavik *et al.*, 1988). Such a procedure assumes constant growth within the interval and is vulnerable for measurement errors which might give false different slopes. Both embryological and sonoembryological studies have shown that the CRL develops in a non-linear fashion (O'Rahilly and Gardner, 1971; Robinson and Fleming, 1975; Drumm and O'Rahilly, 1977; Pedersen, 1982; MacGregor *et al.*, 1987; O'Rahilly and Müller, 1987; Evans, 1991; Kustermann *et al.*, 1992; Grisiola *et al.*, 1993; Lasser *et al.*, 1993; Wisser *et al.*, 1994). Embryology describes a gradual transition from the flexed early embryo to the straight body of the early fetus, where the deflection of the embryonic brain plays an important role (O'Rahilly and Müller, 1987). This developmental process may be partly responsible for the curvi-linear shape of the CRL growth curve. Thus, concerning the CRL the applicability of the procedure proposed by Rossavik is limited.

Rabelink and co-workers analyzed 109 pregnancies longitudinally making a total of 794 CRL and 1795 BPD measurements (Rabelink *et al.*, 1994). For each individual they constructed linear regressions after cutting off measurements of the CRL below 20 mm and above 90 mm, thus analyzing only the straight part of the S-shaped curve. The individual CRL curves showed different slopes and different intercepts on the x-axis (Rabelink *et al.*, 1994). Correlation of the slopes with the intercepts on the x-axis indicated that the individual embryos with a late onset of growth (high x-axis intercept) had a steeper slope as a characteristic for 'catch-up growth'. However, cutting off important measurements of the size and extrapolating curves to the x-axis contributes to significant uncertainty of the results.

Though the plot of the BPD measurements in 108 individuals had a slight bend, Rabelink and co-workers used simple linear regressions for each individual. The correlation of the slopes of the individual BPD curves with the intercepts on the x-axis showed different velocities indicating 'catch-up growth' in embryos with a delayed start (Rabelink *et al.*, 1994). The present study could not confirm any differences of the growth rate of the BPD between the individuals.

The development of the antero-posterior diameter of the head, called occipito-frontal

diameter (OFD), has not been evaluated during the first trimester in other studies and comparisons with previous studies cannot be made.

Rossavik and colleagues did longitudinal studies on the mean chorionic cavity diameter from three perpendicular planes three times each in 19 patients (Rossavik *et al.*, 1988), finding similar slopes for the individuals as in the present study.

Embryologists have shown the close relationship between the amniotic cavity volume and the fetal size (Abramovich, 1968). There is a remarkable similarity of the absolute values of the estimated mean CRL and the estimated mean diameter of the amniotic cavity, such that an embryo of 15 mm CRL has a mean amniotic cavity diameter of approximately 15 mm. This fact may be used in the evaluation of the early pregnancy.

On the ultrasound image, the yolk sac appears as a small ring with rather bright walls lying within the chorionic cavity (extra-embryonic coelom). It is important to consider physical principles of ultrasound imaging when measuring the small yolk sac; this is described in chapter 2.3. Though the wall of the yolk sac is thin ($\approx$ 0.01 mm - 0.3 mm, see above), it appears bright on the ultrasound image and seems to have a considerable thickness depending on the transducer and the gain setting that are used. Many authors neglected to specify where they placed the calipers for the measurement of the yolk sac (Green and Hobbins, 1988; Reece *et al.*, 1988; Schaaps and Hustin, 1988; Jauniaux *et al.*, 1991). In those studies where such information was given and where different ultrasound equipment and different measurement methods were used, relatively large differences of the yolk sac size are found (Rempen, 1991b; Lindsay *et al.*, 1992; Stampone *et al.*, 1996) (Table 5.2.2). Thus, since the imaging of the thickness of the echogenic yolk sac wall varies with the transducer - and frequency-dependent point spread function and the gain setting, we chose to place the calipers on the middle of the yolk sac wall.

The longitudinal plot and the corresponding estimated curves of the yolk sac in the present study showed the slightly increasing parallel course of growth until 10 weeks of gestation followed by disorganized development of the growth in the early fetal period; this probably reflects spontaneous physiological events of normal embryonic development (Jauniaux *et al.*, 1991).

**Table 5.2.2** The diameter of the yolk sac as presented in different studies based on transvaginal ultrasound observations.

| Author | Lindsay et al. 1992 | Stampone et al. 1996⊗ | Blaas et al. 1998 | Rempen 1991⊕ |
|---|---|---|---|---|
| Caliper setting: | inside-inside | inside-inside | middle of the wall | outside-outside |
| Transducer frequency | 6.5 - 7.5 MHz | 6.5 MHz | 7.5 MHz | 5 MHz |
| Study group | N=327 | N=117 | N=29 142 observations | N=219 |
| Design | cross-sectional | cross-sectional | longitudinal | cross-sectional |
| Method of measurements | 3 diameters, decimal of a mm | 2 diameters, decimal of a mm | 3 diameters, decimal of a mm | 3 diameters, full mm |
| LMP-based age | estimated mean diameter (mm) | estimated mean diameter (mm) | estimated mean diameter (mm) | estimated mean diameter (mm) |
| 7 weeks (49 days) | 2.9 | 4.1 | 4.2 | 5.0 |
| 8 weeks (56 days) | 3.1 | 4.5 | 4.3 | 5.5 |
| 9 weeks (63 days) | 3.4 | 4.8 | 4.8 | 5.7 |
| 10 weeks (70 days) | (68 days) 3.8 | 4.9 | 5.3 | 5.8 |
| 11 weeks (77 days) | - | 4.9 | 5.3 | 5.7 |
| 12 weeks (84 days) | - | 4.7 | 4.3 | 5.3 |

⊗ The measurements from Stampone et al.'s study were all presented in complete weeks. It is not commented in the paper, whether the measurements were centered around full weeks or around the middle of a week (e.g. 7 weeks 0 days versus 7 weeks 3.5 days). If they were centered around the middle of the week, the estimated mean would be even smaller than presented in the table. The regression equation presented in their paper is not in accordance with the presented mean values.

⊕ The equation for the regression curve as presented in Rempen's paper is probably not correct as it is not in accordance with his diagram: instead of the constant «-4.642» the constant «-3.642» gives an identical curve as presented in his paper.

## 5.3 Reproducibility of the measurements

The probe used in the 2D studies of the present thesis (Papers I–IV) was a 7.5 MHz slightly curved switched array transvaginal transducer. The imaging of the embryo and fetus for the measurement of the CRL or BPD was highly reproducible as it was expressed in the small intra-observer variation (Table 5.3) with limits of agreement of (-0.9, 0.8) mm for the BPD and (-1.3, 1.3) mm for the CRL. Measurement of small structures was affected by the relatively poorer resolution in the elevation plane and was expressed by a relatively large intra-observer variation. For example, the length, width and height of the cavity of the mesencephalon were at most 5.5 mm, 2.4 mm and 2.8 mm respectively. The intra-observer range of 1.3 mm (length of the mesencephalon), 1.1 mm (width of the mesencephalon) and 1.5 mm (height of the mesencephalon) for these measurements were absolutely very small, but relatively large. For the brain cavities, the largest absolute difference between repeated measurements was 1.6 mm, which was 17% of the total size of the measured structure (9.2 mm hemisphere length, CRL 46 mm). For structures below 3 mm, the largest absolute difference was 0.9 mm, which was 51% of the total size of the measured structure (1.8 mm hemisphere width, CRL 18 mm).

See also Table 5.3 on the next page.

**Table 5.3** Limits of agreement (± 2 SD) in the intra-observer analysis of two different measurements of embryos/fetuses and their brain structures

| | | N | Mean mm | Range mm | Lower limit mm | Upper limit mm |
|---|---|---|---|---|---|---|
| CRL | | 42 | 25.8 | 10.0 - 57.0 | -1.3 | 1.3 |
| BPD | | 42 | 10.0 | 2.8 - 19.0 | -0.9 | 0.8 |
| Hemisphere | length | 17 | 5.9 | 1.5 - 14.0 | -1.0 | 1.4 |
| | width | 17 | 2.7 | 1.1 - 5.3 | -0.6 | 1.3 |
| | height | 17 | 3.7 | 1.2 - 6.5 | -0.8 | 1.2 |
| Choroid plexus | length | 11 | 5.1 | 1.2 - 12.0 | -0.9 | 1.5 |
| of the lateral ventricles | width | 12 | 2.2 | 0.7 - 4.0 | -0.6 | 0.9 |
| | height | 12 | 2.7 | 0.4 - 4.9 | -0.6 | 0.7 |
| Diencephalon | length | 17 | 3.9 | 2.1 - 6.1 | -1.4 | 1.0 |
| | width | 17 | 1.2 | 0.9 - 1.9 | -0.4 | 0.4 |
| | height | 17 | 2.2 | 1.0 - 3.4 | -0.5 | 0.7 |
| Mesencephalon | length | 17 | 3.9 | 2.4 - 5.5 | -0.4 | 0.9 |
| | width | 17 | 1.7 | 1.2 - 2.4 | -0.5 | 0.6 |
| | height | 17 | 1.9 | 1.2 - 2.8 | -0.8 | 0.7 |
| Rhombencephalon | length | 40 | 4.3 | 2.1 - 6.2 | -1.1 | 1.2 |
| | width | 40 | 4.0 | 1.8 - 7.1 | -1.2 | 1.2 |
| | depth | 40 | 2.6 | 0.9 - 3.6 | -0.7 | 0.7 |
| Cerebellum | width | 31 | 6.6 | 4.1 - 10.0 | -1.1 | 1.7 |
| | height | 31 | 1.7 | 0.7 - 2.6 | -0.5 | 0.6 |
| Choroid plexus | width | 29 | 3.6 | 2.3 - 6.4 | -0.9 | 1.3 |
| of the $4^{th}$ ventricle | height | 29 | 0.9 | 0.6 - 2.0 | -0.5 | 0.5 |

## 5.4 3D anatomic and volumetric evaluation

The steps from the original 2D image, to 3D data acquisition and to different 3D visualization modes are shown in Figures 2 A – I in the appendix.

### 5.4.1 Volume of brain cavities (pilot study)

The volumes of the brain cavities expressed in cubic millimeters ($mm^3$) are presented in Table 5.4.1. In this pilot study, volume estimations were neither tested for their validity nor adjusted for the point spread function.

**Table 5.4.1** The estimated volumes of the brain cavities in three specimens (pilot study).

| Cavity | CRL 13 mm | CRL 24 mm | CRL 40 mm |
|---|---|---|---|
| | Volume | | |
| | $mm^3$ | $mm^3$ | $mm^3$ |
| Hemispheres (both) | 2 | 97 | 451 |
| Diencephalon | 3 | 9 | – |
| Mesencephalon | 2 | 15 | 21 |
| Rhombencephalon | 17 | 58 | 85 |

### 5.4.2 Volume of embryonic/fetal bodies and brain cavities

The range of the estimated volumes of the bodies and brain cavities varied from 0.8 $mm^3$ volume of the cavities of the hemispheres in an embryo of 9.3 mm CRL to 4987.6 $mm^3$ body volume of the largest specimen (CRL 39 mm) (Paper VI).

In table 5.4.2 the estimated mean volumes of the brain compartments, the brain and body ($mm^3$) in correlation to the CRL (mm) are shown. The volumes of the cavities of the hemispheres (cubic root transformation), of the total brain cavities and of the bodies (square root transformation) increased exponentially with the embryonic/fetal length (CRL). The best fit of the data for the diencephalic, the mesencephalic and rhombencephalic cavities were square root transformations. The diencephalic cavity increased until the embryos had reached a size of approximately 25 mm CRL. In larger embryos and fetuses, the cavities became smaller. The mesencephalic cavity (future Sylvian aqueduct) increased its volume slightly throughout the first trimester. The rhombencephalic cavity reached its maximal volume at the end of the embryonic period (CRL $\approx$ 30 mm).

**Table 5.4.2** The mean estimated volumes ($mm^3$) of brain cavities and embryonic/fetal bodies in relation to the embryonic/fetal CRL (mm).

| CRL | Hemispheres | Diencephalon | Mes-encephalon | Rhomb-encephalon | Brain, total | Body |
|---|---|---|---|---|---|---|
| mm | $mm^3$ | $mm^3$ | $mm^3$ | $mm^3$ | $mm^3$ | $mm^3$ |
| 10 | 0.6 | 1.7 | 1.1 | 7.3 | 5.3 | 97.8 |
| 15 | 6.8 | 4.4 | 3.6 | 13.3 | 25.6 | 407.0 |
| 20 | 26.2 | 6.7 | 6.6 | 18.8 | 61.2 | 925.0 |
| 25 | 66.1 | 7.6 | 9.3 | 22.6 | 112.1 | 1655.5 |
| 30 | 134.1 | 6.8 | 11.4 | 23.9 | 178.3 | 2562.7 |
| 35 | 239.0 | 4.5 | 12.3 | 22.5 | 260.4 | 3803.5 |
| 39 | 351.2 | 2.4 | 12.2 | 19.6 | 336.1 | 4822.4 |

### 5.4.3 Comments concerning volumetric evaluation

#### 5.4.3.1 Validity of volume estimations

Volume reconstructions of large structures have been tested in-vitro and in-vivo (Gilja *et al.*, 1994; Gilja, 1995; Riccabona *et al.*, 1995; Thune *et al.*, 1996). For volume estimations of small geometrical reconstructions, even small errors in the surface-setting (segmentation) would lead to alterations of the volume estimates. In the test series (Paper VI) we found a relatively high percentage error (mean 15.6%, SE 9.1) in the volume estimation of the test objects of less than 500 $mm^3$. We believe that this error was due to the surface setting in the segmentation procedure, and we may assume that the volumes of embryos up to 17 mm CRL (less than 500 $mm^3$) became overestimated, while the volumes of all brain cavities may represent underestimations. The volume estimations of the embryos of 17 mm CRL and more ($\geq$ 500 $mm^3$) were assumed to be good because the percentage error in the test series was mean - 0.2%, with an acceptable SE of 5.0. In a study on 3D ultrasound measurements of ovarian follicles aspirate volumes (range 1000 $mm^3$ - 14800 $mm^3$) were compared with volumes estimated from 3D ultrasound (range 750 $mm^3$ - 14670 $mm^3$) (Kyei-Mensah *et al.*, 1996). The mean percentage error was -3.3% (range 13% to -26%, SE 9.1), in other words the 3D volume estimates tended to underestimate the fluid volume. One possible source of error for this difference might lie in the segmentation process.

#### 5.4.3.2 Body

The difference between the fetal weight in grams and the volume in cubic millimeters is less than 2% (Meban, 1983). We compared the volumes of the body with measurements of embryos/fetuses with a corresponding size (CRL ≤ 40 mm) from two other studies (Streeter, 1920; Jirásek *et al.*, 1966). The regression curves were best fitted by a square root transformation in all three studies. The regression curve from Streeter's study lay slightly above, while that from Jirásek's study lay a little below the mean curve from our volume estimations. The comparison of these different studies involved several possible biases. Streeter's material had both fresh and formalin-fixed specimens, where the latter were markedly heavier and longer (Streeter, 1920). In addition, the largest fetuses in Streeter's group were reported to be flexed, in other words the true CRL might have been larger. It is known that in-vivo ultrasound measurements of the CRL are not completely comparable with post abortem measurements (Drumm and O'Rahilly, 1977). Thus, the condition of the embryos/fetuses in the different studies is not uniform. This may affect the course of the curves.

#### 5.4.3.3 Brain cavities

Assuming that the mesencephalic cavity has a cylindrical shape, the volume could be calculated by the formula «$\pi r^2$ x length». The embryos in O'Rahilly and Müller's study (O'Rahilly and Müller, 1990) (Carnegie stage 23 ≈ 10 weeks 0 days ≈ CRL 30 mm) would then have a mean volume of 15 $mm^3$ based on the indicated measurements from graphic reconstructions, or 23 $mm^3$ based on values corrected for shrinkage, while the mean volume of the mesencephalic cavity at 10 weeks-0 days in a 2D ultrasound study was only 7.4 $mm^3$ (Paper I). In the present study the mean volume in embryos/fetuses of 30 mm CRL was calculated to be 11.0 $mm^3$, thus, as stated by embryologists (O'Rahilly and Müller, 1990) this cavity was in no sense a narrow aqueduct during the first trimester. While shifting posteriorly, the rhombencephalic cavity shortened in the sagittal section. Already in 1890, His demonstrated the changes of the pontine flexure with a decreasing angle in older fetuses (His, 1890). The growth of the cerebellar hemispheres further restricted the volume of the fourth ventricle, such that the rhombencephalic cavity did not increase in volume in spite of the rapid growth of the brain. In a previous study, the volumes of the lateral ventricles were estimated by the formula of two ellipsoids and the rhombencephalic cavity by the formula of a pyramid (Paper II). The sonographic 3D reconstructions of the lateral ventricles in the present study were in the range of the estimated values from the 2D study; the 3D reconstructions of the rhombencephalic cavity in the present study were significantly larger than the range of the estimated values from

the 2D study, where the measurements of the width involved only the main part of the fourth ventricle, not the lateral recesses. The size of the diencephalic cavity has not been measured before. Through the growth of the dorsal and ventral thalami the lateral walls of this cavity narrow, giving it a slit-like shape. This explains the decreasing volume of the cavity in the older specimens of the present study where only part of the third ventricle was discernible - this was between the dorsal thalamus and the mesencephalon, which is the region near the pineal gland. According to embryologists, the recess of the pineal region and near the infundibulum are distinct in older fetuses (Kostovic, 1990).

Nearly 80 years ago, Jenkins carried out a volumetric study of the developing brain (Jenkins, 1921). Only two of his specimens had a size comparable with the specimens in the 3D study (CRL 16 mm and 25 mm), with the volume of the brain calculated to be 41 $mm^3$ and 126 $mm^3$ respectively. In the present study, the mean volume of the brain cavities in embryos of 16 mm CRL was 37 $mm^3$, and in embryos of 25 mm CRL it was 112 $mm^3$; this must be considered to be in agreement with Jenkins' measurements. Jenkins also looked at the percent growth of the brain compartments, finding a larger share of the diencephalon and the mesencephalon than in the present study. At the same time he found a less marked shift of the share of the telencephalon and the rhombencephalon between the 16 mm and the 25 mm embryo than was shown in the present study.

#### 5.4.3.4 Carnegie staging system

In the Carnegie staging system of classical human embryology, embryos are classified according to the external form and the analysis of the organ system development by light microscope, as summarized in 'Developmental stages in human embryos', and «hence are not directly dependent on either chronological age or on size» (O'Rahilly and Müller, 1987). Such an exact staging by ultrasound is not possible, but an approximate estimation of the stages in the embryos of the present study could be made by comparing the external form of the body and the limbs and the casts of the brain cavities with descriptions from the embryological literature (O'Rahilly and Müller, 1987; O'Rahilly and Müller, 1994) (Table 5.4.3.4).

**Table 5.4.3.4** The distribution of the embryos and fetuses according to the Carnegie staging system

| Carnegie stage | Number of embryos/fetuses | Crown-rump length range (mm) |
|---|---|---|
| 16 | 6 | 9.3 – 12.8 |
| 17 | 5 | 13.5 – 14.8 |
| 18 | 4 | 16.4 – 17.7 |
| 19 | 2 | 19.5 – 19.7 |
| 20 | 4 | 20.4 – 21.0 |
| 21 | 2 | 22.3 – 23.6 |
| 22 | 2 | 25.0 – 26.4 |
| 23 and older | 9 | ≥ 29.0 |

## 5.5 Description of the sonoanatomic development (synopsis)

The studies (Papers I-VI) described embryos and fetuses from about 7 weeks of gestation to 12 weeks of gestation.

### 5.5.1 Gestational age, 7 weeks 0-6 days, CRL 9-14 mm

External form: Sonographically, the embryonic body appeared as a triangle in the sagittal section (Figure 1 A in appendix). The sides consisted of 1) the back, 2) the roof of the rhombencephalon, and 3) the frontal part of the head, the basis of the umbilical cord, and the embryonic tail. The embryonic body was slender in the coronal plane. The limbs were short, paddle-shaped outgrowths.

CNS: The hypoechogenic brain cavities could be identified, including the separated cerebral hemispheres (Figures 1 A, A1 & A2 in appendix). The lateral ventricles were shaped like small round vesicles. The cavity of the diencephalon (future third ventricle) ran posteriorly. In the smallest embryos, the medial telencephalon formed a continuous cavity between the lateral ventricles. The future foramina of Monro were wide during week seven. In the sagittal plane, the height of the cavity of the diencephalon (future third ventricle) was slightly greater than that of the mesencephalon (future Sylvian aqueduct). Thus, the wide border between the cavities of the diencephalon and the mesencephalon was indicated. The curved tube-like mesencephalic cavity (future Sylvian aqueduct) lay anteriorly, its rostral part pointing caudally. It straightened considerably during the

following weeks. By week eight it was regularly identified. The rather broad and shallow rhombencephalic cavity was always visible from 7 weeks 0 days on. It then had a well-defined rhombic shape in the cranial pole of the embryo.

The 3D studies confirmed the previously described features. In these studies the brain cavities were easily delineated in all embryos: The lateral ventricles were small evaginations located lateral and rostral from the cavity of the diencephalon. The cavity of the diencephalon continued directly into that of the mesencephalon. The isthmus rhombencephali represented the connection to the rhombencephalic cavity and future fourth ventricle. The cavity of the rhombencephalon was located superior in the head. In the smallest embryos (CRL 9.3 mm - 17.0 mm), the rather broad and shallow rhombencephalic cavity lay on top, representing the largest brain cavity. The future spine appeared as two parallel lines.

Heart: The heart could easily be recognized by real-time ultrasound as a relatively large beating structure below the embryonic head at seven weeks. It was large and bright, the frequency increasing from 130 bpm to 160 bpm. Details of the heart anatomy were not depictable, but the atrial and the ventricular compartments could sometimes be distinguished by the reciprocal movements of the walls (Paper III).

Intestinal tract: The short umbilical cord showed a large coelomic cavity at its insertion, where the primary intestinal loop could be identified. The initial sign of the herniation of the gut occurred during week seven as a thickening of the cord containing a slight echogenic area at the abdominal insertion. Within a few days this echogenic structure became more distinct.

Extra-embryonic structures: The mean diameter of the amniotic cavity had a value which is approximately identical with the corresponding CRL.

### 5.5.2 8 weeks 0-6 days, CRL 15-22 mm

External form: The body gradually grew thicker and became cuboidal. At the end of the week, the elbows became obvious, the hands angled from the sagittal plane and the fingers were distinguishable.

CNS: The brain cavities were easily seen as large 'holes' in the embryonic head. The hemispheres enlarged, developing via thick round slices originating antero-caudally from

the third ventricle into a crescent shape. The choroid plexus in the lateral ventricles became visible as tiny echogenic areas. The future foramina of Monro became more accentuated during week eight. The third ventricle was still rather wide, as was the mesencephalic cavity. Now, the mesencephalon lay on top of the head. The increased growth of the rostral brain structures and the deepening of the pontine flexure lead to the deflection of the brain. The rhombencephalic cavity (future fourth ventricle) had a pyramid-like shape with the central deepening of the pontine flexure as the peak of the pyramid. The first signs of the bilateral choroid plexuses were lateral echogenic areas originating near the branches of the medulla oblongata caudal to the lateral recesses. Within a short time the choroid plexuses traversed the roof of the fourth ventricle, meeting in the midline and dividing the roof into two portions, about two thirds were located rostrally and one third caudally. In the sagittal section, the choroid plexuses were identified as an echogenic fold of the roof.

3D studies: The lateral ventricles gradually changed shape from small round vesicles (CRL 9.3 mm - 13.6 mm) via thick round slices originating antero-caudally from the third ventricle (CRL 14.6 mm - 17.7 mm) into the crescent shape of the larger embryos (CRL $\geq$ 20.4 mm). The largest volume of the future third ventricle (11.7 $mm^3$) was found in an embryo with 20.5 mm CRL. The future foramina of Monro became distinct in embryos of 19.5 mm CRL. The transition from the third ventricle to the mesencephalic cavity and to the lateral ventricles was wide in the early embryos. The cavity of the mesencephalon was relatively large in all embryos/fetuses. With the increasing size of the specimen, the mesencephalic cavity changed its position, and was found posterior in the large fetuses. The rhombencephalic cavity deepened gradually with the growth of the embryos, at the same time decreasing its length. Its position in the head changed with the increasing size of the specimen, moving posteriorly (CRL 17 mm and larger). The rhombencephalic cavity (future fourth ventricle) had a pyramid-like shape with the central deepening of the pontine flexure as the peak of the pyramid.

Heart: Occasionally it was possible to identify the atrial and ventricular walls moving reciprocally as early as at the end of week eight. The atrial compartment appeared wider than the ventricular compartment, and the heart covered about 50% of the transverse thoracic area. A kind of 4-chamber view of the heart could then be obtained, where the atrial compartment was wider than the ventricular part (Paper III).

Intestinal tract: It was possible to recognize the fluid filled stomach as a small

hypoechogenic area on the left side of the upper abdomen below the heart in a total of 88 examinations. There was no sign of the stomach during week seven (25 examinations). In 31% it could be identified at the end of week eight.

### 5.5.3 9 weeks 0-6 days, CRL 23-31 mm

External form: The body developed an ellipsoid shape with a large head. The foot soles touched in the midline at the end of the week. At the same time it was possible to obtain acceptable images of the profile, thus, it should be possible to examine the mouth. The ventral body wall was well defined.

CNS: The lateral ventricles were always visible. They were best seen in the parasagittal plane, where the C-shape became apparent. The cortex was smooth and hypoechogenic. The bright choroid plexuses of the lateral ventricles were regularly detectable at 9 weeks 4 days (Figure 1 B in appendix). They showed rapid growth, similar to the hemispheres, and soon filled most of the ventricular cavities.

The width of the diencephalic cavity narrowed gradually while the width of the mesencephalon remained wide. A distinct border ("isthmus prosencephali") had developed between the cavity of the mesencephalon and the third ventricle. The wall of the diencephalon, initially very thin, thickened considerably starting from week eight to nine.

The isthmus rhombencephali was always distinct. The cavity of the mesencephalon remained relatively large (Figure 1 C in appendix), especially the posterior part. The height and the width were about the same size.

During weeks eight and nine, the rhombic fossa became deeper due to the progressive flexure of the pons (Figure 1 C in appendix). The lateral corners of the rhombencephalic cavity, called the lateral recesses, were easily identified at seven and eight weeks. During this period the distance between these recesses increased (rhombencephalon width). Later, during weeks nine and ten, the lateral recesses often became covered by the enlarging cerebellar hemispheres. Thus only the central part of the hypoechogenic fourth ventricle, which was divided by the choroid plexuses, was visible. The choroid plexuses of the fourth ventricle were bright landmarks dividing the ventricle into a rostral and caudal compartment. The cerebellar hemispheres were easily detectable. The primordia of cerebellar hemispheres were clearly separated in the midline during the embryonic period.

3D studies: The size of the lateral ventricles increased rapidly (Figure 2 H in appendix). While the third ventricle was still relatively wide at the beginning of this week, its antero-medial part narrowed during this week due to the growth of the thalami. In the fetuses of 25 mm CRL and more there was a clear gap between the rhombencephalic and the mesencephalic cavity due to the growing cerebellum (Figure 2 H in appendix). The isthmus rhombencephali was narrow; in most cases it was not visible in its complete length. The cavity of the diencephalon decreased in the larger embryos and the fetuses (CRL ≥ 25 mm), and became narrow especially at its upper anterior part. The spine was still characterized by two echogenic parallel lines.

Heart: During week 9 the heart rate reached a maximum of mean 175 bpm.

Intestinal tract: From 8 weeks 3 days to 10 weeks 4 days of gestational age all embryos had herniation of the midgut, most distinctive during weeks 9 and 10. At this stage the midgut herniation was presented as a large hyperechogenic mass. The stomach could be detected in 76% of the embryos before 10 weeks 0 days.

### 5.5.4 10 weeks 0-6 days, CRL 32-42 mm, and 11 weeks 0-6 days, CRL 43-54 mm

Early postembryonic period

External form: The human features of the fetus became clearer. In the largest fetuses the soles of the feet rotated from the sagittal plane. The head was still relatively large with a prominent forehead and a flat occiput. The future skull could be distinguished; ossification starts at about 11 weeks with the occipital bone (Zalen-Sprock *et al.*, 1997). 3D: The fetal body elongated, the arms and the legs were developed into upper and lower arms and legs, the hands and fingers and the feet and toes.

CNS: The thick crescent lateral ventricles filled the anterior part of the head and concealed the diencephalic cavity. The thickness of the cortex was about 1 mm at the end of the first trimester. The diencephalon lay between the hemispheres, and the mesencephalon gradually moved towards the center of the head. After an initial increase, the width of the third ventricle became narrow towards the end of the first trimester. The cerebellar hemispheres seemed to meet in the midline during weeks 11 to 12. After 10 weeks 3 days the choroid plexuses of the fourth ventricle could always be visualized. The distance between the choroid plexuses and the cerebellum became shorter during weeks 9 to 11. At the end of the first trimester the choroid plexuses were found close to the caudal border of

the cerebellum. Due to the cerebellar growth, the choroid plexuses approached the caudal border of the cerebellum. Successively the ossification of the spine appeared.

In the 3D pilot study, the lateral ventricles dominated the brain in the fetus of 40 mm CRL. The cavity of the diencephalon was too narrow to be outlined correctly on the 2D images. Both rostrally and caudally, the cavity of the mesencephalon was connected to the neighboring cavities by narrow isthmuses. The cavities of the mesencephalon and rhombencephalon were located posteriorly, while the cavities of the hemispheres occupied the anterior and superior part of the head. The 3D study showed that the thick crescent lateral ventricles filled the anterior part of the head and concealed the diencephalic cavity, which became smaller. The gap between the mesencephalic and the rhombencephalic cavity filled with the growing cerebellum became clear.

Heart: At 10 weeks the moving valves and the interventricular septum could be identified. The heart rate slowed down to 165 bpm at the end of week 11. The ventricles, atria, septa, valves, veins and outflow tracts became identifiable.

Intestinal tract: The midgut herniation had its maximal extension at the beginning of week 10, it returned into the abdominal cavity during weeks 10 to 11. The gut retracted into the abdominal cavity between 10 weeks 4 days and 11 weeks 5 days. Fetuses which were older than 11 weeks 5 days did not demonstrate any sign of the herniation. The esophagus could be identified as an echogenic double line anterior to the aorta, leading into the stomach. The stomach was visible in all specimens before 11 completed weeks.

# 6 Conclusion

1. It was possible to describe the anatomy of the embryo and its organs longitudinally from week seven on.

2. Measuring the embryo, its organs and associated structures made it possible to consider their dimensions such that the development could be followed longitudinally. At week seven all brain compartments were visible. The first sign of the midgut herniation appeared during week seven. The choroid plexuses, the cerebellum, the stomach and the heart chambers became visible during week eight. The other structures could all be evaluated from seven weeks on.

3. The embryos and their associated structures showed virtually identical growth velocities. The growth of the yolk sac mirrored its development with uniform growth until 10 weeks when it degenerated either by shrinking or by enlarging before dissipating; the alteration of the shape is believed to reflect the cessation of the physiological function at that time.

   The clear spread of the parallel growth curves between the individuals varied more than expected. This may have been due to a discrepancy between the LMP-based age and the true age, caused by variations of the time of ovulation, fertilization and nidation, and/or of the growth at very early stages. Once the growth velocity picked up, the embryos seemed to follow the same growth curve.

4. The development of the size of the specimens and the shape both of the body and the brain cavities showed good agreement with images from the embryological literature. The in-vivo 2D and 3D ultrasound findings were in agreement with the descriptions and the «developmental time schedule» of human embryos as described in the Carnegie staging system (O'Rahilly and Müller, 1987).

5. A remarkable uniformity of the development could be registered: Specimens of the same size (CRL) looked virtually identical. The developmental degree and the size of the organs and the relative proportions of these structures to each other were similar in embryos of the same size.

# 7 Future aspects

During recent years, the use of high frequency transvaginal scanning has significantly contributed to the development of sonoembryology, introducing a new area in the use of ultrasound in the early pregnancy. It has become possible to produce ultrasound images with such a quality that the interest has gone beyond the practical diagnostic use towards the use of sonoembryology as a research tool in the basic evaluation of the growing embryo. The embryo can now be followed in vivo and be displayed in both two and three dimensions; these techniques will undoubtedly aid future embryological research. The overview of normal embryological development gives an idea of the manifold dramatic processes that take place during the first trimester. High frequency transvaginal ultrasound will help disclose developmental disorders of the embryo and the early fetus, a technique which already has become invaluable for women with increased risk of hereditary conditions.

There is no reason to believe that the technological development of ultrasound has reached its end-point or even come close to it. An increase of the transmitted ultrasound frequency is to be expected, which additionally will increase the resolution. There is reason to believe the 3D technique, too, will be developed and have practical use in the evaluation of the early pregnancy. Computer technology will be increasingly used to handle the pre- and postprocessing of ultrasound imaging.

We do not know all about the natural history of the development of malformations. Classical embryologists were dependent on the accidental assignments of aborted malformed embryos and fetuses to study abnormal human development. Now, with high-frequency 2D and 3D ultrasound we are able to study the living human embryo longitudinally, and to describe the development and maldevelopment of organs. This may imply a major development in the field of human embryology .

## 8 References


Abramovich, D. R. (1981). Interrelation of fetus and amniotic fluid. *Obstet Gynecol Annu*, 10:27–43.

Abramovich, D. R. (1968). The volume of amniotic fluid in early pregnancy. *J Obstet Gynaecol Br Cwlth*, 75:728–31.

Achiron, R. & Achiron, A. (1991). Transvaginal ultrasonic assessment of the early fetal brain. *Ultrasound Obstet Gynecol*, 1:336–44.

Achiron, R. & Tadmor, O. (1991). Screening for fetal anomalies during the first trimester of pregnancy: transvaginal versus transabdominal sonography. *Ultrasound Obstet Gynecol*, 1:186–91.

Achiron, R., Rotstein, Z., Lipitz, S., Mashiach, S. & Hegesh, J. (1994). First-trimester diagnosis of fetal congenital heart disease by transvaginal ultrasonography. *Obstet Gynecol*, 84:69–72.

AIUM/NEMA. (1992). Standard for real-time display of thermal and mechanical acoustic output indices on diagnostic ultrasound equipment. Rockville Maryland: AIUM, 1992.

Altman, D. G. (1991). Preparing to analyse data. In *Practical Statistics for Medical Research*, ed. D. G. Altman. London: Chapman and Hall, 1991, pp. 122–45.

Altman, D. C. & Chitty, L. S. (1993). Design and analysis of studies to derive charts of fetal size. *Ultrasound Obstet Gynecol*, 3:378–84.

Angelsen, B. A. J., Editor (1996). *Waves, signals and signal processing in medical ultrasound, Vol. 1*. Trondheim: Dep Biomedical Engineering.

Ashhurst, D. E. (1997). Assessing skeletal development. *Ultrasound Obstet Gynecol*, 9:373.

Baba, K., Satoh, K., Sakamoto, S., Okai, T. & Ishii, S. (1989). Development of an ultrasonic system for three-dimensional reconstruction of the fetus. *J Perinat Med*, 17:19–24.

Baba, K. & Okai, T. (1997). Basis and principles of three-dimensional ultrasound. In *Three-dimensional ultrasound in obstetrics and gynecology*, ed. K. Baba & D. Jurkovic. London: Parthenon Publisher, 1997, pp. 1–19.

Bang, J. & Holm, H. H. (1968). Ultrasonics in the demonstration of fetal heart movements. *Am J Obstet Gynecol*, 102:956–60.

Bartelmez, G. W. & Dekaban, A. S. (1962). The early development of the human brain. *Contr Embryol Carnegie Instn*, 253:13–32.

Baum, G., Chester, P. & Greenwood, I. (1961). Orbital lesion localization by three dimensional ultrasonography. *New York State J Med*, Dec 15:4149–57.

Bell, E. T. & Loraine, J. A. (1965). Time of ovulation in relation to cycle length. *Lancet*, 1:1029–30.

Bland, J. M. & Altman, D. G. (1986). Statistical methods for assessing agreement between two methods of clinical measurement. *Lancet*, 1:307–10.

Blumenfeld, Z., Rottem, S., Elgali, S. & Timor-Tritsch, I. E. (1988). Transvaginal sonographic assessment of early embryological development. In *Transvaginal sonography*, ed. I. E. Timor-Tritsch & S. Rottem. London: Heinemann Medical Books, 1988, pp. 87–108.

Bom, N., Lancée, C., Honkoop, J. & Hugenholtz, P. (1971). Ultrasonic viewer for cross-sectional analysis of moving cardiac structures. *Biomed Eng*, 6:500–8.

Bonilla-Musoles, F. M., Raga, F., Osborne, N. & Blanes, J. (1995). The use of three-dimensional (3D) ultrasound for the study of normal and pathologic morphology of the human embryo and fetus: preliminary report. *J Ultrasound Med*, 14:757–65.

Bonilla-Musoles, F. (1996). Three-dimensional visualization of the human embryo: a potential revolution in prenatal diagnosis (Editorial). *Ultrasound Obstet Gynecol*, 7:393–7.

Born, G. (1883). Die Plattenmodellirmethode. *Arch Mikr Anat*, 22:584–99.

Bowerman, R. A. (1993). Sonography of fetal midgut herniation: Normal size criteria and correlation with crown-rump length. *J Ultrasound Med*, 5:251–4.

Boyden, E. A., Cope, J. G. & Bill, A. H. (1967). Anatomy and embryology of congenital intrinsic obstruction of the duodenum. *Am J Surg*, 114:190–202.

Bree, R. L. & Marn, C. S. (1990). Transvaginal sonography in the first trimester: embryology, anatomy, and hCG correlation. *Semin Ultrasound CT MRI*, 11:12–21.

Brinkley, J. F., Moritz, W. E. & Baker, D. W. (1978). A technique for imaging three-dimensional structures and computing their volumes using non-parallel ultrasonic sector scans. *Ultrasonics in Medicine*, 4:471–4.

Brinkley, J. F., McCallum, W. D., Muramatsu, S. K. & Liu, D. Y. (1982). Fetal weight estimation from ultrasonic three-dimensional head and trunk reconstructions: Evaluation in vitro. *Am J Obstet Gynecol*, 144:715–21.

Brinkley, J. F. (1984). *Ultrasonic three-dimensional organ modelling*. Thesis, Stanford University.

Bronshtein, M., Yoffe, N., Brandes, J. M. & Blumenfeld, Z. (1990). First and early second trimester diagnosis of fetal urinary tract anomalies using transvaginal sonography. *Prenat Diagn*, 10:653–66.

Bronshtein, M., Siegler, E., Eshcoli, Z. & Zimmer, E. Z. (1992). Transvaginal ultrasound measurements of the fetal heart at 11 to 17 weeks of gestation. *Am J Perinatol*, 9:38–42.

Brown, D. L., Emerson, D. S., Shulman, L. P. & Carson, S. A. (1989). Sonographic diagnosis of omphalocele during 10th week of gestation. *Am J Roentgenol*, 153:825–26.

Callagan, D. A., Rowland, T. C. & Goldman, D. E. (1964). Ultrasonic Doppler observation of the fetal heart. *Obstet Gynecol*, 23:637.

Campbell, S. (1969). The prediction of fetal maturity by ultrasonic measurement of the biparietal diameter. *J Obstet Gynaecol Br Cwlth*, 76:603–9.

Campbell, S. (1975). Ultrasonic measurements of fetal abdomen circumference in the estimation of fetal weight. *Br J Obstet Gynaecol*, 82:689–97.

Campbell, S. & Thoms, A. (1977). Ultrasound measurement of the fetal to abdominal circumference ratio in the assessment of growth retardation. *Br J Obstet Gynaecol*, 84:165–74.

Chitty, L. S., Altman, D. G., Henderson, A. & Campbell, S. (1994a). Charts of fetal size: 2. Head measurements. *Br J Obstet Gynaecol*, 101:35–43.

Chitty, L. S., Altman, D. G., Henderson, A. & Campbell, S. (1994b). Charts of fetal size: 3. Abdominal measurements. *Br J Obstet Gynaecol*, 101:125–31.

Clark, E. B. (1985). Ventricular function and cardiac growth in the chick embryo. In *Cardiac Morphogenesis*, ed. R. G. Ferrans VJ, Weinstein C. New York: Elsevier, 1985, pp. 238–44.

Cullen, M. T., Green, J., Whetham, J., Salafia, C., Gabrielli, S. & Hobbins, J. (1990). Transvaginal ultrasonographic detection of congenital anomalies in the first trimester. *Am J Obstet Gynecol*, 163:466–76.

Curie, J. & Curie, P. (1880). Développement, par pression, de l'électricité polaire dans les cristaux hémièdres à faces inclinées. *Compt Rend*, 91:294–5.

Cyr, D. R., Mack, L. A., Schoenecker, S. A., Patten, R. M., Shephard, T. H., Shuman, W. P. & Moss, A. A. (1986). Bowel migration in the normal fetus: Ultrasound detection. *Radiology*, 161:119–21.

Cyr, D. R., Mack, L. A., Nyberg, D. A., Shepard, T. H. & Shuman, W. P. (1988). Fetal rhombencephalon: normal US findings. *Radiology*, 166:691–2.

Dalecki, D., Child, S. Z., Raeman, C. H., Cox, C., Penney, D. P. & Carstensen, E. L. (1997). Age dependence of ultrasonically-induced lung hemorrhage in mice. *Ultrasound Med Biol*, 23:767–76.

Davis, C. L. (1927). Development of the human heart from its first appearance to the stage found in embryos of twenty paired somites. *Contrib Embryol Carneg Inst*, 19:245–84.

Day, R. W. (1959). Casts of foetal lateral ventricles. *Brain*, 82:109–15.

Daya, S. (1993). Accuracy of gestational age estimation by means of fetal crown-rump length measurements. *Am J Obstet Gynecol*, 168:903–8.

Desmond, M. E. & Jacobson, A. G. (1977). Embryonic brain enlargement requires cerebrospinal fluid pressure. *Dev Biol*, 57:188–98.

deVries, P. A. & Saunders, J. B. d. C. H. (1962). Development of the ventricles and spiral outflow tract in the human heart. *Contrib Embryol Carneg Inst*, 37:87–114.

deVries, P. A. & Friedland, G. W. (1974). The staged sequential development of the anus and rectum in human embryos and fetuses. *J Pediatr Surg*, 9:755-69.

Diamant, N. E. (1985). Development of esophageal function. *Am Rev Respir Dis*, 131:29–32.

Dickey, R. P. & Gasser, R. F. (1993). Ultrasound evidence for variability in the size and development of normal human embryos before the tenth post-insemination week after assisted reproductive technologies. *Hum Reprod*, 8:331–7.

Donald, I., MacVicar, J. & Brown, T. G. (1958). Investigation of abdominal masses by pulsed ultrasound. *Lancet*, 1:1188–95.

Donald, I. & Brown, T. G. (1961). Demonstration of tissue interfaces within the body by ultrasonic echo sounding. *Br J Radiol*, 34:539–46.

Donald, I. (1964). Ultrasonography in two dimensions. *Med Biol Illustr*, 14:216–24.

Doody, C. (1997). Heating fetal bone. *BMUS Bulletin*, 5:16–18.

Drumm, J. E., Clinch, J. & MacKenzie, G. (1976). The ultrasonic measurement of fetal crown-rump length as a method of assessing gestational age. *Br J Obstet Gynaecol*, 83:417–21.

Drumm, J. E. & O'Rahilly, R. (1977). The assessment of prenatal age from the crown-rump length determined ultrasonically. *Am J Anat*, 148:555–60.

DuBose, T. J., Cunyus, J. A. & Johnson, L. F. (1990). Embryonic heart rate and age. *J Diagn Med Sonogr*, 6:151–7.

Duck, F. A. & Martin, K. (1991). Trends in diagnostic ultrasound exposure. *Phys Med Biol*, 38:1423–32.

Duncker, H.-R. (1990). Respirationstrakt. In *Humanembryologie*, ed. K. V. Hinrichsen. Berlin: Springer-Verlag, 1990, pp. 571–606.

Dussik, K. T. (1942). Über die Möglichkeit, hochfrequente mechanische Schwingungen als diagnostisches Hilfsmittel zu verwenden. *Z Ges Neurol Psychol*, 174:153–68.

ECMUS. (1999). Clinical safety statement for diagnostic ultrasound (Tours 1998). *Eur J Ultrasound*, submitted for publication.

Edler, I. & Hertz, H. (1954). The use of ultrasonic reflectoscope for the continuous recording of the movements of heart walls. *Kungl Fysiogr Sällskap I Lund Förhandl*, 24:1–19.

EFSUMB. (1984). Radiation Safety Committee: Clinical safety statement. *EFSUMB Newsletter*:4.

Eik-Nes, S. H., Grøttum, P., Persson, P.-H. & Marsál, K. (1982). Prediction of fetal growth deviation by ultrasound biometry. I. Methodology. *Acta Obstet Gynecol Scand*, 61:53–8.

England, M. A. (1988). Normal development of the central nervous system. In *Fetal and neonatal neurology and neurosurgery*, ed. M. I. Levene, M. J. Bennett & J. Punt. Edinburgh: Churchill Livingstone, 1988, pp. 3–27.

Ertzeid, G., Storeng, R. & Lyberg, T. (1993). Treatment with gonadotropins impaired implantation and fetal development in mice. *J Assisted Reprod Genet*, 10:286–91.

Evans, J. (1991). Fetal crown-rump length values in the first trimester based upon ovulation timing using the luteinizing hormone surge. *Br J Obstet Gynaecol*, 98:48–51.

Fujiwaki, R., Hata, T., Hata, K. & Kitao, M. (1995). Intrauterine ultrasonographic assessments of embryonic development. *Am J Obstet Gynecol*, 173:1770–4.

Geirsson, R. T. (1997). Ultrasound: the rational way to determine gestational age. *Fetal Matern Med Rev*, 9:133–46.

Gilja, O. H., Thune, N., Matre, K., Hausken, T., Ødegaard, S. & Berstad, A. (1994). In vitro evaluation of three dimensional ultrasonography in volume estimation of organs. *Ultrasound Med Biol*, 20:157–65.

Gilja, O. H. (1995). In vivo comparison of 3D ultrasonography and magnetic resonance imaging in volume estimation of human kidneys. *Ultrasound Med Biol*, 21:25–32.

Goldstein, I., Zimmer, E. A., Tamir, A., Peretz, B. A. & Paldi, E. (1991). Evaluation of normal gestational sac growth: Appearance of embryonic heartbeat and embryo body movements using the transvaginal technique. *Obstet Gynecol*, 77:885–8.

Goldstein, H. (1995). *Multilevel Statistical Models, Vol. 3: Kendall's Library of Statistics*. London: Edward Arnold.

Green, J. J. & Hobbins, J. C. (1988). Abdominal ultrasound examination of the first-trimester fetus. *Am J Obstet Gynecol*, 159:165–75.

Grisiola, G., Milano, V., Pilu, G., Banzi, C., David, C., Gabrielli, S., Rizzo, N., Morandi, R. & Bovicelli, L. (1993). Biometry of early pregnancy with transvaginal sonography. *Ultrasound Obstet Gynecol*, 3:403–11.

Hamilton, W. J. & Mossman, H. W. (1972). Chapter V. The implantation of the blastocyst and the development of the fetal membranes, placenta and decidua. In *Hamilton, Boyd and Mossman's Human Embryology*, ed. W. J. Hamilton & H. W. Mossman. London: The Macmillan Press LTD, 1972, pp. 83–131.

Hansmann, M., Bäker, H., Fabula, S., Müller-Scholtes, H., Nellen, H. J. & Voigt, U. (1972). Biometrische Daten des Feten. Ergebnisse einer modifizierten Methodik der Ultraschall-Diagnostik. In *Perinatale Medizin Bd III, 4. Deutscher Kongreß für Perinatale Medizin*, ed. E. Saling & J. W. Dudenhausen. Stuttgart: Thieme-Verlag, 1972, pp. 136–47.

Hansmann, M. (1976). Ultraschallbiometrie im 2. und 3. Trimester der Schwangerschaft. *Gynäkologe*, 9:133–55.

Hansmann, M., Schmelz, G. & Voigt, U. (1977). Ultraschallmessung der fetalen Scheitel-Steißlänge in der ersten Schwangerschaftshälfte. *Arch Gynecol Obstet*, 224.

Hansmann, M., Schuhmacher, H., Foebus, J. & Voigt, U. (1979). Ultraschallbiometrie der fetalen Scheitelsteißlänge in der ersten Schwangerschaftshälfte. *Geburtshilfe Frauenheilkd*, 39.

Hawass, N. E. D., Al-Badawi, M. G., Fatani, J. A., Meshari, A. A. & Edrees, Y. A. (1991). Morphology and growth of the fetal stomach. *Invest Radiol*, 26:998–1004.

Hellman, L., Kobayashi, M., Fillisti, L., Lavenhar, M. & Cromb, E. (1967). Sources of error in sonographic fetal mensuration and estimation of growth. *Am J Obstet Gynecol*, 99:662–70.

Hellman, L. M., Kobayashi, M., Fillisti, L., Lavenhar, M. & Cromb, E. (1969). The growth and development of the human fetus prior to the twentieth week of gestation. *Am J Obstet Gynecol*, 103:789–800.

Henderson, J., Willson, K., Jago, J. R. & Whittingham, T. A. (1995). A survey of the acoustic output of diagnostic ultrasound equipment in current clinical use. *Ultrasound Med Biol*, 21:699–705.

Henderson, J., Whittingham, T. A. & Dunn, T. (1997). A review of the acoustic output of modern diagnostic ultrasound equipment. *BMUS Bulletin*, 5:10–4.

Hertzberg, B. S., Mahony, B. S. & Bowie, J. D. (1988). First trimester fetal cardiac activity. *J Ultrasound Med*, 7:573–5.

Hesseldahl, H. & Larsen, J. F. (1969). Ultrastructure of human yolk sac: Endoderm, mesenchyme, tubules and meothelium. *Am J Anat*, 126:315–36.

Hinrichsen, K. V., Editor (1990). *Humanembryologie*. Berlin: Springer-Verlag.

His, W. (1880-85). *Anatomie menschlicher Embryonen. Vol 1–3*. Leipzig: Vogel.

His, W. (1887). Über Methoden plastischer Rekonstruktion und über deren Bedeutung für Anatomie und Entwicklungsgeschichte. *Anat Anz*, 2:382–94.

His, W. (1890). Die Entwickelung des menschlichen Rautenhirns vom Ende des ersten bis zum Beginn des dritten Monats. *Abhandl KS Gesellsch Wissensch*, 29:3–74.

His, W. (1904). *Die Entwickelung des menschlichen Gehirns während der ersten Monate. Untersuchungsergebnisse*. Leipzig: Hirzel.

Hochstetter, F. (1919). *Beiträge zur Entwicklungsgeschichte des menschlichen Gehirns*. Wien: Franz Deuticke.

Howry, D. H. & Bliss, W. R. (1952). Ultrasonic visualization of soft tissue structures of the body. *J Lab Clin Med*, 40:579–92.

Howry, D. H., Posakony, G., Cushman, C. R. & Holmes, J. H. (1956). Three-dimensional and stereoscopic observation of body structures by ultrasound. *J Appl Physiol*, 9:304–6.

Howry, D. H. (1957). Techniques used in ultrasonic visualization of soft tissues. In *Ultrasound in Biology and Medicine*, ed. Kelly. Washington: American Institute of Biological Sciences, 1957, pp. 49.

Hubelbank, M. & Tretiak, O. J. (1970). Focused ultrasonic transducer design. *Q Progr Rep Lab Electron MIT*, 98:169–77.

Jauniaux, E., Jurkovic, D., Henriet, Y. & Rodesch, F. (1991). Development of the secondary human yolk sac: correlation of sonographic and anatomical features. *Hum Reprod*, 6:1160–6.

Jauniaux, E. & Moscoso, J. G. (1992). Morphology and significance of the human yolk sac. In *The first twelve weeks of gestation*, ed. E. R. Barnea, J. Hustin & E. Jauniaux. Berlin: Springer-Verlag, 1992, pp. 192–213.

Jenkins, G. B. (1921). Relative weight and volume of the component parts of the brain of the human embryo at different stages of development. *Contr Embryol Carneg Instn*, 13:41–60.

Jirásek, J. E., Uher, J. & Uhrová, M. (1966). Water and nitrogen content of the body of young human embryos. *Am J Obstet Gynecol*, 96:868–71.

Johnson, W. L., Stegall, H. F., Lein, J. N. & Rushmer, R. F. (1965). Detection of fetal life in early pregnancy with an ultrasonic Doppler flowmeter. *Obstet Gynecol*, 26:305–7.

Jouppila, P. (1971). Ultrasound in the diagnosis of early pregnancy and its complications. A comparative study of the A-, B- and Doppler methods. Thesis. *Acta Obstet Gynecol Scand*, 50:3–56.

Keibel, F. & Mall, F. P., Editors (1910). *Handbuch der Entwicklungsgeschichte des Menschen, Vol. 1.* Leipzig: Hirzel.

Keibel, F. & Mall, F. P., Editors (1911). *Handbuch der Entwicklungsgeschichte des Menschen, Vol. 2.* Leipzig: Hirzel.

Kelly, I. M. G., Gardener, J. E. & Lees, W. R. (1992). Three-dimensional fetal ultrasound. *Lancet*, 339:1062–4.

Kier, E. L. (1977). The cerebral ventricles: a phylogenetic and ontogenetic study. Anatomy and pathology. In *Radiology of the skull and the brain*, ed. T. H. Newton & D. G. Potts. Saint Louis: Mosby, 1977, pp. 2787-914.

Kiesselbach, A. (1952). Der physiologische Nabelbruch. *Adv Anat Embryol Cell Biol*, 34:83–143.

Kohorn, E. I. & Kaufman, M. (1974). Sonar in the first trimester of pregnancy. *Obstet Gynecol*, 44:473–83.

Kossoff, G. (1971). Development in ultrasonic echoscopy. In *Digest 9th Internat Conf Med Biol Engineering*. Melbourne, Australia, 1971, pp. 58.

Kossoff, G. (1972). Improved techniques in ultrasonic cross-sectional echography. *Ultrasonics*, 10:221–7.

Kossoff, G., Garrett, W. J. & Radovanovich, G. (1974). Grey scale echography in obstetrics and gynaecology. *Aust Radiol*, 18:62–111.

Kossoff, G. (1976). Technical procedures and imaging. In *Present and future of diagnostic ultrasound*, ed. I. Donald & S. Levi. New York: John Wiley & Sons, 1976, pp. 1–11.

Kostovic, I. (1990). Zentralnervensystem. In *Humanembryologie*, ed. K. V. Hinrichsen. Berlin: Springer-Verlag, 1990, pp. 381–448.

Kratochwil, A. & Eisenhut, L. (1967). Der früheste Nachweis der fetalen Herzaktion durch Ultraschall. *Geburtshilfe Frauenheilkd*, 27:176–80.

Kratochwil, A. (1969). Ein neues vaginales Ultraschall-Schnittbildverfahren. *Geburtshilfe Frauenheilkd*, 29:379–85.

Kratochwil, A. (1992). Versuch der 3 dimensionalen Darstellung in der Geburtshilfe. *Ultraschall Med*, 13:183–6.

Krause, W. & Soldner, R. (1967). Ultraschallbildverfahren (B-scan) mit hoher Bildfrequenz für medizinische Diagnostik. *Electromedica*, 35:8–11.

Krone, S., Wisser, J. & Strowitzki, T. (1989). Anatomie des menschlichen Embryos im vaginalsonographischen Bild. *Ultraschall Klin Prax*, 4:205–9.

Kustermann, A., Zorzoli, A., Spagnolo, D. & Nicolini, U. (1992). Transvaginal sonography for fetal measurement in early pregnancy. *Br J Obstet Gynaecol*, 99:38–42.

Kyei-Mensah, A., Zaidi, J., Pittrof, R., Shaker, A., Campbell, S. & Tai, S.-L. (1996). Transvaginal three-dimensional ultrasound: accuracy of follicular volume measurements. *Fertil Steril*, 65:371–6.

Lamkee, M. J., Huntington, H. W. & deAlvarez, R. R. (1962). Fetal electrocardiography. *Am J Obstet Gynecol*, 83:1622–8.

Larsen, W. J. (1993). *Human Embryology*. New York: Churchill Livingstone.

Lasser, D. M., Peisner, D. B., Vollebergh, J. & Timor-Tritsch, I. (1993). First-trimester fetal biometry using transvaginal sonography. *Ultrasound Obstet Gynecol*, 3:104–8.

Lauge-Hansen, N. (1973). *Developmental anatomy of the human gastro-intestinal tract.* Aarhus: Munksgaard Aarhus Stiftsbogtrykkerie A/S.

Lemire, R. J. (1975). Deep cerebral nuclei. In *Normal and abnormal development of the human nervous system*, ed. R. J. Lemire. Hagerstown, Maryland: Harper&Row, 1975, pp. 169-95.

Liebermann-Meffert, D. (1969). Form und Lageentwicklung des menschlichen Magens und seiner Mesenterien. *Acta Anat*, 72:376-410.

Lindsay, D. J., Lovett, I. S., Lyons, E. A., Levi, C. S., Zheng, X.-H., Holt, S. C. & Dashefsky, S. M. (1992). Yolk sac diameter and shape at endovaginal US: predictors of pregnancy outcome in the first trimester. *Radiology*, 183:115–8.

Ludwig, K. S. (1965). Über die Beziehungen der Kloakenmembran zum Septum urorectale bei menschlichen Embryonen von 9 bis 33 mm SSL. *Z Anat Entwickl Gesch*, 124:401–13.

MacGregor, S. N., Tamura, R. K., Sabbagha, R. E., Minogue, J. P., Gibson, M. E. & Hoffman, D. I. (1987). Underestimation of gestational age by conventional crown-rump length dating curves. *Obstet Gynecol*, 70:344–8.

MacVicar, J. & Donald, I. (1963). Sonar in the diagnosis of early pregnancy and its complications. *J Obstet Gynæcol Br Cwlth*, 70:387–95.

Mall, F. P. (1907). On measuring human embryos. *Anat Rec*, 1:129–40.

Mall, F. P. (1910). Die Altersbestimmung von menschlichen Embryonen und Feten. In *Handbuch der Entwicklungsgeschichte des Menschen, Vol 1*, ed. F. Keibel & F. P. Mall. Leipzig: Hirzel, 1910, pp. 185–207.

Mall, F. P. (1914). On stages in the development of human embryos from 2 to 25 mm. long. *Anat Anz*, 46:78–84.

Mall, F. P. (1918). On the age of human embryos. *Am J Anat*, 23:397–422.

Mantoni, M. & Pedersen, J. F. (1979). Ultrasound visualization of the human yolk sac. *J Clin Ultrasound*, 7:459–60.

Meban, C. (1983). The surface area and volume of the human fetus. *J Anat*, 137:271–8.

Meckel, J. F. (1817). Bildungsgeschichte des Darmkanals der Säugethiere und namentlich des Menschen. *Dtsch Arch Physiol*, 3:1–84.

Merchiers, E. H., Dhont, M., DeSutter, P. A., Beghin, C. J. & Vanderkerckhove, D. A. (1990). Predictive value of early embryonic cardiac activity for pregnancy outcome. *Am J Obstet Gynecol*, 165:11–4.

Moore, G. W., Hutchins, G. M. & O'Rahilly, R. (1981). The estimated age of staged human embryos and early fetuses. *Am J Obstet Gynecol*, 139:500–6.

Moore, K. (1988). The cardiovascular system. In *The developing human*, ed. K. Moore. Philadelphia: Saunders, 1988, pp. 286–333.

Moritz, W. E. & Shreve, P. L. (1976). A microprocessor-based spatial-locating system for use with diagnostic ultrasound. *Proc IEEE*, 64:966–74.

Moutsouris, C. (1966). The "solid stage" and congenital intestinal atresia. *J Pediatr Surg*, 1:446–50.

Müller, K. & Osler, M. (1969). Early detection of foetal life by "Dopplerophonia". *Acta Obstet Gynecol Scand*, 48:130–1.

Müller, F. & O'Rahilly, R. (1990). The human brain at stages 18 - 20, including the choroid plexuses and the amygdaloid and septal nuclei. *Anat Embryol*, 182:285-306.

Nagata, S., Koyanagi, T., Horimoto, N., Satoh, S. & Nakano, H. (1989). Chronological development of the fetal stomach assessed using real-time ultrasound. *Early Hum Dev*, 22:15–22.

Nyberg, D. A., Mack, L. A., Harvey, D. & Wang, K. (1988). Value of the yolk sac in evaluating early pregnancies. *J Ultrasound Med*, 7:129–35.

O'Rahilly, R. & Gardner, E. (1971). The timing and sequence of events in the development of the human nervous system during the embryonic period proper. *Z Anat Entwickl-Gesch*, 134:1–12.

O'Rahilly, R. (1978). The timing and sequence of events in the development of the human digestive system and associated structures during the embryonic period proper. *Anat Embryol*, 153:123–36.

O'Rahilly, R. & Müller, F. (1984). Embryonic length and cerebral landmarks in staged human embryos. *Anat Rec*, 209:265–71.

O'Rahilly, R. & Müller, F. (1987). *Developmental stages in human embryos*. Washington DC: Carneg Instn Publ.

O'Rahilly, R. & Müller, F. (1990). Ventricular system and choroid plexuses of the human brain during the embryonic period proper. *Am J Anat*, 189:285–302.

O'Rahilly, R. & Müller, F. (1994). *The embryonic human brain. An atlas of developmental stages*. New York: Wiley-Liss.

Pedersen, J. F. (1982). Fetal crown-rump length measurement by ultrasound in normal pregnancies. *Br J Obstet Gynaecol*, 89:926–30.

Pernkopf, E. (1923). Die Entwicklung der Form des Magendarmkanals beim Menschen. *Z Anat*, 73:1–144.

Queenan, J. T., O'Brien, G. D. & Campbell, S. (1980). Ultrasound measurement of fetal limb bones. *Am J Obstet Gynecol*, 138:297–302.

Rabelink, I. A. A., Degen, J. E. M., Kessels, M. E. W., Nienhuis, S. J., Ruissen, C. J. & Hoogland, H. J. (1994). Variation in early growth. *Eur J Obstet Gynecol Reprod Biol*, 53:39–43.

Ragavendra, N., McMahon, J. T., Perrella, R. R., Tessler, F. N., Hansen, G. C., Kimme-Smith, C., Grant, E. G. & Crandall, B. F. (1991). Endoluminal catheter-assisted transcervical US of the human embryo. *Radiology*, 181:779–83.

Ramnarine, K. V., Nassiri, D. K., McCarthy, A. & Brown, N. A. (1997). Thresholds for morphological malformations in rat embryos exposed to ultrasound. *BMUS Bulletin*, 5:28–31.

Reece, E. A., Scioscia, A. L., Green, J., O'Connor, T. Z. & Hobbins, J. (1987). Embryonic trunk circumference: a new biometric parameter for estimation of gestational age. *Am J Obstet Gynecol*, 156:713–5.

Reece, E. A., Scioscia, A., Pinter, E., Hobbins, J. C., Green, J., Mahoney, M. J. & Naftolin, F. (1988). Prognostic significance of the human yolk sac assessed by ultrasonography. *Am J Obstet Gynecol*, 159:1191–4.

Rempen, A. (1991a). Biometrie in der Frühgravidität (I. Trimenon). *Frauenarzt*, 32:425–30.

Rempen, A. (1991b). Vaginale Sonographie im ersten Trimenon. II. Quantitative Parameter. *Z Geburtshilfe Perinatol*, 195:163–71.

Riccabona, M., Nelson, T. R. & Pretorius, D. H. (1995). Dreidimensionale Sonographie: zur Genauigkeit sonographischer Volumsbestimmungen. *Ultraschall Klin Prax*, 10:35–9.

Robinson, D. E. (1972). Ultrasonic systems for medical diagnostic visualization. *Q Progr Rep Lab Electron MIT*, 104:289–305.

Robinson, H. P. & Shaw-Dunn, J. (1973). Fetal heart rates as determined by sonar in early pregnancy. *J Obstet Gynaecol Br Cwlth*, 80:805–9.

Robinson, H. P. (1973). Sonar measurement of fetal crown-rump length as means of assessing maturity in first trimester of pregnancy. *Br Med J*, 4:28–31.

Robinson, H. P. & Fleming, J. E. E. (1975). A critical evaluation of sonar "crown-rump length" measurements. *Br J Obstet Gynaecol*, 82:702–10.

Robinson, H. P. (1975). "Gestation sac" volumes as determined by sonar in the first trimester of pregnancy. *Br J Obstet Gynaecol*, 82:100–7.

Rossavik, I. K., Torjusen, G. O. & Gibbons, W. E. (1988). Conceptual age and ultrasound measurements of gestational sac and crown-rump length in in vitro fertilization pregnancies. *Fertil Steril*, 49:1012–7.

Rott, H.-D. (1997). Capillary lung bleeding from exposure to diagnostic ultrasound - a literature review. *BMUS Bulletin*, 5:20–1.

Rottem, S. & Bronshtein, M. (1990). Transvaginal sonographic diagnosis of congenital anomalies between 9 weeks and 16 weeks, menstrual age. *J Clin Ultrasound*, 18:307-14.

Rottem, S., Bronshtein, M., Thaler, I. & Brandes, J. M. (1989). First trimester transvaginal sonographic diagnosis of fetal anomalies. *Lancet*, 1:444–5.

Rubenstein, J. L. R., Shimamura, K., Martinez, S. & Pelles, L. (1998). Regionalization of the prosencephalic neural plate. *Annu Rev Neurosci*, 21:445–77.

Sauerbrei, E., Cooperberg, P. L. & Poland, B. J. (1980). Ultrasound demonstration of the normal fetal yolk sac. *J Clin Ultrasound*, 8:217–20.

Schats, R., Jansen, C. A. M. & Wladimiroff, J. W. (1990). Abnormal embryonic heart rate pattern in early pregnancy associated with Down's syndrome. *Hum Reprod*, 5:877–9.

Schmidt, W., Yarkoni, S., Crelin, E. S. & Hobbins, J. C. (1987). Sonographic visualization of the physiologic anterior wall hernia in the first trimester. *Obstet Gynecol*, 69:911–5.

Schaaps, J. P. & Hustin, J. (1988). In vivo aspect of the maternal-trophoblastic border during the first trimester of gestation. *Trophoblast research*, 3:39–48.

Sohn, C., Stolz, W., Nuber, B., Hesse, A. & Hornung, B. (1991). Die dreidimensionale Ultraschalldiagnostik in Gynäkologie und Geburtshilfe. *Geburtshilfe Frauenheilkd*, 51:335–40.

Somer, J. C. (1978). Transducer arrays. In *Handbook of clinical ultrasound*, ed. M. deVlieger, J. H. Holmes, E. Kazner, G. Kossoff, A. Kratochwil, R. Kraus, J. Poujol & D. E. Strandness. New York: John Wiley & Sons, 1978, pp. 67–74.

Somer, J. C. (1968). Electronic sector scanning for ultrasonic diagnosis. *Ultrasonics*, 6:153–9.

Stampone, C., Nicotra, M., Muttinelli, C. & Cosmi, E. V. (1996). Transvaginal sonography of the yolk sac in normal and abnormal pregnancy. *J Clin Ultrasound*, 24:3–9.

Starritt, H. (1997). Acoustic streaming and other radiation stress effects. *BMUS Bulletin*, 5:24–7.

Steding, G. & Seidl, W. (1990). Cardio-vaskuläres System. Entwicklung der Baumaterialien des Herzens. In *Humanembryologie*, ed. K. V. Hinrichsen. Berlin: Springer-Verlag, 1990, pp. 243–50.

Steen, E. N. (1996). *Analysis and visualization of multi-dimensional medical images.* Thesis, NTNU, Trondheim.

Steen, E. & Olstad, B. (1994). Volume rendering of 3D medical ultrasound data using direct feature mapping. *IEEE Trans Med Imaging*, 13:517–25.

Streeter, G. L. (1920). Weight, sitting height, head size, foot length, and menstrual age of the human embryo. *Contr Embryol Carneg Instn*, 11:143–70.

Streeter, G. L. (1942). Developmental horizons in human embryos. *Contr Embryol Carneg Inst*, 30:211–45.

Streeter, G. L. (1945). Developmental horizons in human embryos. *Contr Embryol Carneg Inst*, 199:27–63.

Streeter, G. L. (1948). Developmental horizons in human embryos. *Contr Embryol Carneg Inst*, 211:133–203.

Streeter, G. L. (1949). Developmental horizons in human embryos (fourth issue). A review of the histogenesis of cartilage and bone. *Contr Embryol Carneg Inst*, 33:150–73.

Sundén, B. (1964). On the diagnostic value of ultrasound in obstetrics and gynecology. Thesis. *Acta Obstet Gynecol Scand*, 43(suppl):1–121.

Szilard, J. (1974). An improved three-dimensional display system. *Ultrasonics*, 76:273–6.

Takashina, T. (1989). Hemopoiesis in the human yolk sac. *Am J Anat*, 184:237–44.

Takeuchi, H., Nakazawa, T., Kusano, R., Kumakiri, K., Nakano, K. & Mizuno, S. (1968). Ultrasonic Doppler method for detecting the fetal heart beat. *Jpn J Med Ultrason*, 6:80–2.

Takeuchi, H. (1992). Transvaginal ultrasound in the first trimester of pregnancy. *Early Hum Dev*, 29:381–4.

Tanner, J. M. (1981). Iatromathematics and the introduction of measurement: the seventeenth and eighteenth centuries. In *A history of the study of human growth*, ed. J. M. Tanner. Cambridge: Cambridge University Press, 1981, pp. 66–97.

ter Haar, G. (1997). Are contrast agents safe? *BMUS Bulletin*, 5:22–3.

Thompson, H. E., Holmes, J. H., Gottesfeld, K. R. & Taylor, E. (1965). Fetal development as determined by ultrasonic pulse echo techniques. *Am J Obstet Gynecol*, 92:44–52.

Thune, N., Gilja, O. H., Hausken, T. & Matre, K. (1996). A practical method for estimating enclosed volumes using 3D ultrasound. *Eur J Ultrasound*, 3:83–92.

Thurstone, F. L. & Melton, J. W. (1970). Biomedical ultrasonics. *IEEE Trans Ind Elect Control Instn*, 17:167–72.

Timor-Tritsch, I. E., Farine, D. & Rosen, M. G. (1988). A close look at the embryonic development with the high frequency transvaginal transducer. *Am J Obstet Gynecol*, 159:678–81.

Timor-Tritsch, I. E., Warren, W. B., Peisner, D. B. & Pirrone, E. (1989). First trimester midgut herniation: A high frequency transvaginal sonographic study. *Am J Obstet Gynecol*, 161:466-76.

Timor-Tritsch, I. E., Peisner, D. B. & Raju, S. (1990). Sonoembryology: an organ-oriented approach using a high-frequency vaginal probe. *J Clin Ultrasound*, 18:286–98.

Timor-Tritsch, I. E., Monteagudo, A. & Warren, W. B. (1991). Transvaginal ultrasonographic definition of the central nervous system in the first and early second trimesters. *Am J Obstet Gynecol*, 164:497-503.

Tsukerman, G. L., Krapiva, G. A. & Kirillova, I. A. (1993). First-trimester diagnosis of duodenal stenosis associated with oesophageal atresia. *Prenat Diagn*, 13:371–6.

Tunón, K., Eik-Nes, S. H. & Grøttum, P. (1996). A comparison between ultrasound and a reliable last menstrual period as a predictor of the day of delivery in 15 000 examinations. *Ultrasound Obstet Gynecol*, 8:178–85.

Warren, W. B., Timor-Tritsch, I. E., Peisner, D. B., Raju, S. & Rosen, M. G. (1989). Dating the pregnancy by sequential appearance of embryonic structures. *Am J Obstet Gynecol*, 161:747–53.

Westergaard, E. (1971). The lateral cerebral ventricles of human foetuses with a crown-rump length of 26-178 mm. *Acta Anat*, 79:409–21.

WFUMB. (1997). World Federation for Ultrasound in Medicine and Biology. *Ultrasound Med Biol*, 23:974.

Willocks, J. (1962). The use of ultrasonic cephalometry. *Proc R Soc Med*, 55:640.

Willocks, J., Donald, I., Duggan, T. C. & Day, N. (1964). Foetal cephalometry by ultrasound. *Br J Obstet Gynaecol*, 71:11–20.

Wisser, J. & Dirschedl, P. (1994). Embryonic heart rate in dated human embryos. *Early Hum Dev*, 37:107–15.

Wisser, J., Dirschedl, P. & Krone, S. (1994). Estimation of gestational age by transvaginal sonographic measurements of greatest embryonic length in dated human embryos. *Ultrasound Obstet Gynecol*, 4:457–62.

Wisser, J. (1995). *Vaginalsonographie im ersten Schwangerschaftsdrittel.* Berlin: Springer-Verlag.

Woollam, D. (1952). Casts of the ventricles of the brain. *Brain*, 75:259–67.

Yokoh, Y. (1975). Early development of the cerebral vesicles in man. *Acta Anat*, 91:455–61.

Zalen-Sprock, R. M. v., Vugt, J. M. G. v. & Geijn, H. P. v. (1996). First-trimester sonographic detection of neurodevelopmental abnormalities in some single-gene disorders. *Prenat Diagn*, 16:199–202.

Zalen-Sprock, R. M. v., Brons, J. T. J., Vugt, J. M. G. v., Harten, H. J. v. d. & Geijn, H. P. v. (1997). Ultrasonographic and radiologic visualization of the developing embryonic skeleton. *Ultrasound Obstet Gynecol*, 9:392–7.

Zalen-Sprock, R. M. v., Vugt, J. M. G. v. & Geijn, H. P. v. (1997). First trimester sonography of physiologic midgut herniation and early diagnosis of omphalocele. *Prenat Diagn*, 17:511–8.

Zalen-Sprock, R. M. v. (1997). *Ultrasound diagnosis of fetal anomalies early in pregnancy.* Thesis, Vrije Universiteit te Amsterdam.

Zorzoli, A., Kustermann, A., Caravelli, E., Corso, F. E., Fogliani, R., Aimi, G. & Nicolini, U. (1994). Measurements of fetal limb bones in early pregnancy. *Ultrasound Obstet Gynecol*, 4:29–33.

# 9 Appendix

## Figure 1

The rapid developmental changes of embryonic brain structures from 7 to 10 weeks of gestation.

A Embryo at 7 1/2 weeks, CRL 11 mm. Sagittal section. The umbilical cord points to the right. The shallow rhombencephalic cavity lies on the top of the head. It leads into the thin, curved mesencephalic cavity and further into the diencephalic cavity, which points dorsally. The lines show the sections as presented in A1 and A2.

A1 Horizontal section through head of embryo, CRL 12 mm, the rhombic shape of the cavity of the rhombencephalon (Rhomb) is shown.

A2 Oblique section through the rhombencephalic cavity (Rhomb), the third ventricle (3) and the hemispheres (Hem).

B Embryo at 9 1/2 weeks, CRL 29 mm. Parasagittal section through hemisphere (Hem) and choroid plexus (ChPl).

C Embryo at the end of the embryonic period at 10 weeks, CRL 33 mm. Sagittal section through the brain (Di = diencephalon; Mes = mesencephalon; Rhomb = rhombencephalon; ChPl-4 = choroid plexus of the fourth ventricle).

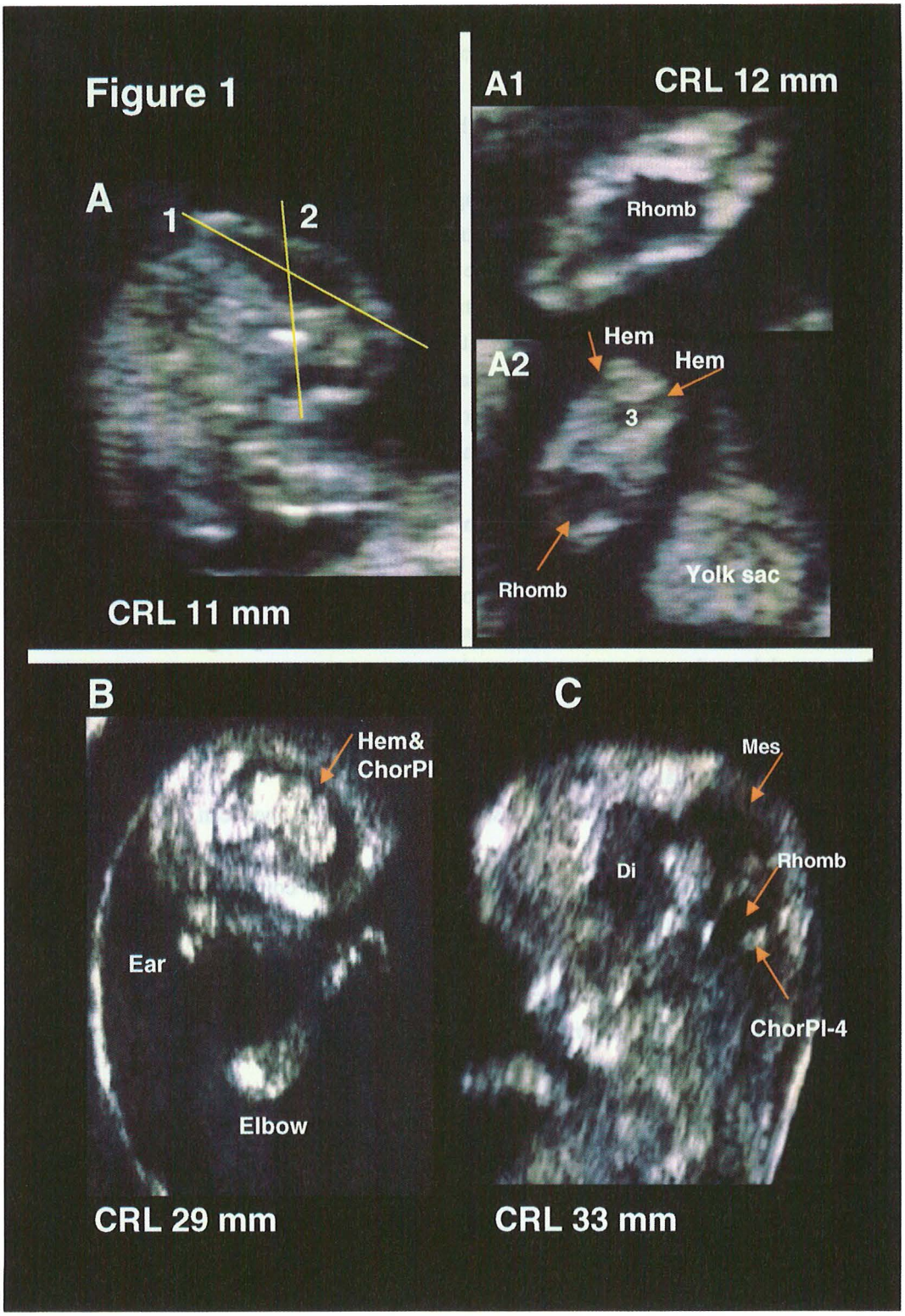
Figure 1
A
1
2
CRL 11 mm
A1
CRL 12 mm
Rhomb
A2
Hem
Hem
3
Rhomb
Yolk sac
B
Hem&
ChorPl
Ear
Elbow
CRL 29 mm
C
Mes
Di
Rhomb
ChorPl-4
CRL 33 mm

Figure 2

Visualization of 3D ultrasound data obtained from transvaginal scan using a transducer rotated by a stepper motor.

A Original coronal scan plane through embryo at the end of the embryonic period, CRL 29 mm.

B 3D navigation: This anyplane tomogram, a sagittal section through the head, was not possible to obtain with the original scan (A). The 2 lines indicate the section of the anyplane tomogram through the isthmus rhombencephali, as it is presented in C (Di = diencephalon; Mes = mesencephalon).

C Oblique coronal anyplane slice through the mesencephalon (Mes), isthmus rhombencephali and rhombencephalon (Cer = cerebellar hemisphere; ChPl-4 = choroid plexuses of the fourth ventricle).

D Sagittal anyplane section through the body. The hypoechogenic brain cavities can be seen.

E Magnification of the head shown in (D). «Where shall we draw the segmentation line?» The figure illustrates that the point spread function resulting from the radial and lateral resolution of the ultrasound system leads to a blurred surface in the ultrasound image. Therefore, the manual segmentation process may be difficult and depends on the operators experience.

F Geometry visualization: Segmentation of the body (white), lateral ventricle (yellow), cavity of the diencephalon (green), mesencephalon (red) and rhombencephalon (blue).

G After the segmentation process, the segmentation lines can be visualized as contours.

H Surface rendering of the embryo from the segmented contours. The opacity of the head is reduced such that the colored brain compartments are visible. The volume calculations are made by the EchoPAC 3D program.

I Volume rendering (surface shading) of the same embryo, made from an intermediate 3D geometrical data set after regional extraction from the original 3D data set.

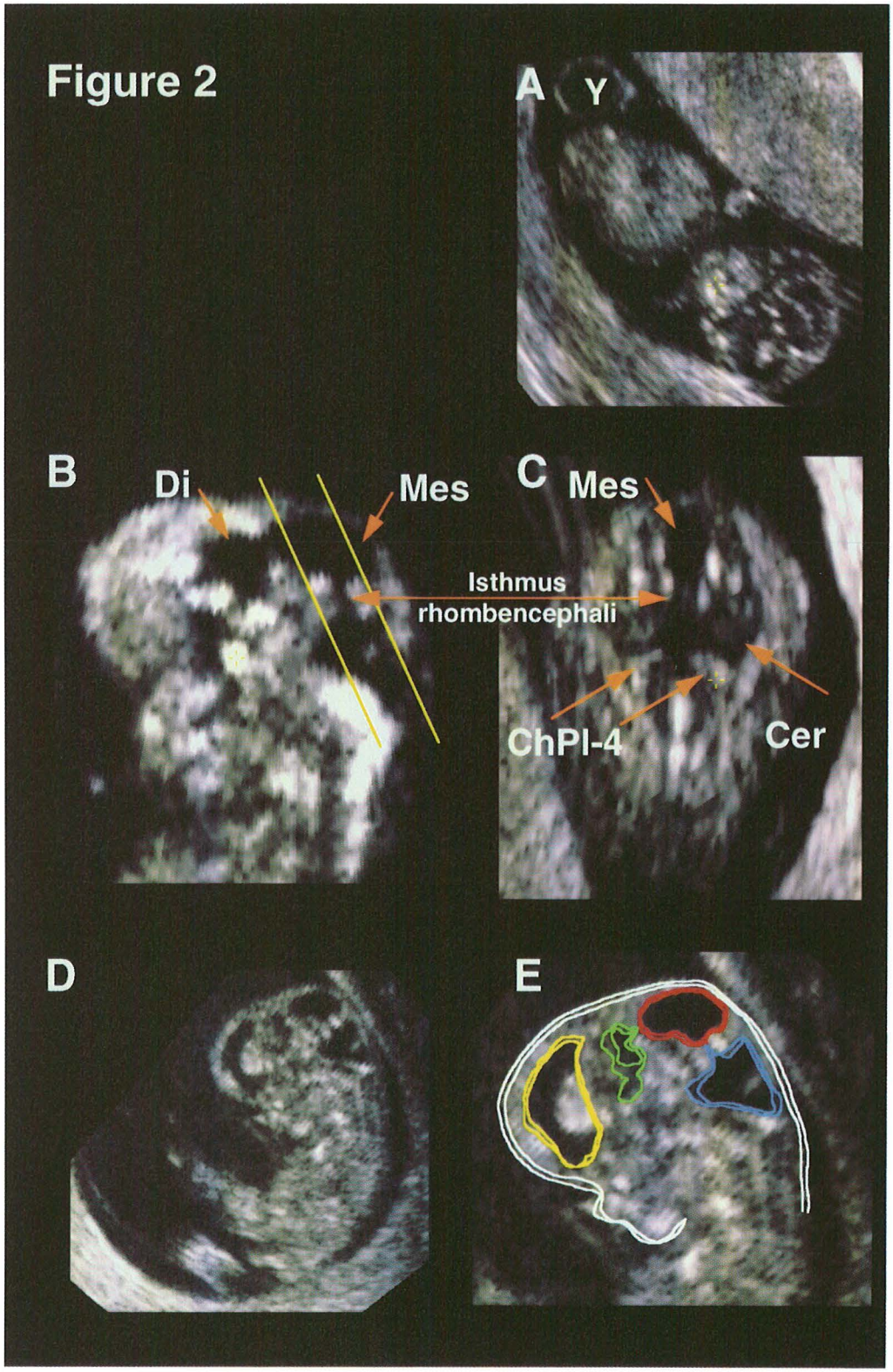
Figure 2
A
Y
B
Di
Mes
C
Mes
Isthmus
rhombencephali
ChPl-4
Cer
D
E

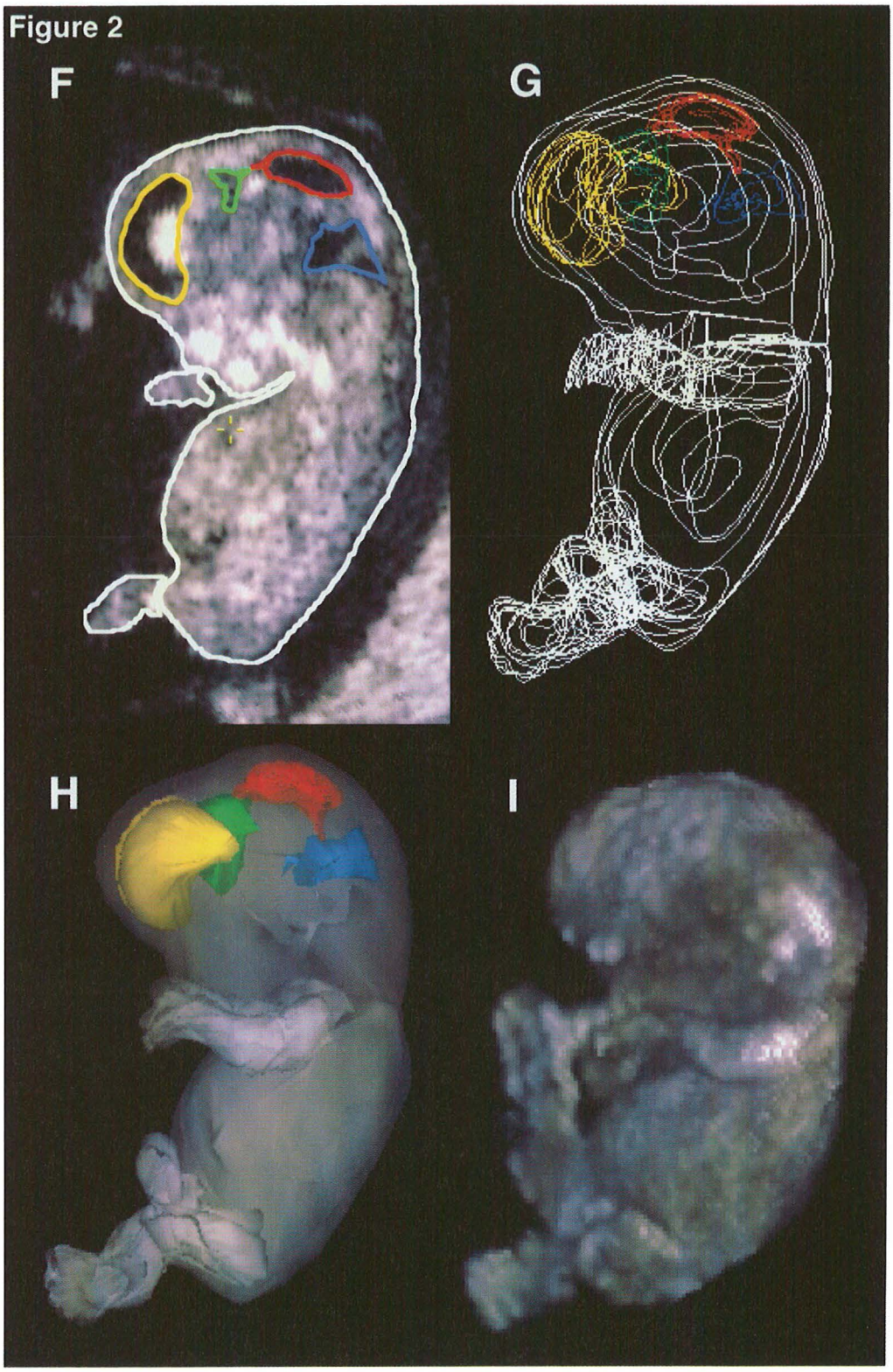
Figure 2
F
G
H
I

## 10 Corrections

Paper I

Figures 9 and 10: The images were switched: The image of Figure 10 belongs to the legend of Figure 9, and vice versa

Page 191, 2. column, 2. paragraph, line 3: «recuitment» should be "recruitment"

Paper II

Page 158, 1. column, 2. paragraph, line 7: "...in our intraobserver study (Table 1)." should be "...in our intraobserver study (Table 3)."

Paper VI

Page 1184, 1. paragraph, line3: "Shapiro Francia W test." should be "Shapiro Francia W' test."

Page 1184, legend of Table 2, should be "*Square root transformed, †cubic root transformed. Residual and multiple $R^2$ are shown."

Page 1184, Figure 3: The 'mean' regression line of the 'Diencephalon' is not visible. The correct Figure 3 is inserted at the end of paper VI.

# Paper I

**Harm-Gerd Blaas, Sturla H. Eik-Nes, Torvid Kiserud, Leif Rune Hellevik. Early development of the forebrain and midbrain: a longitudinal ultrasound study from 7 to 12 weeks of gestation. Ultrasound Obstet Gynecol 1994; 4:183–92**

*Ultrasound Obstet. Gynecol. 4 (1994) 183–192*

# Early development of the forebrain and midbrain: a longitudinal ultrasound study from 7 to 12 weeks of gestation

*H.-G. Blaas, S. H. Eik-Nes, T. Kiserud and L. R. Hellevik*

National Center for Fetal Medicine, Department of Obstetrics and Gynecology, Trondheim University Hospital, Trondheim, Norway

Key words: TRANSVAGINAL ULTRASOUND, CENTRAL NERVOUS SYSTEM, EMBRYONIC BRAIN DEVELOPMENT, SONOEMBRYOLOGY, FIRST TRIMESTER

## ABSTRACT

*The purpose of this longitudinal study was to describe embryonic development* in vivo. *Twenty-nine healthy pregnant women were examined five times with transvaginal ultrasound between 7 and 12 weeks of gestation. Brain structures such as the hemispheres, the choroid plexus of the lateral ventricles, the diencephalon, and the mesencephalon were identified and, if possible, measured.*

*It was possible to identify the cavities of the hemispheres, the diencephalon and the mesencephalon during week 7. The choroid plexus of the lateral ventricles became visible during week 8. The growth of the length, width and height of the hemispheres and the choroid plexus of the lateral ventricles was curvilinear, that of the mesencephalon and diencephalon was linear except for the width of the diencephalon. The width of the diencephalon, the future third ventricle, was 1.1 mm during week 7. It decreased to 0.8 mm at 12 weeks. Apart from the rhombencephalon, the cavity of the diencephalon was the large dominating brain structure during embryonic development. In early fetal life the cerebral hemispheres took over this dominance.*

*The study was in full agreement with descriptions in the embryological literature, both concerning the anatomical features and their chronological formation.*

## INTRODUCTION

In the past few years, the diagnostic potential of high-frequency ultrasound has increased interest in the evaluation of the first-trimester pregnancy. Various authors[1-5] have described the embryonic structures seen by means of this technique and have indicated the possibilities for a new diagnostic field. This has led to a new epoch in the history of medical ultrasound, the age of 'sonoembryology', a term introduced by Timor-Tritsch and colleagues in 1990[1]. So far, all studies on embryology have been cross-sectional, both the classical anatomical work performed by the embryologists, and the recent ultrasound evaluations. These studies have demonstrated that the formation of the human body takes place during a few weeks of hectic development. For instance, it takes only 4½ weeks from the closure of the caudal neuropore in the 3-mm embryo to the completion of the embryonic brain development in the 30-mm embryo. Detailed knowledge about early development is a prerequisite for evaluation of the embryo or fetus at risk for genetic disease, or when abnormal development is suspected.

The safe and non-invasive ultrasound technique offers us a unique possibility to perform a longitudinal study of single embryos with examinations on successive occasions. The aim of this ultrasound study was to describe the morphological development of the embryonic and early fetal central nervous system *in vivo*. We present the development of the forebrain and the midbrain *in vivo* analyzed longitudinally from 7 to 12 weeks.

## SUBJECTS AND METHODS

A total of 36 pregnant women were recruited for a longitudinal vaginal ultrasound study in accordance with a protocol approved by the regional committee of ethics. Written consent was obtained from each woman.

Women had to fulfil the inclusion criteria in that their menstruation had to be regular, no hormonal therapy had been taken 3 months prior to the pregnancy, they were non-smokers, their single pregnancy was natural, and no bleeding had occurred during the pregnancy. Women with conditions that might influence the embryonic growth, such as uterine anomalies, diabetes, and hypertension were not included. The development of diabetes, pre-eclampsia, delivery of a preterm and/or a

Correspondence: Dr H.-G. Blaas, National Center for Fetal Medicine, Department of Obstetrics and Gynecology, Trondheim University Hospital, N-7006 Trondheim, Norway



Received 7–6–93
Revised 18–12–93
Accepted 28–2–94

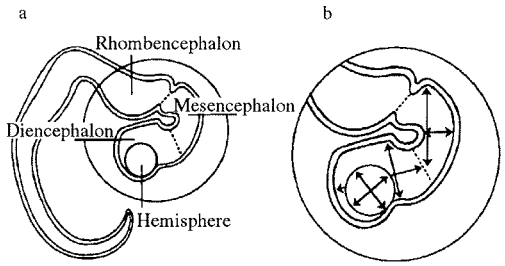


**Figure 1** (a) Sketch of the sagittal plane through the embryonic central nervous system in a 7-week-old embryo (Carnegie stage 16), showing the cavities of the rhombencephalon, mesencephalon, diencephalon, and, parasagittally, the hemisphere; (b) the sagittal measurements of the mesencephalon, diencephalon, and hemisphere are demonstrated by double-headed arrows

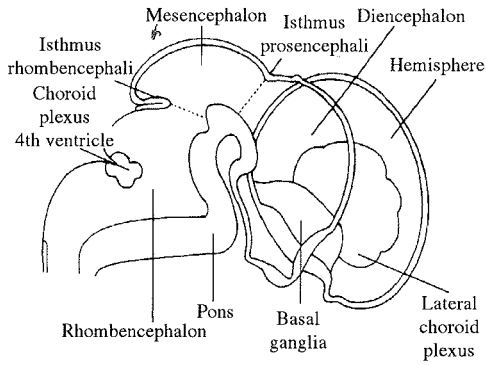


**Figure 2** Sketch of the sagittal plane through the brain at 10 weeks (Carnegie stage 23), including the parasagittal hemisphere. The marked structures are detectable by ultrasound

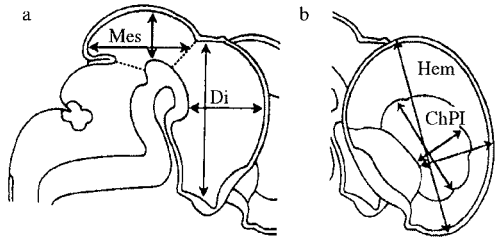


**Figure 3** Measurements of the length and height of the (a) diencephalon, mesencephalon, (b) hemisphere and choroid plexus of the lateral ventricle (Figure 2)

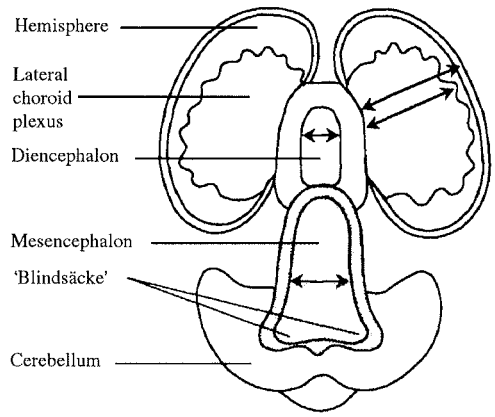


**Figure 4** Sketch of transverse sections through the 10-week-old brain. The mesencephalon (gray shade) lies superior to the other structures. Double-headed arrows indicate measurements of width

growth-retarded infant were exclusion criteria. Five women were excluded (three early pregnancy losses, one bleeding during week 9, one preterm delivery at 36 weeks due to pre-eclampsia), and two women decided to discontinue after the first examination. Thus 29 women were included in the study (mean age 28 years, range 19–38 years).

A high-frequency scanner (Dornier AI 3200) with a 7.5 MHz transvaginal probe was used for all examinations. The emitted energy was set to 0.58 mW/cm$^2$ spatial peak temporal average *in situ*. The magnification on the screen was 3.3 times.

The first examination was performed between 7 and 8 completed gestational weeks according to the last menstrual period. In total, five examinations were carried out, with an interval of approximately 7 days between each. Each examination lasted for 20–30 min.

The brain structures of the embryo were measured as shown in Figures 1–4. In the *sagittal* midline section, the length and height of the cavities of the mesencephalon and the diencephalon were obtained. In a *transverse* section, the widths of the mesencephalon and diencephalon cavities, the hemispheres, and the choroid plexus of the lateral ventricles were measured. The length of the hemisphere was measured in a *parasagittal* section as the longest possible distance from the anterior to the posterior border of the cortex. The height was measured over the frontal horn, not including the basal ganglia. In order to reduce the examination time, only one measurement per target organ was generally performed.

All statements of time are given in completed postmenstrual weeks/days. The measurements are given as predicted mean value (lower and upper 95% prediction limits).

## Statistical evaluation

Cross-sectional regression analysis was used to examine the associations between the measured values and gestational age. For the hemisphere and the choroid plexus data, a square root transformation was done in order to stabilize the variations, to linearize the relationships and normalize the distributions. The diencephalon and mesencephalon measurements were analyzed linearly. The normality of the residuals was evaluated both by visual inspection of the distributions and by the Shapiro Francia $W'$ test[6].

### Intraobserver study

The reproducibility of our measurements was evaluated by an intraobserver study in 17 pregnant women who were not included in the longitudinal study. The size of the measured embryos varied from 14 mm (7 weeks 6 days) to 50 mm (11 weeks 4 days), mean 26 mm (9 weeks 3 days). All measurements were recorded on video print pictures. The participants were scanned, then left the examination room for about 10 min before they were rescanned. Limits of agreement for intraobserver measurements were calculated[7].

## RESULTS

It was possible to visualize the rapid development of the embryonic brain by ultrasound, as demonstrated in Figures 5–14. During week 7, the tiny cavities of the hemispheres, the diencephalon and the mesencephalon were identifiable (Figures 5 and 6). The hemispheres (Figures 7, 10 and 11), the diencephalon (third ventricle) (Figures 7, 8 and 11) and the mesencephalon (Figures 8, 9 and 10) became structures of considerable size during week 8. Additionally, the choroid plexus of the lateral ventricles started to develop (Figure 11). Figures 12–14 illustrate the detailed brain anatomy of 10 and 11-week-old fetuses.

### Hemispheres

The tiny paired buds of the 'telencephalon impar' became visible during week 7 (Figure 6). An oblique transverse section through the embryonic head with an angle of about 45° to the longitudinal axis demonstrated the rhombencephalic cavity posteriorly and the Y-shape of the dividing telencephalon anteriorly (Figures 6 and 7).

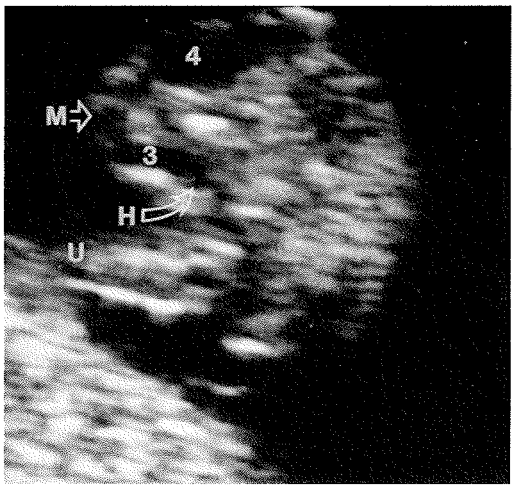


**Figure 5** Sagittal section through an embryo (crown–rump length, 11 mm). The cavities of the rhombencephalon, the future fourth ventricle (4), the mesencephalon (M), the diencephalon, the future third ventricle (3), and of the hemisphere (H) can be identified. U, umbilical cord

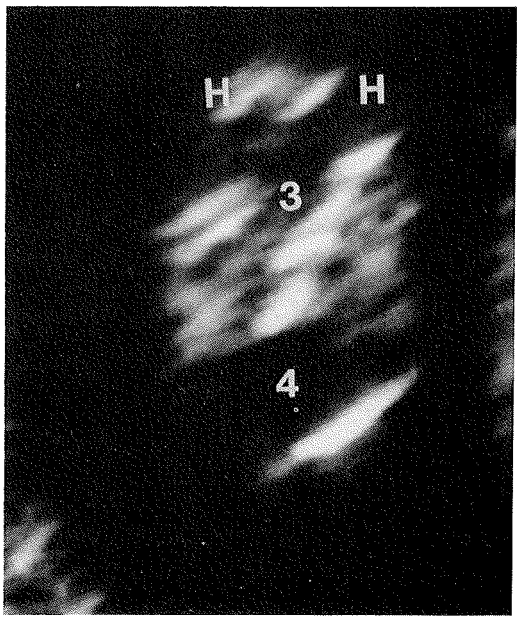


**Figure 6** Transverse/oblique section through the rhombencephalon (4), diencephalon (3) and hemispheres (H) (crown–rump length, 12 mm). The bilateral evaginations of the hemispheres are clearly seen. There is still a wide opening to the third ventricle

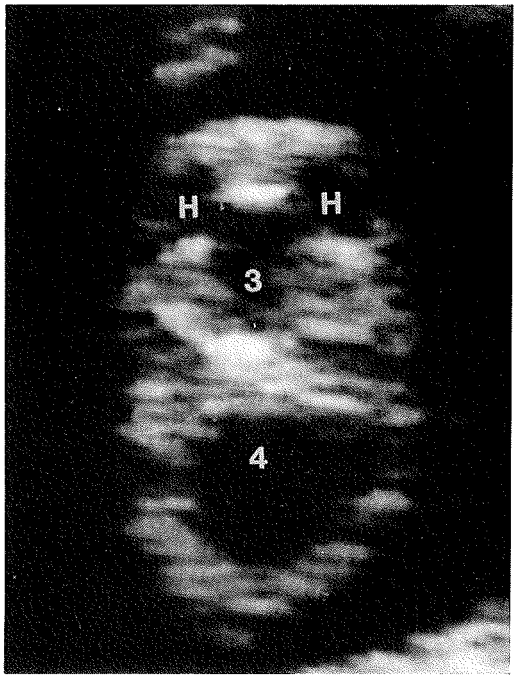


**Figure 7** Identical section as in Figure 6 (crown–rump length, 16 mm). The borders between the hemispheres (H) and the third ventricle (3) remain relatively small and develop into the foramina of Monro

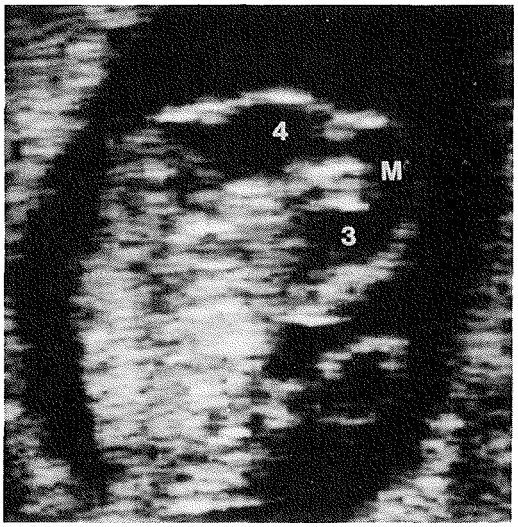


**Figure 8** Sagittal section through an embryo (crown–rump length, 17 mm). On top of the embryo lies the large stretched cavity (4) of the rhombencephalon. Anteriorly (to the right) the crooked cavity of the mesencephalon (M) continues into the relatively large third ventricle (3)

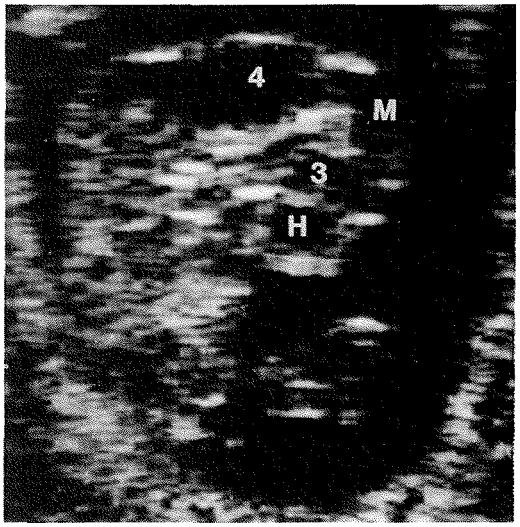


**Figure 9** Slightly parasagittal section through the same embryo (crown–rump length, 17 mm, Figure 8), showing the connections between the rhombencephalon (4), mesencephalon (M), diencephalon (3) and hemisphere (H). The foramen of Monro is clearly seen between (3) and (H)

Before 8 weeks 0 days, the hemispheres could be measured in five embryos (17%), and before 9 weeks 0 days, in 23 (79%) (Figures 9–11). After 9 weeks 0 days, the hemispheres were visualized and measured in all the embryos. They were best seen in the parasagittal plane, where the C-shape became apparent (Figure 12). The cortex was smooth and hypoechogenic. The thickness was about 1 mm at the end of the first trimester.

In a total series of 145 examinations, we achieved 115 measurements of the length, 115 of the width, and 114 of the height. At 7 weeks 4 days, the mean length, width and height of the hemispheres were 1.7 mm (0.6–3.4 mm), 1.0 mm (0.4–2.1 mm), and 1.8 mm (0.8–3.2 mm), respectively. At 12 weeks 0 days, the mean length was 16.4 mm (12.4–20.9 mm), the mean width was 6.1 mm (4.2–8.4 mm), and the mean height 8.2 mm (5.9–10.9 mm). The growth of all these parameters was curvilinear (Figure 15).

## Choroid plexus of the lateral ventricles

The choroid plexus in the lateral ventricles became visible during week 8 as tiny echogenic areas (Figure 11) within the relatively hypoechogenic hemispheres in 16 embryos (53%). They were regularly detectable at 9 weeks 4 days (Figure 12). They showed rapid linear growth, similar to the hemispheres, and soon filled most of the ventricular cavities.

Of a total of 145 examinations, we achieved 108 measurements of the length, 108 of the width, and 108 of the height. At 9 weeks 0 days the mean length, width and height of the choroid plexuses were 2.8 mm (1.2–5.1 mm), 1.3 mm (0.5–2.4 mm), and 1.8 mm (0.9–3.0 mm), respectively. At 12 weeks 0 days, the mean length was 12.7 mm (8.9–17.2 mm), the mean width 4.4 mm (2.8–6.3 mm), and the height 5.4 mm (3.7–7.3 mm) (Figure 16).

## Diencephalon

At week 7, a broad connection had developed between the diencephalon, the mesencephalon and the lateral ventricles. In the sagittal plane, the height of the cavity of the diencephalon (future third ventricle) was slightly higher than that of the mesencephalon (future Sylvian aqueduct) (Figures 5 and 8). Thus, the passage between the cavities of the diencephalon and the mesencephalon was indicated. The diencephalon was detectable in 17 embryos (59%) during week 7, and in all of them before 9 weeks. The future foramina of Monro were wide during week 7 (Figure 6). They became more accentuated during week 8 (Figures 7 and 9). At 9 weeks, a distinct isthmus had developed between the cavity of the mesencephalon and the third ventricle (Figure 13). The wall of the diencephalon, initially very thin, thickened considerably starting from week 8 to 9 (Figure 14). After an initial increase, the width of the third ventricle became narrower towards the end of the first trimester.

In a total of 145 examinations, we achieved 72 measurements of the length, 133 of the width, and 73 of the height. The mean length of the diencephalon at 7 weeks 3 days was 2.1 mm (0.8–3.4 mm) increasing to 3.6 mm (2.3–4.9 mm) at 10 weeks 0 days. The reduction of the mean width was linear, initially 1.2 mm

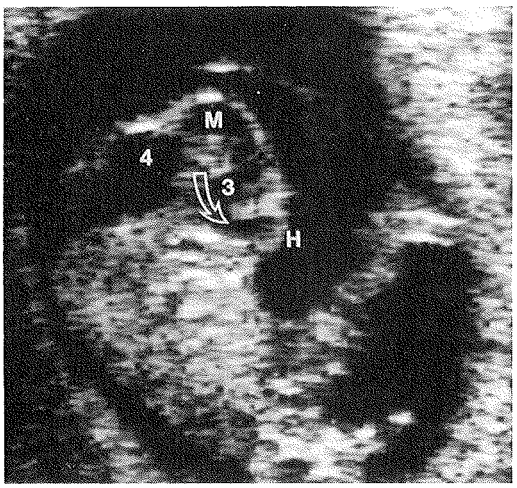


**Figure 10** Oblique parasagittal section in the same embryo (crown–rump length, 17 mm) as in Figures 8 and 9 through the rhombencephalon (4), mesencephalon (M), diencephalon (3), and hemisphere (H). The circle-like hemisphere should not be misinterpreted as the orbit

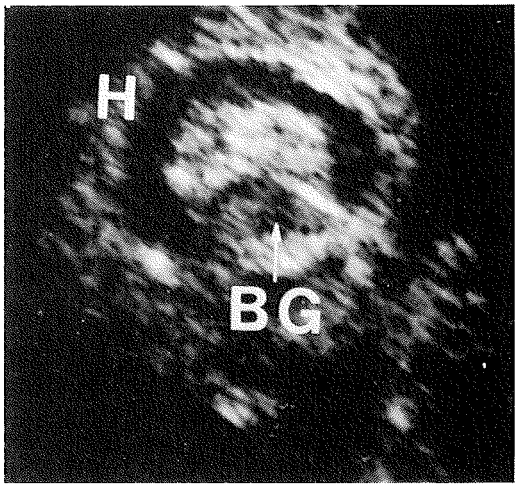


**Figure 12** Parasagittal section through the head (crown–rump length, 30 mm). Above the basal ganglia (BG) lies the hyperechogenic choroid plexus. The surrounding hypoechogenic C-formed area represents the cortex including the cavity of the lateral ventricle

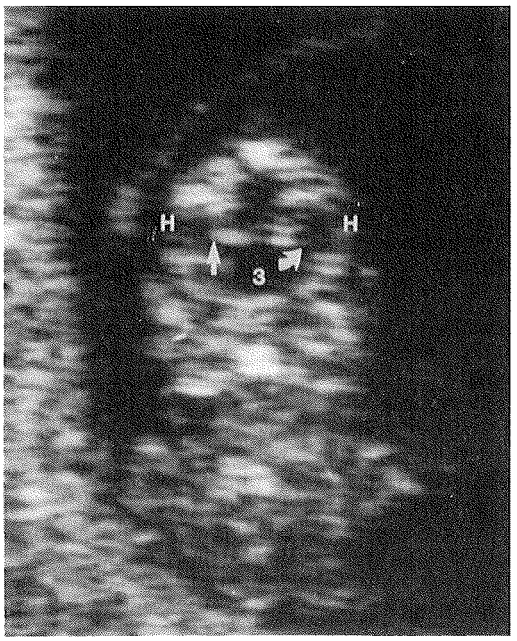


**Figure 11** Coronar section through the third ventricle (3) and hemispheres (H) (crown–rump length, 18 mm). Curved arrow, foramen of Monro; straight arrow, choroid fold, the first sign of the developing choroid plexus

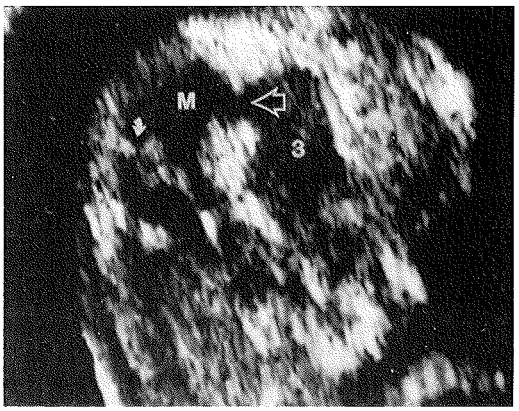


**Figure 13** Sagittal section through the brain (crown–rump length, 33 mm). The same structures as sketched in Figure 2 are identifiable. Mesencephalon (M); curved bold arrow, 'Blindsäcke'; open arrow, isthmus prosencephali; diencephalon (3)

(0.7–1.7 mm) at 7 weeks 0 days, decreasing to 0.8 mm (0.3–1.3 mm) at 12 weeks 0 days. The mean height was 1.1 mm (0.3–1.8 mm) at 7 weeks 0 days, and increased to 1.9 mm (1.2–2.6 mm) at 10 weeks 0 days (Figure 17).

## Mesencephalon

The cavity of the mesencephalon could be recognized during week 7 as a thin arched tube in 17 embryos (57%) (Figure 5). By week 8, it was regularly identified. It straightened considerably during the following weeks (Figures 8, 9 and 13). The isthmus rhombencephali was always distinct, while initially the connection to the diencephalon was wide (Figures 5 and 8). At the end of the embryonic period (9–10 weeks), the border between the di- and mesencephalon had developed into an 'isthmus prosencephali' (Figure 13). During the whole period, the cavity remained relatively large (Figure 14), especially

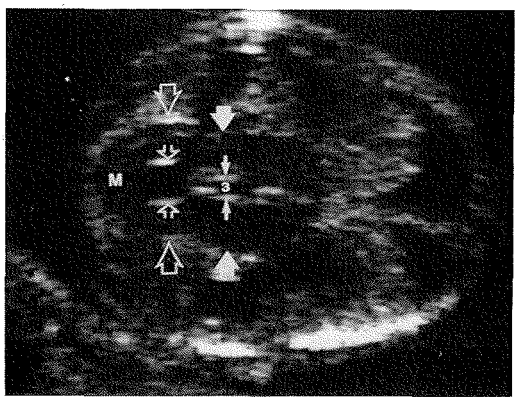


**Figure 14** Transverse section through the brain (crown–rump length, 49 mm). Diencephalon, bold arrows, and its narrow third ventricle, small arrows (3), and through the mesencephalon, large open arrows (M), with its wide cavity, small open arrows

the posterior part. The height and the width were about the same size.

In a total series of 145 examinations, we achieved 134 measurements of the length, 133 of the width, and 136 of the height. The mean length increased from 2.8 mm (1.7–3.9 mm) at 7 weeks 2 days to 4.8 mm (3.7–5.9 mm) at 12 weeks 0 days. At 7 weeks 2 days, the mean width was 1.3 mm (0.7–1.8 mm) and the mean height was 1.2 mm (0.6–1.7 mm). The width increased to 1.7 mm (1.2–2.3 mm) at 12 weeks 0 days, and the height to 2.0 mm (1.4–2.5 mm) (Figure 18).

## Pregnancy outcome

The 29 women included in the study gave birth to 16 male and 13 female children with a mean gestational age of 40 weeks 0 days (range 37 weeks 2 days–42 weeks 1 day postmenstrual age). The mean birth weight was 3610 g (range 2610–4890 g). All but two delivered spontaneously. These two were delivered by Cesarean section at 40 weeks 2 days and 40 weeks 4 days, respectively, because of mechanical disproportion. All children proved to be healthy.

## Intraobserver analysis

For structures with a maximum size of < 4 mm (width and height of the diencephalon and of the mesencephalon), the standard deviation of the differences between repeated measurements was on average 0.27 (range, 0.19–0.36). For structures with a maximum size between 4 mm and 10 mm (length of the mesencephalon and diencephalon, width and height of the hemisphere and its choroid plexus), the standard deviation of the differences was on average 0.46 (range, 0.33–0.59). For both structures with a maximum size ≥ 10 mm (length of the hemisphere and the choroid plexus), the standard

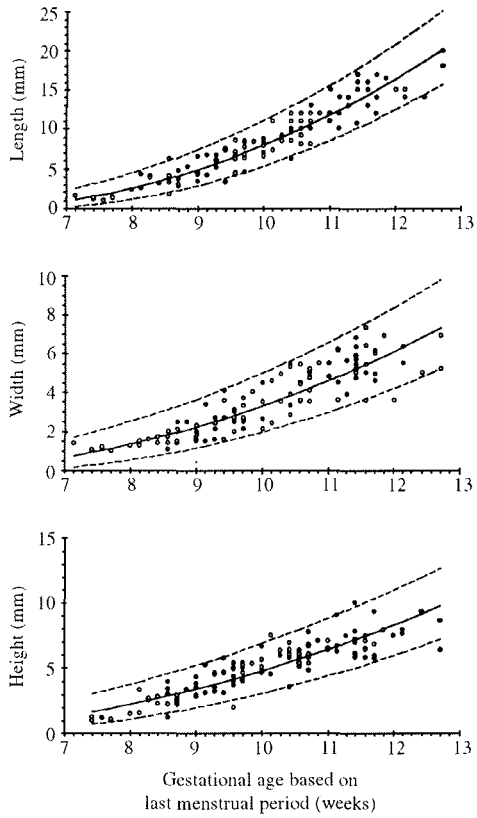


**Figure 15** The length, width and height of the hemisphere, showing the regression line with lower and upper 95% prediction intervals

deviation of the differences was 0.59. The largest absolute difference between repeated measurements was 1.6 mm, which was 17% of the total size of the measured structure (9.2 mm hemisphere length, crown–rump length 46 mm). For structures below 3 mm, the largest absolute difference was 0.9 mm, which was 51% of the total size of the measured structure (1.8 mm hemisphere width, crown–rump length 18 mm). The limits of agreement of the intraobserver study are given in Table 1. The limits of agreement for the length of the hemisphere, the choroid plexus and diencephalon showed a range of ≥ 2 mm. The lowest range was found in the limits of agreement of the diencephalon width.

# DISCUSSION

Detailed knowledge about normal development is a prerequisite for the first-trimester evaluation of pregnancy using ultrasound. Classical human embryology is based on cross-sectional evaluations of aborted embryos. Our intention was to make a thorough longitudinal description of embryonic growth and development *in*

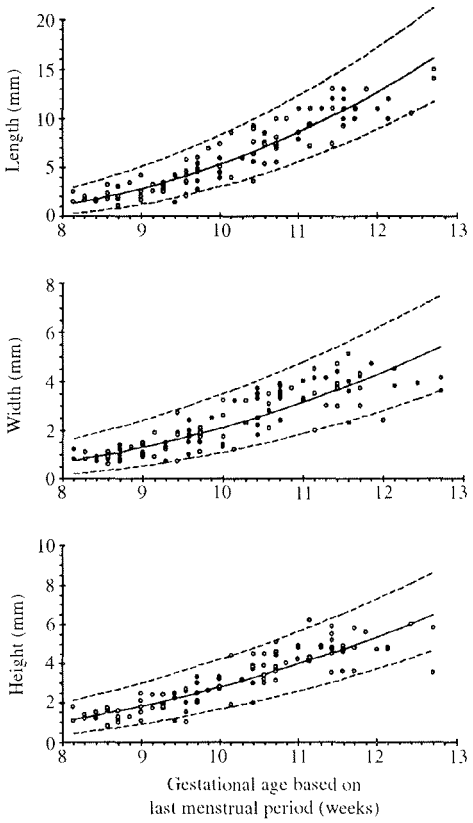


**Figure 16** The length, width and height of the choroid plexus in the lateral ventricle, showing the regression line with lower and upper 95% prediction intervals

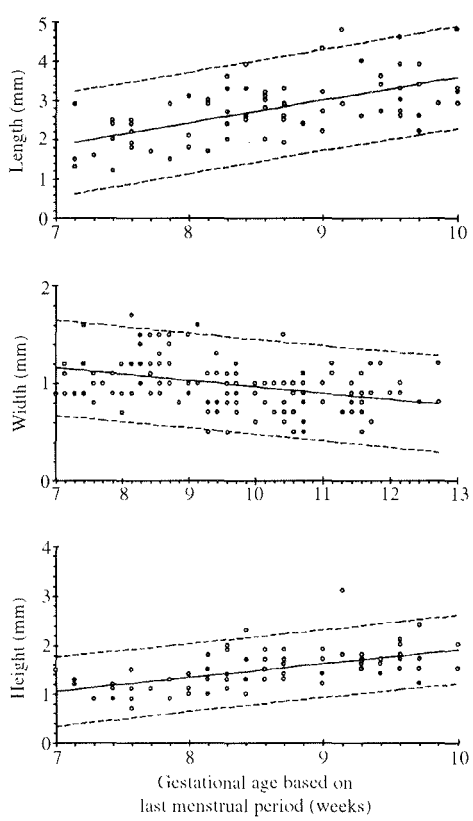


**Figure 17** The length, width and height of the diencephalon, showing the regression line with lower and upper 95% prediction intervals

*vivo*. The presented data of the embryonic brain have shown that such an evaluation is possible, using modern high-resolution ultrasound equipment.

The embryo undergoes certain developmental steps which are expressed in stages. Streeter introduced the 23 embryonic 'horizons'[8], a staging system based on characteristic developmental features of the embryos in the Carnegie Collection of Embryology at Johns Hopkins University. Streeter's work documented the accuracy of embryonic development. His dating system of the embryonic development was later revised by O'Rahilly and Gardner into the 23 'Carnegie stages'[9,10]. This system is generally accepted today for the dating of embryos. The Carnegie staging system starts at fertilization and ends at 10 weeks. In 1981, Moore and colleagues analyzed the anatomical features of 249 well-staged embryos in the Carnegie Collection of Embryology[11]. Of these, 276 were from pregnancies in which the last menstrual period was known. The results supported the concept that embryos of approximately identical size and age go through the same developmental stages and that normal anatomical structures develop within a short space of time.

The central nervous system develops from the ectodermal neural plate. Closure of the caudal neuropore at Carnegie stage 12, at 5 weeks 6 days, heralds the onset of the ventricular system[8,12,13] which, on its cranial pole, divides into five brain regions before the end of week 6: the telencephalon and the diencephalon derive from the prosencephalon (forebrain), the mesencephalon (midbrain) remains undivided, and the metencephalon (future cerebellum and pons) and the myelencephalon (medulla oblongata) derive from the rhombencephalon (hindbrain).

Several papers have been published recently about ultrasound evaluation of embryonic development. In all of these studies[1,5,14] 6.5 MHz transducers have been used. Two of these papers deal exclusively with brain development, one presents a cross-sectional descriptive ultrasound study[14], while the other is an overview article[5]. All studies demonstrated the possibilities of studying embryonic central nervous system structures using the transvaginal approach, and showed that the features changed specifically from week to week. Still, there were divergences in interpreting the appearance and significance of

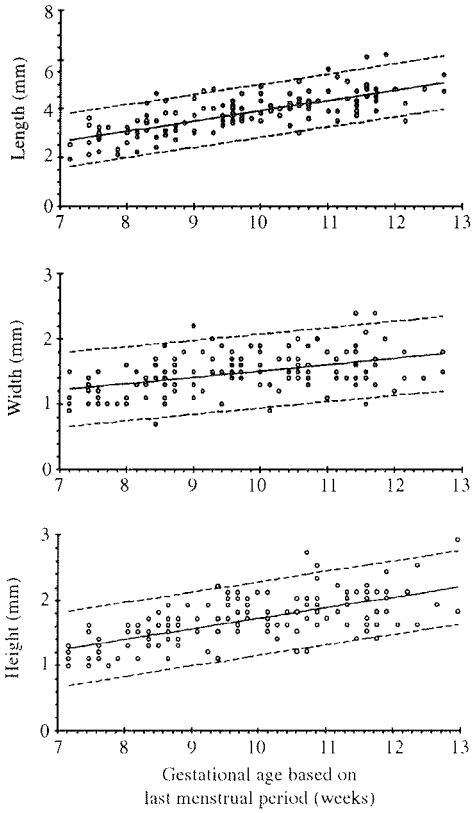


**Figure 18** The length, width and height of the mesencephalon, showing the regression line with lower and upper 95% prediction intervals

certain structures seen by ultrasound, such as the so-called 'single ventricle'[1,5,14].

Acceptable pictures of structures of the central nervous system can be obtained from week 7 by using high-frequency transvaginal ultrasound (7.5 MHz). The rhombencephalon, mesencephalon, diencephalon and telencephalon could all be distinguished and measured early in pregnancy. When the growth of the cerebral cavities is evaluated, it should be taken into consideration that their development starts at about 6 weeks. The cavities could not be visualized before the following week 7. So these structures must have a substantial growth during week 6.

At Carnegie stage 14 (6 weeks 4 days), the future *cerebral hemispheres* appear as bilateral evaginations[8,10,12,15] of the telencephalon impar. At Carnegie stages 17–18 (7 weeks 6 days–8 weeks 4 days), the interventricular foramina (future foramina of Monro) become relatively narrow[12] (Figure 10). In the present study, the small hemispheres were distinguished in an oblique transverse section during week 7 (Figure 6). One week later the hemispheres reached a considerable size (Figures 7, 10 and 11), at which time they might be misinterpreted as the orbits. The walls of the hemispheres

**Table 1** Intraobserver study ($n$ = 17)

| | *Limits of agreement* | |
|---|---|---|
| | *Lower limits* (mm) | *Upper limits* (mm) |
| Hemisphere | | |
| length | −1.0 | 1.4 |
| width | −0.6 | 1.3 |
| height | −0.8 | 1.2 |
| Lateral choroid plexus | | |
| length | −0.9 | 1.5 |
| width | −0.6 | 0.9 |
| height | −0.6 | 0.7 |
| Diencephalon | | |
| length | −1.4 | 1.0 |
| width | −0.4 | 0.4 |
| height | −0.5 | 0.7 |
| Mesencephalon | | |
| length | −0.4 | 0.9 |
| width | −0.5 | 0.6 |
| height | −0.8 | 0.7 |

have a thickness of about 1 mm at the end of the first trimester[16]. Since it was difficult to differentiate between the ventricular cavity and the wall of the cortex, the hypoechogenic wall was generally included in the ultrasound measurements. At Carnegie stages 21–23 (9 weeks 3 days–10 weeks 1 day), the lateral ventricles have become C-shaped (Figure 12). The posterior horns do not develop before the second trimester. O'Rahilly and Müller analyzed the size of the central nervous system structures in four embryos which were 10 weeks old[12], and found the distance from the anterior horn to the future posterior horn to be 9.5 mm with a range from 7.3 mm to 10.9 mm. At 10 weeks 0 days, we found a mean length of 7.9 mm with a 95% prediction interval of 5.3–11.1 mm.

The *choroid plexus of the lateral ventricle* develops from a choroid fold, and can be observed in Carnegie stage 18 (8 weeks 2 days–8 weeks 4 days). The growth is rapid, and at Carnegie stage 23 (10 weeks 0 days–10 weeks 1 day) the choroid plexus occupies approximately one-third or more of the lateral ventricle[12] (Figure 12). By ultrasound it was visible during week 8, and showed a growth corresponding to the growth of the hemisphere.

The posterior part of the forebrain is called the *diencephalon*. Its cavity, the third ventricle, is in continuity with the anterior part of the forebrain. The epithalamus, ventral and dorsal thalamus and hypothalamus are present at Carnegie stage 15 (6 weeks 5 days–7 weeks 1 day), but the wall is still thin at Carnegie stage 17 (7 weeks 6 days–8 weeks 1 day)[8]. The dorsal thalamus grows rapidly after Carnegie stage 20 (9 weeks 0 days–9 weeks 2 days), and in 80% of the brains the two bulges fuse in the midline, forming a bridge of gray matter across the third ventricle called the massa intermedia, and almost fill the third ventricle by 14–15 weeks[17]. The cavity of the diencephalon is easily seen by ultrasound during the embryonic period from week 7 onwards. Its width decreases slowly during the first trimester. This can be explained by the growth of the

wall of the diencephalon, especially the posterior thalamus. Because of the decreasing width, measurement of the height and the length proved to be more difficult after 9–10 weeks. This phenomenon makes the measurements of height and length of the third ventricle less reliable towards 12 weeks. Therefore we included only measurements of the length and height obtained up until 10 weeks 0 days. It might be more appropriate to estimate the extension of the diencephalon by measuring only the length and height of the whole hypoechogenic diencephalon. The third ventricle must not be misinterpreted as the cavum septi pellucidi. According to the embryological literature, the corpus callosum and cavum septi pellucidi are not developed at the end of the first trimester[18].

The *midbrain* cavity is known as the aquaeductus Sylvii in the adult brain. It is relatively wide throughout the embryonic period proper[12]. Originally, the mesencephalon has thin walls, and its lumen is a continuation of the third ventricle[18], separated from the diencephalon by a slight constriction. At Carnegie stages 22–23 (9 weeks 5 days–10 weeks 1 day), this constriction is found immediately rostral to the midbrain, and is called the isthmus prosencephali, which is easily seen by ultrasound (Figure 13). The border towards the rhombencephalon is the distinct isthmus rhombencephali. The midbrain shows bilateral evaginations at Carnegie stage 19 (8 weeks 5 days–8 weeks 6 days) in the caudal part of the cavity (called 'Blindsäcke' by Hochstetter in 1929)[10,19]. O'Rahilly and collaborators[12] measured the cavity of the mesencephalon, the mesocele, and found a mean size of $2.2 \times 2.5 \times 5.3$ mm in preparations of embryos at Carnegie stage 23 (10 weeks 0 days–10 weeks 1 day). This indicates that the cavity 'clearly is still in no sense a narrow aqueduct'[12]. We found both height and width to be slightly increasing throughout the first trimester. The mean inner diameter at 10 weeks in our study (Carnegie stage 23) was $1.5 \times 1.6 \times 3.9$ mm.

In earlier publications, a large cavity called 'single ventricle' appearing during weeks 7 and 8 in the cranial pole of the embryo has been interpreted as the telencephalon, which later divides into the lateral ventricles[1,2,4,5]. In another study, the 'single ventricle' was thought to be the rhombencephalic cavity[3]. From our experience, we consider the rhombencephalon and its cavity to be the largest part of the brain in the embryonic period, lying on top of the embryo during week 7 (Figures 5, 8–10). We found the diencephalon with a width of about 1 mm at the end of week 8 (Figures 8 and 11) as a large hypoechogenic area with the hemispheres lying parasagittally to it (Figures 7, 10 and 11). A study on the size of embryonic and fetal brain compartments was presented by Jenkins as early as in 1921[20]. In the 4.3 mm embryo, the rhombencephalon accounted for 54.4% of the brain, the mesencephalon for 14.3%, the diencephalon for 24.3%, and the telencephalon for 7.0%. In the 25 mm embryo (9 weeks 3 days), these proportions have changed into the rhombencephalon, 36.6%, mesencephalon, 14.8%, diencephalon, 19.8%, and telencephalon, 28.8%.

In the future, sonoembryology will become an important part of prenatal diagnosis. The detailed knowledge that sonoembryology can provide about the normal brain and its altered development carries the potential of diagnosis of conditions like acrania/anencephaly, holoprosencephaly, and anterior encephalocele earlier than is usual today. For example, an alobar holoprosencephaly, which results from failure of the telencephalon impar to divide at 7 weeks[9], theoretically should be detectable during weeks 7–8. It is likely, too, that conditions such as anencephaly or acrania may be detectable at the end of the embryonic period between 8 and 10 weeks. In 1989, Rottem and colleagues suspected a central nervous system malformation in a 9½-week-old embryo: 2 weeks later they described it as an acrania with open cervical spine[21]. We cannot expect to diagnose hydrocephaly caused by acquired aqueduct stenosis before the second trimester. But it is possible that the inherited X-linked aqueduct stenosis could be manifest in the embryonic period if the mesocele is significantly narrower than demonstrated in the present study.

The design of a longitudinal study requires repeated transvaginal examinations of healthy women in early pregnancy. Considering the difficulties of recuitment and the discomfort this procedure imposed on healthy women, we limited the number of participants. We chose to analyze the data cross-sectionally. Serial measurements on an individual embryo are highly correlated. Thus, the effective sample size in this study was likely to be smaller than the total number of observations[22], and therefore the prediction intervals should be interpreted with caution. In a more rigorous statistical analysis, a longitudinal approach would be adopted.

In our study, the objects of interest were very small, often near the limit of the ultrasound resolution and measurability. This was reflected in the intraobserver study. We found small differences, but relatively large limits of agreement. Thus, the reproducibility of the measurement of these small structures was relatively poor, and averaging of repeated measurements seems to be the best way to achieve reliable values.

We conclude that is it possible to study the embryonic development *in vivo* longitudinally by ultrasound. Formation of the central nervous system structures, their size, growth and developmental movements may be evaluated, and growth charts can be established. Correlated to the age based on the last menstrual period, there seems to be a strict regulation in the brain's developmental pattern. The cerebral hemispheres are visible soon after their formation at the beginning of week 7. The choroid plexuses of the lateral ventricles always become visible during week 9. The third ventricle and the midbrain cavity are detectable before 9 weeks 0 days. The third ventricle reaches a maximum width during week 7. It becomes narrow towards the end of the embryonic period. The mesencephalic cavity is relatively large throughout the first trimester. Initially, it is situated in the anterior part of the embryonic head. The deflection of the brain 'transports' the mesencephalic cavity to the top and later to the middle of the head.

## ACKNOWLEDGEMENT

Mrs Nancy Lea Eik-Nes revised the manuscript.

## REFERENCES

1. Timor-Tritsch, I. E., Peisner, D. B. and Raju, S. (1990). Sonoembryology: an organ-oriented approach using a high-frequency vaginal probe. *J. Clin. Ultrasound*, **18**, 286–98
2. Timor-Tritsch, I. E., Farine, D. and Rosen, M. G. (1988). A close look at early embryonic development with the high-frequency transvaginal transducer. *Am. J. Obstet. Gynecol.*, **159**, 676–81
3. Cullen, M. T., Green, J., Whetham, J., Salafia, C., Gabrielli, S. and Hobbins, J. C. (1990). Transvaginal ultrasonographic detection of congenital anomalies in the first trimester. *Am. J. Obstet. Gynecol.*, **163**, 466–76
4. Bree, R. L. and Marn, C. S. (1990). Transvaginal sonography in the first trimester: embryology, anatomy, and hCG correlation. *Sem. Ultrasound, CT, MR*, **11**, 12–21
5. Achiron, R. and Achiron, A. (1991). Transvaginal ultrasonic assessment of the early fetal brain. *Ultrasound Obstet. Gynecol.*, **1**, 336–44
6. Altman, D. G. (1991). *Practical Statistics for Medical Research*, pp. 132–45. (London: Chapman and Hall)
7. Bland, J. M. and Altman, D. G. (1986). Statistical methods for assessing agreement between two methods of clinical measurement. *Lancet*, **1**, 307–10
8. Streeter, G. L. (1948). Developmental horizons in human embryos. *Contributions to embryology, No. 211.* Carnegie Institute of Washington Publications, **32**, 133–203
9. O'Rahilly, R. and Gardner, E. (1977). The developmental anatomy and histology of the human central nervous system. In Vinken, R. J. and Bruyn, G. W. (eds.) *Handbook of Clinical Neurology: Congenital Malformations of the Brain and Skull*, pp. 15–40. (Amsterdam: Myrianthopoulos NC)
10. O'Rahilly, R. and Gardner, E. (1971). The timing and sequence of events in the development of the human nervous system during the embryonic period proper. *Z. Anat. Entwickl.-Gesch.*, **134**, 1–12
11. Moore, G. W., Hutchins, G. M. and O'Rahilly, R. (1981). The estimated age of staged human embryos and early fetuses. *Am. J. Obstet. Gynecol.*, **139**, 500–6
12. O'Rahilly, R. and Müller, F. (1990). Ventricular system and choroid plexuses of the human brain during the embryonic period proper. *Am. J. Anat.*, **189**, 285–302
13. O'Rahilly, R., Müller, F., Hutchins, G. M. and Moore, G. W. (1984). Computer ranking of the sequences of appearance of 100 features of the brain and related structures in staged human embryos during the first 5 weeks of development. *Am. J. Anat.*, **171**, 243–57
14. Timor-Tritsch, I. E., Monteagudo, A. and Warren, W. B. (1991). Transvaginal ultrasonographic definition of the central nervous system in the first and early second trimesters. *Am. J. Obstet. Gynecol.*, **164**, 497–503
15. O'Rahilly, R., Müller, F. and Bossy, J. (1982). Atlas des stades du développement du système nerveux chez l'embryon humain intact. *Arch. Anat. Hist. Embr. norm et exp*, **65**, 57–76
16. Kostovic, I. (1990). Zentralnervensystem. In Hinrichsen, K. V. (ed.) *Humanembryologie, Lehrbuch und Atlas der vorgeburtlichen Entwicklung des Menschen*, pp. 381–448. (Berlin: Springer Verlag)
17. Lemire, R. J. (1975). Deep cerebral nuclei. In Lemire, R. J. (ed.) *Normal and Abnormal Development of the Human Nervous System*, pp. 169–95. (Hagerstown, Maryland: Harper & Row)
18. England, M. A. (1988). Normal development of the central nervous system. In Levene, M. I., Bennett, M. J. and Punt, J. (eds.) *Fetal and Neonatal Neurology and Neurosurgery*, pp. 3–27. (Edinburgh: Churchill Livingstone)
19. Müller, F. and O'Rahilly, R. (1990). The human brain at stages 18–20, including the choroid plexuses and the amygdaloid and septal nuclei. *Anat. Embryol.*, **182**, 285–306
20. Jenkins, G. B. (1921). Relative weight and volume of the component parts of the brain of the human embryo at different stages of development. *Contr. Embryol. Carneg. Instn.*, **13**, 41–60
21. Rottem, S., Bronshtein, M., Thaler, L. and Brandes, J. M. (1989). First trimester transvaginal sonographic diagnosis of fetal anomalies. *Lancet*, **1**, 444–5
22. Altman, D. G. and Chitty, L. S. (1994). Charts of fetal size. 1. Methodology. *Br. J. Obstet. Gynaecol.*, **101**, 29–34

# Paper II

**Harm-Gerd Blaas, Sturla H. Eik-Nes, Torvid Kiserud, Leif Rune Hellevik. Early development of the hindbrain: a longitudinal ultrasound study from 7 to 12 weeks of gestation. Ultrasound Obstet Gynecol 1995; 5:151–60**

*Ultrasound Obstet. Gynecol. 5 (1995) 151–160*

# Early development of the hindbrain: a longitudinal ultrasound study from 7 to 12 weeks of gestation

*H.-G. Blaas, S. H. Eik-Nes, T. Kiserud and L. R. Hellevik*

Department of Obstetrics and Gynecology, National Center for Fetal Medicine, Trondheim University Hospital, Norway

Key words: TRANSVAGINAL ULTRASOUND, CENTRAL NERVOUS SYSTEM, EMBRYONIC BRAIN DEVELOPMENT, SONOEMBRYOLOGY, FIRST TRIMESTER

## ABSTRACT

*Twenty-nine healthy pregnant women were examined by transvaginal ultrasound to evaluate embryonic development* in vivo *between 7 and 12 weeks of gestation. The rhombencephalon with its fourth ventricle, the cerebellum and the choroid plexuses of the fourth ventricle were identified and measured. The cavity of the rhombencephalon, the future fourth ventricle, was always visible from 7 weeks, initially lying superiorly in the head of the embryo. The cerebellum and the choroid plexuses of the fourth ventricle became distinguishable during week 8. The volume of the rhombencephalic cavity was estimated. The shape and size of these rhombencephalic structures, their position in relation to each other and their relation to other brain structures changed specifically during the embryonic and early fetal period. This sonoembryological development corresponded to the descriptions in classical embryological literature.*

## INTRODUCTION

Since imaging ultrasound was introduced, one of its main fields has been the evaluation of the growing fetus. Robinson's classical crown–rump length growth curve from 1975, obtained with compound scanner measurements[1], is still used to date the embryo and the fetus in early pregnancy. The introduction of real-time ultrasound, first the abdominal and later the transvaginal application, improved the assessment of early pregnancy considerably. The technical progress in recent years has led to the development of high-frequency ultrasound equipment that now enables us to approach new diagnostic frontiers.

As described by the classical embryologists, the developing brain with its five secondary vesicles is a striking structure during embryonic life[2–7]. Sonoembryologists have tried to demonstrate this development using ultrasound and have given a detailed description of the embryonic brain[8–13]. Initially there have been divergences in interpreting the early development of the human brain ventricles as seen with ultrasound. The 'single' ventricle that appears during week 7 was interpreted by some authors as the vesicle of the prosencephalon[8–10], while others claimed that it represented the cavity of the rhombencephalon[11].

The aim of this prospective longitudinal ultrasound study was to describe the early development of the brain, with emphasis on the hindbrain, by measuring successively visible structures, such as the rhombencephalic cavity, the choroid plexuses of the fourth ventricle and the cerebellum in the living embryo.

## SUBJECTS AND METHODS

Thirty-six pregnant women were recruited for a longitudinal vaginal ultrasound study, according to a protocol approved by the regional committee of ethics[12]. Written consent was obtained from each woman.

The women who participated in the study had to fulfil the following inclusion criteria: regular menstruation, no hormonal therapy taken 3 months before the pregnancy, non-smoker, natural single pregnancy, and no bleeding during the pregnancy. Women with conditions that might influence the embryonic growth, such as uterine anomalies, subsequent development of diabetes and hypertension were not included. The development of diabetes or pre-eclampsia, or the delivery of a preterm and/or a growth-retarded infant were criteria for exclusion. Five women were excluded (three early pregnancy losses, one bleeding during week 9, one preterm delivery at 36 weeks due to pre-eclampsia), and two women decided to discontinue after the first examination. Thus

Correspondence: Dr H.-G. Blaas, Department of Obstetrics and Gynecology, National Center for Fetal Medicine, Trondheim University Hospital, N-7006 Trondheim, Norway



Received 18–8–94
Revised 3–1–95
Accepted 5–1–95

29 women were included in the study (mean age 28 years, range 19–38).

A high-frequency scanner (Dornier AI 3200) with a 7.5-MHz transvaginal probe was used for all examinations. The emitted energy was set to 0.58 mW/cm$^2$ SPTA *in situ*. The magnification on the screen was × 3.3.

The first examination was performed between 7 and 8 completed gestational weeks according to the last menstrual period. A total of five examinations was carried out in each pregnancy, with an interval of approximately 7 days. Each examination lasted for 20–30 min.

In order to limit the examination time, only one measurement per target organ was taken. A routine fetal examination using ultrasound was additionally performed at 18 weeks (range 16–20).

The brain structures of the embryo were visualized and measured, as shown in Figures 1–3. The planes for the measurement of the length and width of the hindbrain cavity are shown in Figures 1 and 2. They follow the neuroaxis as it bends: during week 7, the section is horizontal (Figure 1), gradually tilting to a coronal section at the end of the embryonic period (Figure 2). In the same sections, the choroid plexuses of the fourth ventricle and the cerebellar thickenings were identified and measured. In the sagittal mid-line section (Figures 1 and 3), the depth of the rhombencephalic cavity was measured from the pontine flexure to the roof of the fourth ventricle.

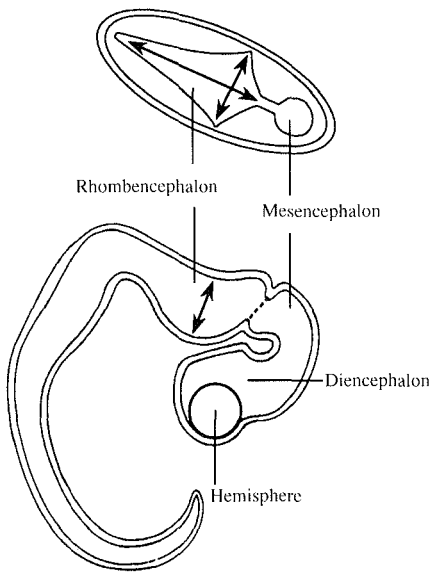


**Figure 1** Sketch of the embryonic central nervous system in a 7-week-old embryo (Carnegie stage 16). The cavities of the rhombencephalon, mesencephalon and diencephalon are shown sagittally; the hemisphere is shown parasagittally. The rhombencephalon and the mesencephalon are delineated in the horizontal plane. The measurements are demonstrated by double-headed arrows

The volume of the rhombencephalon ($V_{Rhomb}$), which has a pyramid-like shape, was estimated by the formula:

$$V_{Rhomb} = \frac{LWD}{6}$$

where $L$ is the length of the rhombencephalic cavity measured in the mid-line from the dividing medulla oblongata to the rhombencephalic isthmus; $W$ is the largest width of either the cavity (in the early period) or the cerebellum; $D$ is the depth of the rhombencephalic cavity.

The volume of the two hemispheres ($V_{2Hem}$), which we used for comparison with the rhombencephalon, was estimated from the basic formula for an ellipsoid:

$$V_{2Hem} = \frac{\pi LWH}{3}$$

where $L$, $W$ and $H$ are the length, width and height of the hemispheres[12]. The growth of the volume of the

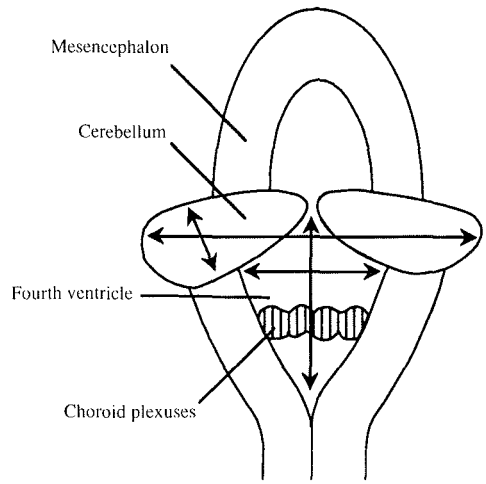


**Figure 2** Coronal section of the head through the rhombencephalon and posterior part of the mesencephalon in a 10-week-old fetus, showing the measurements of the cerebellar hemispheres and the cavity of the rhombencephalon

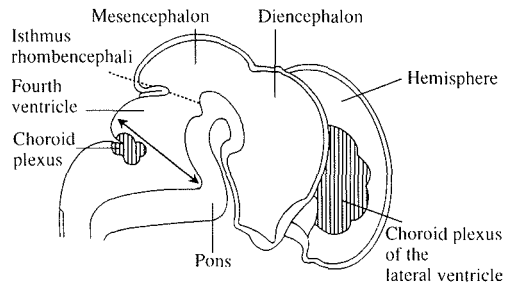


**Figure 3** Sketch of the sagittal plane through the brain at 10 weeks (Carnegie stage 23), including the parasagittal hemisphere. The double-headed arrow indicates the measurement of the depth of the rhombencephalon

rhombencephalon was compared with that of both hemispheres together. A cubic root transformation was used, and the regressions were shown in a logarithmic graph.

Following embryological nomenclature, we called the conceptus younger than 10 weeks 0 days, 'embryo', and the older conceptus, 'fetus'. All statements of time are given in completed weeks and days based on the last menstrual period. The measurements are given as predicted mean value (lower and upper 95% prediction limits).

### Statistical evaluation

Cross-sectional regression analysis was used to examine the associations between the measured values and gestational age. The regressions and the normal distribution of the residuals were evaluated by the Kolmogorov–Smirnov one-sample test, the $\chi^2$ test of goodness of fit (STATISTICA, StatSoft), and the Shapiro Francia W′ test in order to determine the best reference ranges[14].

### Intraobserver study

We evaluated the reproducibility of our measurements by an intraobserver study of 42 pregnant women who did not participate in the longitudinal study. The size of the measured embryos varied from 10 mm (7 weeks 2 days) to 57 mm (11 weeks 6 days), mean 27 mm (9 weeks 4 days). All measurements were recorded on video print pictures. The participants were scanned, then left the examination room for about 5 min before they were rescanned. Limits of agreement (mean difference ± 2 SD) for intraobserver measurements were calculated[15].

## RESULTS

The cavity of the rhombencephalon (Figure 4) was always visible from 7 weeks 0 days on. It then had a well-defined rhombic shape in the cranial pole of the embryo (Figure 5). In the following weeks, this rhombic fossa became deeper due to the progressive flexure of the pons (Figure 6). The lateral corners of the rhombencephalic cavity, called the lateral recesses, were easily identified at 7 and 8 weeks (Figure 1). During this period, the distance between these recesses increased (rhomben-


**Figure 5** Horizontal section superior through the head of a 7-week-old embryo (crown–rump length 12 mm). The rhomboid cavity of the future fourth ventricle (4), the isthmus rhombencephali (open curved arrow) and the cavity of the mid-brain (M) can be identified. The yolk sac (Y) has a diameter of about 4 mm

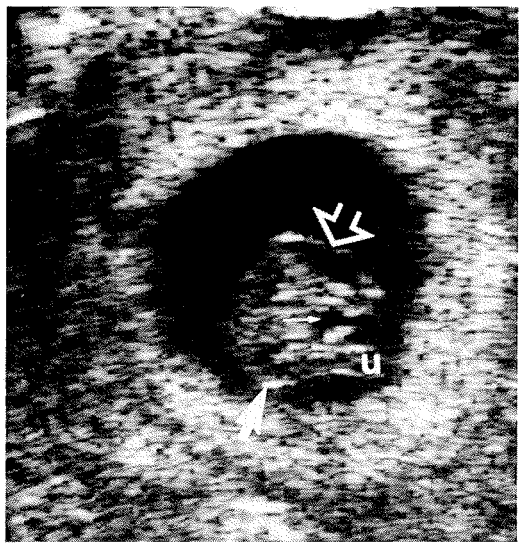


**Figure 4** Sagittal section through a 7-week-old embryo (crown–rump length 10 mm) (see sketch, Figure 1). The open arrow points to the shallow cavity of the rhombencephalon, the small arrow points to the hemisphere, while the bold arrow points to the caudal end of the embryo. The umbilical cord (u) is to the right

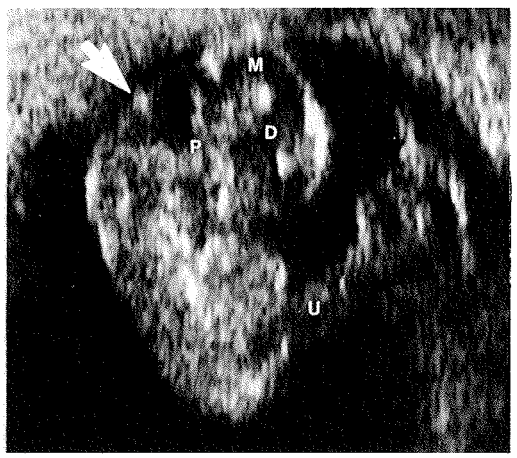


**Figure 6** Sagittal section through an 8-week-old embryo (crown–rump length 18 mm). The mid-brain (M) lies superior; posterior to it, the triangular cavity of the rhombencephalon can be identified. The arrow points to the hyperechogenic choroid plexus in the roof of this cavity. P, pons; D, diencephalon; U, umbilical cord

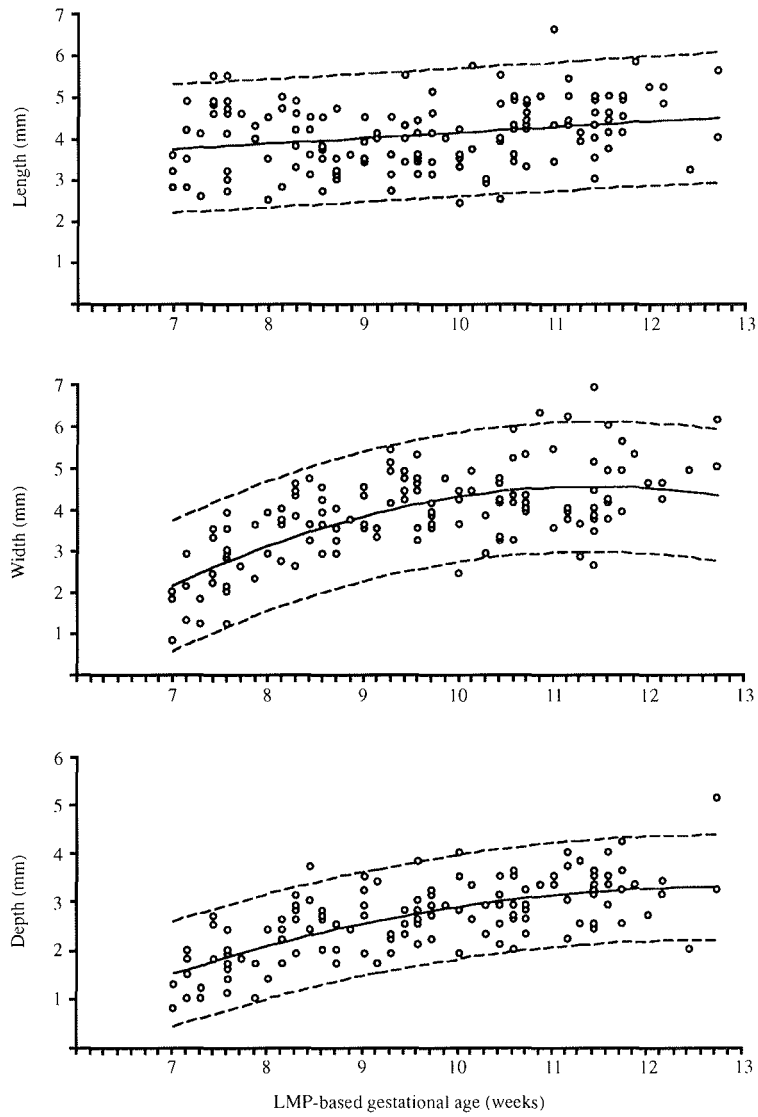


**Figure 7** The length ($n$ = 145), width ($n$ = 145) and depth ($n$ = 141) of the rhombencephalic cavity, showing the regression line with lower and upper 95% prediction intervals. LMP, last menstrual period

cephalic width). Later, during weeks 9 and 10, the lateral recesses often became covered by the enlarging cerebellar hemispheres (Figure 2). Thus, only the central part of the hypoechogenic fourth ventricle, which was divided by the choroid plexuses (see below), was visible and measured.

Measurement of the length of the rhombencephalic cavity ($n$ = 145) showed a relatively large variation with a mean length from 3.8 mm (2.2–5.3 mm) at 7 weeks 0 days to 4.4 mm (2.8–5.9 mm) at 12 weeks 0 days. The mean length increased by only 0.6 mm during 5 weeks (Figure 7). The distribution of the residuals was normal according to the Kolmogorov–Smirnov one-sample test.

With the crown–rump length used as the independent variable, there was an increase and a decrease of the mean length of the cavity from 3.1 mm (crown–rump length 8 mm) to 4.4 mm (crown–rump length 16 mm) and to 2.9 mm (crown–rump length 24 mm) (Figure 8a).

The width of the rhombencephalic cavity ($n$ = 145) increased from 2.1 mm (0.6–3.7 mm) at 7 weeks 0 days to 4.5 mm (2.9–6.1 mm) at 12 weeks 0 days. The data could best be fitted to a polynomial to the second degree (Figure 7).

The depth of the rhombencephalic cavity ($n$ = 141) was 1.5 mm (0.4–2.6 mm) at 7 weeks 0 days. The increase was curvilinear to 3.2 mm (2.2–4.3 mm) at 12 weeks 0

days (Figure 7). These data could also best be fitted to a polynomial to the second degree.

The estimated volume of the rhombencephalon increased slowly. Before week 8, it was larger than the total volume of both hemispheres. The volume of the cerebral hemispheres increased exponentially and exceeded that of the rhombencephalon from week 8 onwards (Figure 8b).

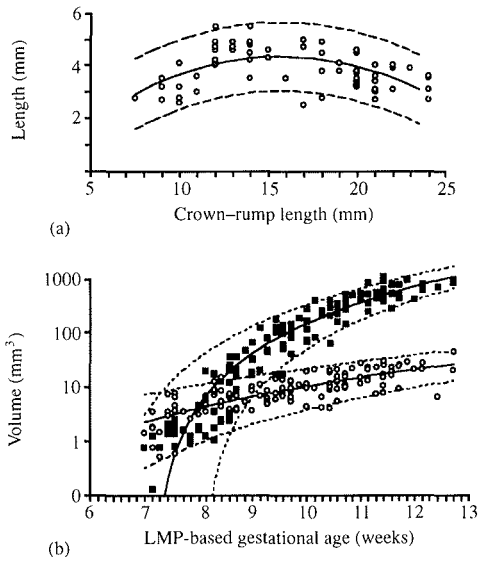


**Figure 8** (a) The length of the rhombencephalon correlated with the crown–rump length of embryos up to 24 mm. (b) The growth of the volume of the rhombencephalon (open circles) and the hemispheres (filled squares) are presented in a logarithmic scale. The regression lines and the lower and upper 95% prediction intervals were obtained by cubic root transformations

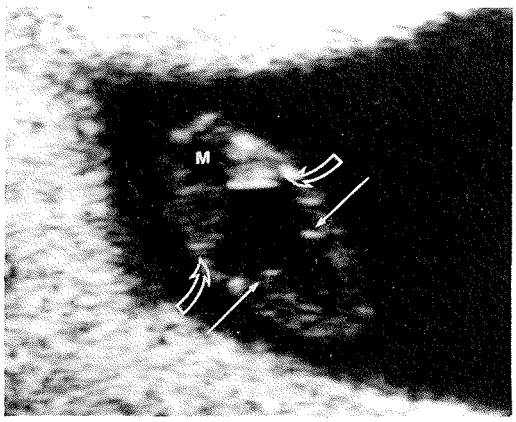


**Figure 9** Section through the rhombencephalon and the mesencephalon of an 8-week-old embryo (crown–rump length, 17 mm; compare with Figure 1). The early choroid plexuses (straight arrows) and the thickenings of the future cerebellum (open curved arrows) are shown. M, mesencephalon

The cerebellum, consisting of the anterior rhombic lips (Figure 9), could be measured in six embryos (20%) before 9 weeks 0 days. Before 10 weeks 0 days, the cerebellum (Figure 10) was distinguishable in 80%, and after 10 weeks 3 days, it could always be seen. The primordia of cerebellar hemispheres were clearly separated in the mid-line during the embryonic period (Figure 10). The cerebellar hemispheres seemed to meet in the mid-line during weeks 11–12 (Figure 11).

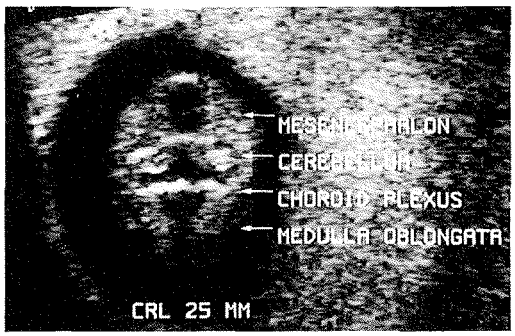


**Figure 10** Coronal section through the hindbrain in a 9-week-old embryo (crown–rump length, CRL 25 mm). The structures are visible as sketched in Figure 2. Both cerebellar hemispheres can be identified. The choroid plexuses traverse the roof of the fourth ventricle, still at a considerable distance from the cerebellar hemispheres

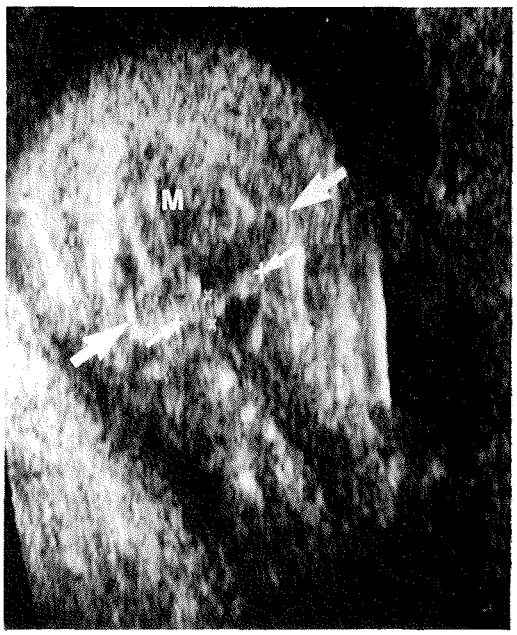


**Figure 11** The same section as in Figure 10; this fetus is 12 weeks old (crown–rump length, 48 mm). The cerebellar hemispheres are hypoechogenic (large arrows), with the hyperechogenic choroid plexuses just beneath the caudal borders. The measurable hypoechogenic cavity of the hindbrain is small, divided by the choroid plexuses. M, mesencephalon

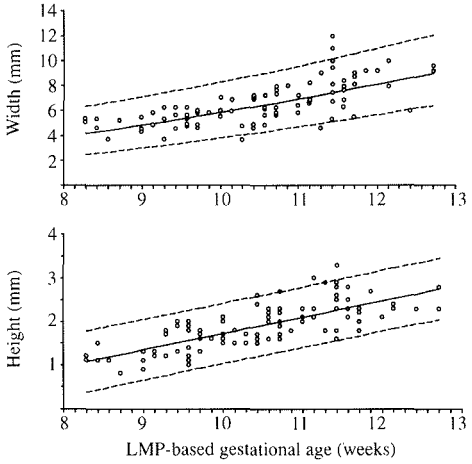


**Figure 12** The width and the height of the cerebellum ($n$ = 93), showing the regression line with lower and upper 95% prediction intervals

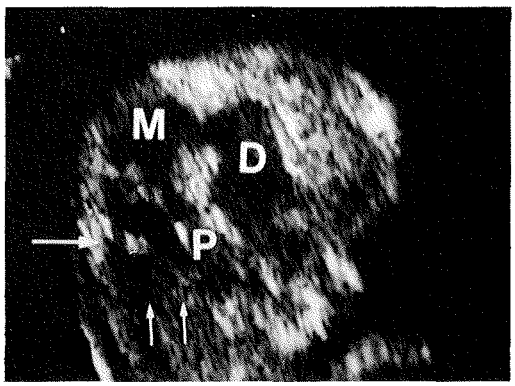


**Figure 13** Sagittal section through the brain of a 10-week-old fetus (crown–rump length, 33 mm). The same structures as sketched in Figure 3 are identifiable. The parallel arrows indicate the posterior and anterior border to the medulla oblongata, which curves anteriorly into the pons (P). The large arrow points to the hyperechogenic choroid plexus in the roof of the fourth ventricle. M, mesencephalon; D, diencephalon

The width of the cerebellum ($n$ = 93) was 4.8 mm (3.0–7.1 mm) at 9 weeks 0 days. At 12 weeks 0 days, the width had increased to 8.1 mm (5.7–11.0 mm). The best fitting regression was obtained by square root transformation (Figure 12).

The height of the cerebellum ($n$ = 93) grew linearly from mean 1.4 mm (0.7–2.1 mm) at 9 weeks 0 days to mean 2.5 mm (1.8–3.2 mm) at 12 weeks 0 days (Figure 12).

The bilateral choroid plexuses of the fourth ventricle became visible in 13 embryos (43%) during week 8 as an echogenic structure in the roof of the rhombencephalon (Figures 6, 9, 10, 11 and 13). After 10 weeks 3 days, they could always be visualized. The first signs of the choroid

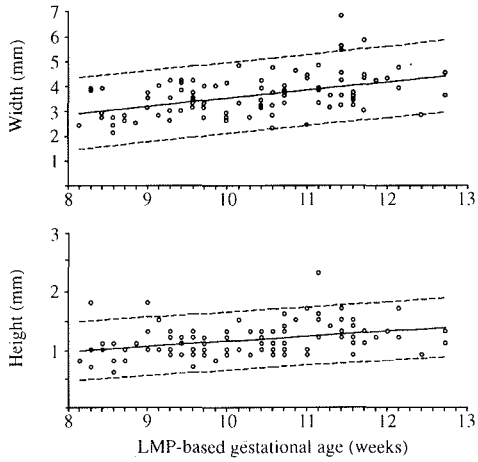


**Figure 14** The width ($n$ = 100) and the height ($n$ = 102) of the choroid plexuses, showing the regression line with lower and upper 95% prediction intervals

plexuses were lateral echogenic areas originating near the branches of the medulla oblongata caudal to the lateral recesses (Figure 9). Within a short time, the choroid plexuses traversed the roof of the fourth ventricle, meeting in the mid-line and dividing the roof into two portions; about two-thirds were located rostrally and one-third caudally. In the sagittal section, the choroid plexuses were identified as an echogenic fold of the roof. The distance between the choroid plexuses and the cerebellum became shorter during the observation period. At the end of the first trimester, the choroid plexuses were found close to the caudal border of the cerebellum.

The width of the choroid plexuses ($n$ = 100) was 3.2 mm (1.8–4.6 mm) at 9 weeks 0 days and increased linearly to 4.1 mm (2.7–5.6 mm) at 12 weeks 0 days (Figure 14).

The height of the choroid plexuses ($n$ = 102) was 1.1 mm (0.6–1.6 mm) at 9 weeks 0 days. The height reached 1.3 mm (0.8–1.8 mm) at 12 weeks 0 days (Figure 14).

Table 1 shows the mean values and the 95% prediction intervals of the rhombencephalic structures, while Table 2 gives the corresponding equations of the regressions, including the prediction limits.

## Pregnancy outcome

Of 29 children (16 males, 13 females), 27 were born spontaneously at a gestational age between 37 weeks 2 days and 42 weeks 1 day postmenstrually (mean 40 weeks 0 days). Two women delivered by Cesarean section because of mechanical disproportion (40 weeks 2 days and 40 weeks 4 days, respectively). The weight ranged from 2610 g to 4890 g (mean 3610 g). All children proved to be healthy and developed normally.

### Intraobserver analysis

The largest absolute difference between two repeated measurements was 1.9 mm in the rhombencephalon width in a fetus with 34 mm crown–rump length, and 1.9 mm in the cerebellum width in a fetus with 50 mm crown–rump length. Table 3 gives the standard deviations of the differences, the maximal measured differences and the limits of agreement. The largest limits of the agreement were found in the width of the rhombencephalon of older embryos and fetuses (crown–rump length of > 25 mm) and in the width of the cerebellum.

**Table 1** Mean size and 95% prediction intervals of the rhombencephalic structures. The gestational age is based on the last menstrual period

| *Gestational age* (weeks/days) | *Rhombencephalon* (mm) | | | *Cerebellum* (mm) | | *Choroid plexuses* (mm) | |
|---|---|---|---|---|---|---|---|
| | *Length* | *Width* | *Depth* | *Width* | *Height* | *Width* | *Height* |
| 7/0 | 3.8 (2.2–5.3) | 2.1 (0.6–3.7) | 1.5 (0.4–2.6) | | | | |
| 8/0 | 3.9 (2.3–5.4) | 3.1 (1.5–4.7) | 2.1 (1.0–3.2) | | | | |
| 9/0 | 4.0 (2.5–5.6) | 3.8 (2.2–5.4) | 2.5 (1.5–3.6) | 4.8 (3.0–7.1) | 1.4 (0.7–2.1) | 3.2 (1.8–4.6) | 1.1 (0.6–1.6) |
| 10/0 | 4.1 (2.6–5.7) | 4.3 (2.7–5.8) | 2.9 (1.8–3.9) | 5.8 (3.8–8.3) | 1.7 (1.0–2.4) | 3.5 (2.1–4.9) | 1.1 (0.6–1.6) |
| 11/0 | 4.3 (2.7–5.8) | 4.5 (2.9–6.1) | 3.1 (2.0–4.2) | 6.9 (4.7–9.6) | 2.1 (1.4–2.8) | 3.8 (2.4–5.2) | 1.2 (0.7–1.7) |
| 12/0 | 4.4 (2.8–5.9) | 4.5 (2.9–6.1) | 3.2 (2.2–4.3) | 8.1 (5.7–11.0) | 2.5 (1.8–3.2) | 4.1 (2.7–5.6) | 1.3 (0.8–1.8) |

**Table 2** Equations of the regressions, including the 95% prediction intervals. The gestational age is based on the last menstrual period

| *Independent variable* | *Dependent variable* | *Equations* |
|---|---|---|
| *Rhombencephalon* | | |
| Gestational age | length | $y = 2.9 + 0.13x \pm 1.96 \cdot 0.78$ |
| Crown–rump length | length | $y = -0.9 + 0.67x - 0.021x^2 \pm 1.96 \cdot 0.65$ |
| Gestational age | width | $y = -11.4 + 2.8x - 0.123x^2 \pm 1.96 \cdot 0.8$ |
| Gestational age | depth | $y = -5.5 + 1.39x - 0.055x^2 \pm 1.96 \cdot 0.54$ |
| *Cerebellum* | | |
| Gestational age | width | $y = (0.2 + 0.22x \pm 1.96 \cdot 0.23)^2$ |
| Gestational age | height | $y = -2.1 + 0.38x \pm 1.96 \cdot 0.35$ |
| *Choroid plexuses* | | |
| Gestational age | width | $y = 0.3 + 0.32x \pm 1.96 \cdot 0.7$ |
| Gestational age | height | $y = 0.3 + 0.085x \pm 1.96 \cdot 0.25$ |
| *Volume* | | |
| Gestational age | rhombencephalon | $y = (0.73 + 0.291x \pm 1.96 \cdot 0.316)^3$ |
| Gestational age | hemispheres | $y = (-13.041 + 1.8368x \pm 1.96 \cdot 0.8178)^3$ |

**Table 3** Intraobserver study ($n$ = 42) CRL, crown–rump length

| | *Crown–rump length* (mm) | *n* | *SD* | *Maximal difference* (mm) | *Limits of agreement* (mm) | |
|---|---|---|---|---|---|---|
| | | | | | *Lower* | *Upper* |
| *Rhombencephalon* | | | | | | |
| Length | 10–57 | 42 | 0.57 | 1.6 | −1.1 | 1.2 |
| | 10–25 | 20 | 0.52 | 1.4 | −1.0 | 1.1 |
| | 26–57 | 22 | 0.62 | 1.6 | −1.2 | 1.3 |
| Width | 10–57 | 42 | 0.62 | 1.9 | −1.2 | 1.2 |
| | 10–25 | 20 | 0.43 | 0.7 | −1.0 | 0.9 |
| | 26–57 | 22 | 0.73 | 1.9 | −1.4 | 1.5 |
| Depth | 10–57 | 40 | 0.35 | 1.1 | −0.7 | 0.7 |
| | 10–25 | 20 | 0.30 | 0.6 | −0.5 | 0.7 |
| | 26–57 | 20 | 0.16 | 1.1 | −0.8 | 0.8 |
| *Cerebellum* | | | | | | |
| Width | | 31 | 0.68 | 1.9 | −1.1 | 1.7 |
| Height | | 31 | 0.25 | 0.6 | −0.5 | 0.6 |
| *Choroid plexuses* | | | | | | |
| Width | | 29 | 0.55 | 1.3 | −0.9 | 1.3 |
| Height | | 29 | 0.24 | 0.8 | −0.5 | 0.5 |

## DISCUSSION

There are few transvaginal ultrasound studies on embryonic brain development. Cullen and colleagues[11] interpreted a single ventricle visible at 8 weeks of gestation as the rhombencephalon. Takeuchi[13], who places the visibility of the fourth ventricle at 7 weeks, used a 7.5-MHz transducer. Timor-Tritsch and colleagues[9] presented a cross-sectional study of 133 observations between 6 and 14 weeks of gestation, examined with a 6.5-MHz transducer. The developing rhombencephalon was clearly imaged at week 8 and later. They described the telencephalic and mesencephalic vesicle during week 7, followed by the occurrence of the myelocele (lower funnelling of the fourth ventricle) at the end of the same week. Both the metocele and the myelocele were registered during week 8. Achiron and Achiron[10] described brain development in a review report, using a 6.5-MHz transducer. They interpreted the single ventricle in the embryonic brain during week 7 as the forebrain, dividing during week 8. We used a 7.5-MHz transducer for ultrasound examinations in a longitudinal study of the fore- and mid-brain development[12] and identified all fore- and mid-brain compartments as the mesencephalon, the diencephalon, and the divided hemispheres during week 7. From the beginning of week 7, we could follow the development of what initially was the largest cavity in the cranial pole of the embryo. We showed that it represented the fourth ventricle.

The objects of interest were very small. This study showed that the hindbrain structures in the coronal section were difficult to define, partly due to the reduced possibility of obtaining the optimal plane by the transvaginal approach. Thus, as expected, we found small absolute differences, but relatively large limits of agreement in our intraobserver study (Table 1). The reproducibility of the measurements of these small structures was poor, and averaging repeated measurements seems to be the best way to achieve acceptable values.

Embryologists differentiate between 23 stages of development (Carnegie stages) from fertilization to 10 weeks 1 day (postmenstrual)[3,4]. During this period, the conceptus is called an embryo. According to this staging system, the closure of the caudal neuropore of the neural tube at Carnegie stage 12, 5 weeks 6 days, creates the ventricular system, which is divided into five brain regions on its cranial pole before the end of week 6[4–6]. The future fourth ventricle becomes apparent at Carnegie stage 14, 6 weeks 4 days, crown–rump length 7 mm, as a large rhomboid shallow cavity in the head of the embryo, while the brain is bent forward by the mesencephalic and cervical flexures[5,6]. The pontine flexure appears at the same age. This flexure deepens during the following weeks.

In our ultrasound study, we could always demonstrate the rhomboid cavity of the rhombencephalon lying superiorly in the head of the embryo at week 7, and measurements could be obtained. The length of this cavity and its relation to the age based on last menstrual period varied considerably during the following weeks. When we used the crown–rump length instead of the age based on last menstrual period as the independent variable (Figure 8a), there seemed to be a certain growth pattern in that we saw a rapid increase of the rhombencephalon length in embryos until 16 mm crown–rump length, followed by an apparent decrease of the rhombencephalon length in embryos until 24 mm crown–rump length. This decrease of length is probably caused by the deflection of the embryonic brain, which is mainly caused by the varying rates of growth of the brain compartments (Figure 8b) and the deepening of the pontine flexure (Figure 7). However, we need larger data samples to verify this hypothesis.

The rhombencephalon as a phylogenetic old brain center[7] developed more rapidly than the prosencephalon during the early embryonic period. At 6 weeks, it was an ultrasonographically invisible structure. Within 1 week, at week 7, when this study started, it had grown to a cavity of measurable size and increased further. The depth and the width showed large variations. There seemed to be no increase of the width from week 9 on (Figure 7). Anatomical changes of the rhombencephalon itself can explain this phenomenon: the cerebellar hemispheres grow while the pontine flexure deepens, hiding the lateral recesses in most cases. Thus, the measurable hypoechogenic cavity becomes smaller. Embryologists have already noted that the growth of the cerebellum leads to narrowing of the isthmic part of the fourth ventricle from stage 23 (crown–rump length 28–30 mm, 10 weeks 0 days–10 weeks 1 day)[6]. Consequently, the cavity becomes smaller and divides into lateral recesses and a progressively diminishing posterior superior recess[7]. Our observations demonstrated that until week 9 the rhombencephalon cavity was easy to visualize and to measure. Thereafter, changes of the border, especially the cerebellum, rendered difficulties in defining the cavity by ultrasound. The relatively large limits of agreement in the intraobserver study illustrate these difficulties.

According to the literature on embryology and anatomic preparations of embryos, the rhombencephalon is the dominating brain structure during the embryonic period. Jenkins stated in 1921[2] that the rhombencephalon amounted to 54% of the whole brain weight at 6 weeks 0 days (stage 13), 46% at 8 weeks 5 days (stage 19), and 37% at 9 weeks 5 days (stage 22). Assuming a pyramid-like shape of the rhombencephalon, we roughly estimated its volume and compared it to that of the ellipsoid-shaped hemispheres. These data confirmed that the rhombencephalon was the largest structure until week 8 (Figure 8). The estimated volume of both cerebral hemispheres together then increased with exponential growth and significantly exceeded that of the rhombencephalon. Jenkins found a less dramatic size difference in the older embryos. The apparent difference between our results and Jenkins' conclusions is probably due to the fact that we estimated the volume including the cavities with the choroid plexuses and cerebrospinal fluid, whereas Jenkins indicated the size by weighing the brain compartments.

Ultrasound papers have described the appearance of the cerebellum at about 10–11 weeks[9,10,13]. The cerebellar plates, the primordium of the cerebellum, begin to form after 46 days (age based on last menstrual period), and become macroscopically visible after 8 completed weeks in embryos of 14–18 mm crown–rump length[5,16]. In 1921, Jenkins found in a 16-mm embryo the rhombic lip constituting the cerebellar rudiment sufficiently differentiated to permit its removal and study[2]. He concluded that, at that stage, it contributed 8% of the total weight of the brain, as opposed to 38% for the medulla–pons, the combined weights giving a total of 46% for the rhombencephalon. Thus, embryological literature indicates that the cerebellar primordium should be visible before 10 weeks. We could define these rhombic lips with ultrasound as slight thickenings during week 8 in six embryos. During the embryonic period, the cerebellar hemispheres were clearly separated in the mid-line (Figure 12). At the end of the embryonic period, the cerebellum covered the rhombencephalon, arching like a horseshoe over the brainstem[6,17]. The cerebellar hemispheres united in the early fetal period[4,6,18], as it could be visualized with ultrasound (Figure 10).

Though the bilateral choroid plexuses of the fourth ventricle are considerable landmarks in the fourth ventricle, visible during week 8, little attention has been devoted to these structures in the ultrasound literature. The choroid plexuses of the fourth ventricle develop during Carnegie stage 17 (7 weeks 6 days–8 weeks 1 day)[18] and stage 18 (8 weeks 2 days–8 weeks 4 days)[6,16,17,19], where the choroid folds form villi in two-fifths of the embryos. In 1890, His[20] described the occurrence of bilateral choroid folds in the fourth ventricle before week 8. It is important to note that the choroid plexuses initially have a horizontal orientation[21]. Their growth starts from the lateral recesses, and at about 9 weeks (last menstrual period)[22,23] the two branches meet in the mid-line, where the future foramen of Magendie is supposed to develop. Thus, the choroid plexuses divide the thin roof of the rhombencephalon into the areae membranaceae superior and inferior[6,7,18,23,24]. In this study, we could recognize the descriptions of the embryologists. We saw echogenic outgrowths from the lateral borders of the rhombencephalic cavity just caudal to the lateral recesses after 8 completed weeks; within 1 week, these outgrowths met in the mid-line. The distance to the cerebellum became shorter with advancing age; the growing cerebellum bulged over the rostral area membranacea superior, thus 'pulling' the superior area membranacea and the choroid plexuses underneath its hemispheres.

Achiron and colleagues described the early detection of a Dandy–Walker cyst in an 11-week-old fetus[25]. Their ultrasound illustration seems to show the rudimentary choroid plexuses separated in the mid-line, and an enlarged area membranacea superior. In the normal 11-week-old fetus, the choroid plexuses lie, as demonstrated in this study, just beneath the inferior border of the cerebellum and cross the cavity of the fourth ventricle (Figure 11). This finding is in accordance with the conclusion of Gardner and co-workers[18] that a defective development of the rostral membranous area is a key factor leading to Dandy–Walker syndrome.

The details that we have described in this longitudinal study may now enable us to use ultrasound to distinguish between normal and abnormal brain development in the first trimester. Effects on brain development by hereditary disease or other irregularities should be detectable early. Occipital encephalocele, as found in Meckel–Gruber syndrome, Dandy–Walker malformation, which is often associated with recessive inherited syndromes, anencephaly, craniorachischisis and other conditions of maldevelopment of the rhombencephalon may soon become first-trimester diagnoses. We may also obtain improved knowledge about the formation and development of the Arnold–Chiari malformation.

## CONCLUSIONS

It is possible to study embryonic brain development longitudinally in great detail with .high-frequency (7.5 MHz) ultrasound scanning in the living human embryo. Formation of hindbrain structures, their size, growth and developmental movements are detectable. The rhombencephalic cavity is always recognizable from week 7 onwards. The choroid plexuses of the fourth ventricle are landmarks in the ultrasound images of the embryonic and early fetal hindbrain. Their formations are demonstrated with ultrasound during week 8. The cerebellar thickenings become identifiable during week 8. The estimated volume of the hindbrain is relatively large during early embryonic development.

It is likely that high-resolution ultrasound images will improve further. Combined with new achievements in three-dimensional ultrasound, this will lead to further development of sonoembryology and the possibility of recognizing embryonic maldevelopment. The application of transvaginal ultrasound in the first-trimester evaluation is widespread. Therefore, there is a great need for further education about this new diagnostic field.

## ACKNOWLEDGEMENT

Mrs Nancy Lea Eik-Nes revised the manuscript.

## REFERENCES

1. Robinson, H. P. and Fleming, J. E. E. (1975). A critical evaluation of sonar 'crown–rump length'. *Br. J. Obstet. Gynaecol.*, **82**, 702–10
2. Jenkins, G. B. (1921). Relative weight and volume of the component parts of the brain of the human embryo at different stages of development. *Contr. Embryol. Carnegie Inst.*, **13**, 41–60
3. O'Rahilly, R. and Gardner, E. (1971). The timing and sequence of events in the development of the human nervous system during the embryonic period proper. *Z. Anat. Entwickl.-Gesch.*, **134**, 1–12
4. O'Rahilly, R. and Gardner, E. (1977). The developmental anatomy and histology of the human central nervous system. In Vinken, R. J. and Bruyn, G. W. (eds.) *Handbook of Clinical Neurology: Congenital Malformations of the*

*Brain and Skull*, pp. 15–40. (Amsterdam: Myrianthopoulos NC)
5. O'Rahilly, R., Müller, F. and Bossy, J. (1982). Atlas des stades du développement du système nerveux chez l'embryon humain intact. *Arch. Anat. Hist. Embr. Norm. Exp.*, **65**, 57–76
6. O'Rahilly, R. and Müller, F. (1990). Ventricular system and choroid plexuses of the human brain during the embryonic period proper. *Am. J. Anat.*, **189**, 285–302
7. Kier, E. L. (1977). The cerebral ventricles: a phylogenetic and ontogenetic study. Anatomy and pathology. In Newton, T. H. and Potts, D. G. (eds.) *Radiology of the Skull and the Brain*, pp. 2787–914. (St. Louis: Mosby)
8. Timor-Tritsch, I. E., Peisner, D. B. and Raju, S. (1990). Sonoembryology: an organ-oriented approach using a high-frequency vaginal probe. *J. Clin. Ultrasound*, **18**, 286–98
9. Trimor-Tritsch, I. E., Monteagudo, A. and Warren, W. B. (1991). Transvaginal ultrasonographic definition of the central nervous system in the first and early second trimesters. *Am. J. Obstet. Gynecol.*, **164**, 497–503
10. Achiron, R. and Achiron, A. (1991). Transvaginal ultrasonic assessment of the early fetal brain. *Ultrasound Obstet. Gynecol.*, **1**, 336–44
11. Cullen, M. T., Green, J., Whetham, J., Salafia, C., Gabrielli, A. and Hobbins, J. C. (1990). Transvaginal ultrasonographic detection of congenital anomalies in the first trimester. *Am. J. Obstet. Gynecol.*, **163**, 466–76
12. Blaas, H.-G., Eik-Nes, S. H., Kiserud, T. and Hellevik, L. R. (1994). Early development of the forebrain and midbrain: a longitudinal ultrasound study from 7 to 12 weeks of gestation. *Ultrasound Obstet. Gynecol.*, **4**, 183–92
13. Takeuchi, H. (1992). Transvaginal ultrasound in the first trimester of pregnancy. *Early Hum. Dev.*, **29**, 381–4
14. Altman, D. G. (1991). *Practical Statistics for Medical Research*. pp. 132–45. (London: Chapman & Hall)
15. Bland, J. M. and Altman, D. G. (1986). Statistical methods for assessing agreement between two methods of clinical measurement. *Lancet*, **1**, 307–10
16. Müller, F. and O'Rahilly, R. (1990). The human brain at stages 18–20, including the choroid plexuses and the amygdaloid and septal nuclei. *Anat. Embryol.*, **182**, 285–306
17. Müller, F. and O'Rahilly, R. (1990). The human rhombencephalon at the end of the embryonic period proper. *Am. J. Anat.*, **189**, 127–45
18. Gardner, E., O'Rahilly, R. and Prolo, D. (1975). The Dandy–Walker and Arnold–Chiari malformations. *Arch. Neurol.*, **32**, 393–407
19. England, M. A. (1988). Normal development of the central nervous system. In Levene, M. I., Bennett, M. J. and Punt, J. (eds.) *Fetal and Neonatal Neurology and Neurosurgery*, pp. 3–27. (Edinburgh: Churchill Livingstone)
20. His, W. (1890). Die Entwicklung des menschlichen Rautenhirns vom Ende des ersten bis zum Beginn des dritten Monats. *Abh. K. S. Ges. Wiss.*, **29**, 1–74
21. Lemire, R. J. (1975). Cerebellum. In Lemire, R. J. (ed.) *Normal and Abnormal Development of the Human Nervous System*, pp. 144–65. (Hagerstown, MD: Harper & Row)
22. Blake, J. A. (1900). The roof and lateral recesses of the fourth ventricle considered morphologically and embryologically. *J. Comp. Neurol.*, **10**, 79–108
23. Brocklehurst, G. (1969). The development of the human cerebrospinal fluid pathway with particular reference to the roof of the fourth ventricle. *J. Anat.*, **105**, 467–75
24. Gardner, W. J. (1973). *The Dysraphic States from Syringomyelia to Anencephaly*, pp. 5–14. (Amsterdam: Excerpta Medica Foundations)
25. Achiron, R., Achiron, A. and Yagel, S. (1993). First trimester transvaginal sonographic diagnosis of Dandy–Walker malformation. *J. Clin. Ultrasound*, **21**, 62–4

# Paper III

**Harm-Gerd Blaas, Sturla H. Eik-Nes, Torvid Kiserud, Leif Rune Hellevik. Early development of the abdominal wall, stomach and heart from 7 to 12 weeks of gestation: a longitudinal ultrasound study. Ultrasound Obstet Gynecol 1995; 6:240–49**

*Ultrasound Obstet. Gynecol. 6 (1995) 240–249*

# Early development of the abdominal wall, stomach and heart from 7 to 12 weeks of gestation: a longitudinal ultrasound study

*H.-G. Blaas, S. H. Eik-Nes, T. Kiserud and L. R. Hellevik*

Department of Obstetrics and Gynecology, National Center for Fetal Medicine, Trondheim University Hospital, Trondheim, Norway

Key words: EMBRYOLOGY, TRANSVAGINAL ULTRASOUND, MIDGUT HERNIATION, ABDOMINAL WALL, STOMACH, HEART, FIRST TRIMESTER

## ABSTRACT

*The purpose of this ultrasound study was to describe longitudinally the normal embryonic development* in vivo. *Twenty-nine healthy pregnant women were examined five times each with transvaginal ultrasound between 7 and 12 weeks of gestation measured from the last menstrual period. Structures such as the midgut herniation into the umbilical cord, the stomach and the heart were recognized and measured.*

*It was possible to identify the physiological midgut herniation during weeks 7–8. It was always present from 8.5 to 10.5 weeks. At 12 completed weeks, the gut was retracted into the abdominal cavity for all the fetuses. We visualized the stomach in nine embryos (31%) during week 8, in 22 embryos (76%) before 10 weeks, and in all fetuses before 11 weeks. The heart rate increased rapidly to a mean of 175 beats per minute (bpm) at the beginning of week 9. Thereafter it decreased slowly to a mean of 166 bpm at 12 weeks. The mean heart diameter was 22% of the crown–rump length at 7 weeks, 17% at 9 weeks and only 13% at 12 weeks.*

## INTRODUCTION

An increasing spectrum of malformations of the body wall and truncal organs can be diagnosed with ultrasound technology in the first trimester[1–8]. Several authors have described cases with abdominal wall defects diagnosed with transabdominal ultrasound before 12 weeks of gestation[1–3]. After the introduction of transvaginal ultrasound, the feasibility of detecting malformations has been evaluated in large series. In 1990, Cullen and colleagues[4] reported three cases with ventral wall defects at 11 and 12 weeks of gestation, and in 1991 Achiron and Tadmor[5] reported the early detection of an epigastric omphalocele at 12 weeks of gestation. Recently, sophisticated diagnoses of heart defects at the end of the first trimester have been described[6–8]. An intestinal tract anomaly consisting of an esophageal atresia combined with a duodenal atresia was diagnosed in a 12-week-old fetus[9].

Transvaginal ultrasound provides better images of the human embryo than transabdominal ultrasound devices are able to present. High-frequency vaginal transducers operating at 7.5 MHz have been developed to increase the resolution of images, and we may expect even earlier diagnoses of pathological embryonic conditions.

A prerequisite for the early diagnosis of malformations is exact knowledge of normal embryonic development and its ultrasound features. Embryologists have given detailed surveys of developmental stages[10–13], but such information can only partially be used by clinicians in evaluating the living embryo. There is a need for detailed anatomical surveys based on ultrasound studies. The object of our interest is the living embryo, whose appearance shows rapid changes during the first trimester[4,14–16].

The developing brain dominates the ultrasound appearance of the embryo, and detailed pictures can be obtained[4,14–16]. In contrast to the brain compartments, only a few truncal structures can be depicted sufficiently clearly for ultrasound evaluation; these include the abdominal wall with its midgut herniation, the stomach and the heart. The object of this study was to follow longitudinally the normal development of these truncal structures from 7 weeks of gestation onwards. We aimed to establish reproducible biometric parameters and descriptions as a contribution to sonoembryology, and, thus, to provide a basis for evaluating the pathological early pregnancy.

Correspondence: Dr H.-G. Blaas, Department of Obstetrics and Gynecology, National Center for Fetal Medicine, Trondheim University Hospital, N-7006 Trondheim, Norway



Received 1–3–95
Revised 5–7–95
Accepted 17–7–95

## SUBJECTS AND METHODS

A total of 36 pregnant women were recruited for a longitudinal vaginal ultrasound study according to a protocol approved by our regional committee of ethics[15,16].

The inclusion criteria were regular menstrual periods, no hormonal therapy during the last 3 months before the pregnancy, non-smoker, natural single pregnancy, and no bleeding during the pregnancy. Women with conditions, such as uterine anomalies, diabetes and hypertension, that might influence embryonic growth, were not included. Diabetes, pre-eclampsia and delivery of preterm or growth- retarded infants were exclusion criteria. Five women were excluded (three early pregnancy losses, one bleeding during week 9, one preterm delivery at 36 weeks due to pre-eclampsia), and two women decided to discontinue after the first examination. Therefore, 29 women were included in the study (mean age 28 years, range 19–38 years).

An ultrasound scanner (Dornier AI 3200) with a 7.5-MHz high-frequency transvaginal probe was used for the examinations. The emitted energy was 0.58 mW/cm$^2$ SPTA (spatial peak temporal average) *in situ*. The magnification rate on the screen was 3.3 times natural size.

The first examination was performed at 7–8 completed weeks according to the last menstrual period (LMP). Five examinations were carried out for each pregnancy, with an interval of approximately 7 days. Each examination lasted for 20–30 min. A routine fetal ultrasound examination was additionally performed between 16 and 20 weeks.

The following parameters were analyzed. The physiological midgut herniation was recorded by measuring the thickness of the umbilical cord close to the abdomen, and by measuring the length of the protruded bowel into the cordal celom. The diameter of the cord was measured additionally in a free loop for comparison with the cord diameter on the level of the midgut herniation. The stomach was measured with its mean diameter in the horizontal abdominal section. The heart size was measured in the largest two perpendicular diameters in the horizontal thoracic section on the real-time image. When the level of the atrioventricular valves became visible (9 weeks and later), the measurements were taken at the level of the valves and through the apex of the heart. The mean diameter was calculated. The heart rate was obtained using M-mode.

### Statistical evaluation

Cross-sectional regression analysis was used to examine the associations of the data. Prediction intervals were calculated to show the uncertainty of using the regression equations to predict new observations at a given age. In order to determine the best fitting curves, we evaluated the normal distribution of the residuals by the Kolmogorov–Smirnov one-sample test, the $\chi^2$ test of goodness of fit (both STATISTICA, StatSoft), and the Shapiro Francia $W'$ test[17] (Excel, Microsoft).

Using embryological nomenclature, we called the conceptus 'embryo' if the gestational age was less than 10 weeks 1 day and 'fetus' if older than this. All time statements are in completed weeks and days, based on the first day of the last menstrual period. The crown–rump length (CRL) measurements cited from the embryological literature were made on aborted embryos that might have been exposed to shrinking; they may therefore differ from ultrasound measurements *in utero*.

## RESULTS

### Midgut herniation

The initial sign of the herniation of the gut occurred during week 7 as a thickening of the cord containing a slight echogenic area at the abdominal insertion

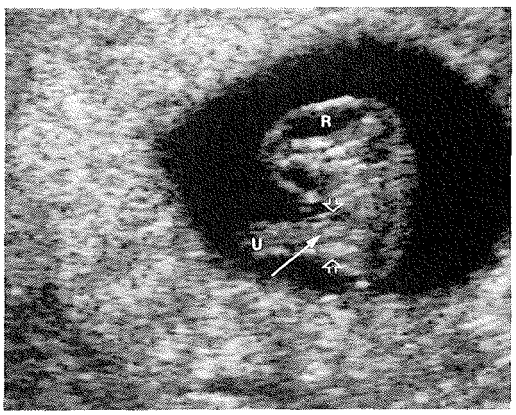


**Figure 1** Sagittal section through a 7-week-old embryo (crown–rump length 11 mm). The thickened abdominal insertion of the umbilical cord (U) is indicated by the open arrows. The peripheral umbilical cord is slim. The long arrow points to the midgut herniation. R, rhombencephalon

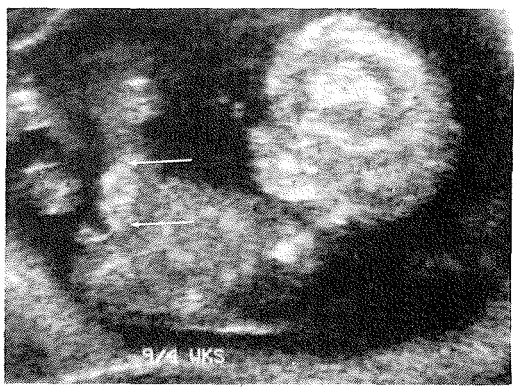

**Figure 2** Sagittal section through a 9-week-old embryo (crown–rump length 27 mm). The profile with the mouth, nose and forehead can easily be outlined. The physiological opening in the ventral wall is large. The arrows mark the echogenic bowel protruding into the cord. Caudal to the umbilicus is the genital tubercle

(Figure 1). Within a few days, this echogenic structure became more distinct. From 8 weeks 3 days to 10 weeks 4 days of gestational age, all embryos had herniation of the midgut, most distinctive during weeks 9 (Figure 2) and 10. At this stage, the midgut herniation was presented as a large hyperechogenic mass (Figure 3). The gut retracted into the abdominal cavity between 10 weeks 4 days and 11 weeks 5 days. Fetuses which were older than 11 weeks 5 days did not demonstrate any sign of the herniation.

The length of the midgut herniation (Table 1) was measured in 96 of 145 examinations. The data could best be fitted to a polynomial of the third degree (Figure 4a, Table 2). According to the regression line, the longest elongation was estimated at 10 weeks 2 days to 10 weeks 4 days (4.1 mm, range 2.4–5.8 mm). The elongated gut projected at the most 6.3 mm into the cord in a 10 week 0 day-old fetus. The measurements of the cord diameter at the level of the abdominal insertion ($n$ = 143) showed an increased thickness between 8 weeks and 11 weeks compared with the thickness of the cord registered at a free loop (Figure 4b).

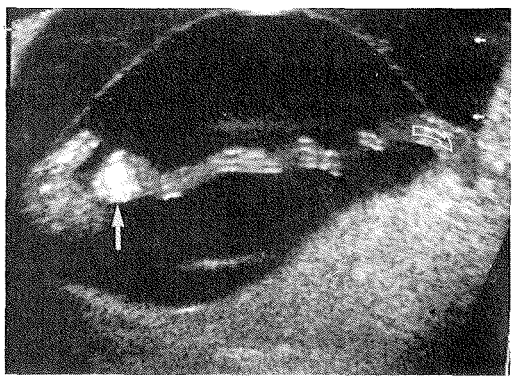

**Figure 3** Horizontal section through the fetal abdomen at 10 weeks (crown–rump length 34 mm). The fetal trunk and part of a femur are obliquely cut by this section. The herniation of the echogenic bowel in the umbilical celom (straight arrow) causes a considerable thickening of the cord. The umbilical cord traverses the amniotic cavity and joins the placenta at the right (open curved arrow)

## Stomach

We could locate a small hypoechogenic area thought to be the stomach on the left side of the upper abdomen below the heart during week 8. Figure 5 shows this feature in a 9 week 1 day-old embryo. With increasing age this hypoechogenic area became more distinct and could be identified as the stomach.

There was no sign of the stomach during week 7 (25 examinations), but it was possible to recognize the fluid-filled stomach totally in 88 of 145 examinations. The stomach was detected in nine of the 29 embryos (31%) before 9 weeks 0 days, in an additional 13 embryos (45%) before 10 weeks 0 days, and in the remaining seven fetuses before 11 weeks (Figure 6).

The mean diameter of the stomach in the transverse section was 1.2 mm (0.5–2.1 mm) of those identified at 9 weeks 0 days, increasing to 2.4 mm (1.4–3.7 mm) at 12 weeks 0 days (Tables 1 and 2, Figure 7).

## Heart

The heart could easily be recognized by real-time ultrasound as a relatively large beating structure below the

**Table 1** The mean values and 95% prediction intervals of the length of the midgut herniation into the cord, the diameter of the cord at a free loop, the stomach diameter and the heart rate in beats per minute (bpm). The gestational age (GA) is based on the last menstrual period

| *GA* (weeks-days) | *Midgut herniation length* (mm) | *Cord, free loop diameter* (mm) | *Stomach diameter* (mm) | *Heart rate* (bpm) |
|---|---|---|---|---|
| 7-0 | 1.9 (0.2–3.6) | 1.8 (1.0–2.7) | — | 138 (122–154) |
| 8-0 | 2.4 (0.7–4.1) | 2.1 (1.3–3.0) | — | 166 (150–182) |
| 9-0 | 3.3 (1.6–5.0) | 2.4 (1.6–3.3) | 1.2 (0.5–2.1) | 175 (159–190) |
| 10-0 | 4.0 (2.3–5.7) | 2.7 (1.9–3.6) | 1.5 (0.8–2.6) | 174 (158–190) |
| 11-0 | 3.9 (2.2–5.6) | 3.0 (2.2–3.9) | 1.9 (1.0–3.1) | 171 (155–187) |
| 12-0 | 0 | 3.3 (2.5–4.2) | 2.4 (1.4–3.7) | 166 (150–182) |

**Table 2** Equations of the regressions, including the 95% prediction intervals. The gestational age is based on the last menstrual period

| *Independent variable* | *Dependent variable* | *Equations* | $R^2$ |
|---|---|---|---|
| Gestational age | midgut herniation length | $y = +61.70 - 22.26x + 2.68x^2 - 0.10x^3 \pm 1.96 \times 0.85$ | 0.42 |
| Gestational age | cord diameter, free loop | $y = -0.23 + 0.30x \pm 1.96 \times 0.43$ | 0.51 |
| Gestational age | stomach diameter | $y = (-0.28 + 0.15x \pm 1.96 \times 0.18)^2$ | 0.49 |
| Gestational age | heart diameter | $y = -5.13 + 1.01x \pm 1.96 \times 0.65$ | 0.85 |
| Crown–rump length | heart diameter | $y = (1.07 + 0.05x - 0.0003x^2 \pm 1.96 \times 0.12)^2$ | 0.91 |
| Mean abdominal diameter | heart diameter | $y = 0.81 + 0.36x \pm 1.96 \times 0.55$ | 0.89 |
| Gestational age | heart rate | $y = -2556.76 + 1014.80x - 141.00x^2 + 8.70x^3 - 0.202x^4 \pm 1.96 \times 8.01$ | 0.54 |

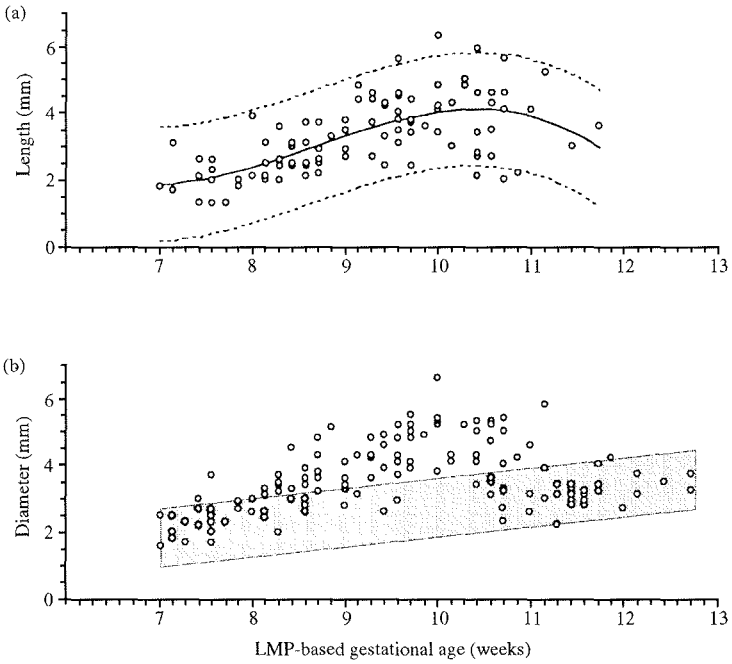


**Figure 4** (a) Measurements ($n$ = 96) of the length of the physiological midgut herniation, as indicated by straight arrows in Figure 2, showing the regression line and the 95% prediction intervals. (b) Measurements ($n$ = 143) of the umbilical cord thickness at the abdominal insertion. The plot shows an increasing thickness between 8 weeks and 11 weeks. The development of the free-loop cord thickness was modelled on a linear regression. The tinted area shows the 95% prediction intervals of the free-loop cord thickness measured in the same embryos/fetuses. LMP, last menstrual period

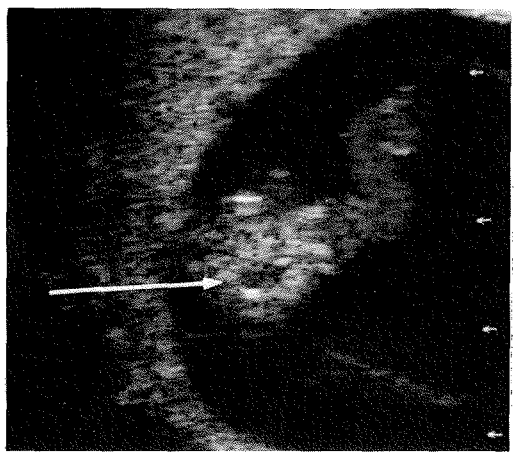

**Figure 5** Horizontal section through the abdomen of a 9-week-old embryo (crown–rump length 24 mm). The arrow points to the hypoechogenic fluid-filled stomach. The umbilical cord near the abdomen is thickened and hyperechogenic, due to the physiological herniation

embryonic head at 7 weeks (Figure 8; crown–rump length 13 mm). Occasionally it was possible to identify the atrial and ventricular walls moving reciprocally as early as the end of week 8. The atrial compartment appeared wider than the ventricular compartment, and the heart covered about 50% of the transverse thoracic area (Figure 9a, crown–rump length 19 mm). At 10 weeks, the moving valves and the interventricular septum could be identified (Figure 10).

The mean diameter of the heart increased linearly with gestational age (Figure 11a, Tables 2 and 3). The relationship of the mean heart diameter to the crown–rump length (Figure 11b, Table 2) could best be expressed by a polynomial regression of the second degree after square root transformation ($R^2$ = 0.91). There was a linear dependence of the mean heart diameter on the mean abdominal diameter (Figure 11c, Table 2).

The ratio of the mean heart diameter to the crown–rump length was 0.22 at 7 weeks 0 days, decreasing to 0.17 at 9 weeks 0 days, and further to 0.13 in the fetus at 12 weeks 0 days (Table 3). We found a similar ratio between the mean heart diameter and the mean abdominal diameter: it fell from 0.57 at 7 weeks 0 days to 0.47 at 9 weeks 0 days, and to 0.42 at 12 weeks 0 days (Table 3).

The most suitable model for the regression of the heart rate data was a fourth-degree polynomial. The

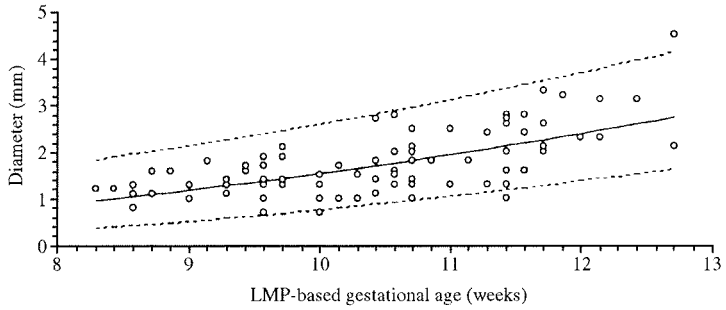


**Figure 6** Measurements ($n$ = 88) of the mean diameter of the stomach, the regression line and the 95% prediction intervals. LMP, last menstrual period

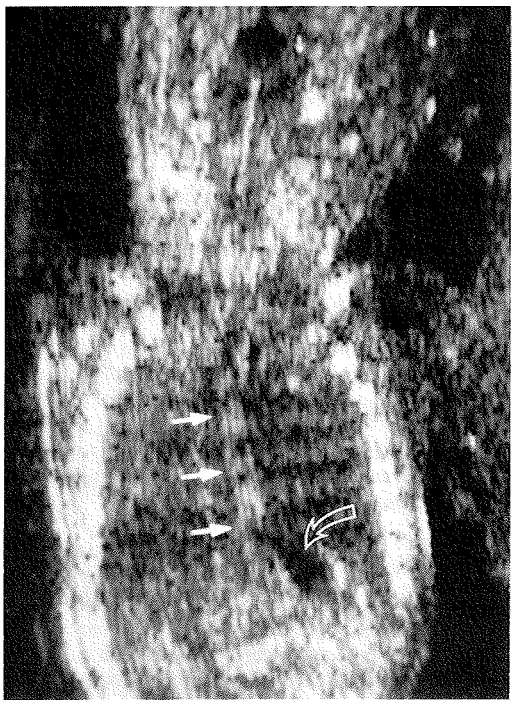

**Figure 7** Coronal section through the trunk of an 11-week-old fetus (crown–rump length 53 mm). The three straight arrows point to the esophagus in the middle of the thoracic cage. The esophagus leads to the fluid-filled stomach on the left side of the upper abdomen (curved open arrow)

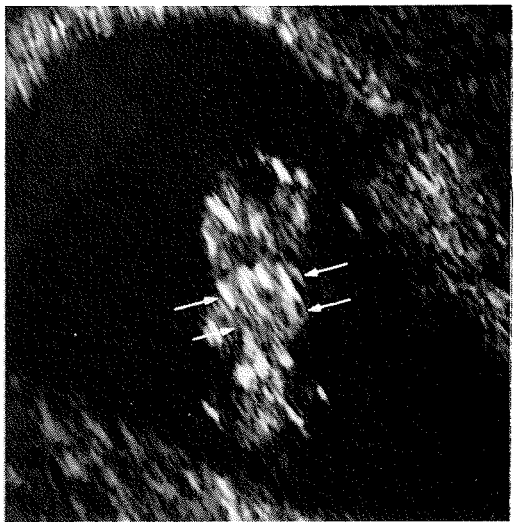

**Figure 8** Coronal section through a 7½-week embryo, crown–rump length 13 mm. The heart is large, with reciprocal movements of the walls (upper vs. lower arrows) during the real-time examination. The upper arrows indicate the wider part of the atrial heart; the lower arrows point to the ventricular part of the heart. It is not yet possible to depict the cardiac structures in more detail

mean heart rate increased from 138 beats per minute (bpm) (122–154 bpm) at 7 weeks 0 days to 166 bpm (150–182 bpm) at 8 weeks 0 days, and to 175 bpm (159–190 bpm) at 9 weeks 0 days (Tables 1 and 2, Figure 12). The peak of the curve, 175 bpm (159–191 bpm), was found at 9 weeks 3 days. At 12 weeks 0 days the mean heart rate had decreased to 166 bpm (150–182 bpm).

## Pregnancy outcome

Twenty-seven children were born spontaneously at a gestational age between 37 weeks 2 days and 42 weeks 1 day postmenstrually, mean 40 weeks 0 days. Two women were delivered by Cesarean section because of mechanical disproportion (at 40 weeks 2 days and 40 weeks 4 days, respectively). The weight of the 29 children (16 males, 13 females) ranged from 2610 g to 4890 g, mean 3610 g. All children proved to be healthy and are developing normally.

## DISCUSSION

Using transvaginal ultrasound with a 7.5-MHz high-resolution transducer, it was possible to reveal embryonic

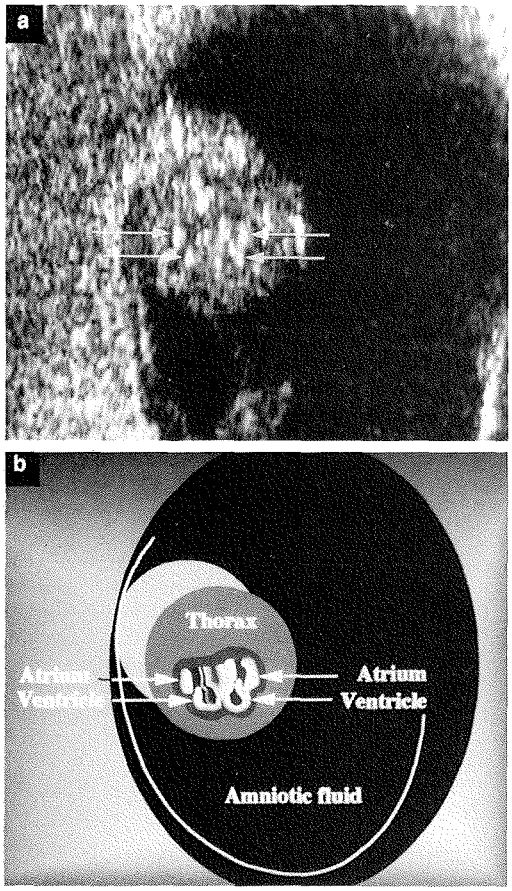


**Figure 9** (a) Obliquely tilted horizontal section through the thorax of an 8½-week-old embryo (crown–rump length 19 mm). The arrows point to the hyperechogenic walls of the atria and the ventricles, which moved reciprocally in the real-time ultrasound examination. (b) Sketch of the ultrasound image shown in (a)

truncal structures at very early stages. It is the advantage of a longitudinal study to follow the development of such embryonic structures and thus to define them more precisely. The number of participants in the present study was limited because of the difficulties of recruitment and the discomfort repeated transvaginal examinations imposed on healthy women.

The data were analyzed cross-sectionally. However, such successive measurements on an individual are correlated: the higher the correlation between successive measurements the lower the effective sample size. In this context a high correlation would manifest itself as each individual's series of values lying on smooth curves. In this study, the objects of interest were very small and often near the limit of measurability, especially during the embryonic period. The ultrasound measurements of such small embryonic structures are associated with an elevated intraobserver variability, as documented in previous studies[15,16]. Therefore, the correlation of these measurements is not likely to be of significant importance. Nevertheless, the effective sample size in the study should be considered smaller than the total number of observations[18], and the prediction intervals should be interpreted with care.

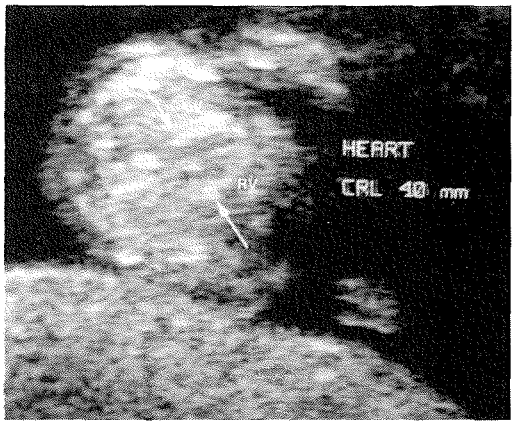


**Figure 10** Horizontal section through the thorax of a fetus at the end of week 10 (crown–rump length 40 mm). The arrows show the plane of the atrioventricular valves. The deep left ventricle (LV), the interventricular septum and the right ventricle (RV) can be recognized

The reduced reproducibility of measuring small embryonic structures and/or the large biological variation of parameters such as the midgut herniation length, the cord diameter, the stomach diameter and the heart rate are manifested in reduced values of $R^2$. Averaging the repeated measurements is recommended to achieve reliable values.

## The midgut herniation

The physiological herniation of the midgut into the celom of the umbilical cord is a normal feature of embryonic intestinal development, leading to elongation and rotation of the bowel. According to Sternberg and Politzer[19], the physiological herniation may already be present in the proximal umbilical cord celom in 7-mm embryos. Streeter[13] found that the primary intestinal loop projected farther into the umbilical cord than the normal umbilical hernia at Carnegie stage 17. This corresponds to 52–54 days' gestational age and a crown–rump length of 11–14 mm. Both Blechschmidt and Kiesselbach believed that this physiological herniation starts as a result of traction from the vitelline duct[20,21]. The herniation of the midgut was present until 11 weeks in fetuses of approximately 40-mm crown–rump length[13], while the elongating and coiling intestine rotated anticlockwise 90°. When returning to the abdomen, the intestine rotated another 180°[22]. Kiesselbach described the returning of the midgut in embryos with crown–rump lengths of 40–42 mm[21], whereas Lauge-Hansen found that the last midgut loop had returned to the abdomen in the embryos of 44-mm

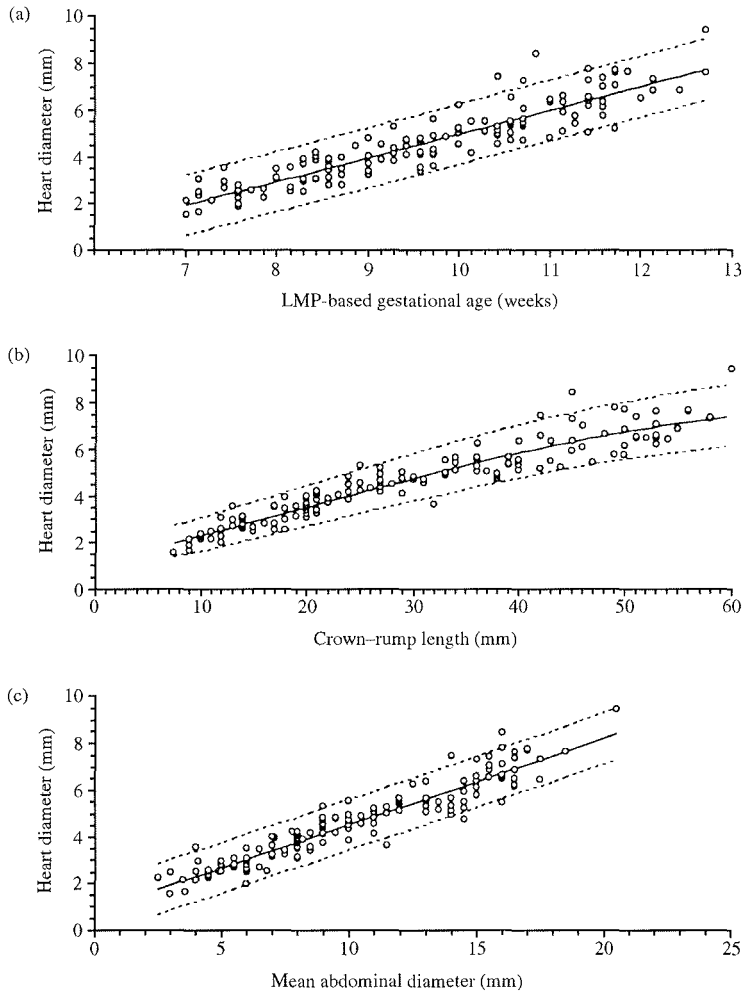


**Figure 11** Measurements of the mean heart diameter correlated with menstrual age (a) ($n$ = 144), crown–rump length (b) ($n$ = 144) and mean abdominal diameter (c) ($n$ = 141), showing the regression lines and the 95% prediction intervals. LMP, last menstrual period

crown–rump length[23]. Thus, relying on the embryological literature, we can expect the physiological herniation of the gut to start during week 7 and to be finished at about 11½–12 weeks, the size of the fetus not being longer than about 45-mm crown–rump length (post-abortem measurement).

The physiological herniation of the midgut has been described in several ultrasound studies. Some used a 5-MHz transabdominal ultrasound transducer[24–26], but Timor-Tritsch and colleagues[27] applied a 6.5-MHz transvaginal probe. Green and Hobbins[26] and Timor-Tritsch and colleagues did not quantify the extension of the herniation. Timor-Tritsch and colleagues suggested that the presence of a midgut herniation was indicated if the diameter of the cord immediately at the abdominal insertion was 1.5 times larger than the cord peripherally. They found the earliest midgut herniation at 8 weeks. Cyr and colleagues[24] examined ten early pregnancies between 7 and 10 weeks transabdominally and in all cases found herniated bowel mass in the umbilical cord with a mean diameter of 6.3 mm (5–10 mm). Schmidt and colleagues[25] examined 14 cases longitudinally. They found larger herniated masses in 8-week-old embryos than in older embryos or fetuses. In their study, the mean diameter of the protruded mass was 6–9 mm at 8 weeks; it decreased to 5–6 mm at 9 weeks. We found the largest mass of the midgut herniation in a 10-week-old fetus, but the length of the mass never exceeded 6.3 mm. In 1989, Brown and colleagues[2] presented the diagnosis of an epigastric omphalocele as early as 10 weeks 2 days (crown–rump length 35 mm). The transverse diameters of the herniated mass measured 8 and 9 mm. Although

**Table 3** The relationship between the mean heart diameter (HD), crown–rump length (CRL) and mean abdominal diameter (MAD) to gestational age (GA)

| *GA* (weeks-days) | *HD* (mm) | *CRL* (mm) | *HD/CRL ratio* | *MAD* (mm) | *HD/MAD ratio* |
|---|---|---|---|---|---|
| 7-0 | 1.9 (0.6–3.2) | 8 | 0.22 | 3.2 | 0.57 |
| 8-0 | 2.9 (1.6–4.2) | 14 | 0.19 | 5.9 | 0.51 |
| 9-0 | 3.9 (2.6–5.2) | 23 | 0.17 | 8.6 | 0.47 |
| 10-0 | 4.9 (3.6–6.2) | 31 | 0.15 | 11.3 | 0.44 |
| 11-0 | 5.9 (4.6–7.2) | 42 | 0.14 | 14.0 | 0.42 |
| 12-0 | 6.9 (5.6–8.2) | 55 | 0.13 | 16.7 | 0.42 |

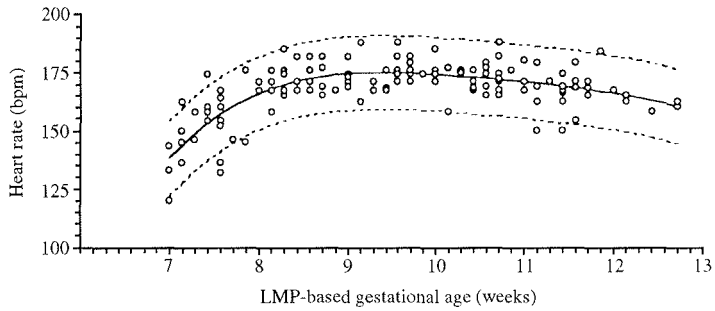


**Figure 12** Measurements ($n$ = 144) of the mean heart rate, the regression line and the 95% prediction intervals. LMP, last menstrual period; bpm, beats per minute

smaller medial omphaloceles may not be detectable during the period of the physiological midgut herniation, we suggest that large omphaloceles, especially the epigastric omphaloceles containing the liver[2], and gastroschises may be detectable towards the end of the embryonic period, namely at 9 weeks of gestation. Larger defects such as the limb–body-wall complex should be detectable even earlier.

## The stomach

The intestine is sufficiently developed during the embryonic period to be filled with fluid. The oropharyngeal membrane ruptures at 38 days[11], while the anal membrane first breaks down after 62[28] to 65 days[11]. The stomach appears fusiform at Carnegie stage 13, which corresponds to 42–45 days, or crown–rump length of 4–6 mm[12]. The lumen of the primitive gut is well defined throughout its length after 6 weeks.

In a study of 162 well-preserved normal embryos and fetuses with crown–rump lengths of 22–250 mm, Hawass and collaborators[29] performed careful measurements of the esophagus and the stomach and demonstrated that the stomach already had a considerable lumen (mean 2.3 mm) in the transverse section in embryos of 22-mm crown–rump length (9 weeks). Liebermann-Meffert[30] studied 75 well-preserved embryos and fetuses with a crown–rump length of 8–200 mm and found that the position of the stomach was fundamentally unaltered from the early stage of the embryonic period. The relative growth rate of the stomach, compared to body length and abdominal cavity volume, was greater in younger embryos. During week 8 (crown–rump length 15–21 mm), she found that the peritoneal cavity was completely occupied by the liver anteriorly and by the growing stomach dorsally, while the intestinal loops were herniated into the umbilical cord. These studies showed that, in the developing embryonic stomach, there is a considerable lumen that may be filled with fluid and, therefore, should be detectable by ultrasound.

We could observe the appearance of the stomach earlier than described by other authors, probably due to the use of the 7.5-MHz transvaginal transducer. Cullen and colleagues[4] and Green and Hobbins[26] identified the stomach at 10 weeks, but they did not measure its size. The human fetus initiates swallowing movements at 11 gestational weeks[31]. We found fluid in the stomach of embryos as early as 8½ weeks. Since the embryo does not swallow amniotic fluid at that stage, fluid production from the intestinal epithelium is most likely already present in the embryonic period. Thus, the physiology of the intestinal tract fluid production in the first-trimester conceptuses is different from that in older fetuses. As demonstrated, the finding of an empty stomach during the first trimester is a normal feature. Developmental disorders of the intestinal tract, such as intestinal or esophageal atresia, may affect the amount of fluid in the stomach during the first trimester and thus provide a sign for detection. Tsukerman and colleagues[9] described a 12-week-old fetus with a grossly dilated stomach and duodenum. This fetus had a complete atresia of both the esophagus and the duodenum. Here the fluid

accumulation probably originated from the gastric and duodenal epithelium itself.

### The heart

During the embryonic period, the heart undergoes profound developmental changes that transform its simple tubular cavity at 5 weeks into the four chambers of the heart, usually completed at the end of week 8 by the closure of the interventricular foramen. The formation of the foramen ovale by the septum secundum is completed during week 9[32]. The innervation of the heart starts in the embryo of 10–13-mm crown–rump length (7 weeks) where branches of the vagal nerve and cervical sympathicus are found in the region of the sinus venosus and with the trunks of the aorta and the pulmonary artery[33]. The expansion of the cardiac nerves and ganglions is completed late in the fetal period. At the same time as these complex changes are taking place, the developing heart pumps blood supplying the embryonic and the extraembryonic circulation.

As expected, the size of the human embryonic heart was correlated with that of the crown–rump length and the abdominal diameter. There was a considerable change in the relationship between the heart size and the body size. Compared to the body size, the heart was relatively large in the early embryonic period. The heart size became a relatively smaller part of the embryo with increasing age. Clark described similar conditions in chick embryos[34]. He found a 15-fold increase of the embryonic dry weight compared to a nine-fold increase of the heart weight from 3 days to 6 days of gestational age, and he concluded that the larger the embryo, the smaller the relative size of the heart. Bronshtein and colleagues[35] presented biometric data of the fetal heart in a cross-sectional study of 120 normal fetuses from 10 to 17 weeks. The estimated heart size at 11–12 weeks was lower than in our study, probably because the heart diameter was only measured at the level of the atrioventricular valves. The size increased by about 1.2 mm a week. They also calculated the heart size/chest diameter ratio, which probably corresponds to our heart size/mean abdominal diameter ratio, finding a slight increase of this ratio instead of a decrease.

The heart rate of the embryo has been analyzed with ultrasound by various authors. In general, the heart rate obtained by visual counting is lower[36,37] than the heart rate obtained by M-mode measurements[38,39]. Hertzberg and co-workers[36] counted visually and found the highest mean frequency of 144 bpm at 8 weeks, while Merchiers and associates[37] recorded the highest mean frequency of 157 bpm during week 10. DuBose and colleagues[38] suggested using M-mode measurements to improve the accuracy of the counting. Similar to our findings, DuBose and colleagues[38] and Robinson and Shaw-Dunn[39] recorded the highest mean heart rates of 175 bpm and 177 bpm, respectively, at the beginning of week 9.

The regularity found in the pattern of the initial increase of the heart rate (Table 1, Figure 12), the initial distinct decrease of heart size to crown–rump length ratio and heart size to abdominal diameter ratio, followed by the slow decrease of these parameters (Table 3, Figure 11), suggest a fundamental association in the anatomical and physiological development of the heart. The size of the heart and the intrinsic frequency of the heart activity are factors that are modified by developmental factors and physiological demands of the early blood circulation. In the early embryo, with its developing heart architecture, a certain heart size and muscle mass may be necessary to maintain a sufficient pump power. Clark assumed that the energy delivered to the intracardiac blood may be relatively less in the complex heart than in the early muscular tube[34]. It is remarkable that the time of the highest heart rate coincided with the aorta having fully connected with the left ventricle, with closure of the foramen interventriculare tertium, with the start of differentiation of the membranous portion of the ventricular septum and with the development of the septal leaflet of the tricuspid valve in the setting of a four-chamber organ. It may be speculated that developmental changes in the embryonic period have improved the function of the heart and peripheral vasculature and made them more economical, and optimized the heart rate so that, at 9 weeks and later, proportionally less muscle mass and fewer heart beats are required to meet the demands of the fetal blood circulation.

It is known that alterations of the heart rate can be associated with embryonic maldevelopment. Gross defects of the heart such as an ectopia cordis may be detectable at the end of the embryonic period, while defects such as a large atrioventricular canal may be detectable at the very beginning of the fetal period.

## CONCLUSION

The results of the present sonographic study of the embryonic and early fetal development *in vivo* are in accordance with research done by embryologists. The physiological midgut herniation started during week 7, was always present between 8½ and 10½ weeks, and resolved at the end of week 11. The size of the herniated bowel mass did not exceed 6.3 mm. The stomach became detectable during week 8. Before 11 completed weeks, it had been visualized in all fetuses. Its mean diameter did not exceed 3.5 mm before 12 weeks. The relative size of the heart compared to body size decreased with age. The heart rate showed considerable changes during development with the highest rate during week 9. This peak coincided with the completion of the structural development of the embryonic heart.

It is likely that the technique of ultrasound will continue to improve and that the use of three-dimensional ultrasound, Doppler techniques and particularly higher-frequency ultrasound devices will provide more detailed information about normal and abnormal sonoembryonic development.

## ACKNOWLEDGEMENTS

Jim Huhta gave valuable comments on the heart development. Mrs Nancy Lea Eik-Nes revised the manuscript.

## REFERENCES

1. Curtis, J. A. and Watson, L. (1988). Sonographic diagnosis of omphalocele in the first trimester of fetal gestation. *J. Ultrasound Med.*, **7**, 97–100
2. Brown, D. L., Emerson, D. S., Shulman, L. P. and Carson, S. A. (1989). Sonographic diagnosis of omphalocele during 10th week of gestation. *Am. J. Roentgenol.*, **153**, 825–6
3. Gray, D. L., Martin, C. M. and Crane, J. P. (1989). Differential diagnosis of first trimester ventral wall defect. *J. Ultrasound Med.*, **8**, 255–8
4. Cullen, M. T., Green, J., Whetham, J., Salafia, C., Gabrielli, S. and Hobbins, J. (1990). Transvaginal ultrasonographic detection of congenital anomalies in the first trimester. *Am. J. Obstet. Gynecol.*, **163**, 466–76
5. Achiron, R. and Tadmor, O. (1991). Screening for fetal anomalies during the first trimester of pregnancy: transvaginal versus transabdominal sonography. *Ultrasound Obstet. Gynecol.*, **1**, 186–91
6. Bronshtein, M., Zimmer, E. Z., Gerlis, L. M., Lorber, A. and Drugan, A. (1993). Early ultrasound diagnosis of fetal congenital heart defects in high-risk and low-risk pregnancies. *Obstet. Gynecol.*, **82**, 225–9
7. Gembruch, U., Knöpfle, G., Bald, R. and Hansmann, M. (1993). Early diagnosis of fetal congenital heart disease by transvaginal echocardiography. *Ultrasound Obstet. Gynecol.*, **3**, 310–17
8. Achiron, R., Rotstein, Z., Lipitz, S., Mashiach, S. and Hegesh, J. (1994). First-trimester diagnosis of fetal congenital heart disease by transvaginal ultrasound. *Obstet. Gynecol.*, **84**, 69–72
9. Tsukerman, G. L., Krapiva, G. A. and Kirillova, I. A. (1993). First-trimester diagnosis of duodenal stenosis associated with oesophageal atresia. *Prenat. Diagn.*, **13**, 371–6
10. O'Rahilly, R. and Gardner, E. (1971). The timing and sequence of events in the development of the human nervous system during the embryonic period proper. *Z. Anat. Entwickl.-Gesch.*, **134**, 1–12
11. O'Rahilly, R. (1978). The timing and sequence of events in the development of the human digestive system and associated structures during the embryonic period proper. *Anat. Embryol.*, **153**, 123–36
12. Streeter, G. L. (1945). Developmental horizons in human embryos. *Carnegie Inst. Washington, Contrib. Embryol.*, **199**, 27–63
13. Streeter, G. L. (1948). Developmental horizons in human embryos. *Carnegie Inst. Washington, Contrib. Embryol.*, **211**, 32, 133–203
14. Timor-Tritsch, I. E., Peisner, D. B. and Raju, S. (1990). Sonoembryology: an organ-oriented approach using a high-frequency vaginal probe. *J. Clin. Ultrasound*, **18**, 286–98
15. Blaas, H.-G., Eik-Nes, S. H., Kiserud, T. and Hellevik, L. R. (1994). Early development of the forebrain and midbrain: a longitudinal ultrasound study from 7 to 12 weeks of gestation. *Ultrasound Obstet. Gynecol.*, **4**, 183–92
16. Blaas, H.-G., Eik-Nes, S. H., Kiserud, T. and Hellevik, L. R. (1995). Early development of the hindbrain: a longitudinal ultrasound study from 7 to 12 weeks of gestation. *Ultrasound Obstet. Gynecol.*, **5**, 151–60
17. Altman, D. G. (1991). Preparing to analyse data. In Altman, D. G. (ed.) *Practical Statistics for Medical Research*, pp. 122–45. (London: Chapman & Hall)
18. Altman, D. G. and Chitty, L. S. (1994). Charts of fetal size. 1. Methodology. *Br. J. Obstet. Gynaecol.*, **101**, 29–34
19. Sternberg, H. and Politzer, G. (1931). Über die formale Genese der Fehlbildungen des Nabelstranges und der ventralen Körperwand, nebst Beschreibung eines einschlägigen Falles. *Beitr. Path. Anat.*, **88**, 150–92
20. Blechschmidt, E. (1974). *Humanembryologie, Prinzipien und Grundbegriffe*, p. 40. (Stuttgart: Hippokrates Verlag)
21. Kiesselbach, A. (1952). Der physiologische Nabelbruch. *Adv. Anat. Embryol. Cell Biol.*, **34**, 83–143
22. Moore, K. (1988). The digestive system, rotation of the midgut. In Moore, K. (ed.) *The Developing Human*, pp. 228–9. (Philadelphia: Saunders)
23. Lauge-Hansen, N. (1973). *Developmental Anatomy of the Human Gastro-intestinal Tract*, p. 48. (Aarhus: Munksgaard Aarhus Stiftsbogtrykkerie A/S)
24. Cyr, D. R., Mack, L. A., Schoenecker, S. A., Patten, R. M., Shephard, T. H., Shuman, W. P. and Moss, A. A. (1986). Bowel migration in the normal fetus: ultrasound detection. *Radiology*, **161**, 119–21
25. Schmidt, W., Yarkoni, S., Crelin, E. S. and Hobbins, J. C. (1987). Sonographic visualization of the physiologic anterior wall hernia in the first trimester. *Obstet. Gynecol.*, **69**, 911–15
26. Green, J. J. and Hobbins, J. C. (1988). Abdominal ultrasound examination of the first-trimester fetus. *Am. J. Obstet. Gynecol.*, **159**, 165–75
27. Timor-Tritsch, I. E., Warren, W. B., Peisner, D. and Pirrone, E. (1989). First trimester midgut herniation: a high frequency transvaginal sonographic study. *Am. J. Obstet. Gynecol.*, **161**, 466–76
28. deVries, P. A. and Friedland, G. W. (1974). The staged sequential development of the anus and rectum in human embryos and fetuses. *J. Pediatr. Surg.*, **9**, 755–69
29. Hawass, N. E. D., Al-Badawi, M. G., Fatani, J. A., Meshari, A. A. and Edrees, Y. A. (1991). Morphology and growth of the fetal stomach. *Invest. Radiol.*, **26**, 998–1004
30. Liebermann-Meffert, D. (1969). Form und Lageentwicklung des menschlichen Magens und seiner Mesenterien. *Acta Anat.*, **72**, 376–410
31. Diamant, N. E. (1985). Development of esophageal function. *Am. Rev. Respir. Dis.*, **131**, 29–32
32. Moore, K. (1988). The cardiovascular system. In Moore, K. (ed.) *The Developing Human*, pp. 286–333. (Philadelphia: Saunders)
33. Steding, G. and Seidl, W. (1990). Cardio-vaskuläres System. Entwicklung der Baumaterialien des Herzens. In Hinrichsen, K. V. (ed.) *Humanembryologie*, pp. 243–50. (Berlin: Springer-Verlag)
34. Clark, E. B. (1985). Ventricular function and cardiac growth in the chick embryo. In Ferrans, V. J., Rosenquist, G. and Weinstein, C. (eds.) *Cardiac Morphogenesis*, pp. 238–44. (New York: Elsevier)
35. Bronshtein, M., Siegler, E., Eshcoli, Z. and Zimmer, E. Z. (1992). Transvaginal ultrasound measurements of the fetal heart at 11 to 17 weeks of gestation. *Am. J. Perinatol.*, **9**, 38–42
36. Hertzberg, B. S., Mahony, B. S. and Bowie, J. D. (1988). First trimester fetal cardiac activity. *J. Ultrasound Med.*, **7**, 573–5
37. Merchiers, E. H., Dhont, M., DeSutter, P. A., Beghin, C. J. and Vanderkerckhove, D. A. (1990). Predictive value of early embryonic cardiac activity for pregnancy outcome. *Am. J. Obstet. Gynecol.*, **165**, 11–14
38. DuBose, T. J., Cunyus, J. A. and Johnson, L. F. (1990). Embryonic heart rate and age. *J. Diagn. Med. Ultrasound*, **6**, 151–7
39. Robinson, H. P. and Shaw-Dunn, J. (1973). Fetal heart rates as determined by sonar in early pregnancy. *J. Obstet. Gynaecol. Br. Commonw.*, **80**, 805–9

# Paper IV

**Harm-Gerd Blaas, Sturla H. Eik-Nes, John Bjørnar Bremnes. The growth of the human embryo. A longitudinal biometric assessment from 7 to 12 weeks of gestation. Ultrasound Obstet Gynecol 1998; 12:346–54**

*Ultrasound Obstet Gynecol 1998;12:346–354*

# The growth of the human embryo. A longitudinal biometric assessment from 7 to 12 weeks of gestation

*H.-G. Blaas, S. H. Eik-Nes and J. B. Bremnes*

National Center for Fetal Medicine, Department of Obstetrics and Gynecology, Trondheim University Hospital, Trondheim, Norway

Key words: HUMAN EMBRYO, LONGITUDINAL STUDY, FIRST TRIMESTER, CROWN-RUMP LENGTH, BIPARIETAL DIAMETER, OCCIPITOFRONTAL DIAMETER, ABDOMINAL DIAMETER, CHORIONIC CAVITY, AMNIOTIC CAVITY, YOLK SAC

## ABSTRACT

***Objectives*** *Longitudinal studies of multiple parameters in the first trimester for assessment of embryonic growth are lacking. This study's aim was to register changes in growth over time, by taking several measurements of embryos on successive occasions and evaluating these changes by longitudinal analysis.*

***Design*** *This prospective longitudinal study describes the normal embryonic growth* in vivo. *Inclusion criteria were non-smoking women with single uneventful pregnancies, regular menstrual periods (28–30 days) and no hormone therapy in the 3 months prior to the pregnancy. Exclusion criteria were pregnancy complications such as diabetes, pre-eclampsia, delivery of preterm or growth-restricted infants. Of 36 recruited pregnant women, 29 met these criteria. Each pregnancy was examined five times between 7 and 12 weeks of gestation. This resulted in a two-level data set, where level 1 consisted of the observations and level 2 consisted of the individuals. The longitudinal data were analyzed with a software package specially created for multilevel analysis.*

***Results*** *The growth of the biparietal diameter (BPD), occipitofrontal diameter (OFD), mean abdominal diameter (MAD), chorionic cavity diameter and amniotic cavity diameter was constant; the growth of the crown–rump length (CRL) and the yolk sac diameter was not constant. Variation in the data sets was mainly caused by variation between the embryos/fetuses.*

***Conclusions*** *The measured parameters except for the yolk sac showed a high degree of uniformity with virtually the same growth velocities. The yolk sac demonstrated uniform growth until week 10 only. Differences between the gestational age based on the last menstrual period and the true gestational age, and/or differences in the early growth of the embryos before the start of the study at 7 weeks, may have contributed to the variation between the individuals.*

## INTRODUCTION

The increase in size of a living individual over a period of time is defined as growth. Classical human embryology is based on aborted conceptuses and the analysis of growth of individual embryos has not been possible. The development of a staging system by O'Rahilly and Müller[1], where the measurements and the structural and morphological features of aborted embryos of the first 8 postovulatory weeks were divided into 23 stages based on the external and internal morphological status of the embryos, helped to draw indirect conclusions about growth.

The introduction of ultrasound has opened new possibilities for describing and measuring the growing conceptus *in vivo*. There have been many studies of biometric parameters such as the crown–rump length, biparietal diameter, abdominal diameter, limb length, diameter of the chorionic cavity, the amniotic cavity and the yolk sac[2–7]. Such studies were usually designed as single-level models, in which each individual was measured on a single occasion, and analyzed cross-sectionally. With the increased resolution offered by high-frequency transvaginal ultrasound equipment, very detailed images of embryonic structures could be obtained, and the scope of biometric measurements has been extended to the evaluation of embryonic organs[8–10]. Mixed studies involve both single and repeated measurements and are not recommended for either cross-sectional or longitudinal statistical analysis[11].

In order to register changes in growth over time, at least two measurements of the individual must be made on successive occasions. The measurements should be evaluated

Correspondence: Dr H.-G. Blaas, National Center for Fetal Medicine, Department of Obstetrics and Gynecology, Trondheim University Hospital, N-7006 Trondheim, Norway



Received 8–4–98
Revised 3–7–98
Accepted 6–7–98

by longitudinal analysis, which requires special analytical methods[11–14]. Therefore, charts derived from single-level studies describing the relationship of the size to the age of individuals should not be used for the evaluation of growth[11]. Longitudinal studies of multiple parameters in the first trimester for assessing embryonic growth are lacking.

The aim of the present paper was to examine the living human conceptus longitudinally to observe and analyze its growth.

## SUBJECTS AND METHODS

Thirty-six pregnant women were recruited for a longitudinal transvaginal ultrasound study according to a protocol approved by the regional committee of ethics[8–10]. The inclusion and exclusion criteria were strict, as we wanted to avoid bias which could affect the study group: non-smoking women with single uneventful pregnancies were included in the study if they had had regular menstrual periods (28–30 days) and no hormone therapy in the 3 months prior to pregnancy. Diabetes, pre-eclampsia and delivery of preterm or growth-restricted infants were exclusion criteria. Five women were withdrawn from the study: three of them experienced early pregnancy loss, one had bleeding during week 9, and one had a preterm delivery at 36 weeks due to pre-eclampsia. Two women chose to discontinue participation in the trial after the first examination. Thus, the pregnancies of 29 women were analyzed (mean age 28 years, range 19–38). All children were delivered between 37 weeks 2 days and 42 weeks 1 day postmenstrually (mean 40 weeks 0 days). The birth weight ranged from 2610 g to 4890 g (mean 3610 g).

An ultrasound scanner (Dornier AI 3200, Phoenix, AZ, USA) with a 7.5-MHz high-frequency transvaginal probe was used for the examinations. The emitted energy was reduced to 30% (0.58 mW/cm$^2$ spatial peak temporal average (SPTA)) of the maximal intensity of 1.92 mW/cm$^2$ SPTA *in situ*.

The first examination was performed at between 7 and 8 completed gestational weeks according to the last menstrual period (LMP). Five examinations were carried out for each pregnancy (in total 145 observations in 29 individuals), with an interval of approximately 7 days between each examination. Each examination lasted for 20–30 min. To limit the examination time, only one measurement per parameter was performed. All ultrasound examinations were made by one person to reduce measurement bias by interobserver variation.

The greatest length and the crown–rump length (CRL) of the embryo and fetus are different measurements[15,16]. We chose the widely used term CRL even though we measured the greatest length in a straight line from the cranial to the caudal end of the body in the straightest possible position of the embryo/fetus.

The width of the head was measured in the horizontal section perpendicular to the body axis. At 7 weeks this plane involved the rhombencephalon and the posterior part of the mesencephalon. The largest width was found at the height of the rhombic lips, the future cerebellum. Owing to the development of the brain characterized by differences in growth of the brain compartments and by the 'deflection' of the brain, the largest width alters its position in relation to cerebral landmarks during the embryonic and early fetal period. In the early fetal period the future cranium becomes successively distinguishable so that the biparietal diameter (BPD) can be obtained by placing the calipers at the outer border of the not-yet-ossified cranium in a horizontal section at the level of the thalamus. We chose the designation BPD for the measurements during the embryonic period as well as for the fetal period. The anteroposterior diameter of the embryonic head, designated as the occipitofrontal diameter (OFD), was obtained in the same section perpendicular to the BPD.

The mean abdominal diameter (MAD)[17] was measured in the horizontal section through the embryonic body below the heart and above the umbilicus.

The mean diameter of the chorionic cavity and the amniotic cavity was calculated by the arithmetic mean of three diameters measured perpendicular to each other. For these measurements, the calipers were placed on the thin membranes of the chorionic and amniotic cavities. The imaging of the thickness of the echogenic wall of the yolk sac varies with the transducer-dependent point spread function and with the gain setting. Therefore, we placed the calipers not on the outside but in the middle of the yolk sac wall, to avoid this possible measurement bias.

All statements of age, including the citations from embryological literature, are made in completed weeks and completed days and based on the last menstrual period.

### Statistical analysis

The variation of the data[13] was differentiated into two levels: the variation of each individual (level 1) and th variation between the individuals (level 2). The progran MLn[18] was used for the statistical evaluation of these hierarchical data.

The method of longitudinal analysis is similar to fitting a straight line for each individual. To examine the basic relationship between the response variable and the explanatory variable a longitudinal plot was evaluated visually to obtain information on the trend and possible heteroscedasticity. A linear curve was suitable in most of the cases.

The statistical model for the data had to take into account the difference in size between the individuals:

$$Y_{ij} = \alpha + \alpha_i + \alpha_{ij} + \beta x_{ij} \qquad (A)$$

where the index $ij$ meant observation number $i$ on the $j$th individual. Here $\alpha_{ij}$ was the intercept residuals for observations and $\alpha_i$ the intercept residuals for individuals. Both residuals were assumed to be independent and normally distributed, with zero means and constant variances $\sigma^2_{1\alpha}$ and $\sigma^2_{2\alpha}$, respectively. Levels 1 and 2 were assumed to be independent.

The next step was to check whether the slope for each individual was identical; this was done by adding slope

residuals for individuals ($\beta_j$) at level 2 to the slope coefficient ($\beta$). The model became

$$Y_{ij} = \alpha + \alpha_j + \alpha_{ij} + (\beta + \beta_j)x_{ij} \quad (B)$$

The new random coefficients $\beta_j$ were assumed to be independent and normally distributed, with zero mean and variance $\sigma^2_{2\beta}$. Since there were two random variables ($\alpha_j$ and $\beta_j$) at level 2, a possible covariance $\sigma^2_{2\alpha\beta}$ was included.

The $-2 \times \log$ likelihoods for models (A) and (B) were computed. It was possible to test the significance of the parameters $\beta_j$ since the difference in the likelihoods was $\chi^2$ with the number of new parameters as degree of freedom[13]. In this case there were two degrees of freedom ($\sigma^2_{2\beta}$ and $\sigma^2_{2\alpha\beta}$).

The described procedure was applied for the analysis of the BPD, OFD, MAD, chorionic cavity diameter, amniotic cavity diameter and, after square root transformation, of the CRL.

The longitudinal plot of the yolk sac diameter gave information about the trend of the data and hints about the variance structure. The stepwise analysis resulted in the model

$$Y_{ij} = \alpha + \alpha_j + \alpha_{ij} + (\beta + \beta_j + \beta_{ij})x_{ij} + (\gamma + \gamma_j)x_{ij}^2 + \eta x_{ij}^3 \quad (C)$$

where $\alpha$, $\beta$, $\gamma$ and $\eta$ are regression coefficients, $\alpha_j$, $\beta_j$ and $\gamma_j$ are residuals for individuals, and $\alpha_{ij}$ and $\beta_{ij}$ are residuals for observations.

The model assumptions were examined visually by constructing normal and residual plots for all random variables.

The statistical analysis was based on the LMP-based gestational age. The LMP values of the study were centered at 9 weeks 4 days (9.5862 weeks) before the statistical analysis. Thus, the constants $\alpha$ (Tables 1–7) are not related to the $y$-axis in $x = 0$ days, but in $x = 9.5862$ days.

## Intraobserver study

We evaluated the reproducibility of the measurements of the BPD and the CRL by an intraobserver study of 42 pregnant women who did not participate in the longitudinal study. The age of the measured embryos/fetuses varied from 7 weeks 2 days to 11 weeks 6 days, mean 9 weeks 4 days (9.5862 weeks). All measurements were recorded on video print pictures, the values hidden from the examiner. The participants were scanned, then left the examination room for about 5–10 min before they were rescanned. Limits of agreement (mean difference ± 2SD) for intraobserver measurements were calculated[19].

# RESULTS

As a rule we obtained five observations per analyzed parameter in each of the 29 individuals with a few exceptions, where only four observations were made. Figures 1–7 show the longitudinal plots of the original measurements and the corresponding estimated curves for all individuals based on model B except for the yolk sac (Figure 7) where model C was applied.

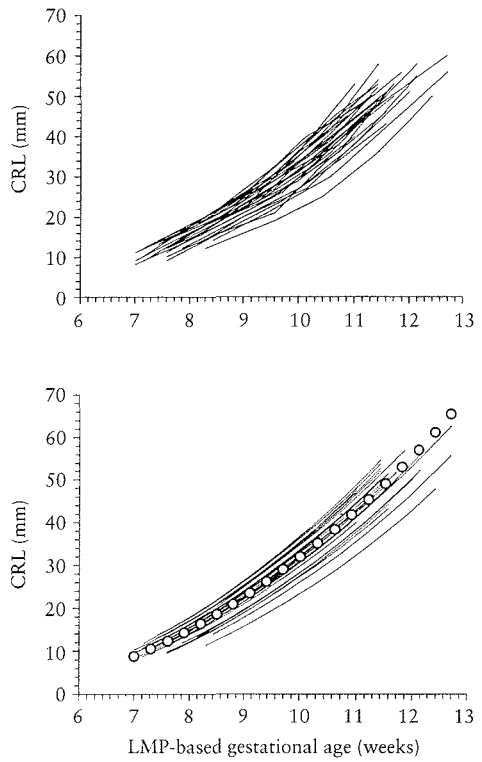


**Figure 1** Longitudinal plot of the measurements of the crown–rump length (CRL) (above), and the corresponding estimated curves based on the individual residuals (below). The circles represent the mean curve

The CRL values at the first examination varied from 8 to 18 mm. In embryos of 12 mm in CRL, the age range of the LMP-based age was at most 8 days (Figure 1). Correspondingly the BPD values varied from 3 to 8 mm, with the largest age range of 9 days in embryos with a BPD of 4 mm (Figure 2).

The longitudinal plot of the CRL measurements (145 observations) were curvilinear and showed a heteroscedastic distribution of the data (Figure 1). For the analysis of the CRL development, a square root transformation of the data was performed. The variation of the slope between the individuals was hardly visible using model B (Figure 1) and did not describe the data significantly better than model A ($p = 0.08$) (Table 1). The total variation of the data consisted of 85% variation in level 2 (between the individuals), and 15% variation in level 1 (of each individual).

The longitudinal plots of the measurements of the BPD (139 observations), the OFD (139 observations), the MAD (142 observations), the chorionic cavity diameter (145 observations) and the amniotic cavity diameter (143 observations) revealed a linear flow of the data (Figures 2–6). The statistical analysis showed non-significant differences of the slopes at level 2 (Tables 2–6). The corresponding

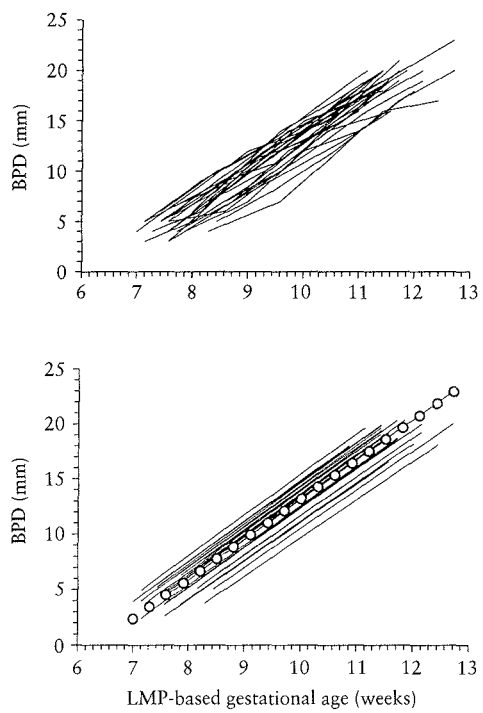


**Figure 2** Longitudinal plot of the measurements of the biparietal diameter (BPD) (above), and the corresponding estimated curves based on the individual residuals (below). The circles represent the mean curve

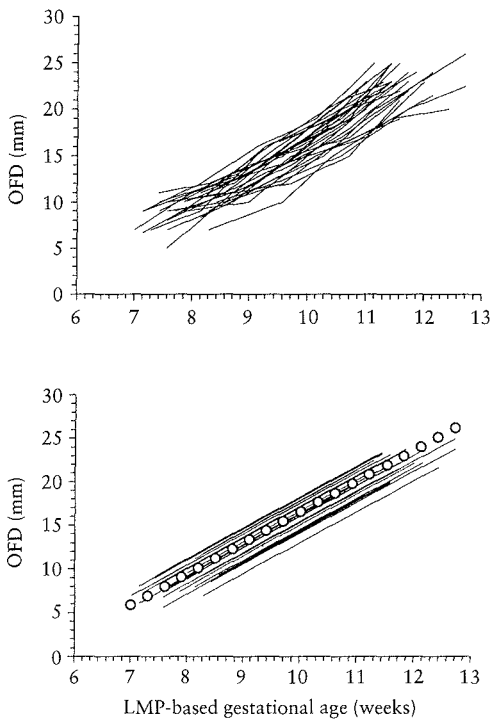


**Figure 3** Longitudinal plot of the measurements of the occipitofrontal diameter (OFD) (above), and the corresponding estimated curves based on the individual residuals (below). The circles represent the mean curve

**Table 1** Estimates of crown–rump length, 145 observations. Square root transformation applied. SE shown in parentheses

| *Parameter* | *Model (A)* | *Model (B)* |
|---|---|---|
| *Fixed* | | |
| Intercept α | 5.277 (0.058) | 5.282 (0.057) |
| Slope β | 0.8986 (0.0073) | 0.8991 (0.0087) |
| *Random* | | |
| Level 1 (individuals) | | |
| $\sigma^2_{1\alpha}$ | 0.01616 (0.0021) | 0.01399 (0.0021) |
| Level 2 (between individuals) | | |
| $\sigma^2_{2\alpha}$ | 0.09371 (0.025) | 0.09233 (0.025) |
| $\sigma^2_{2\beta}$ | | 0.0008691 (0.00061) |
| $\sigma^2_{2\alpha\beta}$ | | 0.003895 (0.0028) |
| −2 log likelihood | −88.05 | −93.04 |

**Table 2** Estimates of biparietal diameter, 139 observations. SE shown in parentheses

| *Parameter* | *Model (A)* | *Model (B)* |
|---|---|---|
| *Fixed* | | |
| Intercept α | 11.64 (0.27) | 11.66 (0.26) |
| Slope β | 3.598 (0.041) | 3.599 (0.044) |
| *Random* | | |
| Level 1 (individuals) | | |
| $\sigma^2_{1\alpha}$ | 0.4632 (0.062) | 0.4434 (0.069) |
| Level 2 (between individuals) | | |
| $\sigma^2_{2\alpha}$ | 1.957 (0.54) | 1.915 (0.53) |
| $\sigma^2_{2\beta}$ | | 0.00856 (0.016) |
| $\sigma^2_{2\alpha\beta}$ | | 0.0749 (0.064) |
| −2 log likelihood | 376.02 | 374.06 |

$p$ values were $p = 0.375$ (BPD), $p = 1$ (OFD), $p = 0.45$ (MAD), $p = 0.067$ (chorionic cavity diameter) and $p = 0.062$ (amniotic cavity diameter). Therefore, model A was used for the description of the data. The variation of the data at level 2 expressed as percentage of the total variation, was 81% for BPD, 69% for OFD, 59% for MAD, 56% for the chorionic cavity diameter and 75% for the amniotic cavity diameter. Thus, for the most part the variation consisted of variation between individuals.

The mean growth curve of the CRL and that of the mean amniotic cavity diameter showed very similar absolute values in millimeters throughout the observation period from 7 weeks to 12 weeks (Figures 1 and 6).

The yolk sac (142 observations) appeared as a round structure with a rather echogenic wall during the embryonic period. The longitudinal plot of the yolk sac diameter initially showed a slightly increasing linear course of the growth until 10 weeks of gestation. During weeks 10 to 11

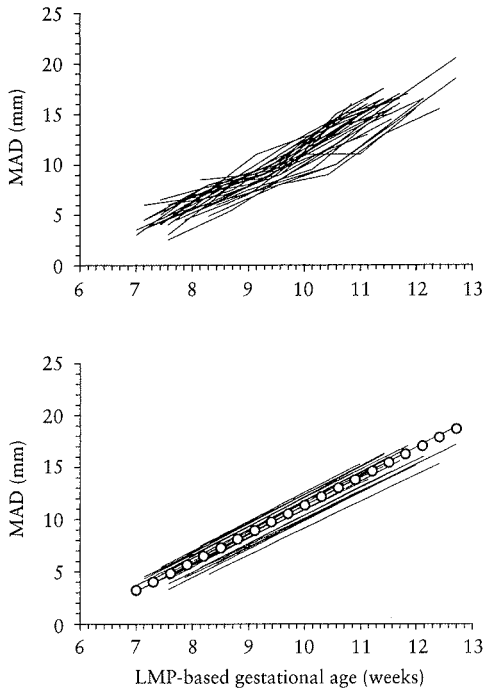


**Figure 4** Longitudinal plot of the measurements of the mean abdominal diameter (MAD) (above), and the corresponding estimated curves based on the individual residuals (below). The circles represent the mean curve

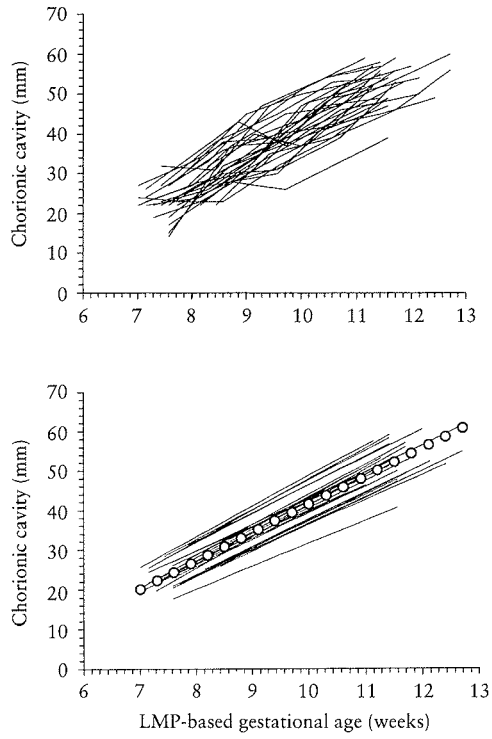


**Figure 5** Longitudinal plot of the measurements of the chorionic cavity diameter (above), and the corresponding estimated curves based on the individual residuals (below). The circles represent the mean curve

**Table 3** Estimates of occipitofrontal diameter, 139 observations. SE shown in parentheses

| *Parameter* | *Model (A)* | *Model (B)* |
|---|---|---|
| *Fixed* | | |
| Intercept α | 15.05 (0.30) | 15.05 (0.30) |
| Slope β | 3.555 (0.063) | 3.555 (0.063) |
| *Random* | | |
| Level 1 (individuals) | | |
| $\sigma^2_{1\alpha}$ | 1.080 (0.15) | 1.080 (0.15) |
| Level 2 (between individuals) | | |
| $\sigma^2_{2\alpha}$ | 2.382 (0.69) | 2.382 (0.69) |
| $\sigma^2_{2\beta}$ | | 0 |
| $\sigma^2_{2\alpha\beta}$ | | 0 |
| −2 log likelihood | 476.06 | 476.06 |

**Table 4** Estimates of mean abdominal diameter, 142 observations. SE shown in parentheses

| *Parameter* | *Model (A)* | *Model (B)* |
|---|---|---|
| *Fixed* | | |
| Intercept α | 10.21 (0.19) | 10.22 (0.19) |
| Slope β | 2.808 (0.047) | 2.81 (0.051) |
| *Random* | | |
| Level 1 (individuals) | | |
| $\sigma^2_{1\alpha}$ | 0.6364 (0.085) | 0.5968 (0.091) |
| Level 2 (between individuals) | | |
| $\sigma^2_{2\alpha}$ | 0.9271 (0.28) | 0.9108 (0.27) |
| $\sigma^2_{2\beta}$ | | 0.04456 (0.053) |
| $\sigma^2_{2\alpha\beta}$ | | 0.01633 (0.022) |
| −2 log likelihood | 399.54 | 397.94 |

the shape of the yolk sac altered and its wall became thinner. The yolk sac became enlarged in some cases, while it shrank in other cases. The data were fitted by a polynomial of third degree (Figure 7). Estimates are shown in Table 7.

The limits of agreement were (−0.9,0.8) mm for the BPD and (−1.3,1.3) mm for the CRL.

## DISCUSSION

A growth study with several individuals who are examined serially on different occasions has a hierarchical two-level structure, where the repeated measurements of one individual represent the level 1 units and the individuals represent the level 2 units[13]. The statistical analysis of

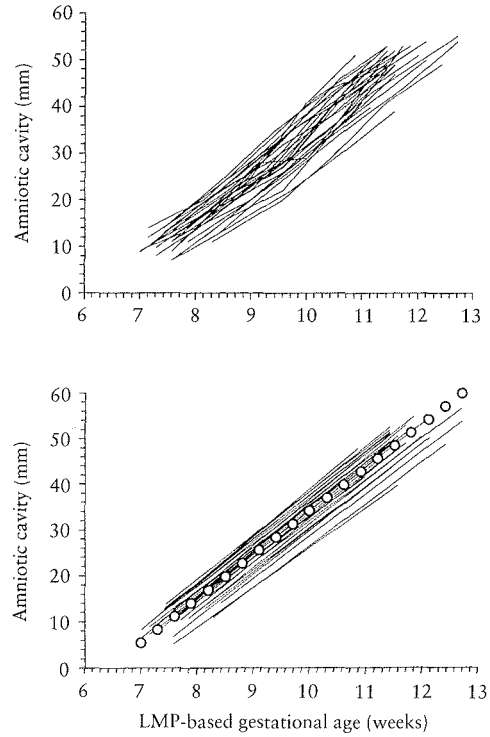


**Figure 6** Longitudinal plot of the measurements of the amniotic cavity diameter (above), and the corresponding estimated curves based on the individual residuals (below). The circles represent the mean curve

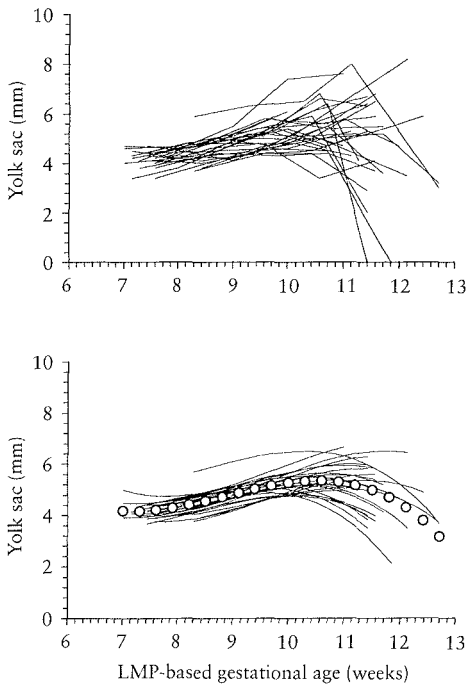


**Figure 7** Longitudinal plot of the measurements of the yolk sac diameter (above), and the corresponding estimated curves based on the individual residuals (below). The circles represent the mean curve

**Table 5** Estimates of chorionic cavity diameter, 145 observations. SE shown in parentheses

| *Parameter* | *Model (A)* | *Model (B)* |
|---|---|---|
| *Fixed* | | |
| Intercept α | 38.4 (0.78) | 38.5 (0.78) |
| Slope β | 7.101 (0.20) | 7.112 (0.24) |
| *Random* | | |
| Level 1 (individuals) | | |
| $\sigma^2_{1\alpha}$ | 12.07 (1.6) | 10.25 (1.6) |
| Level 2 (between individuals) | | |
| $\sigma^2_{2\alpha}$ | 15.24 (4.6) | 15.62 (4.7) |
| $\sigma^2_{2\beta}$ | | 1.440 (1.0) |
| $\sigma^2_{2\alpha\beta}$ | | 0.7012 (0.46) |
| –2 log likelihood | 830.35 | 824.94 |

**Table 6** Estimates of amniotic cavity diameter, 143 observations. SE shown in parentheses

| *Parameter* | *Model (A)* | *Model (B)* |
|---|---|---|
| *Fixed* | | |
| Intercept α | 30.02 (0.67) | 30.07 (0.67) |
| Slope β | 9.487 (0.12) | 9.490 (0.14) |
| *Random* | | |
| Level 1 (individuals) | | |
| $\sigma^2_{1\alpha}$ | 4.00 (0.53) | 3.406 (0.52) |
| Level 2 (between individuals) | | |
| $\sigma^2_{2\alpha}$ | 12.15 (3.4) | 12.18 (3.4) |
| $\sigma^2_{2\beta}$ | | 0.2383 (0.16) |
| $\sigma^2_{2\alpha\beta}$ | | 0.8051 (0.52) |
| –2 log likelihood | 684.38 | 678.81 |

the present study on 29 individuals considered the longitudinal structure of the data. We found a high degree of uniformity of the growth velocities of the analyzed parameters from 7 to 12 weeks of gestation where the individual curves virtually run parallel, although there was a considerable spread of values for a specific gestational age.

The prerequisite for analyzing growth is the knowledge of the age. In obstetric studies, the determination of the gestational age has been a recurrent problem. The time interval between the onset of the last menstrual period and the day of conception may vary from 1 to 42 days[20], and from the history of menstrual cyclicity, even when regular, there is no certain way of determining the exact age[21].

Many of the first-trimester biometric studies have chosen patients from assisted reproductive treatment programs, where the exact timing of the ovulation and fertilization is known[7, 22–24]. Dickey and Gasser[23] analyzed,

**Table 7** Estimates of yolk sac diameter, 142 observations. SE shown in parentheses

| *Parameter* | *Model (C)* |
|---|---|
| *Fixed* | |
| $\alpha$ | 5.109 (0.097) |
| $\beta$ | 0.4359 (0.086) |
| $\gamma$ | −0.1377 (0.039) |
| $\eta$ | −0.06392 (0.017) |
| *Random* | |
| Level 1 (individuals) | |
| $\sigma^2_{1\alpha}$ | 0.2297 (0.045) |
| $\sigma^2_{1\beta}$ | 0.1061 (0.032) |
| $\sigma^2_{1\alpha\beta}$ | 0.1444 (0.033) |
| Level 2 (between individuals) | |
| $\sigma^2_{2\alpha}$ | 0.1528 (0.047) |
| $\sigma^2_{2\beta}$ | 0.09213 (0.039) |
| $\sigma^2_{2\gamma}$ | 0.01555 (0.0087) |
| $\sigma^2_{2\beta\gamma}$ | 0.04014 (0.017) |

cross-sectionally, the data obtained from 107 pregnancies from an assisted fertilization program. They registered a ten-fold difference in the level of human chorionic gonadotropin (hCG) on post-insemination days 13 to 16. Later they found differences of the CRL in embryos of the same age. For example, at post-insemination day 41, the CRL in ten embryos varied from 7 to 15 mm, and at the approximate age of Carnegie stage 18 (post-insemination days 43–46) the CRL in 15 embryos varied from 8 to 19 mm. Other CRL studies based on populations derived from assisted reproductive treatment programs analyzed the accuracy of age assessment by measuring the embryonic length, and found relatively large 95% prediction intervals of 12.8 days[25], 9.8 days[26] and 9.3 days[27]. These variations indicated developmental differences of the early conceptuses. In a subfertile population intervention is necessary to achieve pregnancy, and these pregnancies do not meet the criterion of 'normal', although they develop uneventfully in most cases. Such intervention may include hormonal treatment, harvesting of the ovum, external fertilization and artificial transfer of the embryo into the uterus or tube. Animal studies have indicated that treatment with gonadotropin as it is used in *in vitro* fertilization may have adverse effects such as delayed implantation and impaired embryonic/fetal development[28].

Embryological studies have implied uniform development of the human embryo with small differences in size and age at different stages. In the Carnegie staging system for embryonic development[1], the time range for stages 16–18 is approximately 3–4 days, and that for stage 19 is approximately 3 days. These are the four stages at which the measurements of the embryos in the present study started. The length of the embryos from Appendix I of the Carnegie Collection[1] ranged from 7 to 12.2 mm ($n$ = 48) at stage 16 (mean approximately 7 weeks 2 days), 10.1 to 14.5 mm ($n$ = 30) at stage 17 (mean approximately 7 weeks 6 days), 12 to 18 mm ($n$ = 40) at stage 18 (mean approximately 8 weeks 2 days) and 16 to 21.4 mm ($n$ = 28) at stage 19 (mean approximately 8 weeks 5–6 days). When considering the measurement of the length of the embryo one must keep in mind the fact that, owing to the fixation procedures, the length of embryos as measured in embryological studies may be different from equivalent *in vivo* CRL measurements[29]. Moore and co-workers[30], who studied the size, stage and age of 276 embryos, concluded that normal anatomic structures probably develop within a short space of time.

The population of the present study was small, but had strict inclusion and exclusion criteria. The development of these pregnancies and the outcomes were normal with respect to the date of delivery, the birth weight, the sex distribution (16 males : 13 females) and the health of the infants. Except for the yolk sac diameter, the raw longitudinal plots of the measurements showed a high degree of uniformity with a parallel rather than intersecting course of the individual curves. The small level 1 variation and the intraobserver study on CRL and BPD measurements demonstrated that the measurements were exact and the reproducibility was high. The calculation of the longitudinal plots by the statistical program MLn gave smoothed individual curves that ran virtually parallel without any crossing over. If we assume the Carnegie stage 18 to extend from approximately 8 weeks 1 day to 8 weeks 4 days, the variation of 12 mm between the CRL values of this period (10.5–22.5 mm) in the present study seemed very large and was probably not an expression of simple variation in size of individuals of the same age alone (Figure 1, CRL, smoothed curve). According to the embryological literature, nearly two-thirds of the embryos at stage 18 had a CRL of 14 to 16 mm, with a maximum variation of only 6 mm (12–18 mm) (Appendix I[1]).

Several facts may be responsible for the discrepancy. Embryos of the same age may have reached different developmental stages. Variations of the moment of ovulation[31], fertilization or nidation may result in differences between the true age and the LMP-based age, or there may be variations of the very early development and growth velocity of the human embryo, as suggested by the studies of Dickey and Gasser[23]. The finding of parallel growth curves from 7 weeks to 12 weeks may indicate that, once the embryos start to grow, they all follow the same growth velocity, which implies that embryos of the same size have approximately the same 'true' age. In a large-scale study of 15 241 women, the ultrasound-based and LMP-based estimates of the day of delivery were compared[32]. A total of 9240 women with spontaneous onset of labor had reliable data of the LMP and regular menstrual cycles. This study showed that the size (BPD) of the young fetus correlated better with the day of delivery than with LMP-based age.

There have been only a few longitudinal studies addressing growth in early pregnancy[22,33]. Rossavik and co-workers[22] used two CRL measurements to calculate growth. Such a procedure assumes constant growth within the interval and is vulnerable to measurement errors, which might give falsely different slopes. Both embryological and sonoembryological studies have shown that the CRL develops in a non-linear fashion[1,4,5,7,24–27,29,34–36]. Embryology describes a gradual transition from the flexed early embryo to the straight body of the early fetus, where the

deflection of the embryonic brain plays an important role[1]. This may be partly responsible for the curvilinear development of the CRL. Thus, concerning the CRL the applicability of the procedure proposed by Rossavik and colleagues is limited.

Rabelink and co-workers[33] analyzed 109 pregnancies longitudinally, producing a total of 794 CRL and 1795 BPD measurements. For each individual they constructed linear regression curves after cutting off measurements of the CRL below 20 mm and above 90 mm, thus analyzing only the straight part of the S-shaped curve. The individual CRL curves showed different slopes and different intercepts on the $x$ axis[33]. Correlation of the slopes with the intercepts on the $x$ axis indicated that the individual embryos with a late onset of growth (high $x$-axis intercept) had a steeper slope as a characteristic of 'catch-up growth'. However, cutting off important measurements of the size and extrapolating curves to the $x$ axis contributes to significant uncertainty of the results.

Although the plot of the BPD measurements in 108 individuals had a slight bend, Rabelink and co-workers[33] used simple linear regression curves for each individual. The correlation of the slopes of the individual BPD curves with the intercepts on the $x$ axis showed different velocities, indicating 'catch-up growth' in embryos with a delayed start. The present study could not confirm any differences of the growth rate of the BPD between the individuals.

The development of the anteroposterior diameter of the head, the OFD, has not been evaluated during the first trimester in other studies, so comparisons with previous studies cannot be made.

Rossavik and colleagues[22] carried out longitudinal studies on the mean chorionic cavity diameter from three perpendicular planes three times each in 19 patients, finding similar slopes for the individuals to those in the present study.

Embryologists have shown the close relationship between amniotic cavity volume and fetal size[37]. There is a remarkable similarity in the absolute values of the estimated mean CRL and the estimated mean diameter of the amniotic cavity (Figures 1 and 6).

The longitudinal plot and the corresponding estimated curves of the yolk sac in the present study showed the slightly increasing parallel course of growth until 10 weeks of gestation, followed by disorganized development of growth in the early fetal period; this probably reflects spontaneous physiological events of normal embryonic development[3].

## CONCLUSION

In the present longitudinal biometric study on 29 embryos from 7 to 12 weeks of gestation, the observations around the curve for each individual lay close together, but there were considerable variations between different individuals. The measured parameters (CRL, BPD, OFD, MAD, chorionic cavity diameter and amniotic cavity diameter) showed a high degree of uniformity with virtually the same growth velocities. The yolk sac also demonstrated uniform growth until 10 weeks, when it degenerated either by shrinking or by enlarging before dissipating; the alteration of the shape is believed to reflect the cessation of the physiological function at that time.

The clear spread of the parallel growth curves between the individuals varied more than expected. This might be due to a discrepancy between the LMP-based age and the true age, caused by variations of the time of ovulation, fertilization and nidation, and/or of the growth at very early stages. Once the growth begins, the embryos seem to follow the same growth curve.

Further research should be directed towards very early human embryonic growth in normal pregnancy in order to shed light on human development between the last menstrual period and the late embryonic period.

## ACKNOWLEDGEMENT

Mrs Nancy Lea Eik-Nes revised the manuscript.

## REFERENCES

1. O'Rahilly R, Müller F. *Developmental Stages in Human Embryos*. Washington DC: Carnegie Institution Publications, 1987:637
2. Goldstein I, Zimmer EA, Tamir A, Peretz BA, Paldi E. Evaluation of normal gestational sac growth: appearance of embryonic heartbeat and embryo body movements using the transvaginal technique. *Obstet Gynecol* 1991;77:885–8
3. Jauniaux E, Jurkovic D, Henriet Y, Rodesch F. Development of the secondary human yolk sac: correlation of sonographic and anatomical features. *Hum Reprod* 1991;6:1160–6
4. Kustermann A, Zorzoli A, Spagnolo D, Nicolini U. Transvaginal sonography for fetal measurement in early pregnancy. *Br J Obstet Gynaecol* 1992;99:38–42
5. Grisiola G, Milano V, Pilu G, Banzi C, David C, Gabrielli S, Rizzo N, Morandi R, Bovicelli L. Biometry of early pregnancy with transvaginal sonography. *Ultrasound Obstet Gynecol* 1993;3:403–11
6. Zorzoli A, Kustermann A, Caravelli E, Corso FE, Fogliani R, Aimi G, Nicolini U. Measurements of fetal limb bones in early pregnancy. *Ultrasound Obstet Gynecol* 1994;4:29–33
7. Lasser DM, Peisner DB, Vollebergh J, Timor-Tritsch I. First-trimester fetal biometry using transvaginal sonography. *Ultrasound Obstet Gynecol* 1993;3:104–8
8. Blaas H-G, Eik-Nes SH, Kiserud T, Hellevik LR. Early development of the forebrain and midbrain: a longitudinal ultrasound study from 7 to 12 weeks of gestation. *Ultrasound Obstet Gynecol* 1994;4:183–92
9. Blaas H-G, Eik-Nes SH, Kiserud T, Hellevik LR. Early development of the hindbrain: a longitudinal ultrasound study from 7 to 12 weeks of gestation. *Ultrasound Obstet Gynecol* 1995; 5:151–60
10. Blaas H-G, Eik-Nes SH, Kiserud T, Hellevik LR. Early development of the abdominal wall, stomach and heart from 7 to 12 weeks of gestation: a longitudinal ultrasound study. *Ultrasound Obstet Gynecol* 1995;6:240–9
11. Altman DC, Chitty LS. Design and analysis of studies to derive charts of fetal size. *Ultrasound Obstet Gynecol* 1994;4: 308–13
12. Rutter CM. Analysis of longitudinal data: random coefficient regression modelling. *Stat Med* 1994;13:1211–31
13. Goldstein H, ed. *Multilevel Statistical Models*. London: Edward Arnold, 1995;3:178

14. Royston P. Calculation of unconditional and conditional reference intervals for fetal size and growth from longitudinal measurements. *Stat Med* 1995;14:1417–36
15. Mall FP. On measuring human embryos. *Anat Rec* 1907;1: 129–40
16. O'Rahilly R, Müller F. Embryonic length and cerebral landmarks in staged human embryos. *Anat Rec* 1984;209:265–71
17. Eik-Nes SH, Grøttum P, Persson P-H, Marsál K. Prediction of fetal growth deviation by ultrasound biometry. I. Methodology. *Acta Obstet Gynecol Scand* 1982;61:53–8
18. Woodhouse G, Rasbash J, Goldstein H, Yang M, Howarth J, Plewis I. Program Multi-Level n. *MLn Command Reference*. London: Institute of Education, 1995
19. Bland JM, Altman DG. Statistical methods for assessing agreement between two methods of clinical measurement. *Lancet* 1986;1:307–10
20. Pryll W. Kohabitationstermin und Kindsgeschlecht. *Münch Med Wochenschr* 1916;45:1579–82
21. Geirsson RT. Ultrasound instead of last menstrual period as the basis of gestational age assignment. *Ultrasound Obstet Gynecol* 1991;1:212–19
22. Rossavik IK, Torjusen GO, Gibbons WE. Conceptual age and ultrasound measurements of gestational sac and crown–rump length in *in vitro* fertilization pregnancies. *Fertil Steril* 1988; 49:1012–17
23. Dickey RP, Gasser RF. Ultrasound evidence for variability in the size and development of normal human embryos before the tenth post-insemination week after assisted reproductive technologies. *Hum Reprod* 1993;8:331–7
24. Evans J. Fetal crown–rump length values in the first trimester based upon ovulation timing using the luteinizing hormone surge. *Br J Obstet Gynaecol* 1991;98:48–51
25. MacGregor SN, Tamura RK, Sabbagha RE, Minogue JP, Gibson ME, Hoffman DI. Underestimation of gestational age by conventional crown–rump length dating curves. *Obstet Gynecol* 1987;70:344–8
26. Daya S. Accuracy of gestational age estimation by means of fetal crown–rump length measurements. *Am J Obstet Gynecol* 1993;168:903–8
27. Wisser J, Dirschedl P, Krone S. Estimation of gestational age by transvaginal sonographic measurements of greatest embryonic length in dated human embryos. *Ultrasound Obstet Gynecol* 1994;4:457–62
28. Ertzeid G, Storeng R, Lyberg T. Treatment with gonadotropins impaired implantation and fetal development in mice. *J Assist Reprod Genet* 1993;10:286–91
29. Drumm JE, O'Rahilly R. The assessment of prenatal age from the crown–rump length determined ultrasonically. *Am J Anat* 1977;148:555–60
30. Moore GW, Hutchins GM, O'Rahilly R. The estimated age of staged human embryos and early fetuses. *Am J Obstet Gynecol* 1981;139:500–6
31. Bell ET, Loraine JA. Time of ovulation in relation to cycle length. *Lancet* 1965;1:1029–30
32. Tunón K, Eik-Nes SH, Grøttum P. A comparison between ultrasound and a reliable last menstrual period as a predictor of the day of delivery in 15 000 examinations. *Ultrasound Obstet Gynecol* 1996;8:178–85
33. Rabelink IAA, Degen JEM, Kessels MEW, Nienhuis SJ, Ruissen CJ, Hoogland HJ. Variation in early growth. *Eur J Obstet Gynecol Reprod Biol* 1994;53:39–43
34. Robinson HP, Fleming JEE. A critical evaluation of sonar 'crown–rump length' measurements. *Br J Obstet Gynaecol* 1975;82:702–10
35. Pedersen JF. Fetal crown–rump length measurement by ultrasound in normal pregnancies. *Br J Obstet Gynaecol* 1982;89: 926–30
36. O'Rahilly R, Gardner E. The timing and sequence of events in the development of the human nervous system during the embryonic period proper. *Z Anat Entwickl-Gesch* 1971;134: 1–12
37. Abramovich DR. The volume of amniotic fluid in early pregnancy. *J Obstet Gynaecol Br Cwlth* 1968;75:728–31

# Paper V

**Harm-Gerd Blaas, Sturla H. Eik-Nes, Torvid Kiserud, Sevald Berg, Bjørn Angelsen, Bjørn Olstad. Three-dimensional imaging of the brain cavities in human embryos. Ultrasound Obstet Gynecol 1995; 5:228–32**

*Ultrasound Obstet. Gynecol. 5 (1995) 228–232*

# Three-dimensional imaging of the brain cavities in human embryos

*H.-G. Blaas, S. H. Eik-Nes, T. Kiserud, S. Berg, B. Angelsen* and B. Olstad†*

National Center for Fetal Medicine, Department of Obstetrics and Gynecology, Trondheim University Hospital, Trondheim; *Department of Biomedical Engineering, University of Trondheim, Trondheim; †Department of Computer Systems and Telematics, The Norwegian Institute of Technology, Trondheim, Norway

Key words: TRANSVAGINAL ULTRASOUND, CENTRAL NERVOUS SYSTEM, EMBRYONIC BRAIN, FIRST TRIMESTER, THREE-DIMENSIONAL ULTRASOUND

## ABSTRACT

*A system for high-resolution three-dimensional imaging of small structures has been developed, based on the Vingmed CFM-800 annular array sector scanner with a 7.5-MHz transducer attached to a PC-based TomTec Echo-Scan unit. A stepper motor rotates the transducer 180° and the complete three-dimensional scan consists of 132 two-dimensional images, video-grabbed and scan-converted into a regular volumetric data set by the TomTec unit. Three normal pregnancies with embryos of gestational age 7, 9 and 10 weeks received a transvaginal examination with special attention to the embryonic/fetal brain. In all three cases, it was possible to obtain high-resolution images of the brain cavities. At 7 weeks, both hemispheres and their connection to the third ventricle were delineated. The isthmus rhombencephali could be visualized. At 9 weeks, the continuous development of the brain cavities could be followed and at 11 weeks the dominating size of the hemispheres could be depicted. It is concluded that present ultrasound technology has reached a stage where structures of only a few millimeters can be imaged* in vivo *in three-dimensions with a quality that resembles the plaster figures used in embryonic laboratories. The method can become an important tool in future embryological research and also in the detection of early developmental disorders of the embryo.*

## INTRODUCTION

Modern embryology was established about 100 years ago when Wilhelm His developed the method of using microscopic sections to reconstruct the human embryo in three-dimensional form[1]. The three-dimensional approach remains a method for understanding the anatomy of the human embryo, and today we are aided by advanced technology.

Ultrasound technology, since its introduction in the 1960s, has greatly improved the clinical practice of the gynecologist, and is still undergoing technical refinement. In its early development, only a crude image of the relatively large fetus was possible. The introduction of the computer scanners and, later, the intravaginal ultrasound transducers improved the quality of the images to such an extent that the developing human embryo could be described in detail *in vivo*[2–5]. The introduction of high-frequency ultrasound has contributed to the further refinement of image quality[6,7].

The three-dimensional reconstruction of structures outlined by the ultrasound technique has been refined since its introduction[8,9]. Recently, we have been presented with three-dimensional images of second-trimester fetuses. The purpose of this study was to explore the usefulness of a newly developed high-resolution system for making three-dimensional images of small structures such as the developing embryo *in vivo*.

## MATERIAL AND METHOD

The ultrasound scans were collected using a sector scanner, Vingmed CFM-800 (Vingmed Sound, Horten, Norway) with a mechanical 7.5-MHz annular array transvaginal transducer. The diameter of the transducer was 11.5 mm, the emitted ultrasound waves had a focal length of 25 mm, while the received waves were focused dynamically. With a wave length of 0.2 mm, the lateral resolution was 0.8 mm and the axial resolution 0.4 mm at a depth of 25 mm. The transducer was attached to a rotating stepper motor coupled to a PC-based TomTec Echo-Scan unit (Boulder, Co, USA). During a period of 4 s, the stepper motor rotated the transducer 180°. Thus a complete three-dimensional scan consisted of 132 two-dimensional sector images rotated around the central axis of the transducer. During the scan, the output video signal from the Vingmed scanner was converted into digital representation by the TomTec unit. The

Correspondence: Dr H.-G. Blaas, National Center for Fetal Medicine, Department of Obstetrics and Gynecology, Trondheim University Hospital, N-7006 Trondheim, Norway



Received 5–1–95
Revised 24–2–95
Accepted 27–2–95

images were then scan-converted into a regular volumetric data set by the TomTec unit. This volume consisted of a block of unit volume cells, called voxels, with interpolated values in the regions between the captured sector images. The dimensions of the volumes, consisting of about $256 \times 256 \times 256$ voxels, varied slightly. The resolution of the voxels was between 0.1 and 0.2 mm. The data of interest were analyzed on a subvoxel level by interpolating the voxels with the factor 3.

During the scanning, the transducer unit was held in the vagina by hand. To ensure the quality of the data, it was therefore important that the pistol-like device supporting the transducer was kept stable and that the scanned object did not move during the examination time of 4 s.

The regular volumetric data set acquired by the TomTec unit was transferred to a UNIX workstation running AVS, a general purpose computer graphics system from Advanced Visual Systems. The visualization and volume calculation reported in this paper were performed with a prototype AVS module developed by Chr. Michelsen Research, Bergen, Norway. An *in vitro* evaluation of this volume estimation method has been described[10].

To obtain the three-dimensional representation of the scanned structures, the contours were interactively drawn in the successive two-dimensional slices of the three-dimensional data set. An algorithm, where polyhedrons were created from these contours, defined the surface of the object. The volume was calculated from the closed object. By using the visualization tools in AVS, the three-dimensional object could be scaled, rotated and shaded.

The three-dimensional scans were made on three women without any pregnancy complications referred for an ultrasound evaluation to confirm and date the pregnancy. Each woman had given her informed consent. The normal development of the pregnancies was confirmed by transvaginal ultrasound examination of the embryonic or fetal anatomy. The gestational age was based on the crown–rump length. The central nervous system was evaluated as previously described[6,7].

In our outlining of the lateral ventricles and the future fourth ventricle, we included the choroid plexuses in the volume.

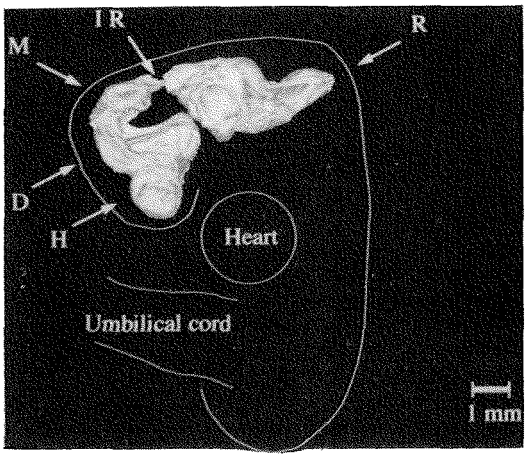


**Figure 1** Lateral view of the brain cavities in an embryo of 13-mm crown–rump length (Case 1). The outline shows the embryonic shape with the head and the umbilical cord. H, hemisphere; D, diencephalon; M, mesencephalon; R, rhombencephalon; IR, isthmus rhombencephali

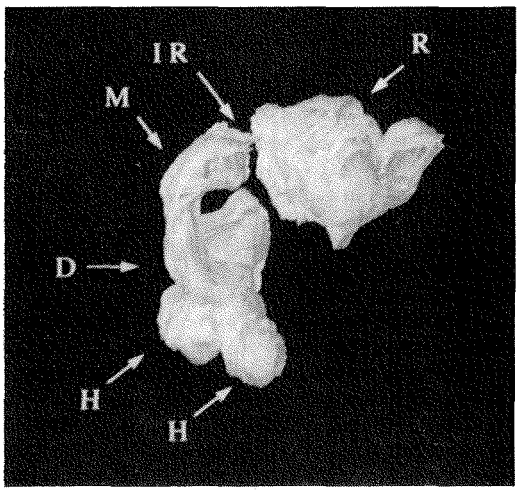


**Figure 2** The brain cavities of the same embryo (crown–rump length, 13 mm) as in Figure 1, oblique view. H, hemisphere; D, diencephalon; M, mesencephalon; R, rhombencephalon; IR, isthmus rhombencephali

## RESULTS

### Case 1

The embryo had a crown–rump length of 13 mm, corresponding to a gestational age of 7 weeks 5 days (Figures 1 and 2). The cavities of both hemispheres and their connections to the third ventricle were easily delineated. Compared to the neural axis, the cavities of the hemispheres were small evaginations located lateral and rostral from the cavity of the diencephalon. The cavity of the diencephalon continued directly into that of the mesencephalon. The isthmus rhombencephali represented the connection to the rhombencephalic cavity and future fourth ventricle. The cavity of the rhombencephalon was located superior in the head.

### Case 2

The cavities of the hemispheres were clearly depicted on an embryo with a crown–rump length of 24 mm, corresponding to a gestational age of 9 weeks 1 day (Figures 3 and 4). The rhombencephalic cavity appeared shorter than that of the embryo with a 13-mm crown–rump length. The passage from the cavity of the diencephalon

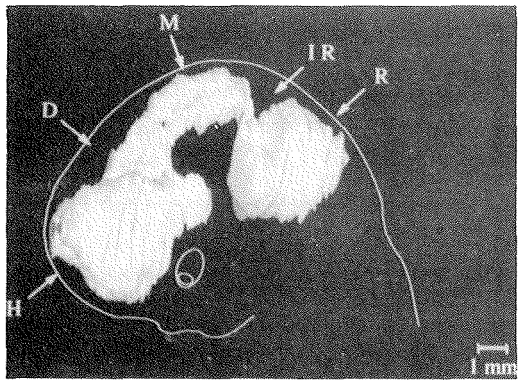


**Figure 3** Lateral view of the brain cavities in an embryo of 24-mm crown–rump length (Case 2). The outline shows the embryonic head and eye. H, hemisphere; D, diencephalon; M, mesencephalon; R, rhombencephalon; IR, isthmus rhombencephali

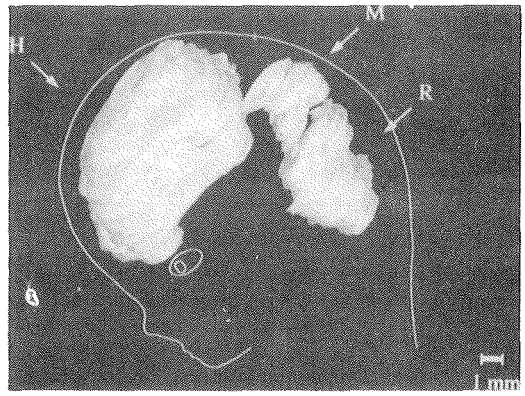


**Figure 5** Lateral view of the brain cavities in a fetus of 40-mm crown–rump length (Case 3). The outline shows the fetal head and eye. H, hemisphere; M, mesencephalon; R, rhombencephalon

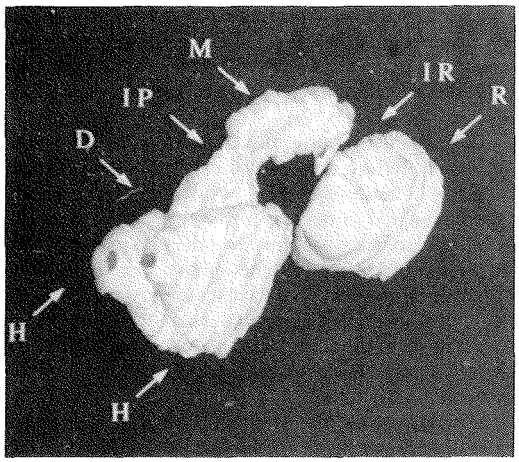


**Figure 4** Oblique view of the brain cavities in the same embryo as in Figure 3 (crown–rump length, 24 mm). H, hemisphere; D, diencephalon; M, mesencephalon; R, rhombencephalon; IR, isthmus rhombencephali; IP, isthmus prosencephali

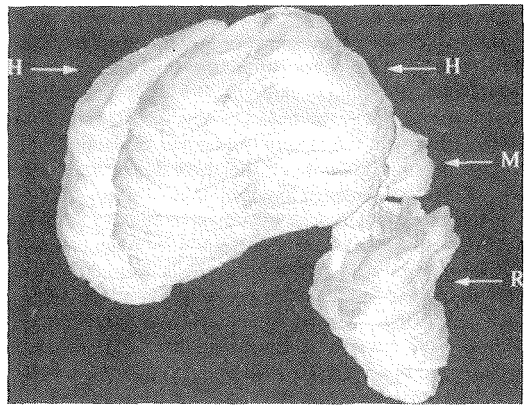


**Figure 6** Oblique view of the brain cavities in the same fetus as in Figure 5 (crown–rump length, 40 mm). H, hemisphere; M, mesencephalon; R, rhombencephalon

to the mesencephalon had become more distinct and developed into the isthmus prosencephali. The mesencephalon lay superior in the head.

### Case 3

The fetus had a crown–rump length of 40 mm, corresponding to a gestational age of 10 weeks 6 days (Figures 5 and 6). The cavities of the hemispheres dominated the brain. The cavity of the diencephalon was too narrow to be outlined correctly on the two-dimensional images. Both rostrally and caudally, the cavity of the mesencephalon was connected to the neighboring cavities by narrow isthmuses. The cavities of the mesencephalon and rhombencephalon were located posteriorly, while the cavities of the hemispheres occupied the anterior and superior part of the head.

The values of the volumes are presented in Table 1.

## DISCUSSION

Embryologists have classified embryonic development into 23 stages, the Carnegie stages, starting with fertilization and ending at 10 postmenstrual weeks with the completion of the embryonic period. The brain development of the embryo has been described in detail, showing the stereotype formation and growth of the different cerebral structures[11,12]. High-frequency ultrasound scanning of the brain has demonstrated the possibilities this technique can provide in basic embryological research in the living human embryo[5–7]. The present three-dimensional reconstruction of the developing embryonic brain shows that ultrasound technology has now been

**Table 1** The volumes of the brain cavities expressed in cubic centimeters ($cm^3$)

| | *Volume* ($cm^3$) | | |
|---|---|---|---|
| *Cavity* | *Crown–rump length 13 mm* | *Crown–rump length 24 mm* | *Crown–rump length 40 mm* |
| Hemispheres (both) | 0.002 | 0.097 | 0.451 |
| Diencephalon | 0.003 | 0.009 | — |
| Mesencephalon | 0.002 | 0.015 | 0.021 |
| Rhombencephalon | 0.017 | 0.058 | 0.085 |

developed to such a stage that structures measuring a few millimeters in size can be adequately presented. In this context, the three-dimensional ultrasound technique will represent an important contribution to the research of the developing embryo *in vivo*. The idea of a three-dimensional reconstruction of the human embryo is not new. Already by the 1880s, the three-dimensional image of the total embryo[13] was introduced by the stacking of wax plates to form solid reconstructions. That technique has been refined and plaster reconstructions have been made of the various stages of the embryonic brain. These reconstructions have been important to the understanding of the developmental stages of the embryo. Recently, there has been improvement in the three-dimensional reconstruction of human embryos. O'Rahilly and Müller reconstructed the embryonic brain with a 'Perspektomat'[12,13]. But with the present ultrasound technique[9,10], it is now possible to monitor the three-dimensional development of an embryo longitudinally *in vivo*.

Each of the three pregnancies represented a specific developmental stage. Case 1 corresponded to an embryo of Carnegie stage 17. At this stage the hemispheres have become distinct[11] and tower rostrally about the telencephalon impar, and the interventricular foramina of Monro have become relatively smaller[12]. The border between the cavities of the diencephalon and the mesencephalon is not distinct at this stage, while the connection from the mesencephalon to the rhombencephalon consists of the isthmus rhombencephali. All these characteristics could be seen in our three-dimensional reconstruction (Figures 1 and 2). Similarly, characteristic features and proportions, as described in the classical embryological literature, are detectable in the reconstructions in the other two cases: Case 2 corresponded to an embryo of Carnegie stage 21, where the hemispheres began to overlap the third ventricle considerably[12], and the first sign of the isthmus prosencephali became evident[12] (Figures 3 and 4). Case 3 represented a fetus at a postembryonic stage, where the most remarkable changes were the dominating size of the hemispheres and the narrow third ventricle (Figures 5 and 6).

In a previous longitudinal study, the volumes of the cavities of the hemispheres and the rhombencephalon were estimated by the formula for the volume of two ellipsoids and the formula for the volume of a pyramid, respectively[7]. The measured volumes in the present three-dimensional reconstructions of the hemispheres were in the range of the estimated values in the longitudinal study, while the measured volumes for the rhombencephalon were greater than the range of the estimated values. Knowledge of the volumes of various structures is of importance for the early diagnosis of specific conditions. For example, the occipital encephalocele in the Meckel–Gruber syndrome may be expressed by an early enlargement of the rhombencephalic cavity.

The present three-dimensional images of the complex developing human brain cavities give important information about the form and the volume; however, the symmetry of the brain was not completely preserved in our reconstructions. For the evaluation of the brain compartments by two-dimensional ultrasound, optimal sections for each brain compartment can be chosen[6,7]. In three-dimensional imaging, the embryos or fetuses were scanned from a given angle so that some brain compartments became clearly depicted, while others were slightly blurred.

The software was originally intended to present larger and more uniform organs such as a fluid-filled porcine stomach[10]. The software used in this study was a prototype. It suffered from some inconveniences, such as not being able to draw arbitrary two-dimensional slices, so we were unable to choose the optimal slice through an organ. Thus, the quality of the ultrasound data depended not only on the two-dimensional scanning angle but also on the angle of the slices in the data volume. This led to slightly skewed and not completely symmetrical images of the brain cavities.

In this presentation, no smoothing techniques were used to improve the image quality of the data. All the same, the surface of the brain cavities showed only small grooves between the slices (Figures 1–6), illustrating the high resolution obtained with this scanning and processing system.

## CONCLUSION

By using high-resolution ultrasound and the described technique, three-dimensional images of the embryonic brain cavities were constructed. The present ultrasound technology has reached the stage where structures of only a few millimeters can be imaged *in vivo* in three dimensions with a quality that resembles the meticulously assembled wax and plaster figures used in the embryonic laboratories. By increasing the basic ultrasound frequency to 10 MHz and making further improvements to the presented hardware and software technique, we believe this method can become an important tool in future embryological research and also in the detection of early developmental disorders of the embryo.

## ACKNOWLEDGEMENT

Mrs Nancy Lea Eik-Nes revised the manuscript.

## REFERENCES

1. His, W. (1880–85). *Anatomie menschlicher Embryonen.* (Leipzig: Vogel)
2. Achiron, R. and Achiron, A. (1991). Transvaginal ultrasonic assessment of the early fetal brain. *Ultrasound Obstet. Gynecol.*, **1**, 336–44
3. Cullen, M. T., Green, J., Whetham, J., Salafia, C., Gabrielli, S. and Hobbins, J. (1990). Transvaginal ultrasonographic detection of congenital anomalies in the first trimester. *Am. J. Obstet. Gynecol.*, **163**, 466–76
4. Timor-Tritsch, I. E., Peisner, D. B. and Raju, S. (1990). Sonoembryology: an organ-oriented approach using a high-frequency vaginal probe. *J. Clin. Ultrasound*, **18**, 286–98
5. Timor-Tritsch, I. E., Monteagudo, A. and Warren, A. (1991). Transvaginal ultrasonographic definition of the central nervous system in the first and early second trimesters. *Am. J. Obstet. Gynecol.*, **164**, 497–503
6. Blaas, H.-G., Eik-Nes, S. H., Kiserud, T. and Hellevik, L. R. (1994). Early development of the forebrain and midbrain: a longitudinal ultrasound study from 7 to 12 weeks of gestation. *Ultrasound Obstet. Gynecol.*, **4**, 183–92
7. Blaas, H.-G., Eik-Nes, S. H., Kiserud, T. and Hellevik, L. R. (1995). Early development of the hindbrain: a longitudinal ultrasound study from 7 to 12 weeks of gestation. *Ultrasound Obstet. Gynecol.*, **5**, 151–60
8. Brinkley, J. F., McCallum, W. D., Muramatsu, S. K. and Liu, D. Y. (1982). Fetal weight estimation from ultrasonic three-dimensional head and trunk reconstructions: evaluation *in vitro*. *Am. J. Obstet. Gynecol.*, **144**, 715–21
9. Steen, E. and Olstad, B. (1994). Volume rendering of 3D medical ultrasound data using direct feature mapping. *IEEE Trans. Med. Imaging*, **13**, 517–25
10. Gilja, O. H., Thune, N., Matre, K., Hausken, T., Ødegaard, S. and Berstad, A. (1994). *In vitro* evaluation of three dimensional ultrasonography in volume estimation of organs. *Ultrasound Med. Biol.*, **20**, 157–65
11. O'Rahilly, R. and Gardner, E. (1971). The timing and sequence of events in the development of the human nervous system during the embryonic period proper. *Z. Anat. Entwickl.-Gesch.*, **134**, 1–12
12. O'Rahilly, R. and Müller, F. (1990). Ventricular system and choroid plexuses of the human brain during the embryonic period proper. *Am. J. Anat.*, **189**, 285–302
13. O'Rahilly, R. and Müller, F. (1992). General embryology and teratology. Introduction and general concepts. In O'Rahilly, R. and Müller, F. (eds.) *Human Embryology and Teratology*, pp. 5–11. (New York: Wiley-Liss)

# Paper VI

**Harm-Gerd Blaas, Sturla H. Eik-Nes, Sevald Berg, Hans Torp. In-vivo three-dimensional ultrasound reconstructions of embryos and early fetuses. Lancet 1998; 352:1182–6**

THE LANCET

# In-vivo three-dimensional ultrasound reconstructions of embryos and early fetuses

Harm-Gerd Blaas Sturla H Eik-Nes
Sevald Berg Hans Torp

**Reprinted from** THE LANCET **Saturday 10 October 1998**
**Vol. 352 No. 9135 Page 1182–1186**

THE LANCET 42 BEDFORD SQUARE LONDON WC1B 3SL UK

Early reports

# In-vivo three-dimensional ultrasound reconstructions of embryos and early fetuses

*Harm-Gerd Blaas, Sturla H Eik-Nes, Sevald Berg, Hans Torp*


## Summary

**Background** Three-dimensional (3D) imaging of the living human embryo has become possible in the monitoring of embryological development, as described by classic human embryology. We aimed to create 3D images of organs in embryos on early pregnancy.

**Methods** We used a specially developed 7·5 MHz annular array 3D transvaginal probe to examine embryos. We included 34 women at 7–10 weeks' gestation. We measured the crown-rump length (CRL) of the embryos and fetuses and transferred the 3D ultrasound data to an external computer for further processing to calculate volume.

**Findings** The CRLs ranged from 9·3 mm to 39·0 mm. The quality of the images of the embryos and fetuses made it possible to outline in detail the outer contours and the contours of the brain cavities, and the calculated volumes corresponded well to the descriptions from classic human embryology.

**Interpretation** Our 3D imaging system allowed visualisation of structures of less than 10 mm. Therefore, development and abnormal development of fetuses can be monitored.


*Lancet* 1998; 352: 1182–86

**National Center for Fetal Medicine, Department of Obstetrics and Gynaecology, Trondheim University Hospital, N-7006 Trondheim, Norway** (H G Blaas MD, S H Eik-Nes MD), **and Department of Physiology and Biomedical Engineering, University of Trondheim** (S Berg MSc, H Torp Drtech)

**Correspondence to:** Dr Harm-Gerd Blaas

## Introduction

Classic human embryology was established by Wilhelm His in 1880–85.[1] His realised the need for magnified three-dimensional (3D) imaging and the need for a model of the dissected object.[1] He made 3D reconstructions from free-hand drawings of histological slices.[2] Born,[3] who in 1876 was the first to describe the technique of making solid reconstructions by stacking wax plates of histological slices, made use of the camera lucida, a device that aided the accurate sketching of small objects. Wax was later substituted by more durable materials such as wood, plaster, glass, or plastic.[4]

Imaging by graphic reconstructions with the aid of special devices has commonly been used in modern human embryology.[5–8] The development of computer technology has opened new possibilities for 3D reconstructions.[9] The first attempt at constructing 3D images of the fetus from ultrasound recordings was made in the early 1980s.[10] The introduction of real-time high-frequency ultrasonography with transvaginal transducers led to improved resolution and allowed detailed imaging of the living embryo.[11,12] The subsequent longitudinal ultrasound studies of the embryological development[13–15] were in agreement with the descriptions from human embryology.[16] Real-time ultrasonography linked with computer technology has made 3D representation of embryonic structures feasible.[17]

We aimed to design a system that used a specially developed transvaginal transducer to enable the study of small embryonic organs in 3D from 7 weeks' to 10 weeks' gestation. We also wanted to describe the development of the living human embryo with emphasis on the shape and the volume of the body and of the brain compartments.

## Methods

We developed a 7·5 MHz annular array 3D transvaginal probe to enable the creation of 3D images of very small structures. The probe had an axial resolution of 0·4 mm and a lateral resolution of 0·8 mm. The scan-plane of the transducer was tilted 45° from the end-fire position, rotating inside a fixed dome. The data acquisition (181 frames/volume, range 89–297) took an average of 5·3 s (2·3–8·6). We stored the digital data in the frame buffer of the scanner (System Five, Vingmed Sound, Horten, Norway) and transferred them to an external computer for further processing with Vingmed EchoPAC-3D software (version 1.1). The rotated 2D planes were converted into a 3D dataset. The objects to be studied were segmented by manual drawing of contours in several parallel 2D slices. The parallel 2D slices could be obtained in any plane, so optimum drawing positions for each object could be determined. From these contours, polyhedrons were created to define the surface and the volume of the objects.[18] The objects could be rotated, scaled, and visualised with different colours and different opacity values.

We recruited 35 healthy pregnant women without any previous pregnancy complications from among women who were referred early in their pregnancy for a routine second-trimester

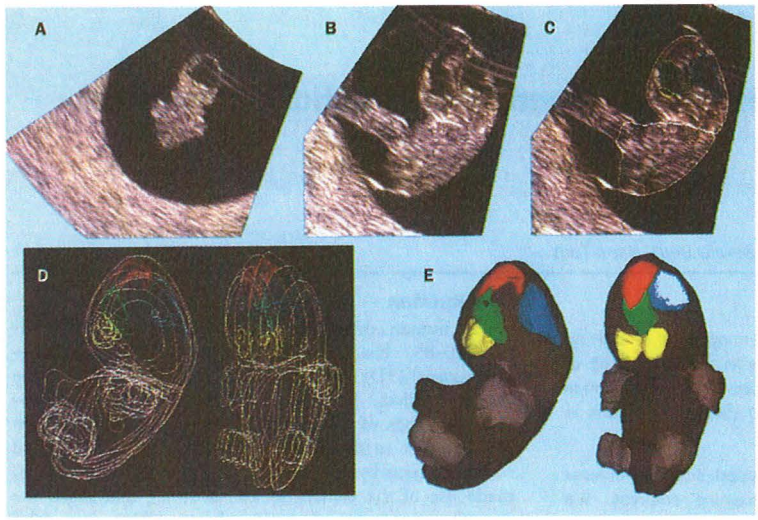


Figure 1: **3D reconstruction of embryo with CRL 17 mm (8 weeks 2 days)**
A=original scan plane through gestational sac and embryo; oblique horizontal section through head with hypoechogenic fourth ventricle, and upper part of thorax. B=rotated 2D sagittal section through embryo in amniotic cavity; umbilical cord leads to left. C=contours drawn manually around head and body (white), lateral ventricles (yellow), third ventricle (green), cavity of mesencephalon (red), and fourth ventricle (blue). D=3D graph of contours. E=3D graph of volumes of body and brain cavities. Opacity of volume reconstruction of body is decreased to show brain cavities.

ultrasonography at our centre. None of the women had used any hormonal treatment during the 3 months before the pregnancy. All were non-smokers. All women gave written informed consent, and the study was approved by the regional committee for medical ethics. We excluded one woman because the baby died of anomalous pulmonary venous return a few days after delivery. The 34 women included in the study gave birth to 17 boys and 17 girls at a mean of 40 weeks 3 days' gestation (range 38–43 weeks), based on the crown-rump length (CRL). The mean birthweight was 3652 g (2770–4970). All but three women delivered spontaneously. Two babies were delivered by caesarean section at 39 weeks 2 days and at 39 weeks 4 days, respectively; the first because of pre-eclampsia, the second because of mechanical disproportion. For one woman with a fetus in breech presentation, delivery was induced with oxytocin at 39 weeks 3 days. All children were healthy.

The gestational age at imaging ranged from 7 weeks to 10 weeks. The CRL measurement is the greatest length of the embryo or fetus from the top of the head to the caudal end of the body. We included the limbs and the physiological midgut herniation in the measurement of the volume of the embryonic or fetal body. We chose the hypoechogenic brain cavities for reconstruction of 3D casts of the brain compartments (figure 1). We included the choroid plexuses in the outlining of the brain cavities. All ultrasound examinations and 3D reconstructions were done by the same person. All statements of gestational age are made in completed weeks and days, based on the date of the last menstrual period. The sonographic appearance of the surface of an object in a fluid is defined by the point-spread function that depends on the resolution of the ultrasound beam. The surface of an embryo will appear, therefore, not as a sharp silhouette, but as a blurred line. Especially small structures will appear larger than they are on the scan, and the outlining will result in overestimation of volume proportional to the surface of the object being scanned, whereas cavities with inner surfaces may be underestimated. We corrected for the point-spread function by modelling the surface with the formula for a cube.

We tested the validity of the volume measurements with ten cylindrical objects of known volumes ranging from 24·8 $mm^3$ to 3362·5 $mm^3$ (table 1). The cylinders had different radii and heights, and were made from a mixture of agar gel and kaolin. Each object was measured three times from different positions in a water bath at 21°C; adjustments were made to allow for ultrasound velocity in water bath at 21°C. The deviation distance for the point spread function was calculated to be 0·2 mm, and all volume estimations were corrected by this factor. The correlation between the volume estimates and the true volumes gave a linear regression with a slope of 0·994 (SE 0·0087), and $R^2$=0·998. The percentage error of the volume estimations was mean 15·6% (9·1) for the three smallest test volumes (<500 $mm^3$), and mean –0·2% (5·0) for the seven largest test volumes (≥500 $mm^3$).

We used cross-sectional regression analysis to assess the relation between the estimated volumes and CRL. Simple models to fit the data were searched for, but transformation

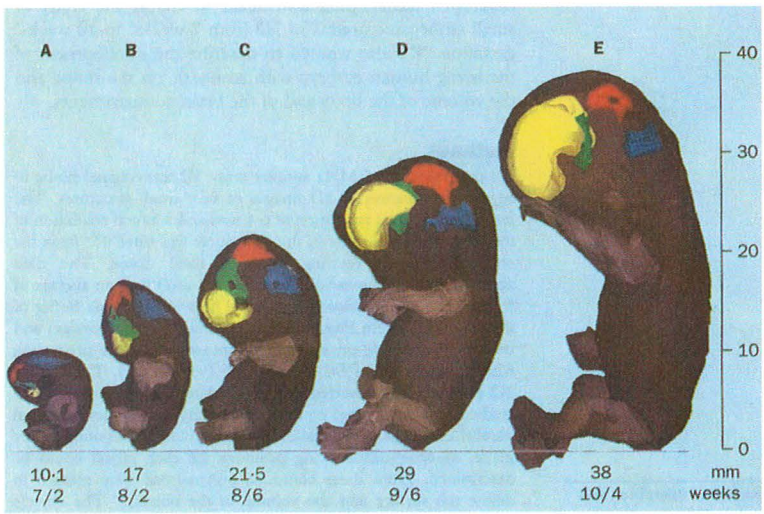


Figure 2: **3D graph of five embryos and fetuses showing development of shape and size from 7 to 10 weeks of gestation**
Cavities of hemispheres (lateral ventricles)=yellow, cavity of diencephalon (third ventricle)=green, cavity of mesencephalon=red, cavity of rhombencephalon (fourth ventricle)=blue.

| Measured volumes ($mm^3$) | Estimated volumes ($mm^3$) | | |
|---|---|---|---|
| | A | B | C |
| 24·8 | 27·8 | 30·6 | 28·1 |
| 132·3 | 175·8 | 159·6 | 149·8 |
| 449·3 | 509·6 | 492·8 | 454·6 |
| 950·8 | 892·6 | 1039·6 | 1007·6 |
| 1458·0 | 1406·2 | 1385·9 | 1448·4 |
| 2029·0 | 2112·7 | 2201·5 | 1989·7 |
| 2483·1 | 2480·4 | 2440·6 | 2383·0 |
| 2607·5 | 2531·2 | 2514·4 | 2528·2 |
| 3094·7 | 2991·6 | 3341·9 | 3252·5 |
| 3362·5 | 3166·9 | 3418·7 | 3173·0 |

Table 1: **Comparison of measured volumes with 3D volume estimates of test objects**

of the responses were necessary in all six analyses to remove the heteroscedasticity. The normality of the residuals was confirmed by visual inspection and by the Shapiro Francia W test. The assumption of independency and constant variance of the residuals was confirmed by the residual plots.

## Results

The CRL of the 34 embryos or fetuses ranged from 9·3 mm to 39 mm. It was possible to describe the development of the embryo based on the assessment of the 3D reconstructions from the 34 individuals. The shape of the embryonic bodies altered substantially from the smallest to the largest embryos and fetuses (figure 2). Initially, the embryonic body was slender in the coronal plane. In embryos with 16–24 mm CRL (figure 2), the body gradually grew thicker, becoming cuboidal and finally ellipsoid shaped with a large head in embryos of 25 mm or more CRL. The limbs were short paddle-shaped outgrowths in the smallest embryos. In an embryo of CRL 14·8 mm, the hands were distinct; the elbows became obvious in an embryo of CRL 20·6 mm (figure 2). The hand angled from the sagittal plane in embryos of 20·5 mm CRL and larger. The soles of the feet touched in the midline in 25 mm embryos. In the largest fetuses, the soles of the feet rotated from the sagittal plane. In the smallest embryos (CRL 9·3–17·0 mm), the rhombencephalic cavity was broad and shallow and lay on top, representing the largest brain cavity (figure 2). The cavity deepened gradually with the growth of the embryos, simultaneously decreasing in length. The position in the head changed as embryos grew, moving posteriorly (CRL 17 mm and larger, figure 2). The rhombencephalic cavity (future fourth ventricle) had a pyramid-like shape with the central deepening of the pontine flexure as the peak of the pyramid. In the fetuses of 25 mm CRL and more, there was a clear gap between the rhombencephalic and the mesencephalic cavity due to the growing cerebellum (figure 2). The isthmus rhombencephali was thin; in most cases it was not visible in its complete length.

In the small embryos, the curved tube-like mesencephalic cavity (future Sylvian aqueduct) lay anteriorly, its rostal part pointing caudally. The cavity of the diencephalon (future third ventricle) ran posteriorly. As the size of the embryos increased, the mesencephalic cavity changed its position posteriorly. The transition from the third ventricle to the mesencephalic cavity and to the lateral ventricles was wide in the early embryos. The cavity of the mesencephalon was large in relation to total volume in all embryos or fetuses. The largest volume of the future third ventricle (11·7 $mm^3$) was found in an embryo with 20·5 mm CRL (figure 3), but was smaller in the larger embryos and fetuses (CRL≥25 mm) with a narrow upper anterior part.

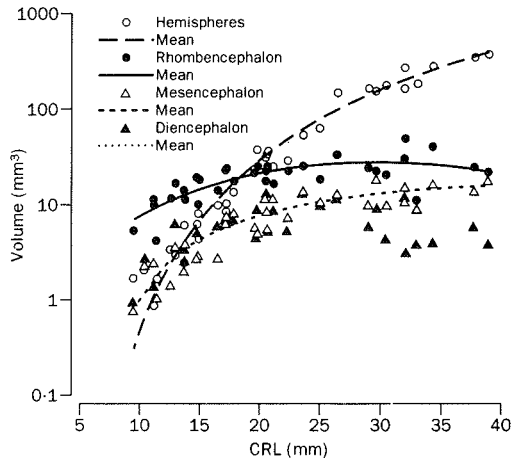


Figure 3: **Measurements and mean volume of lateral ventricles, cavities of diencephalon, mesencephalon, and rhombencephalon**

In the smallest embryos, the medial telencephalon formed a continuous cavity between the lateral ventricles. The future foramina of Monro became distinct in embryos of 19·5 mm CRL. The lateral ventricles gradually changed shape from small round vesicles (CRL 9·3–13·6 mm) via thick round slices originating anterocaudally from the third ventricle (CRL 14·6–17·7 mm) into the crescent shape of the larger embryos (CRL≥20·4 mm, figure 2). In the early fetuses, the thick crescent lateral ventricles filled the anterior part of the head and concealed the diencephalic cavity (figure 2), which became smaller.

The range of the estimated volumes was: bodies 122·0–4987·6 $mm^3$; all cavities of the brain 6·6–354·1 $mm^3$; cavities of the hemispheres 0·8–323·8 $mm^3$; cavities of the diencephalon 0·9–11·7 $mm^3$; cavities of the mesencephalon 0·7–15·9 $mm^3$, and cavities of the rhombencephalon 3·8–42·4 $mm^3$. The estimates of the regression coefficients are shown in table 2.

We combined the measurement of the CRL with the external form of the embryos and the casts of the brain cavities;[8,16] this approach gave an estimate of the development stages (table 3). The correlation of the volumes of the embryo/fetuses and their brain cavities to the CRL are presented in figures 3 and 4.

| Response | Intercept | CRL | $CRL^2$ | Residual SE | $R^2$ |
|---|---|---|---|---|---|
| Body* | −10·7 (1·1) | 2·05 (0·048) | · · | 2·33 | 0·983 |
| Cavities of brain* | −3·25 (0·47) | 0·554 (0·020) | · · | 0·986 | 0·958 |
| Cavity of hemispheres† | −1·34 (0·14) | 0·215 (0·0061) | · · | 0·293 | 0·975 |
| Cavity of diencephalon* | −1·22 (0·59) | 0·316 (0·056) | −0·0063 (0·0012) | 0·446 | 0·526 |
| Cavity of mesencephalon* | −1·17 (0·51) | 0·257 (0·048) | −0·0035 (0·0010) | 0·385 | 0·826 |
| Cavity of rhombencephalon* | · · | 0·325 (0·017) | −0·0054 (0·0006) | 0·641 | 0·978 |

*Square root transformed, cubic root transformed. †Residual and multiple $R^2$ are shown.

Table 2: **Estimates (SE) of regression coefficients by linear regression analysis**

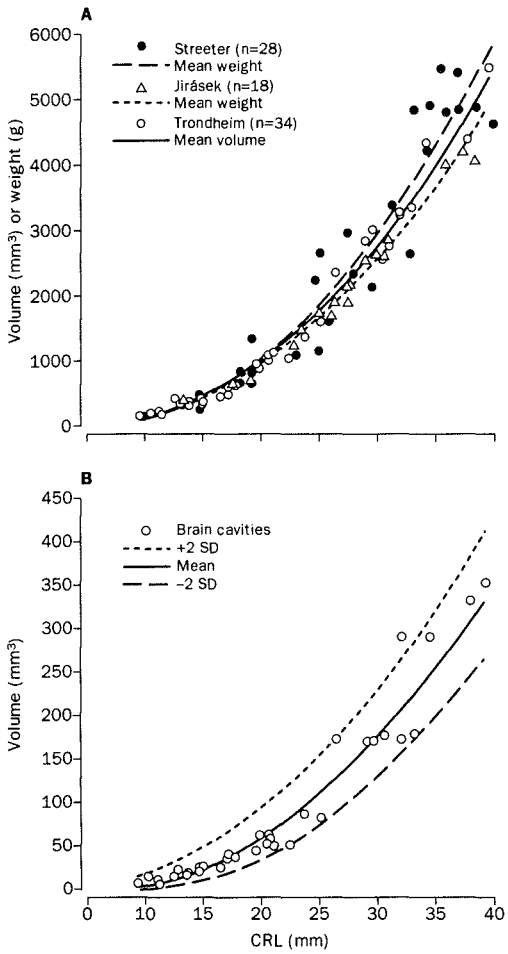


Figure 4: **Volumes of embryos and fetuses and brain cavities**
A=mean volume of embryos and fetuses compared with mean weights from Streeter[23] and Jirásek[24] in embryos CLR ≤40 mm.
B=measurements of total volume of brain cavities, regression line, and ±2 SD.

## Discussion

3D reconstructions and measurements of embryos and their brain cavities showed similar results to those from classic embryology, and estimations of the stage of embryos could be made. We confirmed the classic descriptions of the external appearance of the embryonic body and limbs, and of the shape, size, and position of the brain compartments.[6,8]

In previous studies, volume reconstruction of large structures was tested in vitro and in vivo.[18-21] The objects we measured were small, some of them near the limits of the ultrasonographic resolution. Therefore, even small errors in the surface-setting would lead to incorrect volumes. Our test study showed that 3D reconstructions were acceptable, with only a small correction to account for the point-spread function. We believe that the relatively high percentage error in the volume estimation of the small test object of less than 500 mm³ was due to the surface setting in the segmentation procedure, and we may assume that the volumes of embryos up to 17 mm CRL (<500 mm³) became overestimated, whereas volumes of all brain cavities may have been underestimated. We assume that the volume estimations of the embryos of 17 mm CRL and more (≥500 mm³) are good, since the percentage error in the test study only was mean −0·2%, with an acceptable SE of 5·0.

Because of the difference between the embryonic tissue and the amniotic fluid and between the brain tissue and the fluid-filled brain cavities we could analyse the embryonic structures very early, despite their small size. Limitations were set mainly by the resolution of the ultrasonographic equipment. The short duration of the recordings (2·3–8·6 s) was enough to obtain pictures of the fetuses in a quiet phase. Movements of the pregnant woman, such as breathing or pulsation of the abdominal aorta, did not affect the quality of the images.

The difference between the fetal weight (g) and the volume (mm³) is less than 2%.[22] We compared the volumes of the body with measurements of embryos and fetuses that had a corresponding size (CRL ≤40 mm) from two other studies.[23,24] The regression curves were best fitted by a square-root transformation in all three studies (figure 4). The comparison of these different studies involved several possible biases. Streeter[23] studied fresh and formalin-fixed samples; the latter were substantially heavier and longer.[23] In addition, the largest fetuses in Streeter's group were reported to be flexed, and the CRL might have been larger. Drumm and O'Rahilly[25] analysed the relation between measurements of the CRL in vivo by ultrasonography and measurement of the embryo or fetus after abortion. They found that the lengths of embryos in embryological studies was about 1–5 mm less than equivalent in-vivo CRL measurements.[25] Therefore, the condition of the embryos and fetuses in the different studies was not uniform, which may have affected the shape of the curves.

If the mesencephalic cavity had a cylindrical shape, the volume could be calculated by the formula $\pi r^2 \times$length. The embryos in O'Rahilly and Müller's study[6] (Carnegie stage 23 is about 10 weeks 0 days gestational age and CRL 30 mm) would then have a mean volume of 15 mm³ based in the measurements indicated from graphic reconstructions, or 23 mm³ based on the values corrected for shrinkage, whereas the mean volume of the mesencephalic cavity at 10 weeks 0 days in a 2D ultrasound study was only 7·4 mm³.[13] In our study the mean volume in embryos and fetuses of 30 mm CRL was calculated to be 11 mm³ (figure 3). As the rhombencephalic cavity moved posteriorly, it shortened in the sagittal section. In 1890, His showed the changes of the pontine flexure with a decreasing angle in older fetuses.[26] The growth of the cerebellar hemispheres further restricted the volume of the fourth ventricle. In this way, the rhombencephalic cavity did not increase in volume despite the rapid growth of the brain (figure 3). In a previous study, the volumes of the lateral ventricles were estimated

| Carnegie stage | Number of embryos and fetuses | CRL range (mm) |
|---|---|---|
| 16 | 6 | 9·3–12·8 |
| 17 | 5 | 13·5–14·8 |
| 18 | 4 | 16·4–17·7 |
| 19 | 2 | 19·5–19·7 |
| 20 | 4 | 20·4–21·0 |
| 21 | 2 | 22·3–23·6 |
| 22 | 2 | 25·0–26·4 |
| ≥23 | 9 | ≥29·0 |

Table 3: **Distribution of embryos and fetuses according to Carnegie staging system**

by the formula of two ellipsoids and the rhombencephalic cavity by the formula of a pyramid.[14] Our sonographic 3D reconstructions of the lateral ventricles were in the range of the estimated values from the 2D study; our 3D reconstructions of the rhombencephalic cavity were larger than the range of the estimated values from the 2D study, in which the measurements of the width involved only the main part of the fourth ventricle, not the lateral recesses. The size of the diencephalic cavity has not been measured before. Through the growth of the dorsal and ventral thalami, the lateral walls of this cavity narrow, giving it a slit-like shape. This change in shape explains the decreasing volume of the cavity in the older embryos and fetuses in our study, in which only part of the third ventricle between the dorsal thalamus and the mesencephalon, which is the region near the pineal gland, was discernible. According to embryologists, the recesses of the pineal region and near the infundibulum are distinct in older fetuses.[27]

In 1921, Jenkins[28] carried out a volumetric study of the developing brain. Only two of the embryos he studied were smaller than 40 mm (CRL 16 mm and 25 mm), and the volumes of the brains were calculated to be 41 $mm^3$ and 126 $mm^3$. In our study, the mean volume of the brain cavities (figure 4) was 37 $mm^3$ at 16 mm CRL, and 112 $mm^3$ at 25 mm CRL; these measurements must be taken to be in agreement with Jenkins' measurements. Jenkins also looked at the proportional growth of the brain compartments, finding a larger share of the diencephalon and the mesencephalon than our measurements showed. At the same time he found less of a shift of the share of the telencephalon and the rhombencephalon between the 16 mm and the 25 mm embryo than we showed (figure 4).

Classic human embryology is based on aborted human embryos and fetuses, as previously summarised.[16] In the Carnegie staging system, embryos are classified by external form and development of the organ system analysed by light microscopy. Such exact staging by ultrasonongraphy is not possible, but we could estimate the stages in the embryos by comparing the external form of the body, the limbs, and the casts of the brain cavities with embryological descriptions.

We showed that it was possible to develop a dedicated transducer system and additional software for 3D imaging of objects of less than 10 mm. The quality of the images allowed description of the outer contours and the development of organ systems, as well as the staging of the embryos between 7 weeks' and 10 weeks' gestation. Our system will also make possible study of abnormal development of the embryo or early fetus and elucidate its progression. The 3D imaging system will help in the avoidance of artefacts and other difficulties in in-vitro assessment of the aborted embryos and may revitalise human embryology.

*Contributors*

Harm-Gerd Blaas planned the study, did the ultrasound examinations and the 3D-reconstructions, and wrote the paper. Sturla H Eik-Nes supervised the planning and revision of the study and its results. Sevald Berg assisted with the technical performance of the 3D reconstructions of the test series and of the study objects. Hans Torp assisted with the mathematical assessment of the 3D analysis and the validity of the method.

*Acknowledgments*

We thank Nancy Lea Eik-Nes for revision of the paper.

**References**

1 His W. Anatomie menschlicher Embryonen. Leipzig: Vogel: 1880–85.
2 His W. Über Methoden plastischer Rekonstruktion und über deren Bedeutung für Anatomie und Entwicklungsgeschichte. *Anat Anz* 1887; **2:** 382–94.
3 Born G. Die Plattenmodellirmethode. *Arch Mikr Anat* 1883; **22:** 584–99,
4 Gaunt PN, Gaunt WA. Solid reconstruction. In: Gaunt PN, Gaunt WA, eds. Three dimensional reconstruction in biology. Kent: Pitman Medical, 1978: 63–73.
5 Müller F, O'Rahilly R. The human brain at stages 21–23, with particular reference to the cerebral cortical plate and the development of the cerebellum. *Anat Embryol* 1990; **182:** 375–400.
6 O'Rahilly R, Müller F. Ventricular system and choroid plexuses of the human brain during the embryonic period proper. *Am J Anat* 1990; **189:** 285–302.
7 O'Rahilly R, Müller F. General embryology and teratology: introduction and general concepts. In: O'Rahilly R, Müller F, eds. Human embryology and teratology. New York: Wiley-Liss, 1992.
8 O'Rahilly R, Müller F. The embryonic human brain: an atlas of developmental stages. New York: Wiley-Liss, 1994.
9 el-Gammal S. ANAT3D: a computer program for stereo pictures of three dimensional reconstructions from histological serial slices. In: Elsner N, Creutzfeld O, eds. New frontiers in brain research. Stuttgart, New York: Thieme, 1987: 46.
10 Brinkley JF, McCallum WD, Muramatsu SK, Liu DY. Fetal weight estimation from ultrasonic three-dimensional head and trunk reconstructions: evaluation in vitro. *Am J Obstet Gynecol* 1982; **144:** 715–21.
11 Timor-Tritsch IE, Farine D, Rosen MG. A close look at the embryonic development with the high frequency transvaginal transducer. *Am J Obstet Gynecol* 1988; **159:** 678–81.
12 Timor-Tritsch IE, Peisner DB, Raju S. Sonoembryology: and organ-oriented approach using a high-frequency vaginal probe. *J Clin Ultrasound* 1990; **18:** 286–98.
13 Blaas HG, Eik-Nes SH, Kiserud T, Hellevik LR. Early development of the forebrain and midbrain: a longitudinal ultrasound study from 7 to 12 weeks of gestation. *Ultrasound Obstet Gynecol* 1994; **4:** 183–92.
14 Blaas HG, Eik-Nes SH, Kiserud T, Hellevik LR. Early development of the hindbrain: a longitudinal ultrasound study from 7 to 12 weeks of gestation. *Ultrasound Obstet Gynecol* 1995; **5:** 151–60.
15 Blaas HG, Eik-Nes SH, Kiserud T, Hellevik LR. Early development of the abdominal wall, stomach and heart from 7 to 12 weeks of gestation: a longitudinal ultrasound study. *Ultrasound Obstet Gynecol* 1995; **6:** 240–49.
16 O'Rahilly R, Müller F. Developmental stages in human embryos. Washington: Carnegie Institution Publishing, 1987.
17 Blaas HG, Eik-Nes SH, Kiserud T, Berg S, Angelsen B, Olstad B. Three-dimensional imaging of the brain cavities in human embryos. *Ultrasound Obstet Gynecol* 1995; **5:** 228–32.
18 Thune N, Gilja OH, Hausken T, Matre K. A practical method for estimating enclosed volumes using 3D ultrasound. *Eur J Ultrasound* 1996; **3:** 83–92.
19 Gilja OH, Thune N, Matre K, Hausken T, Ødegaard S, Berstad A. In vitro evaluation of three dimensional ultrasonography in volume estimation of organs. *Ultrasound Med Biol* 1994; **20:** 157–65.
20 Gilja OH. In vivo comparison of 3D ultrasonography and magnetic resonance imaging in volume estimation of human kidneys. *Ultrasound Med Biol* 1995; **21:** 25–32.
21 Riccabona M, Nelson TR, Pretorius DH. Dreidimensionale Sonographie: zur Genauigkeit sonographischer Volumsbestimmungen. *Ultraschall Klin Prax* 1995; **10:** 35–39.
22 Meban C. The surface area and volume of the human fetus. *J Anat* 1983; **137:** 217–78.
23 Streeter GL. Weight, sitting height, head size, foot length, and menstrual age of the human embryo. *Contr Embryol Carneg Instn* 1920; **11:** 143–70.
24 Jirásek JE, Uher J, Uhrová M. Water and nitrogen content of the body of young human embryos. *Am J Obstet Gynecol* 1966; **96:** 868–71.
25 Drumm JE, O'Rahilly R. The assessment of prenatal age from the crown-rump length determined ultrasonically. *Am J Anat* 1977; **148:** 555–60.
26 His W. Die Entwickelung des menschlichen Rautenhirns vom Ende des ersten bis zum Beginn des dritten Monats. *Abhandl KS Gesellsch Wissensch* 1890; **29:** 3–74.
27 Kostovic I. Zentralnervensystem. In: Hinrichsen KV, ed. Humanembryologie. Berlin: Springer-Verlag, 1990: 381–448.
28 Jenkins GB. Relative weight and volume of the component parts of the brain of the human embryo at different stages of development. *Contr Embryol Carneg Instn* 1921; **13:** 41–60.

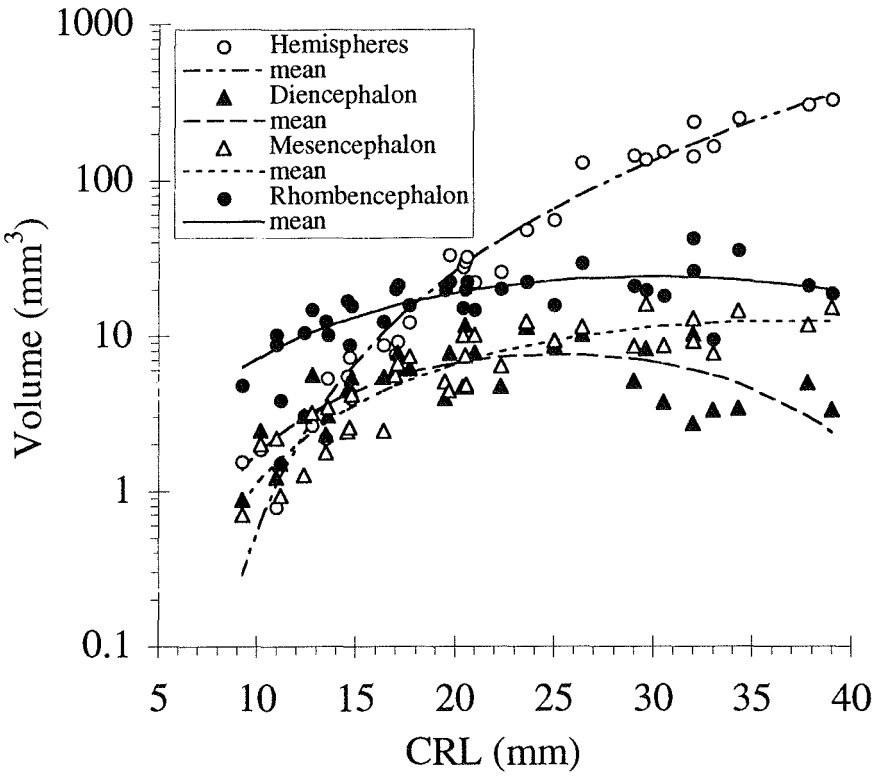


Figure 3: **Measurements and mean volume of lateral ventricles, cavities of diencephalon, mesencephalon, and rhombencephalon**

The Lancet is a weekly subscription journal. For further information on how to subscribe please contact our Subscription Department
Tel: +44 (0)171 436 4981 Fax: +44 (0)171 580 8175
North America Tel: +1 212 633 3800 Fax: +1 212 633 3850

Printed in UK
by Robquest Ltd

# ACTA UNIVERSITATIS NIDROSIENSIS FACULTATIS MEDICINAE

## Series A: Dissertations

1. Knut Joachim Berg: EFFECT OF ACETYLSALICYLIC ACID ON RENAL FUNCTION. 1977.
2. Karl Erik Viken and Arne Ødegaard: STUDIES ON HUMAN MONOCYTES CULTURED *IN VITRO*. 1977.
3. Karel Bjørn Cyvin: CONGENITAL DISLOCATION OF THE HIP JOINT. 1978.
4. Alf O. Brubakk: METHODS FOR STUDYING FLOW DYNAMICS IN THE LEFT VENTRICLE AND THE AORTA IN MAN. 1978.
5. Geirmund Unsgaard: CYTOSTATIC AND IMMUNOREGULATORY ABILITIES OF HUMAN BLOOD MONOCYTES CULTURED IN VITRO. 1979.
6. Størker Jørstad: URAEMIC TOXINS. 1980.
7. Arne Olav Jenssen: SOME RHEOLOGICAL, CHEMICAL AND STRUCTURAL PROPERTIES OF MUCOID SPUTUM FROM PATIENTS WITH CHRONIC OBSTRUCTIVE BRONCHITIS. 1980.
8. Jens Hammerstrøm: CYTOSTATIC AND CYTOLYTIC ACTIVITY OF HUMAN MONOCYTES AND EFFUSION MACROPHAGES AGAINST TUMOUR CELLS *IN VITRO*. 1981.
9. Tore Syversen: EFFECTS OF METHYLMERCURY ON RAT BRAIN PROTEIN. 1983.
10. Torbjørn Iversen: SQUAMOUS CELL CARCINOMA OF THE VULVA. 1983.
11. Tor-Erik Widerøe: ASPECTS OF CONTINUOUS AMBULATORY PERITONEAL DIALYSIS. 1984.
12. Anton Hole: ALTERATIONS OF MONOCYTE AND LYMPHOCYTE FUNCTIONS IN RELATION TO SURGERY UNDER EPIDURAL OR GENERAL ANAESTHESIA. 1984.
13. Terje Terjesen: FRACTURE HEALING AND STRESS-PROTECTION AFTER METAL PLATE FIXATION AND EXTERNAL FIXATION. 1984.
14. Carsten Saunte: CLUSTER HEADACHE SYNDROME. 1984.
15. Inggard Lereim: TRAFFIC ACCIDENTS AND THEIR CONSEQUENCES. 1984.
16. Bjørn Magne Eggen: STUDIES IN CYTOTOXICITY IN HUMAN ADHERENT MONONUCLEAR BLOOD CELLS. 1984.
17. Trond Haug: FACTORS REGULATING BEHAVIORAL EFFECTS OF DRUGS. 1984.
18. Sven Erik Gisvold: RESUSCITATION AFTER COMPLETE GLOBAL BRAIN ISCHEMIA. 1985.
19. Terje Espevik: THE CYTOSKELETON OF HUMAN MONOCYTES. 1985.
20. Lars Bevanger: STUDIES OF THE Ibc (c) PROTEIN ANTIGENS OF GROUP B STREPTOCOCCI. 1985.
21. Ole-Jan Iversen: RETROVIRUS-LIKE PARTICLES IN THE PATHOGENESIS OF PSORIASIS. 1985.
22. Lasse Eriksen: EVALUATION AND TREATMENT OF ALCOHOL DEPENDENT BEHAVIOUR. 1985.
23. Per I. Lundmo: ANDROGEN METABOLISM IN THE PROSTATE. 1985.
24. Dagfinn Berntzen: ANALYSIS AND MANAGEMENT OF EXPERIMENTAL AND CLINICAL PAIN. 1986.
25. Odd Arnold Kildahl-Andersen: PRODUCTION AND CHARACTERIZATION OF MONOCYTE-DERIVED CYTOTOXIN AND ITS ROLE IN MONOCYTE-MEDIATED CYTOTOXICITY. 1986.
26. Ola Dale: VOLATILE ANAESTHETICS. 1986.
27. Per Martin Kleveland: STUDIES ON GASTRIN. 1987.
28. Audun N. Øksendal: THE CALCIUM PARADOX AND THE HEART. 1987.
29. Vilhjalmur R. Finsen: HIP FRACTURES. 1987.
30. Rigmor Austgulen: TUMOR NECROSIS FACTOR: A MONOCYTE-DERIVED REGULATOR OF CELLULAR GROWTH. 1988.
31. Tom-Harald Edna: HEAD INJURIES ADMITTED TO HOSPITAL. 1988.
32. Joseph D. Borsi: NEW ASPECTS OF THE CLINICAL PHARMACOKINETICS OF METHOTREXATE. 1988.
33. Olav F.M. Sellevold: GLUCOCORTICOIDS IN MYOCARDIAL PROTECTION. 1988.
34. Terje Skjærpe: NONINVASIVE QUANTITATION OF GLOBAL PARAMETERS ON LEFT VENTRICULAR FUNCTION: THE SYSTOLIC PULMONARY ARTERY PRESSURE AND CARDIAC OUTPUT. 1988.
35. Eyvind Rødahl: STUDIES OF IMMUNE COMPLEXES AND RETROVIRUS-LIKE ANTIGENS IN PATIENTS WITH ANKYLOSING SPONDYLITIS. 1988.
36. Ketil Thorstensen: STUDIES ON THE MECHANISMS OF CELLULAR UPTAKE OF IRON FROM TRANSFERRIN. 1988.
37. Anna Midelfart: STUDIES OF THE MECHANISMS OF ION AND FLUID TRANSPORT IN THE BOVINE CORNEA. 1988.
38. Eirik Helseth: GROWTH AND PLASMINOGEN ACTIVATOR ACTIVITY OF HUMAN GLIOMAS AND BRAIN METASTASES – WITH SPECIAL REFERENCE TO TRANSFORMING GROWTH FACTOR BETA AND THE EPIDERMAL GROWTH FACTOR RECEPTOR. 1988.
39. Petter C. Borchgrevink: MAGNESIUM AND THE ISCHEMIC HEART. 1988.
40. Kjell-Arne Rein: THE EFFECT OF EXTRACORPOREAL CIRCULATION ON SUBCUTANEOUS TRANSCAPILLARY FLUID BALANCE. 1988.
41. Arne Kristian Sandvik: RAT GASTRIC HISTAMINE. 1988.
42. Carl Bredo Dahl: ANIMAL MODELS IN PSYCHIATRY. 1988.
43. Torbjørn A. Fredriksen: CERVICOGENIC HEADACHE. 1989.
44. Rolf A. Walstad: CEFTAZIDIME. 1989.
45. Rolf Salvesen: THE PUPIL IN CLUSTER HEADACHE. 1989.

46. Nils Petter Jørgensen: DRUG EXPOSURE IN EARLY PREGNANCY. 1989.
47. Johan C. Ræder: PREMEDICATION AND GENERAL ANAESTHESIA IN OUTPATIENT GYNECOLOGICAL SURGERY. 1989.
48. M. R. Shalaby: IMMUNOREGULATORY PROPERTIES OF TNF-α AND RELATED CYTOKINES. 1989.
49. Anders Waage: THE COMPLEX PATTERN OF CYTOKINES IN SEPTIC SHOCK. 1989.
50. Bjarne Christian Eriksen: ELECTROSTIMULATION OF THE PELVIC FLOOR IN FEMALE URINARY INCONTINENCE. 1989.
51. Tore B. Halvorsen: PROGNOSTIC FACTORS IN COLORECTAL CANCER. 1989.
52. Asbjørn Nordby: CELLULAR TOXICITY OF ROENTGEN CONTRAST MEDIA. 1990.
53. Kåre E. Tvedt: X-RAY MICROANALYSIS OF BIOLOGICAL MATERIAL. 1990.
54. Tore C. Stiles: COGNITIVE VULNERABILITY FACTORS IN THE DEVELOPMENT AND MAINTENANCE OF DEPRESSION. 1990.
55. Eva Hofsli: TUMOR NECROSIS FACTOR AND MULTIDRUG RESISTANCE. 1990.
56. Helge S. Haarstad: TROPHIC EFFECTS OF CHOLECYSTOKININ AND SECRETIN ON THE RAT PANCREAS. 1990.
57. Lars Engebretsen: TREATMENT OF ACUTE ANTERIOR CRUCIATE LIGAMENT INJURIES. 1990.
58. Tarjei Rygnestad: DELIBERATE SELF-POISONING IN TRONDHEIM. 1990.
59. Arne Z. Henriksen: STUDIES ON CONSERVED ANTIGENIC DOMAINS ON MAJOR OUTER MEMBRANE PROTEINS FROM ENTEROBACTERIA. 1990.
60. Steinar Westin: UNEMPLOYMENT AND HEALTH: Medical and social consequences of a factory closure in a ten-year controlled follow-up study. 1990.
61. Ylva Sahlin: INJURY REGISTRATION, a tool for accident preventive work. 1990.
62. Helge Bjørnstad Pettersen: BIOSYNTHESIS OF COMPLEMENT BY HUMAN ALVEOLAR MACROPHAGES WITH SPECIAL REFERENCE TO SARCOIDOSIS. 1990.
63. Berit Schei: TRAPPED IN PAINFUL LOVE. 1990.
64. Lars J. Vatten: PROSPECTIVE STUDIES OF THE RISK OF BREAST CANCER IN A COHORT OF NORWEGIAN WOMEN. 1990.
65. Kåre Bergh: APPLICATIONS OF ANTI-C5a SPECIFIC MONOCLONAL ANTIBODIES FOR THE ASSESSMENT OF COMPLEMENT ACTIVATION. 1991.
66. Svein Svenningsen: THE CLINICAL SIGNIFICANCE OF INCREASED FEMORAL ANTEVERSION. 1991.
67. Olbjørn Klepp: NONSEMINOMATOUS GERM CELL TESTIS CANCER: THERAPEUTIC OUTCOME AND PROGNOSTIC FACTORS. 1991.
68. Trond Sand: THE EFFECTS OF CLICK POLARITY ON BRAINSTEM AUDITORY EVOKED POTENTIALS AMPLITUDE, DISPERSION, AND LATENCY VARIABLES. 1991.
69. Kjetil B. Åsbakk: STUDIES OF A PROTEIN FROM PSORIATIC SCALE, PSO P27, WITH RESPECT TO ITS POTENTIAL ROLE IN IMMUNE REACTIONS IN PSORIASIS. 1991.
70. Arnulf Hestnes: STUDIES ON DOWN'S SYNDROME. 1991.
71. Randi Nygaard: LONG-TERM SURVIVAL IN CHILDHOOD LEUKEMIA. 1991.
72. Bjørn Hagen: THIO-TEPA. 1991.
73. Svein Anda: EVALUATION OF THE HIP JOINT BY COMPUTED TOMOGRAPHY AND ULTRASONOGRAPHY. 1991.
74. Martin Svartberg: AN INVESTIGATION OF PROCESS AND OUTCOME OF SHORT-TERM PSYCHODYNAMIC PSYCHOTHERAPY. 1992.
75. Stig Arild Slørdahl: AORTIC REGURGITATION. 1992.
76. Harold C Sexton: STUDIES RELATING TO THE TREATMENT OF SYMPTOMATIC NON-PSYCHOTIC PATIENTS. 1992.
77. Maurice B. Vincent: VASOACTIVE PEPTIDES IN THE OCULAR/FOREHEAD AREA. 1992.
78. Terje Johannessen: CONTROLLED TRIALS IN SINGLE SUBJECTS. 1992.
79. Turid Nilsen: PYROPHOSPHATE IN HEPATOCYTE IRON METABOLISM. 1992.
80. Olav Haraldseth: NMR SPECTROSCOPY OF CEREBRAL ISCHEMIA AND REPERFUSION IN RAT. 1992.
81. Eiliv Brenna: REGULATION OF FUNCTION AND GROWTH OF THE OXYNTIC MUCOSA. 1992.
82. Gunnar Bovim: CERVICOGENIC HEADACHE. 1993.
83. Jarl Arne Kahn: ASSISTED PROCREATION. 1993.
84. Bjørn Naume: IMMUNOREGULATORY EFFECTS OF CYTOKINES ON NK CELLS. 1993.
85. Rune Wiseth: AORTIC VALVE REPLACEMENT. 1993.
86. Jie Ming Shen: BLOOD FLOW VELOCITY AND RESPIRATORY STUDIES. 1993.
87. Piotr Kruszewski: SUNCT SYNDROME WITH SPECIAL REFERENCE TO THE AUTONOMIC NERVOUS SYSTEM. 1993.
88. Mette Haase Moen: ENDOMETRIOSIS. 1993.
89. Anne Vik: VASCULAR GAS EMBOLISM DURING AIR INFUSION AND AFTER DECOMPRESSION IN PIGS. 1993.
90. Lars Jacob Stovner: THE CHIARI TYPE I MALFORMATION. 1993.
91. Kjell Å. Salvesen: ROUTINE ULTRASONOGRAPHY IN UTERO AND DEVELOPMENT IN CHILDHOOD. 1993.
92. Nina-Beate Liabakk: DEVELOPMENT OF IMMUNOASSAYS FOR TNF AND ITS SOLUBLE RECEPTORS. 1994.
93. Sverre Helge Torp: *erb*B ONCOGENES IN HUMAN GLIOMAS AND MENINGIOMAS. 1994.
94. Olav M. Linaker: MENTAL RETARDATION AND PSYCHIATRY. Past and present. 1994.